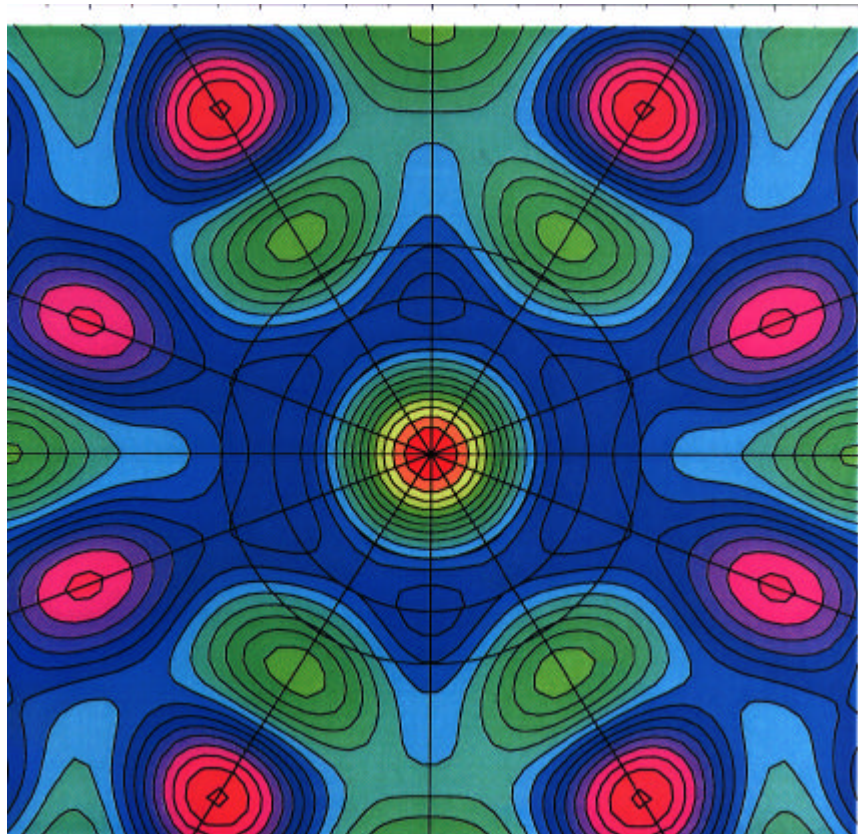


SCIENTIFIC REPORT

1997-1998



Laboratoire Léon Brillouin

CONTENTS

FOREWORD.....	1
PRESENTATION OF LLB.....	3
SCIENTIFIC HIGHLIGHTS.....	15
- MAGNETISM AND SUPERCONDUCTIVITY.....	17
- STRUCTURES AND PHASE TRANSITIONS.....	39
- DISORDERED SYSTEMS AND MATERIALS SCIENCE.....	56
- CHEMICAL PHYSICS AND BIOLOGY.....	76
- TECHNICAL AND INSTRUMENTAL DEVELOPMENTS.....	96
EXPERIMENTAL PROGRAMME AND USER ACTIVITIES.....	115
PUBLICATIONS	125

FOREWORD

This year, we adopt a new presentation of the activities of the Laboratoire Léon Brillouin (LLB), which emphasizes the scientific highlights and the more recent developments accomplished both by the researchers of the laboratory and by external users.

The LLB is a laboratory dependent both on the Centre National de la Recherche Scientifique (CNRS) and the Commissariat à l'Energie Atomique (CEA). It has been created with a triple purpose :

- a) to be a large national facility where neutron scattering experiments proposed by external users can be realised in the best conditions,
- b) to train young researchers, in particular, giving the opportunity of preparing PhD thesis essentially based on neutron scattering techniques and instrumentation,
- c) to have its own research activity based on the work of permanent or semi-permanent groups having a coherent organisation of their research activities, centred on the use of neutron scattering.

Certainly, the three types of activities largely overlap each other, and the scientific evolution of the laboratory since its creation shows that it adapted constantly to the more recent developments both in research and in technology. It is even such overlap that originates some original studies based, for example, in new instruments or in extended researches less compatible with short time periodic applications.

It is worth mentioning in this context the various relations established with several partners in France and in many European countries. In particular, the participation of the LLB to the Large Scale Facilities Programme of the European Union increased substantially the number of European users since 1993. As a consequence, the LLB is recognized as one of the best medium flux neutron sources of the world.

The following pages illustrate some of the activities of the LLB. The report focuses mainly on the research activities performed, totally or in collaboration, by the teams of the laboratory, but it shows as well some highlights of experiments totally performed by external users. The examples are far to be exhaustive and cannot cover all the domains of research studied by neutron scattering. Other reports summarize the ensemble of the activity performed at the LLB.

The LLB, the only French national neutron scattering facility, benefits of the quality of one of the most recent neutron sources in the world, almost exclusively dedicated to research and run in a remarkable way by the Commissariat à l'Energie Atomique. In this way, the LLB can ensure the important responsibility of keeping alive and active a large community of researchers in many different domains, for whom neutron scattering represents an essential tool of research. This large community of French users issued from Physics, Chemistry, Biology, Geophysics and Material Sciences is aware of the importance of this neutron source and its 25 spectrometers.

We believe, with others, that neutron scattering will develop still more in France and in Europe as one of the major techniques of fundamental and applied research and that the LLB will continue to occupy, in the future, a central role in this development.

José Teixeira

Charles-Henri de Novion

PRESENTATION OF LLB

The Laboratoire Léon Brillouin (LLB) is a facility that depends on both the Commissariat à l'Energie Atomique (CEA) and the Centre National de la Recherche Scientifique (CNRS). Its aim is to carry out fundamental and applied research in the field of condensed matter using neutron beams supplied by the reactor Orphée.

As a national laboratory, the LLB facility is opened to external users (via a written proposal and Selection Panel procedure), coming in priority from french laboratories, but also to some extent from foreign countries (mainly of European Union and Central and Eastern Europe).

The LLB both carries its own scientific research programme covering different fields of condensed matter physics, and collaborates closely with many scientists of the french and foreign communities, coming mainly from fundamental research laboratories, but also from applied research and industry. The synthesis of activities and the highlights presented in this Report, as well as the list of publications (more than 250 per year), show that the ensemble of research performed at LLB encompasses a very large scientific domain, in physics, chemistry, biology, materials science and geosciences.

The reactor Orphée and the LLB instruments

Orphée (which operates since december 1980) is the most recent and the highest flux medium size reactor, especially designed to produce thermal neutron beams for fundamental research. It is managed by the Direction of Nuclear Reactors of CEA.

Orphée has a very compact highly enriched ^{235}U - 34% Al core, a heavy water reflector and a light water swimming pool.

The variety of problems studied by neutron scattering requires a neutron wavelength (and energy) distribution as broad as possible : small wavelength to explore a large volume of the reciprocal space for atomic structure resolution, large wavelength (and therefore low energy) to study large scale structures up to a fraction of μm and to perform high resolution energy spectroscopy (neV to meV scale). This is solved by local thermalization of 3 neutron beams by a hot source (heated graphite, 1400 K), of 8 others by two cold sources (liquid hydrogen, 20 K), the 6 remaining ("thermal" beams) being thermalized at the temperature of the D_2O moderator (300 K). This makes available incident neutrons of any wavelength ranging from 0.5 to 15 Å. 6 cold neutron beams are distributed in a guide hall via neutron guides. The design of the 9 horizontal neutron beam tubes (which point tangentially towards the core) and of the 6 curved neutron guides, has allowed to considerably reduce the background due to fast neutrons and γ -rays coming from the reactor, and to optimize the signal-to-background ratio measured on the spectrometers.

The Orphée reactor is maintained at the best possible working order and safety requirements : in 1997, the zircaloy housing core has been replaced; the safety authority undertook a detailed examination of the reactor, and declared itself quite satisfied with it.

A layout of the reactor hall and the neutron guide hall instrumentation is shown in the joined figure. The characteristics of the 24 neutron scattering instruments opened to external users are given in Table 1. Two other new instruments (a small-angle diffractometer with polarized neutrons "PAPOL", and a neutron resonance spin-echo spectrometer in G1bis, see below) will be partly opened to users at the next Selection Panel.

In addition to neutron scattering, a part of Orphée reactor activity is devoted to other utilizations : non-destructive testing by neutron radiography, chemical analysis by neutron activation, irradiation of silicon for the industry and elaboration of isotopes for medical use. These activities are not described in the present Report.

Collaborations

Several collaborations with other countries, particularly European, have been developed, and the international character of the laboratory appears clearly in the large number of publications where, for example, several researchers (worldwide) appear as co-authors. The LLB is consequently an ideal place for the exchange of scientific ideas and for the establishment of collaborations.

Among the international collaborations, it is worth mentioning some particularly intense and fruitful ones.

1) Germany. An agreement exists since 1979 with the Kernforschungszentrum of Karlsruhe, following the CRG principle. It concerns two spectrometers : the triple-axis 2T and the 4-circles 5C2. The latter is supervised by the University of Aachen (prof. G. Heger). Two german physicists and one technician work on a permanent basis at LLB.

The Technical University of Munich has built between 1995 and 1998 a spectrometer of the resonant spin-echo type; one physicist is supported by this University.

2) Austria. Since 1980, a 3-axis spectrometer works also in the conditions of a CRG. This collaboration was initiated by Prof. O. Blaschko, unfortunately deceased in 1997. The responsibility of the scientific programme is now assumed by Prof. P. Fratzl (University of Leoben) and Dr. G. Krexner (University of Wien), and one physicist is permanently at LLB.

3) Italy. One of the largest users, Italy established an agreement with LLB that corresponds to a financial participation. Another agreement concerns the renewal and the utilisation of the diffractometer DIANE (G5.2), that studies residual stresses in the field of materials science.

4) Russia. Three agreements of scientific collaboration have been signed in 1994 by the CNRS and the CEA with the Petersburg Nuclear Physics Institute of the Russian Academy of Sciences, the Kurchatov Institute at Moscow, and the Joint Institute of Nuclear Research at Dubna.

A new diffractometer for the study of the structure of powders at high resolution, built at Gatchina, is now at LLB (in G4.2 in the guide hall), where it has been inaugurated in 1997 (see photographs).

5) Hungary. A collaboration has been established with the Neutron Physics Department of the Research Institute for Solid State Physics at Budapest (Prof. L. Rosta).

6) Other international operations concern Morocco, Korea and China.

The LLB continues also a very fruitful collaboration with the Institute Laue-Langevin (ILL), namely in the domain of instrumentation, in particular on the elaboration of polarizing Heusler single crystals.

It participates also (since July 1998) in the pool that uses as a CRG the backscattering spectrometer IN13 at ILL, mostly used for biological studies.

Finally, in the international domain, the LLB benefits since 1993 from the funds of the "Large Scale Facilities" access programmes ("Human Capital and Mobility" (1993-96) and "Training and Mobility of Researchers" (1997-2000)) for the countries of the European Union and associated states, extended in the case of HCM to PECO countries. Within this frame, the LLB participates in the network XENNI (The 10-Member European Network for Neutron Instrumentation).

Undertaking an important role in the training of young scientists, the LLB participates in the European course HERCULES, organises and participates in many workshops, schools, educational meetings, and organises visits of its installations. Some of the visits, during specific days, are addressed to a more general public.

The tables and statistics shown at the end of this Introduction (list of LLB staff, of long-term visitors and post-docs, and of PhD students) and in the chapter "Experimental Programme and User Activities" give a numerical idea of the ensemble of the activities. Even non exhaustive, they show how much the LLB is a tool used by several hundreds of researchers and students coming from many different places and disciplines. More than the numbers, the scientific production, as mirrored by the list of publications, shows the richness of the research activity, and the devotion of all the staff : permanent researchers, engineers and technicians of LLB and Orphée, administrative staff, associated researchers, post-docs and PhD's. It is due to their work and competence that the LLB can be considered among the most recognised places for neutron scattering research.

**Inauguration of the high-resolution powder diffraction built in Gatchina
and installed in the guide hall (G4.2) of Orphée Reactor
June 12, 1997**

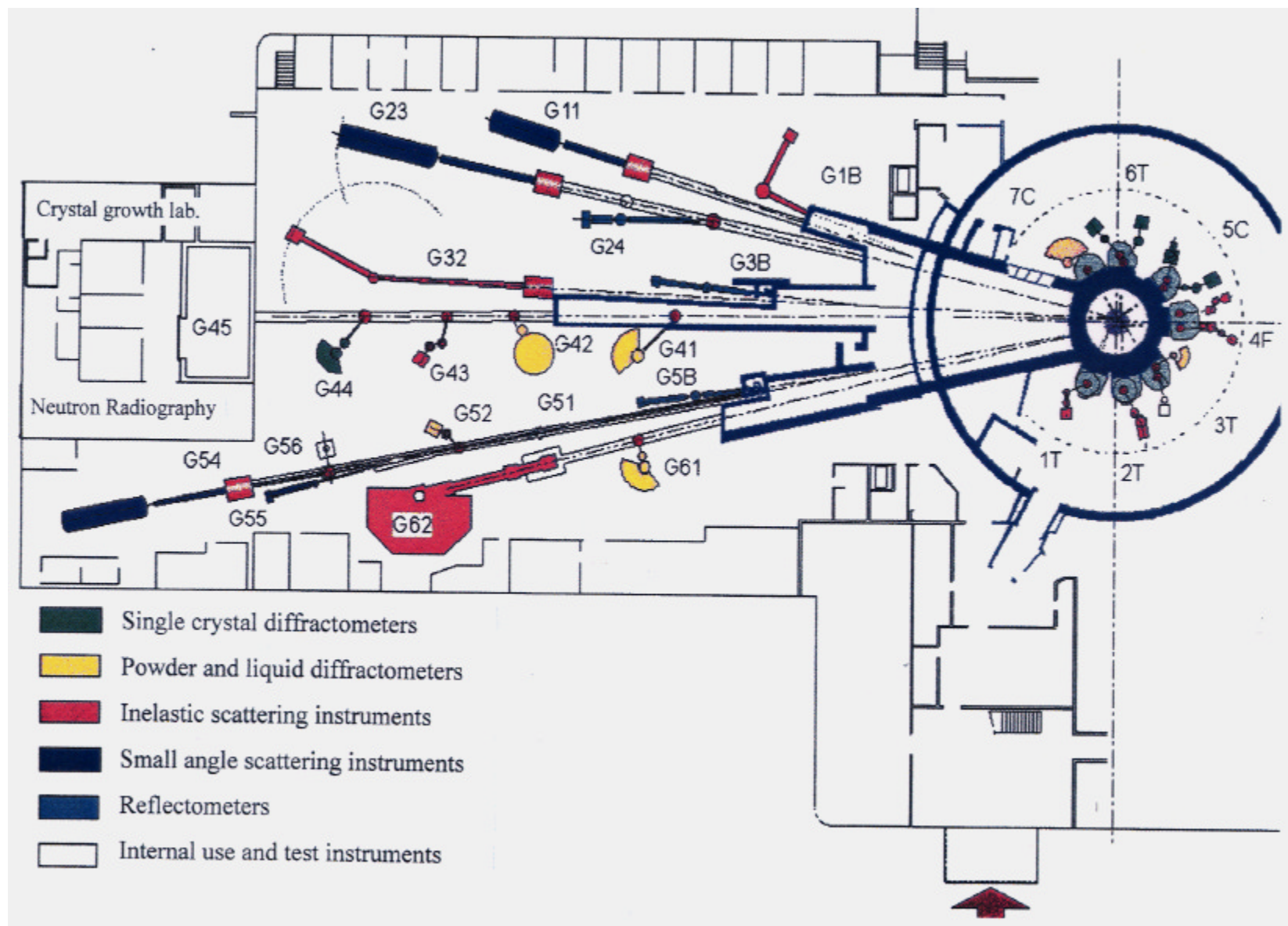


*Standing from left : J. Rodriguez-Carvajal, C.H. de Novion, F. Bourée, G. Pépy, V. Nazarenko, J. Teixeira,
Sitting : A. Kurbakov, T. Roisnel*



*The party !
From left : A. Goukassov, C.H. de Novion, V. Nazarenko, A. Kurbakov*

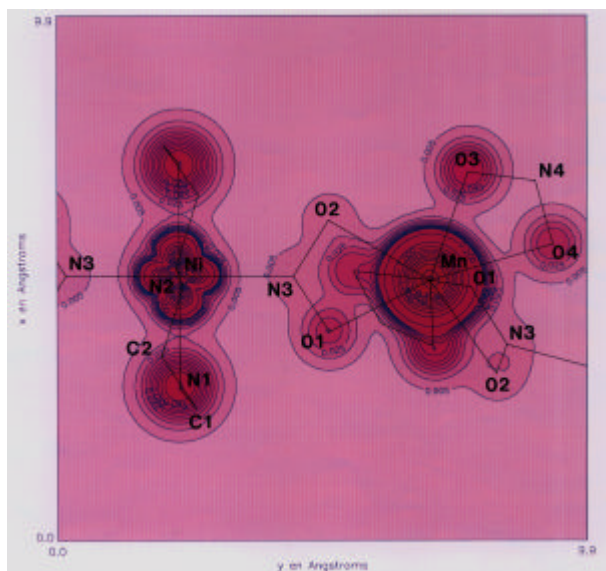
GENERAL IMPLANTATION OF LLB INSTRUMENTS



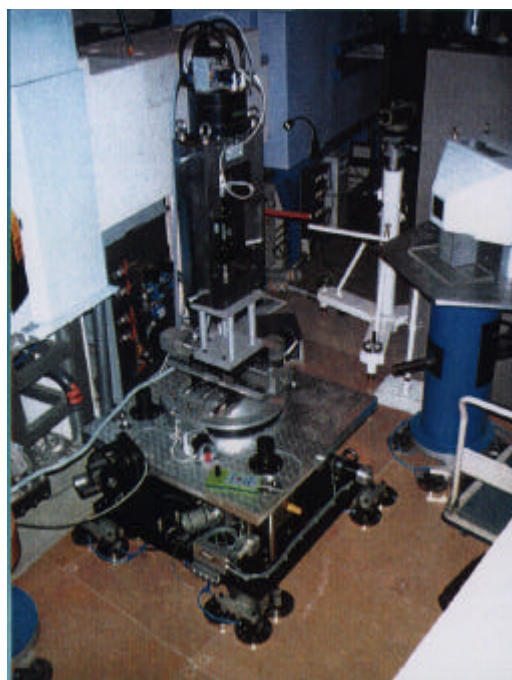
List of LLB instruments scheduled for external users

	Powder diffractometers 3T2 "Thermal neutrons" 2-axis (20 detectors) high resolution, mainly for nuclear structure determination G4.1 "Cold neutrons" 2-axis (multidetector 800 cells) high flux, mainly for magnetic structure determination G4.2 "Cold neutrons" 2-axis (7x10 detectors) high resolution, for structure determination on polycrystalline samples with large unit cell. MICRO (G6.1) "Cold neutrons" 2-axis (multidetector 400 cells) with long wavelength ($\sim 5\text{\AA}$) and high flux, for the study of very small powder samples ($< 1\text{ mm}^3$). Very high pressure cell available (40 GPa). Diffractometers for material science studies 6T1 "Thermal neutrons" 4-circle for texture determination DIANE (G5.2) "Cold neutrons" 2-axis for internal strain mapping in bulk samples with spatial resolution $\sim 1\text{ mm}^3$. Single crystal diffractometers 5C1 "Hot neutrons" 2-axis with lifting arm, polarised neutrons, magnetic field (8 Tesla) for spin-density maps determination 5C2 "Hot neutrons" 4-circle for nuclear structure determination. 6T2 "Thermal neutrons" 2-axis, lifting arm and 4-circle, mainly for magnetic structure determination. 12 Tesla magnetic field available Diffuse scattering instruments 7C2 "Hot neutrons" 2-axis (multidetector 640 cells) for local order studies in liquid or amorphous systems. Cryostat and furnace available (1.2K to 1300°C). G4.4 "Cold neutrons" 2-axis (48 detectors, elastic/inelastic discrimination by time-of-flight technique) for local order studies in single crystals. Furnace available (1400°C). Small-angle scattering instruments PACE (G1.1) "Cold neutrons" (annular detector, 30 rings) for study of large scale structures in isotropic systems (mainly polymers and colloids). PAXY (G2.3) "Cold neutrons" (X-Y detector, 128x128 cells) for study of large-scale structures (10 to 500 Å) in anisotropic systems (polymers under stress, metallurgical samples, vortex in superconductors ...). PAXE (G5.4) "Cold neutrons" (X-Y detector, 64x64 cells) for multipurpose studies of large scale structures	Reflectometers DESIR (G5bis) "Cold neutrons" reflectometer operating in time-of-flight mode (X-Y multidetector 128x128 cells) for horizontal samples (liquids). EROS (G3bis) "Cold neutrons" reflectometer operating in time-of-flight mode for multipurpose surface studies. PADA (G2.4) "Cold neutrons" reflectometer with polarised neutrons and polarisation analysis for the study of magnetic layers. Triple-axis instruments 1T "Thermal neutrons" high-flux 3-axis instrument with focusing monochromator and analyser, mainly devoted to spin-waves and magnetic excitations studies (1.5 to 80 meV). 2T "Thermal neutrons" high-flux 3-axis instrument with focusing monochromator and analyser, mainly devoted to phonon dispersion curves measurements. Very high pressure cell (100 Kbar) available. 4F1 "Cold neutrons" high flux 3-axis instrument with double monochromator and analyser, mainly devoted to the study of low-energy (15µeV to 4meV) magnetic excitations. Polarised neutrons and polarisation analysis option available. 4F2 "Cold neutrons" high-flux 3-axis instrument for the study of low-energy excitations (e.g. soft modes) or modulated structural studies in single crystals. G4.3 "Cold neutrons" high resolution and low background 3-axis instrument, mainly devoted to elastic diffuse scattering studies. Quasi-elastic instruments MIBEMOL G6.2 "Cold neutrons" high resolution ($\sim 15\text{ }\mu\text{eV}$ at 10Å) time-of-flight instrument for the study of low energy excitations, mainly in disordered systems. MESS (G3.2) "Cold neutrons" small-angle high resolution spin-echo instrument, for the study of slow dynamics (Fourier time $\sim 40\text{ ns}$) of disordered matter (movements of large molecules in biology or physical chemistry, relaxation of magnetic moments).
--	--	---

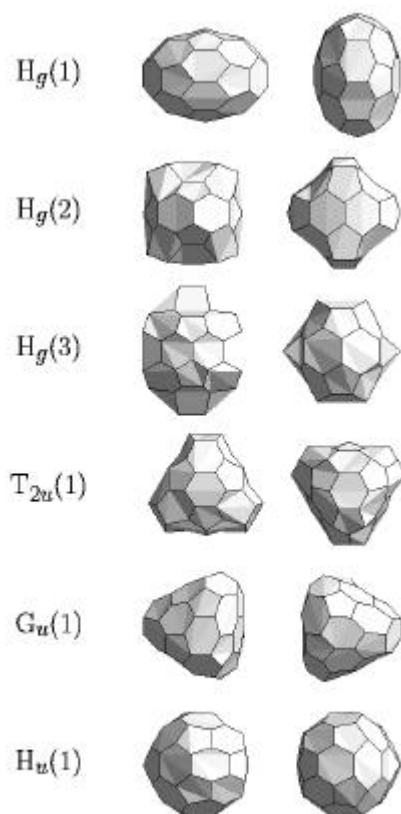
SCIENTIFIC HIGHLIGHTS



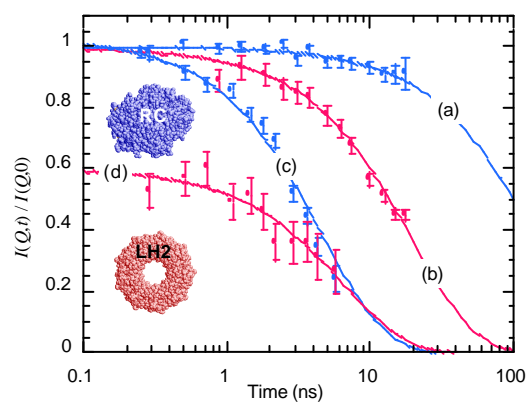
Induced spin density map in the ferromagnetic chain compound $\text{MnNi}(\text{NO}_2)_4(\text{en})_2$



The Italian-French strain scanner installed at the Orphée reactor



Displacement patterns for six different eigenmodes of the C_{60} molecule.



Time dependence of the intermediate scattering function for the RC and LH2 proteins measured by spin-echo spectroscopy

MAGNETISM AND SUPERCONDUCTIVITY

The research related to magnetism is progressing steadily as shown by the number of new pertinent results of high quality at the international level and the large number of scientists involved coming from the Laboratoire Léon Brillouin and from other national and international laboratories. Let us mention as an example the "hot" result obtained recently which concerns the new rather unexpected discovery of **strong incommensurate magnetic fluctuations in the ruthenate** Sr_2RuO_4 (brother compound of the cuprate La_2CuO_4), a potent candidate for p-wave superconductivity.

The field covered is rich and in constant evolution with emergence of new subjects (spin ladders, ruthenates). The activities can be grouped into several subfields :

The first one (the largest) is entitled **Strongly Correlated Electron Systems**. After having got a strong impulse from the physics of high T_c cuprates, it progresses rapidly and becomes more unified. It includes the **Mixed Valence** and heavy fermions rare earth compounds, the **Low Dimensional** systems (spin Peierls system CuGeO_3 and spin ladder compound $(\text{Sr,Ca})_{14}\text{Cu}_{24}\text{O}_{41}$), the "colossal magnetoresistance" **Manganites**, and naturally the **High T_c Cuprates** (and related materials such as the **ruthenates**).

The second one is the **Molecular Magnetism** developed in collaboration with the Chemistry group of O. Kahn at Bordeaux University.

The third one concerns **Magnetic Nanostructures**, a rapidly progressing theme which includes small aggregates, superlattices and thin layered nanostructures.

The activity concerning **Magnetism in the frustrated Laves hydrides** RMnH_x is rising rapidly .

Finally magnetic structure determination in various families of d and f intermetallic compounds constitutes an important activity in collaboration with several Solid State Chemistry Laboratories.

1. STRONGLY CORRELATED ELECTRON SYSTEMS

There are mainly two classes of strongly correlated electron systems : the rare earth (actinide) systems where the localised f electrons are strongly interacting with themselves and with the conduction electrons, and the d electron oxides where the d electrons are strongly interacting. Because of the strong interactions, Mott insulator-metal transitions are expected, new magnetic properties are obtained and Fermi liquid behavior of metals may break down. These strong interactions can lead to new types of superconductivity, charge and spin orderings. Neutron scattering is a good tool to study the new orderings and the fluctuations in their vicinity or at low dimension when ordering is suppressed and replaced by a **spin liquid** phase. This field is rapidly expanding both experimentally and theoretically. LLB takes part in this adventure.

1.a Mixed valence and Kondo systems (J.-M. Mignot)

This activity is developed by J.-M. Mignot together with postdocs in collaboration with French groups in Grenoble (Boucherle, Fak, Schweizer, Givord), a Russian group at Kurchatov Institute in Moscow (Aleksiev, Clementyev, Goncharenko) and two Japanese groups, one at Tohoku University Sendai (Matsumara, Suzuki) and one at Tokyo Metropolitan University (Kohgi, Iwasa).

Antiferroquadrupolar order in TmTe

The most interesting result obtained in collaboration with the Japanese group at Sendai and with a postdoc (P. Link) is the determination by neutron diffraction of antiferroquadrupolar long range ordering in the mixed valence compound TmTe. This determination is indirect. Detailed information of the ordered state of quadrupolar moments is derived from the symmetry properties of the response to an applied magnetic field.

Mixed valence systems

In mixed valence systems such as Yb_4As_3 or Sm_3Te_4 , the rare earth ion is not fluctuating between two valences but is either in one valence state or in the other. The number of ions in each valence state is fixed by charge neutrality. At low temperature, **charge ordering** occurs in Yb_4As_3 . The ions with the valence corresponding to a magnetic ion order along one-dimensional chains which then behave as **spin 1/2 Heisenberg antiferromagnetic chains**. The excitation spin fluctuation spectrum has been studied by inelastic neutron scattering and the expected two-spinon

continuum spectrum has been recovered (in collaboration with the Tokyo Metropolitan University Japanese group (Iwasa, Kohgi)).

In the other mixed valence system Sm_3Te_4 , it seems that the different valence ions are not ordered even at very low temperature, but could form a **charge glass** with magnetic properties reminiscent of a spin glass of a new type (collaboration with Grenoble group : Boucherle, Givord, Schweizer).

Kondo systems

YbB_{12} is known to behave as a **Kondo insulator** with a small **charge gap** seen by photoemission. Neutron inelastic scattering on a powder sample have revealed a complex excitation spectrum with a well defined **spin gap**.

In heavy fermion systems (Kondo lattice) the border between the magnetic phase and the non-magnetic one is marked by the presence of a $T=0$ **quantum critical point (QCP)** which may be responsible for **non-Fermi liquid behavior**. The vicinity of such a QCP has been studied by inelastic neutron scattering in $\text{Ce}_{1-x}\text{La}_x\text{Ru}_2\text{Si}_2$ with x close to .1 (collaboration with S. Raymond, L.P. Regnault, B. Fak (CENG)). The behavior seems to be different from another well studied compound $\text{Ce}(\text{Cu}_{1-x}\text{Au}_x)_6$ (Schröder)

1.b Low Dimensional systems

The renewal of interest in low dimensional systems is stimulated by the physics of high T_c cuprates for which the active electrons are located in $D=2$ dimensional CuO_2 planes and where **pseudogap** and non-Fermi liquid phenomena have been observed in the normal state, which are reminiscent of low dimensional electron systems (Luttinger liquid). Two quasi one-dimensional systems have been studied : the spin Peierls system CuGeO_3 and the spin ladder system $(\text{Sr},\text{La})_{14-x}\text{Ca}_x\text{Cu}_{24}\text{O}_{41}$.

Spin Peierls system CuGeO_3

(M. Braden, B. Hennion, M. Ain (LLB), G. Dhalenne and A. Revcolevschi (Laboratoire de Chimie des Solides d'Orsay))

In this quasi one-dimensional system, the spin-Peierls dimerisation structural transition is based on the spin-phonon coupling. This aspect has been investigated in LLB for recent years by M. Braden. Contrary to the usual view which assumes an adiabaticity with fast magnetic excitations and slow phonons (soft modes), the situation has been shown to be the opposite. There are no soft modes, the phonons become harder so that there is non-adiabaticity. The spin excitations are slow and the phonon modes fast so that non-adiabaticity leads to a new effective spin Hamiltonian. This could explain (P. Pfeuty) the **recently discovered new excitation** by inelastic neutron scattering just above the two spinon continuum and independently of the spin-Peierls transition.

Spin Ladder system $(\text{Sr},\text{La})_{14-x}\text{Ca}_x\text{Cu}_{24}\text{O}_{41}$

(L.P. Regnault (CENG), H. Moudden (LLB), J.E. Lorenzo (Laboratoire de Cristallographie de Grenoble)).

2-3-n legs ladders are one-dimensional systems which become closer to two dimensions when n becomes large. Such systems may constitute a link between one and two-dimensional electron systems and thus help to better understand the high T_c cuprate two dimensional physics. $(\text{Sr},\text{La})_{14-x}\text{Ca}_x\text{Cu}_{24}\text{O}_{41}$ is a doped two-leg ladder system which becomes **superconductor** under pressure. The magnetic excitation spectrum has been studied by neutron scattering with clear evidence of a singlet-triplet excitation. Measurements as a function of doping show that the **spin gap** does not vary with doping. Experiments under pressure in the superconducting phase are expected soon. The samples are prepared by the Laboratoire de Chimie des Solides in Orsay (A. Revcolevschi)

1.c Manganites.

The oxides of perovskite structure with Mn ions have recently attracted a strong interest due to the discovery of a giant negative magnetoresistance. The doping of the family RMnO_3 (R: lanthanide) with divalent ions introduces holes in the d band that give rise to interesting interrelated magnetic, transport and structural properties.

Three projects are actually developed :

Inhomogeneities and magnetic excitations in $\text{La}_{1-x}\text{Ca}_x\text{MnO}_3$

(M. Hennion, F. Moussa, G. Biotteau [PhD student])

Pure LaMnO_3 is an insulator with a well defined antiferromagnetic structure at low temperature. When hole doping reaches a certain threshold around $x=.3$, the system becomes metallic and ferromagnetic and acquires new interesting transport properties. In order to understand this state, it is interesting to approach it from the low doping side $0 < x < .2$. New unexpected properties have been discovered, some of which are not yet understood.

First, new **well defined low energy excitations** have been discovered from inelastic neutron scattering studies on single crystals (prepared by the Laboratoire de Chimie des Solides in Orsay).

Secondly, from small angle neutron scattering, **magnetic inhomogeneities** have been identified and characterized. These could be associated with **charge inhomogeneities** which are the object of much debate in the scientific community.

The same phenomena have been observed in the brother compound $\text{La}_{1-x}\text{Sr}_x\text{MnO}_3$.

Parallel studies (structural Jahn-Teller transitions) have been pursued on the same samples (J.Rodriguez-Carvajal).

Charge ordering phenomena

(J. Rodriguez-Carvajal, A. Daoud-Aladine [PhD student])

For specific doping elements and specific concentrations of these dopants a **charge ordered** state can be realized. This is the case for **$\text{Pr}_{0.5}\text{Ca}_{0.5}\text{MnO}_3$** and **$\text{Nd}_{0.5}\text{Ca}_{0.5}\text{MnO}_3$** which have been studied by neutron diffraction to reveal charge orderings (single crystals were grown by the Laboratoire de Chimie des Solides at Orsay). New experiments are planned with Ca replaced by Sr.

Another project led by C. Martin (Crismat-Caen; collaboration LLB: G. André, F. Bourée) deals with the relations between the nuclear and magnetic structures of some GMR manganites and their associated macroscopic (magnetic, transport...) properties. For the family $\text{Pr}_{0.5}\text{Sr}_{0.5-x}\text{Ca}_x\text{MnO}_3$ ($0 < x < 0.5$), the complete nuclear and magnetic phase diagram has been obtained from neutron powder diffraction showing the influence of the A cation size on the magnetic properties of the compounds. The influence of the doping on the Mn site on the charge and orbital ordering of the $\text{Pr}_{0.5}\text{A}_{0.5}\text{Mn}_{1-x}\text{M}_x\text{O}_3$ (A=Sr,Ca; M=Cr,Al; $x=0.05$) compounds has been studied for Cr and Al doping.

1.d Magnetism and Superconductivity in cuprates and ruthenates.

High T_c cuprates

LLB Neutron group (Y. Sidis [new CNRS recruitment], P. Bourges, D. Petitgrand, B. Hennion, M. D'Astuto [PhD student]), LLB Crystallography group (G. Collin, P. Gautier-Picard [Postdoc], L. Manificier [PhD student]), LLB Theory group (F. Onufrieva, P. Pfeuty, M. Kisselev [post doc], F. Bouis [PhD student])

High T_c cuprates constitute the motor of the actual development of the field of strongly correlated electron systems. After more than ten years of intense experimental and theoretical efforts, the secrets of those highly complex electronic systems are still not yet unraveled and we should pursue our efforts.

High T_c cuprates are characterized by global anomalies : the very existence of high T_c anomalies observed for all properties in the underdoped regime above T_c , anomalies observed in the superconducting state. There are more and more arguments that all of them are somehow related to anomalous magnetism. This is why the study of details of magnetic properties becomes today a key point for understanding the physics of high T_c cuprates.

In LLB we follow a strategy combining three interrelated actions : **preparation** of large good quality single crystals; **inelastic neutron scattering** experiments giving access to the spatio-temporal magnetic response in both the normal metallic state and the superconducting state; **theoretical** developments trying to give a unified picture for both charge and spin properties.

The **underdoped** regime has been extensively studied. In the superconducting state, the existence of a **resonance peak** has recently been confirmed in a new system **$\text{Bi}_2\text{Sr}_2\text{CaCu}_2\text{O}_{8+\delta}$ (BiSCO)**, in collaboration with B. Keimer and H.F. Fong (University of Princeton and MPI Stuttgart), for which the electronic spectra are known from photoemission experiments. The neutron resonance peak has larger momentum and energy width in BiSCO than in YBCO.

New experiments have been realized with **Zn** and **Ni** doped YBCO samples prepared by the LLB crystallography group (G. Collin, P. Gautier-Picard). The effect of these two impurities seems to be rather different : Zn affects strongly the resonance peak, whereas Ni only shifts it slightly with a broadening in both wave vector and energy .

New results obtained in underdoped YBCO both in LLB and abroad (Mook, Hayden, Aeppli) show that for energy below the energy of the commensurate resonance peak there exists an **incommensurate** dynamic response. This has been explained by the LLB theory group (F. Onufrieva, P. Pfeuty) based on the general theory of two dimensional electron systems close to an Electronic Topological Transition (ETT). It is shown that the superconducting state in the two-dimensional electron system in the proximity of ETT (i.e. a long range ordered state with respect to charge degrees of freedom) is at the same time a **quantum spin liquid** state with respect to spin degrees of freedom and that both the resonance peak and the incommensurability are signatures of such a **mixed state**. As we already noticed, this is only part of a general theory developed by the theory group (F. Onufrieva, P. Pfeuty, M. Kisselev, F. Bouis). This theory being developed for different properties and for both normal and superconducting states allows to understand crucial anomalies observed experimentally in high T_c cuprates by NMR, inelastic neutron scattering, photoemission, tunneling... More generally it shed light on the nature of the new anomalous metallic state observed in the high T_c cuprates and on the very existence of high T_c superconductivity with d-wave symmetry.

Two other important situations remain to be understood : the **overdoped** regime for which actually no neutron scattering study exists; and the case of **electron doped** cuprates for which the phase diagram is different.

The electron doped system $\text{Nd}_{2-x}\text{Ce}_x\text{CuO}_4$ has been investigated (thesis submitted in 1998 by M.D'Astuto (under the direction of D. Petitgrand)). Samples were not good enough to study dynamic magnetic fluctuations in the superconducting state. The magnetism of rare earth Nd has been studied both in the pure non-superconducting sample Nd_2CuO_4 and in the superconducting sample ($T_c=10\text{K}$) $\text{Nd}_{1.85}\text{Ce}_{0.15}\text{CuO}_4$. In Nd_2CuO_4 , quasi-elastic scattering due to Nd has been measured with the existence of two components : a three dimensional one and a two dimensional one. This could be due to the nature of the interactions between the Nd and Cu ions. To better understand these interactions, magnetic excitations of Nd have been analysed at low temperature. In $\text{Nd}_{1.85}\text{Ce}_{0.15}\text{CuO}_4$, magnetic order of Nd has been studied and it is shown that the effect of the presence of superconducting CuO_2 planes is to induce bidimensional order of Nd magnetic moments.

Finally the role of the reservoir planes in the high T_c cuprates has been considered in a recent PhD thesis work (L. Manificier 1998 under G. Collin supervision) by crystallographic (structural refinements) and magnetic (diamagnetic susceptibility) studies performed on lead and rare-earth substitutions in Bi-2212 systems. The main conclusion reached is that "overdoped", "underdoped", and insulating phases would depend altogether on the carrier concentration in the CuO_2 planes, their mobility, and the physical state of the charge reservoirs.

Ruthenates

(M. Braden, W. Reichardt, (Kf. Karlsruhe) , Y. Sidis, P. Bourges, B. Hennion, G. André (LLB), Y. Maeno (Kyoto University))

A few years after the discovery of superconductivity in CuO_2 systems, a new **oxide superconductor** has been found : **Sr_2RuO_4** . This system has the same layered perovskite structure as La_2CuO_4 , but behaves otherwise very differently. In its stoichiometric composition it is metallic and becomes superconductor at 1.5 K. The electronic properties are determined by the three 4d t_{2g} orbitals (d_{yz}, d_{zx}, d_{xy}) of the Ru^{4+} ion which form the bands that cross the Fermi level resulting in two electron-like quasi-one-dimensional Fermi Surfaces (FS) and one hole-like quasi-two dimensional FS (analogous to the 2D FS of cuprates). Some experiments suggest that superconductivity is rather unconventional of **p-wave symmetry** and could be due to the coupling with ferromagnetic fluctuations. To confirm this view it was essential to study the magnetic fluctuations by neutron scattering on a single crystal which was available (Maeno). Existing NMR results are difficult to interpret making neutron data essential. Recent results reveal unambiguously intense dynamic **spin fluctuations** at low energy (8 meV) and for an **incommensurate** wave vector $(.3,.3,0) 2\pi/a$. This can be interpreted in an itinerant picture as a dynamic quasi-nesting effect due to the two quasi-one dimensional electron like FS (Mazin, Pfeuty). These experiments have been made in the normal metallic state with temperature $10\text{K} < T < 300\text{K}$. Further experiments are planned to explore the superconducting state.

Lattice dynamics has been also explored. If the modes associated with an intra-plane charge ordering behave normally, an anomaly is observed for the vibrations associated with an inter-plane charge ordering .

When Sr is replaced by Ca, the system orders antiferromagnetically at low temperature. With excess oxygen, structural studies by neutron diffraction have shown that **Ca_2RuO_4** presents a first order structural transition associated with a metal-insulator transition.

2. MOLECULAR MAGNETISM

Molecular magnetism is at the borderline between magnetism and organic condensed matter chemistry. It constitutes an activity developed for many years in LLB by B. Gillon in collaboration with O. Kahn and his laboratory at the Institut de Chimie de la Matière Condensée in Bordeaux. Recently an English postdoc (John Stride) joined B. Gillon's group.

The main project developed actually consists in the study of the **ferromagnetic interaction mechanisms** in molecular compounds through the determination of the spin density map which is obtained from diffraction by polarized neutrons. The study of the organic radical triazole nitronyl nitroxide has not been completed because of the lack of sample. A complete study of the bimetallic compound **$\text{MnNi}(\text{NO}_2)_4(\text{en})_2$** (en=ethylenediamine) has been realized. In this compound ferromagnetic chains are formed. The spin density map has been determined and the main result is the low apparent spin transfer from the metallic ions to the bridge NO_2 with a larger spin delocalization towards the outside atoms. This could be due to a compensation effect between two opposite effects, delocalization and spin polarization. Actually a similar study is in progress with the ferromagnetic bimetallic compound **$\text{Mn}_2\text{H}_2\text{OMo}(\text{CN})_7\text{H}_2\text{O}$** .

The informations coming from spin density measurements are completed with charge density measurements from X-ray diffraction and compared to quantum chemistry calculations.

3. MAGNETIC NANOSTRUCTURES

Because of new fabrication tools (epitaxy, nanolithography), small size architectures are designed and a study of their fundamental properties is a challenge for future technological applications.

3.a Molecular nanomagnets : low energy excitations of the Mn_{12} acetate spin cluster

(I. Mirebeau, M. Hennion)

Molecular nanomagnets consist of a few (10-20) paramagnetic ions coupled by exchange interactions. The study of these large magnetic molecules has both fundamental and practical interest (information storage).

New data of very high precision concerning the low energy magnetic excitations of the Mn_{12} acetate spin cluster have been obtained by inelastic neutron scattering at LLB and ILL. This enables to separate the energy sublevels of the ground state and determine through a simple quantum mechanical calculation the value of a very small non- diagonal term which presence in the spin Hamiltonian is necessary to explain the excitation spectrum. This term which produces quantum tunneling between the different magnetic quantum levels is then responsible of the observed finite relaxation time of the magnetization at low temperature.

3.b Neutron Diffraction of rare earth superlattices and epitaxial films

(M. Hennion (LLB) and C. Dufour, K. Dumesnil, P. Mangin (Laboratoire de Physique des Matériaux, Nancy))

Spin reorientation in Laves phases (RE)Fe₂ (RE=rare earth).

Laves phases (RE)Fe₂ present a giant magnetostriction effect at room temperature with potential applications. An epitaxial film of the ternary compound Dy₇Tb₃Fe₂ has been prepared and studied by neutron diffraction to follow the spin reorientation as a function of temperature. An actual project concerns the polarized neutron study of the superlattice DyFe₂/YFe₂ to determine the spin density and follow the spin reorientation as a function of temperature and magnetic field.

Light rare earth films and superlattices

Neutron diffraction of Sm films with thickness of 4000 Å show that the magnetic order of the Sm in the hexagonal sites seems to be the same as in the bulk, but with a higher magnetic moment. The nature of long range interactions between magnetic Sm through non magnetic Nd phase should be studied on superlattices Sm/Nd.

3.c Magnetic structure of superlattices, thin films and regular nanostructures from polarized neutron specular and off-specular reflectometry and surface diffraction

(C. Fermon, F. Ott)

These three different techniques are developed at LLB. When applied together to regular magnetic nanostructures of sufficient size, they give a full 3D magnetic structure determination both parallel and perpendicularly to the surface of the nanostructure. These techniques have been applied to different examples of nanostructures : this necessitates large regular samples (1cm ×1cm) with repetitive motives (alternate lines, alternate layers, lattice of magnetic motives). Only a few laboratories prepare such samples and collaborate with the LLB : SPEC Saclay, CENG Grenoble, CRISMAT Caen, IEF Orsay, IPCMS Strasbourg. The systems studied are Fe/Mn/Fe sandwich structures, (LaMnO)_m(SrMnO)_n superlattices, FePd and Co thin layers with magnetic domains, Pt/Co irradiated interfaces and M/Co/M (M=Au,Pt) sandwiches, Co/Mn superlattices, La_{0.7}Sr_{0.3}MnO₃/SrTiO₃ interface, La(Sr,Ca)MnO₃/YBa₂Cu₃O₇ interface, Si/SiO₂/Co systems with an electric field.

4. MAGNETISM IN THE FRUSTRATED LAVES HYDRIDES RMnH_x

(I. Mirebeau (LLB), I. Goncharenko and A. Irodova (Kurchatov Institute, Moscow))

The RMn_2 compounds where R is Y or a rare earth metal, have been studied during the recent years for several interests : the magnetism of Mn at the border between localized and itinerant; the interplay between R and Mn magnetism; quantum frustration effects for the Mn sublattice with antiferromagnetic interactions.

When hydrogen is added and occupies the interstitial site in the metal sublattices, new interesting effects can be studied : hydrogen acts as a negative pressure on the magnetism of Mn; hydrogen can order and the H ordering can affect the magnetic ordering of Mn and R.

In recent studies of the magnetic and crystal structures of $\text{YMn}_2\text{H}_{4.3}$, a peculiar interplay between the magnetic and hydrogen order has been observed. Mn magnetic moments and hydrogen atoms order simultaneously through a first order structural transition.

Further neutron diffraction (and eventually inelastic neutron scattering) studies of the interplay between hydrogen and magnetic orders are in preparation using chemical substitution, applied pressure and varying the hydrogen content.

Similar structural and magnetic phase determinations have been pursued on the same hydrides but for lower hydrogen concentration (specifically $x=1.1$) by M. Latroche, V. Paul-Boncour from CNRS-Thiais and F. Bourée, G. André (LLB).

5. DETERMINATION OF MAGNETIC STRUCTURES IN MAGNETIC SYSTEMS WITH D AND F ELECTRONS

When new families of magnetic compounds are synthesized, it is essential to determine their magnetic structure in order to have access to the microscopic magnetic interaction at work. This is done in close collaboration with solid state chemistry laboratories in France (Bordeaux, Rennes, Paris VI, Clermont-Ferrand...) and abroad (Spain, Germany, Poland, Russia, Switzerland). Many different compounds are studied, ranging from transition metal, rare earth to actinide compounds. Among these, let us consider three typical examples:

With the ICMCB Bordeaux (B. Chevalier) and the LLB (F. Bourée and T. Roisnel), the study of the family R_2T_2X (R =rare earth or U; T =transition metal; X =Sn or In) has been pursued (PhD thesis of D. Laffargue) mainly for X =Sn, T =Pd and R =Tb,Dy,Ho,Er. Two magnetic structures (commensurate and incommensurate) have been determined at low temperature for all of these four compounds but with different magnetic moments depending on the rare earth element and reflecting the competition between the magnetic RKKY exchange and the crystalline field anisotropy.

The magnetic structures of different and new Uranium compounds (UGe_2 , U_3Ge_5 , U_3TiGe_5 , $U_3Ga_2Ge_3$) synthesized by the group of H. Noël at Rennes (collaboration with LLB (G. André and F. Bourée)) have been obtained, stressing the key role of the local Uranium ion environment (nature and ligand position in the cell) on the Uranium magnetic properties.

A study on a new Terbium fluoride family has begun with the compound KTb_3F_{12} (D. Avignant from Clermont-Ferrand in collaboration with the LLB (F. Bourée and G. André)) where Tb is present in two valence states : Tb^{4+} and Tb^{3+} (ratio $Tb^{3+}/Tb^{4+}=1/2$). Neutron diffraction gave two main results : the precise localization of the light F atoms leads to correct the X-ray space-group determination (from $I4/mmm$ to $I4/m$); the compound is antiferromagnetic below $T_N \approx 3.65K$ with only the Tb^{4+} moments magnetically ordered.

CONCLUSION

Six years after the impulse given by Jean Rossat-Mignod when he joined the LLB from 1991 to 1993, the activity in magnetism is progressing well with a large spectrum of research themes.

It benefits from a close collaboration with chemists : O. Kahn (Bordeaux) for molecular magnetism, A. Revcolevschi (Orsay) for the preparation of single crystals of Strongly Correlated Electron Systems and G. Collin and P. Gautier-Picard (crystallogenes group at LLB) for the preparation of single crystals of high T_c compounds.

Efforts are made to get better instruments (new polarized neutron triple-axis 2T) with a better environment (high pressure and high magnetic field).

The coupling with theory is good especially on high T_c cuprates and is progressively extending to other subjects.

SPIN DENSITIES IN FERROMAGNETIC Mn(II)Ni(II) BIMETALLIC CHAINS : POLARIZED NEUTRON DIFFRACTION

B. Gillon

Laboratoire Léon Brillouin (CEA-CNRS)

In the field of molecular magnetism, the determination of spin density maps provides crucial information about phenomena such as spin delocalization and spin polarization that play a role in magnetic interactions between metallic ions through organic bridges. The compound $\text{MnNi}(\text{NO}_2)_4(\text{en})_2$ (with « en » = ethylenediamine) constitutes the first bimetallic ferromagnetic chain compound to be fully characterized,

both magnetically and structurally. The chains present a zig-zag structure formed by alternating Mn(II) and Ni(II) ions bridged by a bidendate NO_2^- group, as shown by Figure 1. The two oxygen atoms of the bridging nitro group are linked to Manganese and the nitrogen atom is bonded to Nickel.

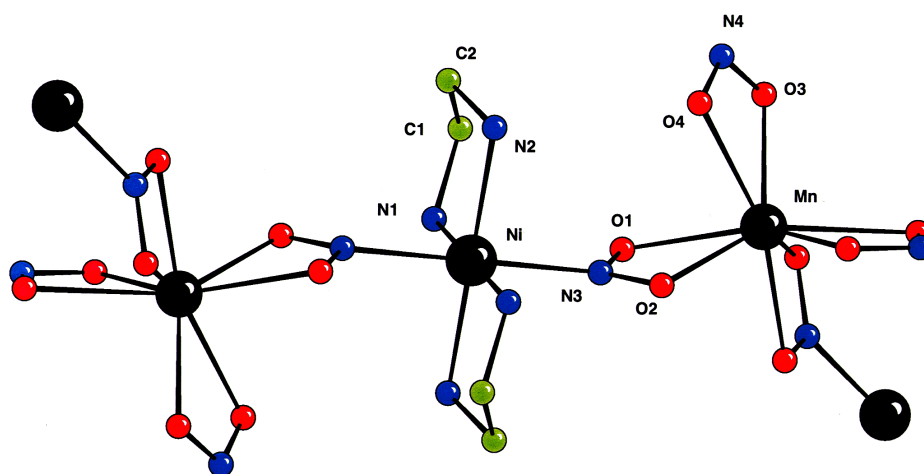


Figure 1 Structure of the chain in $\text{MnNi}(\text{NO}_2)_4(\text{en})_2$ at low temperature from unpolarized neutron measurements at 20K on 5C2

The Nickel ion is located on an inversion center, in a nearly perfect octahedral environment. It is surrounded by four nitrogen atoms coming from the two ethylenediamine groups and by two NO_2^- bridging nitrogen atoms. The Manganese ion resides on a two-fold symmetry axis and presents an unusual coordination sphere consisting of eight oxygen atoms, with two non-bonding oxygen atoms at a slightly larger distance than the six others. The intrachain Mn ... Ni distance is equal to 4.817 Å.

The structure can be described as a superimposition of ABAB layers perpendicular to the [001] direction: in the A layer the chains are parallel to [110] while in the B layer they are directed along the [-110] direction. Magnetic susceptibility measurements give evidence for a weak intrachain ferromagnetic coupling $J = 1.33$

cm^{-1} . A long range antiferromagnetic ordering between the chains occurs at $T_N = 2.35\text{K}$. The behaviour of the magnetization versus magnetic field is characteristic of

a metamagnetic compound with a threshold field of 1.2 KOe.

Figure 2 shows the induced spin density map, in projection perpendicular to the N1-Ni-N3 plane. The spin density is positive over all the map including on the

NO_2^- bridge. This map was obtained by a multipole model refinement on a set of 127 independent magnetic structure factors measured on the polarized neutron diffractometer 5C1 of the L.L.B. In this model the spin density is assumed to be the sum of atomic spin densities centered on the metal ions and on their first neighbours.. Spherical atomic spin densities were assumed for all atoms except Nickel, for which a 3d-type spin density was refined. The refined spin populations are normalized to 7 μ_B for each MnNi unit which corresponds to a system of local spins $S_{\text{Mn}^{2+}} = +5/2$ and $S_{\text{Ni}^{2+}} = +1$.

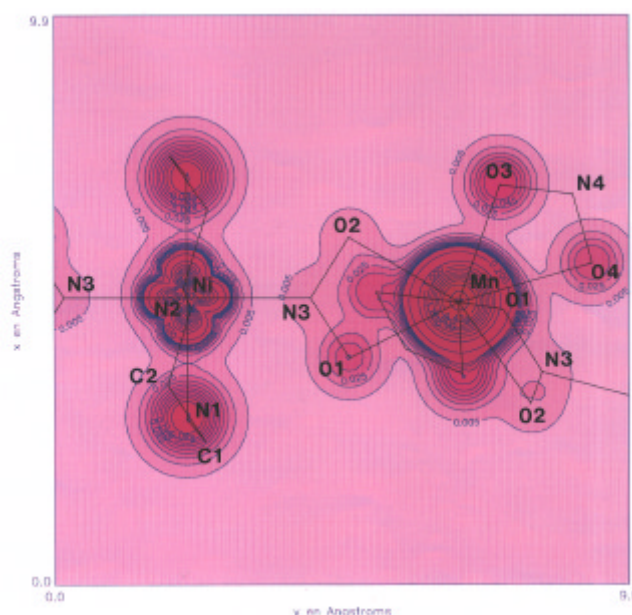


Figure 2 Induced spin density integrated along the perpendicular to the N1-Ni-N3 plane in the ferromagnetic chain compound $\text{MnNi}(\text{NO}_2)_4(\text{en})_2$ at 4K under an applied field of 2 Teslas. Positive spin density is in red. Different intervals are used for the low density and high density levels: low levels (from 0.005 to 0.095 $\mu\text{B}/\text{\AA}^2$ by steps of 0.010 $\mu\text{B}/\text{\AA}^2$) and high levels (from 0.2 to 4.2 $\mu\text{B}/\text{\AA}^2$ by steps of 0.4 $\mu\text{B}/\text{\AA}^2$)

The Mn^{2+} and Ni^{2+} spin populations are respectively equal to 4.48(4) and 1.62(3) μB . The unpaired spin on Ni^{2+} is found to be essentially located in the $d_{x^2-y^2}$

and d_{2x} orbitals. For Mn^{2+} , equal populations of the five 3d orbitals were assumed. The quantity of spin transferred from Mn^{2+} to its neighbours only amounts to 8 per cent of the moment associated to the manganese region while the spin delocalization from Ni^{2+} represents 24 per cent of the total moment on the nickel site, reflecting the stronger covalent character of the nickel than that of the manganese ion.

The delocalization from the nickel ion towards the bridging N3 atom of the nitro group (0.01(3) μB) is clearly weaker than towards the atoms of the ethylenediamine groups N1 (0.16(3) μB) and N2 (0.09(3) μB). Similarly the spin transfer from Mn^{2+} is smaller on both oxygen atoms of the bridge O1 (0.04(3) μB) and O2 (0.01(2) μB) than on the O3 atom (0.08(2) μB) of the non-bridging NO_2^- groups. The weak spin population on the oxygen atom O4 (0.05(2) μB) may be explained by the larger Mn-O4 distance.

The apparently negligible spin transfer from both metallic ions towards the atoms of the NO_2^- bridging group, compared to the significant spin transfer towards the external ligands is quite paradoxical. The interpretation that we propose is a balance between two phenomena which act in opposite ways: spin delocalization responsible for s type positive spin density on the neighbours of the metallic ions and spin polarization responsible for negative spin density of p type on the second neighbours. On the spin density map, the positive spin actually delocalized from each metallic ion towards its first neighbours belonging to the bridge would then be compensated for by a negative contribution due to the presence of the other metallic ion.

Acknowledgments

The author thanks Professor O. Kahn, from the Institut de Chimie de la Matière Condensée de Bordeaux (I.C.M.C.B.), who initiated this work, C. Mathonière and T. Rajendiran (I.C.M.C.B.) for the single crystal elaboration and A. Cousson (L.L.B.) for the low temperature structural study.

^[1]O. Kahn, E. Bakalbassis, C. Mathonière, M. Hagiwara, K. Katsumata and L. Ouahab, *Inorg. Chem.* **36** (1997) 1530.

^[2]E. Ressouche, A. Zheludev, J.X. Boucherle, B. Gillon, P. Rey and J. Schweizer, *Mol. Cryst. Liq. Cryst.* **233** (1993) 13.

OBSERVATION OF A FERROMAGNETIC MODULATION IN DOPED Mn PEROVSKITES: AN ELECTRONIC PHASE SEPARATION

G. Biotteau¹, M. Hennion¹, F. Moussa¹, J. Rodriguez-Carvajal¹,
L. Pinsard² and A. Revcolevschi²

¹Laboratoire Léon Brillouin, CEA-CNRS,

²Laboratoire de Chimie des Solides, Université Paris-Sud, 91405 Orsay Cedex, France

In manganites $\text{La}_{1-x}\text{A}_x\text{MnO}_3$, where the divalent ions ($\text{A}=\text{Sr}, \text{Ca}, \text{Ba}$) induce a hole doping, the coupling between the hole mobility and the ferromagnetism provides spectacular effects. Close to the magnetic transition where the metal-insulator transition occurs, an applied field induces a variation of the resistivity by several orders of magnitude (giant magnetoresistance), the largest effect being for $x \approx 0.3$. On a fundamental basis, the parameters leading to these effects are still not clearly understood. For several years, the existence of magnetic inhomogeneities has been suggested^[1-3], associating the ferromagnetic transition and likely the metal-insulator transition to a percolation effect. Several experiments^[4-5] have reported unusual fluctuations close to the ferromagnetic transition $T \approx T_c$, suggesting a picture of fluctuating ferromagnetic clusters.

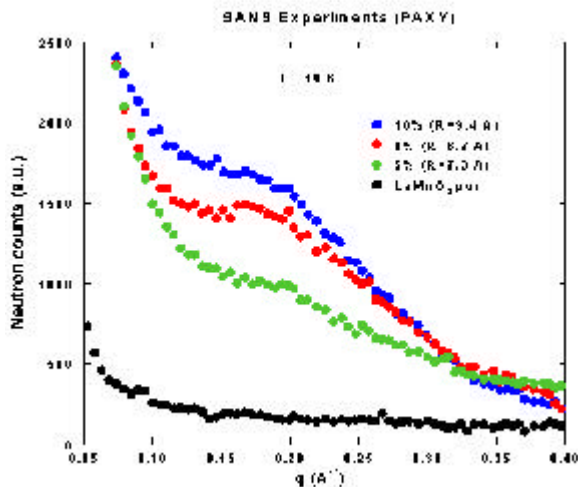


Figure 1. Scattering Intensities versus q observed using the diffractometer PAXY with an incident wavelength $\lambda=6\text{\AA}$ for $x=0, 0.05, 0.08$, and 0.1 of Ca doping. The intensities, renormalised by the volume, taking account of the sample transmission are readily comparable.

We have undertaken a small angle scattering study, using a small angle diffractometer (PAXY) in a first step, and then, a three-axis spectrometer (4F1), in an elastic configuration. The first one (PAXY), thanks to the multidetector device, provides measurements with an isotropic q resolution. However, any static ($\omega=0$) spin correlations cannot be observed as a function of temperature (contamination by the spin excitations) so that the magnetic contribution cannot be separated from the nuclear one. By contrast, the

three axis spectrometer allows to determine any $\omega \neq 0$ scattering intensity at any temperature, and, by subtracting the nuclear contribution determined at high temperature, allows to select the purely magnetic contribution.

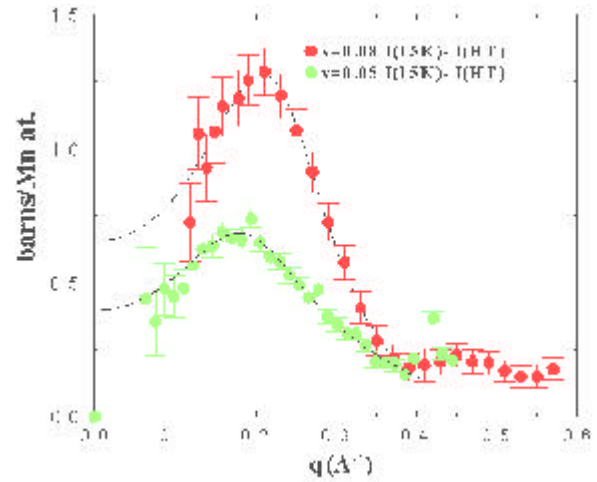


Figure 2. Scattering Intensities of magnetic origin, $I(q)=I_{15K}-I_{HT}$, versus q , calibrated in barns per Mn atom, observed using a three axis spectrometer for $x=0.05$ and $x=0.08$. The dashed line is a calculated curve according to the model described in the text

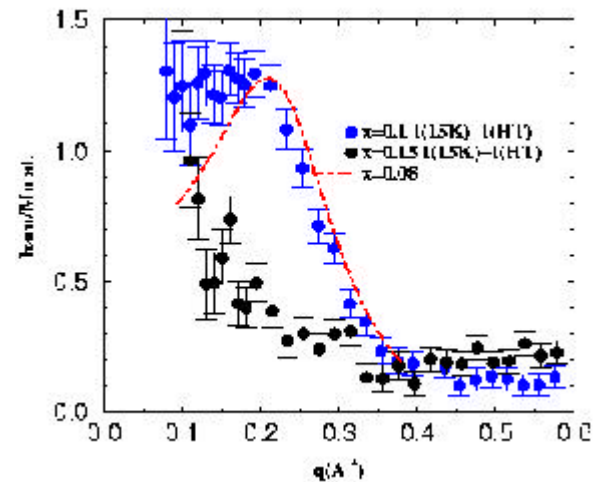


Figure 3. Scattering Intensities of magnetic origin $I(q)=I_{15K}-I_{HT}$, versus q , calibrated in barns per Mn, observed using a three-axis spectrometer for $x=0.1$ and $x=0.15$. The dashed line is a guide for the eye.

In the $0 \leq x \leq 0.15$ range studied, both experiments reveal the occurrence of a ferromagnetic modulation, in all the q directions. We have shown that it can be interpreted in terms of magnetic inhomogeneities,

with a liquid-like distribution, and therefore in repulsive interaction. Both the size of the inhomogeneities and their characteristic distance can be quantitatively determined. Such an experimental result, observed for the first time, likely originates from a purely electronic effect^[6].

In the range $0 \leq x \leq 0.15$, the compounds are insulating at all temperatures and, depending on x , undergo either a transition from a paramagnetic to a canted-antiferromagnetic state at T_{CA} ($T_{CA}=122\text{K}$ at $x=0.08$) or a transition from a paramagnetic to a ferromagnetic state at $T_C=155\text{K}$ for $x=0.15$.

In figure 1, the SANS scattering intensities obtained at 10K for $x=0, 0.05, 0.08$ and 0.1 are compared. The new experimental feature occurring in doped samples is a q -modulation, growing with x and superposed on a large scattering intensity (see the weak scattering intensity in the pure LaMnO_3). The multidetector device allows in principle, to check the q -isotropy of this modulation, but here, the complication related to the twinning domains prevents any definitive conclusion. A similar study on a three-axis spectrometer allows to separate the contribution of nuclear origin (dislocations or any structural defects induced by Ca doping) determined above the magnetic transition T_{CA} , where the intensity $I(q)$ is temperature independent, from the intensity of magnetic origin that grows below T_{CA} . This magnetic contribution is reported in figure 2 at 15K, for $x=0.05$ and $x=0.08$ of Ca. It reveals clearly that the modulation observed around $q \approx 0.2 \text{ \AA}^{-1}$ using PAXY has a magnetic origin and its intensity evolves strongly in this small concentration range. The magnetic contribution is also shown at higher doping value in figure 3. At $x=0.1$ the scattering intensity is close to that observed for $x=0.08$ (represented by the red dot-dashed line) except at small q , where a flat plateau instead of a true modulation is observed. At $x=0.15$, the modulation is no more observed in our experimental window. We have also studied the temperature evolution of the scattering. In figure 4, the evolution with temperature observed in the sample with $x=0.05$ is reported. It shows that as the intensity decreases, there is a slight shift of the modulation towards smaller q values. Since the studied samples are single crystals, all the experimental features observed close to the direct beam also exist around Bragg peaks. For example, in Figure 5, the intensity observed around (110) Bragg peak is reported for $x=0.08$ at several temperatures. There, the q -modulation is clearly observed, without any subtraction. It disappears above the magnetic transition ($T_{CA}=122\text{K}$), where a monotoneous decreasing scattering intensity, nearly temperature independent, persists. In addition, a study at small angle scattering using X-rays, for which a large contrast between La and Ca scattering exists, has been performed. It allows to check that there is no scattering in this small q range, which

excludes any chemical clustering related to Ca impurities associated to the magnetic scattering observed by neutrons.

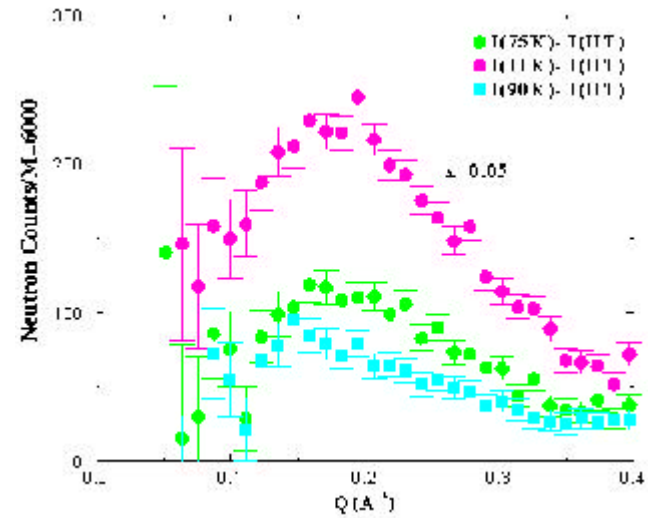


Figure 4. Diffuse scattering intensity versus Q along $[110]$ at several temperatures obtained at $x=0.08$ of Ca doping.

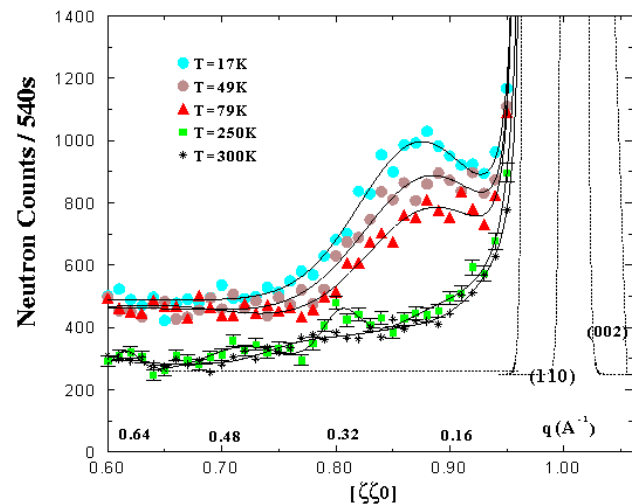


Figure 5. Diffuse scattering intensity versus Q along $[110]$ at several temperatures obtained at $x=0.08$ of Ca doping.

The existence of such an isotropic modulation, suggests a typical characteristic distance between similar magnetic inhomogeneities as in a liquid-like distribution. These inhomogeneities can be seen thanks to the contrast between their magnetization density and that of the surrounding matrix. To get a more quantitative description, a hard sphere model has been used with a liquid function for the distribution and excluded volumes, assuming a perfect isotropy. The corresponding calculated curves which fit the experimental data are shown also in Figure 2 for $x=0.05$ and $x=0.08$. They determine a typical size of 15 \AA for $x=0.05$, increasing to 18 \AA for $x=0.08$ with a typical distance of 38 \AA . The most striking result is that the density of these inhomogeneities, or "droplets", is smaller by more

than an order of magnitude than the density of Ca atoms. Such a result gets rid of a picture of magnetic polarisation surrounding each Ca or hole defects, but rather suggests a purely electronic effect of hole rich regions in repulsive interaction within a hole poor medium. This segregation would occur on a small spatial scale of some tens of Å. The temperature dependence reported for $x=0.05$ reflects a decrease of the size of the inhomogeneity and of their spatial density. However, the fall down of the intensity may be also related to a change of the magnetic contrast which must become nul in the paramagnetic state. The calibration of the intensities in barns per Mn atom, allows in principle, an estimation of the difference between the magnetization densities of the two magnetic regions at low temperature. This determination is model dependent. In particular, the isotropy of the structure, which could not be checked with accuracy because of twinned domains, is assumed.

The present determination of the magnetic contrast, $0.7 \mu_B$, does not agree with a ferromagnetic state within the hole rich regions. This conclusion apparently disagrees with NMR experiments performed on the same samples. These latter experiments indicate that some Mn spins follow the applied field as expected for spins within a

ferromagnetic state. Both findings can be conciliated in a more complex picture of magnetic clusters with a small ferromagnetic core, therefore not observable by neutrons (the intensity is proportional to the square of the volume).

Very recently, a similar study has also been performed in a $x=0.06$ Sr doped compound. A ferromagnetic modulation with characteristics close to those found for Ca doping has been also observed. This suggests the general character of these observations.

The disappearance of the modulation in the scattering intensity for $x=0.15$, where the compound is fully ferromagnetic, could be explained by a percolation of the magnetic inhomogeneities or by an homogeneization of the electronic density. In the first case, one expects the intensity to be restricted within a much smaller q scale, out of the present experimental window.

The role of such an electronic phase separation in the metal-insulating transition, is still unclear. At $x=0.15$, where one can expect a percolation of these inhomogeneities, the compound keeps insulating properties. This stresses out that the magnetic state alone is insufficient to explain the metal-insulating transition.

References

- [1] E. L. Nagaev, *Phys. Status Solidi B* **186**, 9 (1994)
- [2] M.Kagan, M.Mostovoy and D.Khomskii, cond-mat/9804213 Los Alamos April 1998
- [3] S. Yunoki, J. Hu, A.L. Malvezzi, A. Moreo, N. Furukawa and E. Dagotto, *Phys. Rev. Lett.* **80**, 845 (1998)
- [4] J. M. De Teresa M. R. Ibarra, P. A. Algarabel, C. Ritter, C. Marquina, J. Blasco, J. Garcia, A. Del Moral, Z. Arnold, *Nature* **386**, 256 (1997)
- [5] J. W. Lynn, R. W. Erwin, J. A. Borchers, Q. Huang and A. Satoro, *Phys. Rev. Lett.* **76**, 4046 (1996)
- [6] M. Hennion, F. Moussa, G. Biotteau, J. Rodriguez-Carvajal, L. Pinsard, A. Revcolevschi, *Phys. Rev. Lett.* **81**, 1957 (1998)

INTERPLAY OF ANTIFERROQUADRPOLAR AND ANTIFERROMAGNETIC ORDER IN TmTe

P. Link¹, J.-M. Mignot¹, A. Gukasov¹, T. Matsumura² and T. Suzuki²

¹Laboratoire Léon Brillouin (CEA-CNRS)

²Tohoku University, Sendai, Japan

Neutron diffraction is the reference technique for probing long-range order formed on a lattice of atoms or magnetic moments. It is shown that, under certain conditions, it can also be invaluable for studying more exotic types of ordered structures involving electron charge distributions. Although the determination is indirect in this case, detailed information on the ordered state of quadrupole moments can be derived from the symmetry properties of the response to an applied magnetic field. This method is demonstrated in the case of the antiferroquadrupolar phase of TmTe.

Besides their magnetic dipole moments, lanthanide elements with incomplete $4f$ electron shells are known to also possess higher-order moments (quadrupole, octupole, etc.). In a classical picture, this reflects the non-sphericity of the electron charge distribution. In the case of solids, pair interactions between $4f$ quadrupoles located at neighboring sites can occur either directly through their electrostatic potentials (usually weak), or indirectly through various channels such as lattice strains (cooperative Jahn-Teller effect), conduction electrons in metals (RKKY-type coupling), higher-order exchange terms, etc. For most real systems, conventional magnetic interactions dominate, and the $4f$ dipole-moment lattice orders in a long-range magnetic structure at low temperature. Accordingly, the quadrupole moments will have non-zero values in the magnetic state, but this is only the result of dipole ordering. More rarely, quadrupole interactions can prevail and produce a phase transition on their own, whose primary order parameter is a component, or combination of components, of the quadrupole moment tensor. In some intermetallic compounds (TmZn, CeAg), as well as in typical Jahn-Teller systems (rare-earth zircons), the value of the order parameter is uniform at all sites, and the order is thus denoted “ferroquadrupolar” in analogy with magnetism. On the other hand, staggered types of quadrupole order, loosely termed “antiferroquadrupolar” (AFQ), have been reported so far only for a small number of metallic compounds (TmGa₃, CeB₆). However, their study is of particular interest because the tensor nature of the quadrupole moment operator, as well as the possible interplay between magnetic and quadrupole order parameters, may result in a rich variety of physical situations. To characterize these phases, microscopic information is even more crucial than in the case of magnetism because one has to determine not only the wave-vectors and Fourier components of the structure, but also which components of the quadrupole moment tensor constitute the order parameter.

At first sight, neutron experiments do not seem well suited to probing quadrupole order because the

neutron does not interact directly with electrostatic charge distributions. However, as was shown in the work of Effantin et al. on CeB₆ [1], this obstacle can be partly circumvented by concentrating on the response of the *dipole* moment lattice to a magnetic field applied along a high-symmetry direction in a single-crystal: indeed, this response is strongly constrained by the preexisting quadrupole order, and therefore contains relevant information, in the first place concerning the wave-vector of the quadrupole structure. We have applied this strategy to the magnetic semiconductor TmTe, which was recently reported to undergo a phase transition at $T_Q \sim 1.8$ K [2] (far above the Néel temperature of approximately 0.4 – 0.6 K) whose characteristics are suggestive of quadrupole order.

High-field measurements have been performed on the lifting detector diffractometer 6T2 using the Saclay-Grenoble 12-tesla split-pair cryomagnet. The data shown in Figure 1 clearly indicate that superstructure magnetic peaks associated with the zone-boundary wave-vector $\mathbf{k} = (1/2, 1/2, 1/2)$, which were absent in zero field, grow below T_Q as H is increased parallel to the $[110]$ direction.

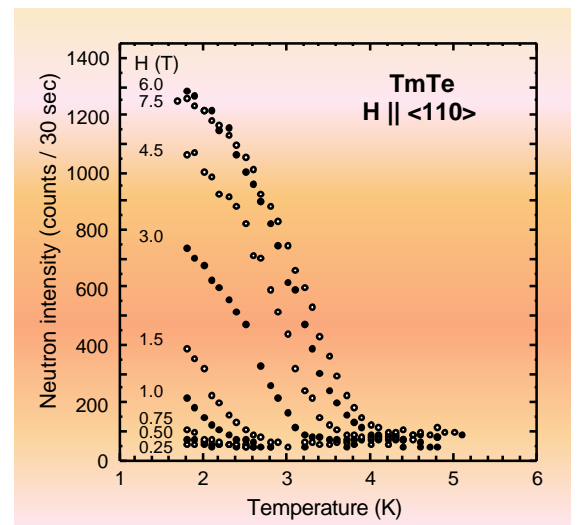


Figure 1. Intensity of the magnetic Bragg peak $(3/2, -1/2, 1/2)$ induced by the external field $H \parallel [110]$.

This result is very important because it establishes the possibility for a *uniform* field to induce a *staggered* magnetic component in the ordered state below T_Q , whereas it induces only a component at $\mathbf{q} = 0$ in the paramagnetic state. This lends considerable support to the above assumption of an underlying quadrupole order. By tracing these intensities as a function of temperature for different values of H , we were able to delineate the quadrupolar phase diagram for the three main symmetry directions, $H \parallel [001]$, $[110]$, and $[111]$ (Figure 2), and found good agreement with existing specific-heat results.

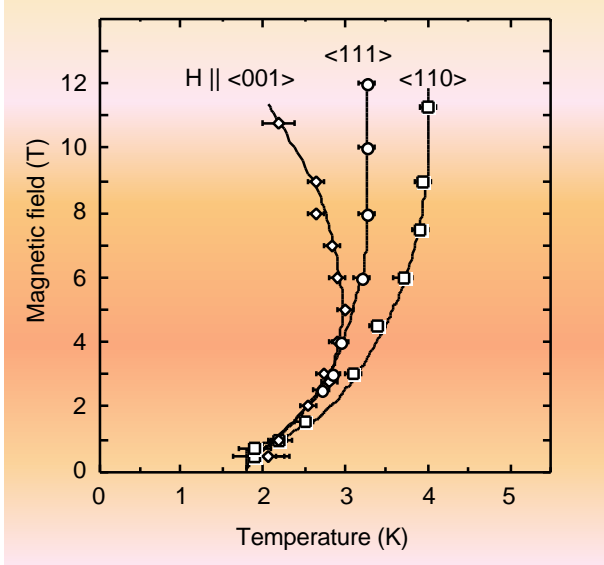


Figure 2. Quadrupolar phase diagram from the neutron diffraction results.

Furthermore, the quality of the data allowed us to fully disentangle the contribution of the different k - and S -domains, and to establish the direction of the staggered magnetic component μ_{AF} for $H \parallel [110]$, and $[111]$. In both cases, the best refinement was obtained by assuming μ_{AF} to be oriented along the two-fold axis $[\bar{1}0]$ perpendicular to both the wave-vector \mathbf{k} and the field direction. For $H \parallel [001]$, on the other hand, the induced magnetic component is much weaker and the direction of μ_{AF} cannot be reliably determined. Using the group-theoretical analysis developed by Shiina et al. [3], it can be concluded that the latter results are compatible with only one type of order parameter, namely O_2^2 . A schematic illustration of the field response for H applied along (110) is given in Figure 3.

Recently, the measurements have been extended to temperatures around 0.1 K and it was found that the magnetic phase forming below T_N is of the canted

type: it gives rise to two magnetic components, one antiferromagnetic with the same wave-vector $\mathbf{k} = (1/2, 1/2, 1/2)$ as the quadrupolar structure, and the other ferromagnetic. This effect had actually been predicted by Shiina et al. [3] for the case where “in-plane” magnetic couplings (*i. e.* bilinear interactions involving the x and y components of the dipole moment) dominate. Its experimental observation further supports the type of quadrupole order suggested above.

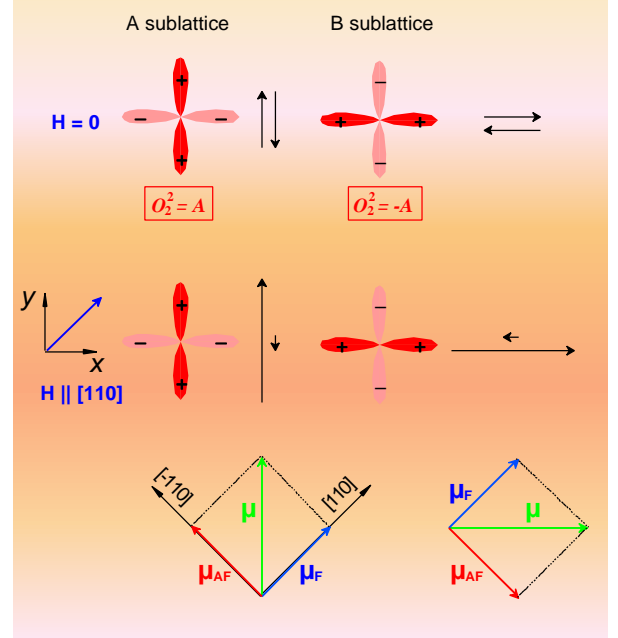


Figure 3. Schematic representation of the effect of a magnetic field $H \parallel [110]$ on the AFQ phase of TmTe; for $H \parallel [001]$, the symmetry is not broken and, ideally, only a uniform magnetic component is expected.

The results of this work [4] demonstrate that neutron diffraction, combined with a large external magnetic field, can provide a very powerful, albeit indirect, tool for studying quadrupole order in solids. Depending on systems, other techniques, such as synchrotron x-ray scattering may offer attractive alternatives. In the case of TmTe, however, the relatively low value of T_Q , as well as the risk of surface oxidation, make neutron diffraction the most straightforward method at the present time.

Further developments of this work, in particular measurements of the excitations in an applied field, will be aimed at clarifying the nature of the interactions responsible for the quadrupole ordering. Higher-order superexchange interactions have been suggested in Reference [3] but this assumption remains to be confirmed.

- [1] J.M. Effantin, J. Rossat-Mignod, P. Burlet, H. Bartholin, S. Kunii and T. Kasuya, J. Magn. Magn. Mat. 47&48 (1985) 145.
- [2] T. Matsumura, Y. Haga, Y. Nemoto, S. Nakamura, T. Goto and T. Suzuki, Physica B 206&207 (1995) 380.
- [3] R. Shiina and H. Shiba, Physica B 259-261 (1999) 322.
- [4] P. Link, A. Gukasov, J.-M. Mignot, T. Matsumura and T. Suzuki, Phys. Rev. Lett. 80 (1998) 4779.

MAGNETIC EXCITATIONS IN THE SPIN LADDER COMPOUNDS

$\text{Sr}_{14-x}\text{Ca}_x\text{Cu}_{24}\text{O}_{41+d}$

H. Moudden¹, L.P. Regnault², J.P. Boucher³, L.E. Lorenzo⁴, A. Revcolevschi⁵

¹Laboratoire Leon Brillouin (CEA-CNRS)

²Département de Recherche Fondamentale sur la Matière Condensée, CEA-Grenoble, 38054 Grenoble cedex 9, France

³Laboratoire de Spectrométrie Physique, Université Joseph Fourier, BP87, 38042 Saint Martin d'Hères cedex, France

⁴Laboratoire de Cristallographie, CNRS Grenoble, BP.166, 38042 Grenoble, France

⁵Laboratoire de Chimie des Solides, CNRS URA 446, Université Paris Sud, Bât. 414, 91405 Orsay, France

At the boundary between dimensions one and two, spin-ladder systems are conceptually very interesting as they exhibit rather "exotic" properties. In particular, the spin-pairing expected to develop in a 2-leg ladder gives rise, upon doping, to a charge pairing and finally to a non conventional (i.e. non phonon mediated) superconductivity. In this report, we present recent neutron inelastic scattering results obtained on a single crystal of the undoped $\text{Sr}_{14}\text{Cu}_{24}\text{O}_{41+\delta}$ and doped $\text{Sr}_{14-x}\text{Ca}_x\text{Cu}_{24}\text{O}_{41+\delta}$ 2-leg spin-ladder compounds.

After the discovery of the high- T_c superconductivity, a renewed interest in low-dimensional quantum magnetism has emerged, motivated by the possible role played by the magnetic interactions in the charge-pairing mechanism. One-dimensional antiferromagnets are particularly interesting to consider as they often exhibit unconventional phenomena. The first striking effect was discovered in the early 80's by Haldane^[1], who suggested that Heisenberg antiferromagnetic chains with half-integer ($S=1/2, 3/2, \dots$) and integer ($S=1, 2, \dots$) spin values behave quite differently at low temperatures. Whereas the former is expected to be gapless, the latter should have a non-magnetic singlet ground state and a quantum gap should open in the magnetic excitation spectrum. This non-intuitive prediction has been further very comprehensively verified from neutron-inelastic-scattering experiments performed on the spin-1 antiferromagnetic chain compound $\text{Ni}(\text{C}_2\text{H}_8\text{N}_2)_2\text{NO}_2\text{ClO}_4$.^[2] On the other side, the spin-1/2 square lattice with antiferromagnetic nearest-neighbour Heisenberg exchange couplings exhibits a quasi-ordered gapless ground state at $T=0$. Spin-ladders can be viewed as an array of a finite number of coupled chains, allowing therefore to study the crossover between space dimensions 1 and 2. While spin ladders with an odd number of legs behave like the spin-1/2 antiferromagnetic chain (gapless excitation spectrum, power-law spin correlations, ...), those with an even number of legs exhibit an exponential decay of the spin-correlations due to the opening of a spin-gap (with energy Δ) in the excitation spectrum^[3]. Of particularly high interest is the 2-leg spin-ladder system, since the prediction that charge doping could induce a non-conventional superconductivity, in which a d-wave pairing could be achieved, driven by the magnetic fluctuations^[3]. Indeed, superconductivity has been recently discovered in the Ca-doped spin-ladder family $\text{Sr}_{14-x}\text{Ca}_x\text{Cu}_{24}\text{O}_{41+\delta}$ for $x>11$, under high pressure in the range 30-45 kbar.^[4] The understanding of the

mechanism yielding to superconductivity in this material requires an accurate determination of both the temperature and doping dependencies of the magnetic excitation spectra. This can be achieved by neutron-inelastic-scattering investigations on undoped and doped single crystals.

As a first step, we have recently undertaken such a determination on the undoped $\text{Sr}_{14}\text{Cu}_{24}\text{O}_{41+\delta}$ and doped $\text{Sr}_{14-x}\text{Ca}_x\text{Cu}_{24}\text{O}_{41+\delta}$ compounds. The structure of this material is a misfit stacking of layers of two distinct quantum spin systems : linear CuO_2 chains and 2-leg Cu_2O_3 ladders^[5]. Figure 1 shows a "3D" view of the crystallographic structure, which emphasizes the chain and ladder subsystems. Quite interestingly, the pure material contains a large amount of holes mainly localized in the CuO_2 -chains (0.6 hole/Cu), which play the role of a charge reservoir.

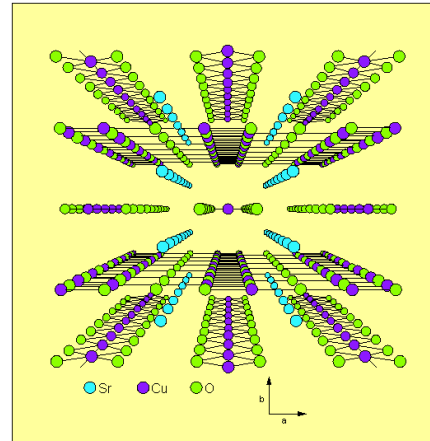


Figure 1: Crystal structure of $\text{Sr}_{14}\text{Cu}_{24}\text{O}_{41+d}$ showing the chain and ladder subsystems (viewed along the c axis).

Following the theoretical predictions, the ground state of a 2-leg spin-ladder system in the case $J_{\perp} < J_{\parallel}$, where J_{\parallel} and J_{\perp} represent respectively the exchange coupling constants along the legs and along the rungs, should be a non magnetic singlet ground state, well separated from the first excited states by an energy gap $\Delta \approx 0.4$

J_{\perp} . These two features have been unambiguously observed from neutron-inelastic-scattering experiments carried out on the 3-axes spectrometers (TAS) IN8/ILL, 1T/LLB and IN22/CRG-ILL. We show in Figure 2 two typical energy scans performed on TAS 1T/LLB at the scattering vectors $\mathbf{Q}=(4.5, 0, 0.5)$ (where one expects a strong signal originating from the ladders) and $\mathbf{Q}=(4.5, 0, 0.65)$ (where one expects a vanishing contribution of the ladders). The observed line shape is characteristic of a gapped magnetic response, with no signal detected at low energy and a gap value $\Delta=33$ meV. The magnetic response can be understood from the existence of "two" contributions: one narrow contribution peaked at Δ and a second one, persisting at much higher energy and peaked around 40-50 meV. The temperature dependence of the magnetic response reveals several interesting and new features:

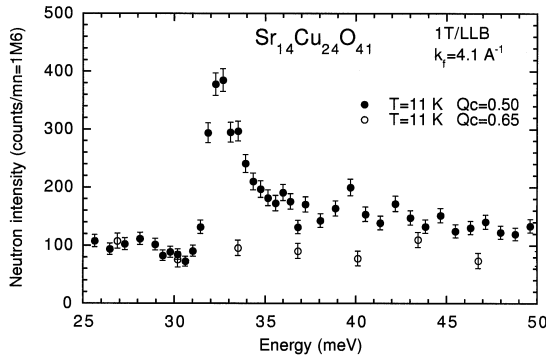


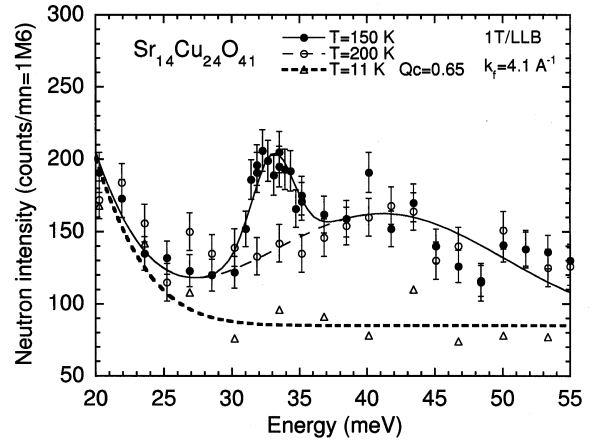
Figure 2: Inelastic neutron scattering response of the ladder subsystem at 1.5 K, showing the presence of a quantum spin-gap with energy 33 meV.

Figure 3: Dynamical magnetic response at 150K and 200K showing the existence of two distinct contributions in $\text{Sr}_{14}\text{Cu}_{24}\text{O}_{41+d}$

- the "33 meV-peak" disappears above roughly 200K, without strong renormalization nor damping below 150K. Figure 3 displays constant-Q scans at the scattering vector $\mathbf{Q}=(4.5, 0, 0.5)$ and two temperatures $T=150\text{K}$ and 200K which demonstrate the presence of two distinct contributions.

- the second contribution is wealdy temperature dependent above 200K and extends at least up to 90 meV (data taken on IN1 and IN8/ILL).

We have presently no definitive explanation for these results, which however bear some resemblance with those obtained on, e.g., $\text{YBa}_2\text{Cu}_3\text{O}_{6.5}$ in the normal state [6].



Upon Ca-doping, holes are progressively transferred from the CuO_2 chains to the Cu_2O_3 ladders which become metallic. Our neutron data show that the spin dynamics in the ladders is little affected by hole doping. The magnetic response, despite well visible broadening effects, remains peaked at 33 meV. At the reverse, the spin dynamics in the chain is much more affected, as a result of the partial destruction of the charge ordering in the chain subsystem.

References:

- [1] F.D.M. Haldane, Phys. Lett. **A93** (1983) 464.
- [2] L.P. Regnault, I. Zalitznyak, J.P. Renard and C. Vettier, Phys. Rev. **B53** (1994) 5579.
- [3] E. Dagotto and T.M. Rice, Science **271** (1996) 618.
- [4] M. Uehara, T. Nagata, J. Akimitsu, H. Takahashi, N. Môri and K. Kinoshita, J. Phys. Soc. Japan **65** (1996) 2764.
- [5] E.M. McCarron, M.A. Subramanian, J.C. Calabrese and R.L. Harlow, Mat. Res. Bull. **23** (1988) 1355.
- [6] P. Bourges et al, Phys. Rev. **B56** (1997) 1439.
- [7] M. Matsuda, K. Katsumata, H. Eisaki, N. Motoyama, S. Uchida, S.M. Shapiro and G. Shirane, Phys. Rev. **B54** (1996) 12199.
- [8] L.P. Regnault et al, Phys. Rev. **B59** (1999) 1055.

NEUTRON SCATTERING FROM MAGNETIC EXCITATIONS IN $\text{Bi}_2\text{Sr}_2\text{CaCu}_2\text{O}_{8+\delta}$

H. F. Fong¹, P. Bourges², Y. Sidis², L. P. Regnault³, A. Ivanov⁴, G. D. Gu⁵,
N. Koshizuka⁶ and B. Keimer^{1,7}

¹ Department of Princeton University, Princeton, NJ 08544, USA.

² Laboratoire Léon Brillouin (CEA-CNRS)

³ CEA Grenoble, DRFMC, 38054 Grenoble cedex 9, France.

⁴ Institut Laue Langevin, 156X, 38042 Grenoble cedex 9, France.

⁵ Department of Advanced Electronic Materials, University of New South Wales, Sydney 2052, Australia.

⁶ SRL/ISTEC, 10-13, Shinomone 1-chome, Koto-ku, Tokyo 135, Japan.

⁷ Max-Planck-Institut für Festkörperforschung, 70569 Stuttgart, Germany.

Many of the physical properties of the copper oxides high-temperature superconductors appear to defy the conventional "one-electron" theory of metals. The development of alternative theories incorporating strong electron correlations is currently at the forefront of research in condensed matter physics. In this context inelastic neutron scattering can provide valuable insight into collective magnetic excitations in copper oxide superconductors and so guide these theoretical efforts.

For lack of suitably large single crystals, inelastic neutron scattering (INS) measurements have thus far proven possible for only two of the many families of high temperature superconductors, $\text{YBa}_2\text{Cu}_3\text{O}_{6+x}$ and $\text{La}_{2-x}\text{Sr}_x\text{CuO}_4$. While the magnetic spectra of both materials bear certain similarities, there are also pronounced differences that have hampered an unified description of the spin dynamics in the cuprates. In particular, the magnetic resonance peak that dominates the spectrum in the superconducting state of $\text{YBa}_2\text{Cu}_3\text{O}_{6+x}$, is not found in $\text{La}_{2-x}\text{Sr}_x\text{CuO}_4$.

In the optimally doped $\text{YBa}_2\text{Cu}_3\text{O}_{6+x}$ (superconducting transition temperature $T_c=93$ K), the magnetic resonance peak is a sharp collective mode that occurs at 40 meV and at the two-dimensional wave vector $(\pi/a, \pi/a)$, where a is the nearest neighbour Cu-Cu distance (Fig.a). Its intensity decreases continuously and vanishes above T_c (Fig.b). In the underdoped $\text{YBa}_2\text{Cu}_3\text{O}_{6+x}$, the mode energy decreases monotonically with decreasing hole concentration. Such a collective excitation mode has not been observed in conventional superconductors. Several microscopic models have been proposed, ranging from band structure singularities to interlayer pair tunnelling. In all these models, the interactions that give rise to the resonance mode are the same that cause pairing of electrons in the superconducting state, so that this phenomenon provides a direct clue to the mechanism of high- T_c superconductivity.

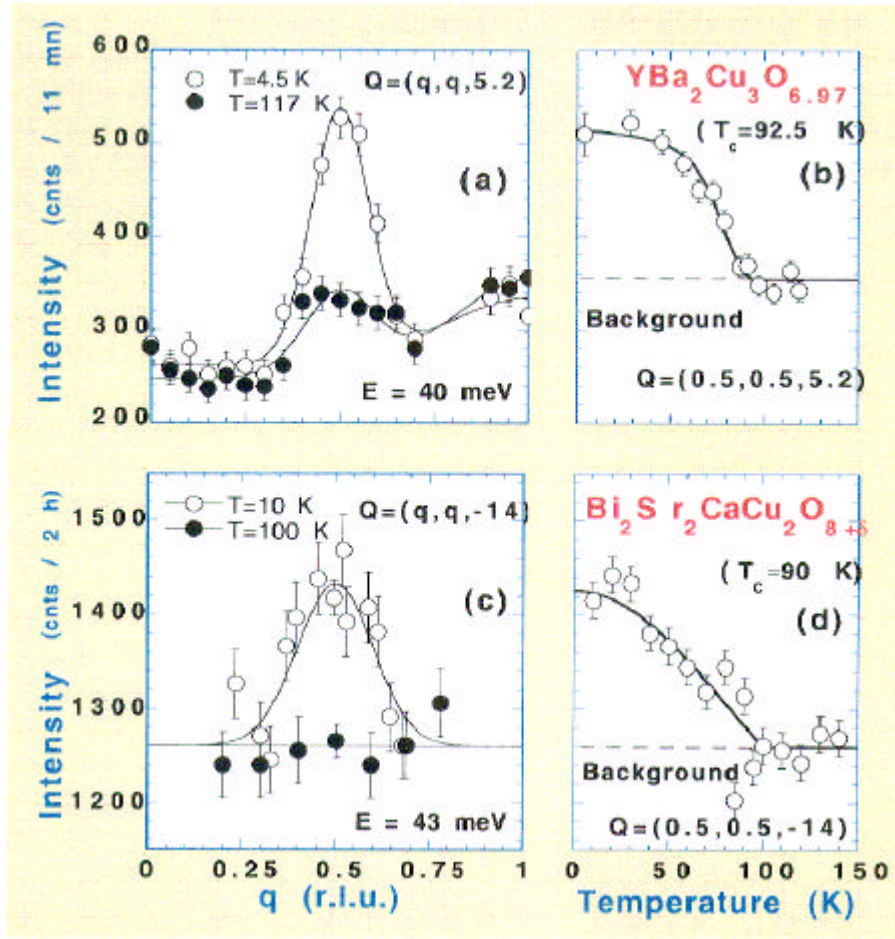
A very sensitive test of the disparate models is whether they are capable of providing a detailed

description of both the INS results and those of angle resolved photoemission measurements (ARPES), a complementary momentum resolved experimental technique that primarily probes single electron excitations. By far the best ARPES data have been obtained in $\text{Bi}_2\text{Sr}_2\text{CaCu}_2\text{O}_{8+\delta}$, a material for which no INS data have been available for experimental difficulties ($\text{Bi}_2\text{Sr}_2\text{CaCu}_2\text{O}_{8+\delta}$ cleaves easily along CuO_2 layers, which facilitates surface sensitive techniques such as ARPES, but this property is also responsible for the lack of large single crystal required in INS measurements). This situation that has precluded a direct quantitative comparison of both techniques is remediated by the present study.

We have performed the first INS measurements on a 60 mm³ single crystal of $\text{Bi}_2\text{Sr}_2\text{CaCu}_2\text{O}_{8+\delta}$ ($T_c=91$ K). Measurements have been carried out on the triple-axis spectrometers 2T located at the reactor Orphée at Saclay and IN8 located at Institut Laue Langevin at Grenoble (France)

The magnetic excitation spectra of $\text{Bi}_2\text{Sr}_2\text{CaCu}_2\text{O}_{8+\delta}$ and optimally doped $\text{YBa}_2\text{Cu}_3\text{O}_{6+x}$ exhibit an unmistakable similarity. In the superconducting state, the magnetic intensity is sharply concentrated around a single point in energy (~ 43 meV, with a width of ~ 10 -15 meV) and wave vector ($\mathbf{Q}=(\pi/a, \pi/a)$) (Fig.c). In the normal state, the intensity is either too broad or too weak to be observable above background. Fig. d shows the temperature dependence of the peak amplitude which vanishes above the superconducting transition temperature to within the experimental uncertainty. There is also no indication of magnetic intensity above the background level at other energies or wavevectors. In particular, an extensive search for magnetic excitations at 10 meV has thus far been fruitless in $\text{Bi}_2\text{Sr}_2\text{CaCu}_2\text{O}_{8+\delta}$.

In both $\text{Bi}_2\text{Sr}_2\text{CaCu}_2\text{O}_{8+\delta}$ and $\text{YBa}_2\text{Cu}_3\text{O}_7$, the magnetic resonance peak is thus by far the most predominant feature in the magnetic excitation spectrum.



Figures : Resonance peaks in $\text{YBa}_2\text{Cu}_3\text{O}_{6.97}$ (a,b) [$E=40$ meV] and $\text{Bi}_2\text{Sr}_2\text{CaCu}_2\text{O}_{8+\delta}$ (c,d) [$E=43$ meV]. The resonance peak is centered at the antiferromagnetic wave vector $q = 0.5$ (in reciprocal lattice units $2\pi/a$). Its intensity vanishes above T_c (b,d)

A further comparison between both compounds is made possible by a calibration of the absolute neutron cross-section against a vanadium standard. The energy integrated spectral weight of the resonance peak is $1.9 \pm 1 \mu_B^2$, in close agreement with $1.6 \mu_B^2$ found in $\text{YBa}_2\text{Cu}_3\text{O}_7$. The width of the resonance peak at the $(\pi/a, \pi/a)$ wavevector is much larger in $\text{Bi}_2\text{Sr}_2\text{CaCu}_2\text{O}_{8+\delta}$ (0.53 \AA^{-1} , full width at half maximum) than in $\text{YBa}_2\text{Cu}_3\text{O}_7$ (0.25 \AA^{-1}). If averaged over the Brillouin zone, in addition to integrating over energy, the resonant spectral weight is clearly larger in $\text{Bi}_2\text{Sr}_2\text{CaCu}_2\text{O}_{8+\delta}$ ($0.23 \mu_B^2$) than in $\text{YBa}_2\text{Cu}_3\text{O}_7$ ($0.043 \mu_B^2$).

Such a quantitative comparison between different materials are required for a microscopic, quantitative description of the origin of the magnetic resonance peak. In the framework of the models proposed for the resonance peak, it should be now possible to relate the different Q -width measured in $\text{YBa}_2\text{Cu}_3\text{O}_7$ and $\text{Bi}_2\text{Sr}_2\text{CaCu}_2\text{O}_{8+\delta}$ to their different Fermi surfaces as measured by ARPES.

References:

H. F. Fong, P. Bourges, Y. Sidis, L. P. Regnault, A. Ivanov, G. D. Gu, N. Koshizuka et B. Keimer, *Nature* **398**, 588 (1999)

Our study opens the way to a variety of further neutron experiments, in particular in the overdoped regime which is easily accessible in $\text{Bi}_2\text{Sr}_2\text{CaCu}_2\text{O}_{8+\delta}$ over a wide range of hole concentrations. It has also left open questions that can only be answered by neutron scattering work on other families of high- T_c superconductors. For instance, as both $\text{YBa}_2\text{Cu}_3\text{O}_{6+x}$ and $\text{Bi}_2\text{Sr}_2\text{CaCu}_2\text{O}_{8+\delta}$ are bilayer materials, the present study does not provide further insight into the role of interlayer interactions in the resonance peak. Most importantly, the observation of the resonance peak in $\text{Bi}_2\text{Sr}_2\text{CaCu}_2\text{O}_{8+\delta}$ rules out the possibility that this phenomenon is due to a conspiracy of structural and chemical parameters in $\text{YBa}_2\text{Cu}_3\text{O}_{6+x}$. It is in fact an intrinsic feature of copper oxides superconductors and an explanation of this feature needs to be an integral part of any theory of high-temperature superconductivity.

OFF-SPECULAR REFLECTIVITY MEASUREMENTS ON PERIODIC MAGNETIC STRIPE DOMAINS IN $\text{Fe}_{0.5}\text{Pd}_{0.5}$ THIN FILMS.

B. Gilles¹, A. Marty², C. Fermon³, F. Ott⁴

¹LTPCM, ENSEEG, B.P.75, 38 042 Grenoble, France

²CEA-Grenoble, DRFMC, 17 rue des Martyrs, 38 054 Grenoble Cedex 9, France.

³Service de Physique de l'Etat Condensé, CEA-Saclay, 91191 Gif-sur-Yvette cedex

⁴Laboratoire Léon Brillouin (CEA-CNRS)

Specular polarised neutron reflectometry with polarisation analysis allows one to probe in-depth magnetic profiles of thin films (along the normal to the film). In the case of homogeneous films, the neutron is sensitive only to the in-plane magnetisation and all the intensity is reflected in the specular direction. In the case of non homogeneous films, all the directions of the magnetisation can be explored and intensity is scattered off the specular direction. The convention is to call « off-specular » the intensity measured in the incidence plane and « surface diffraction » the intensity measured out of the incidence plane. The incidence plane is defined by the incident wave vector and the perpendicular of the surface. Off-specular reflectometry gives information about lateral structures (in the plane of the film) with typical length scales ranging from 2 μm to 100 μm . Furthermore, surface diffraction at grazing angle gives access to transverse dimensions between 10 nm and 300 nm with a resolution in that direction of a few nanometers. The combination of these three types of signals (specular, off-specular and surface diffraction) applied to magnetic systems can lead to a 3D magnetic structure measurement. Off-specular measurements are however not applicable to the study of a single magnetic dot, but it can generate unique results in several cases including patterns of domain walls in thin films with perpendicular anisotropy, arrays of magnetic dots or patterned lines in magnetic thin films.

To demonstrate the potential of non-specular neutron scattering, we have measured magnetic surface diffraction on magnetic stripe domains appearing in FePd thin films. The sample was prepared by Molecular Beam Epitaxy under ultra-high vacuum (10^{-7} Pa). A 2 nm seed layer of Cr was deposited onto a MgO (001)-oriented substrate in order to allow the epitaxial growth of the 60 nm single crystal Pd buffer layer. A 50 nm thick FePd alloy layer was then deposited at room temperature using a mono-layer by mono-layer growth method in order to induce a chemical order similar to the one found in the tetragonal structure L_{10} . This structure consists in alternate atomic layers of Fe and Pd on a body centred tetragonal lattice [1]. After a magnetisation along the

easy axis, a magnetic stripe domain structure is observed [2] (see bottom picture on Figure 1).

The diffraction measurement has been performed using a small angle neutron scattering spectrometer (the spectrometer PAPOL at the Laboratoire Léon Brillouin) in a reflectivity configuration [3]. In the experiment, the stripes were aligned along the plane of incidence. An example of diffraction is shown on figure 1. One can observe a bright specular spot and two weaker (10^{-3}) off-specular peaks. The position of these peaks along the q_{\parallel} direction reflects the periodicity of the stripe domains (100 nm). The diffraction peaks are reflected with an angle θ_o equal to the critical angle θ_c of the layer whatever the incidence angle is.

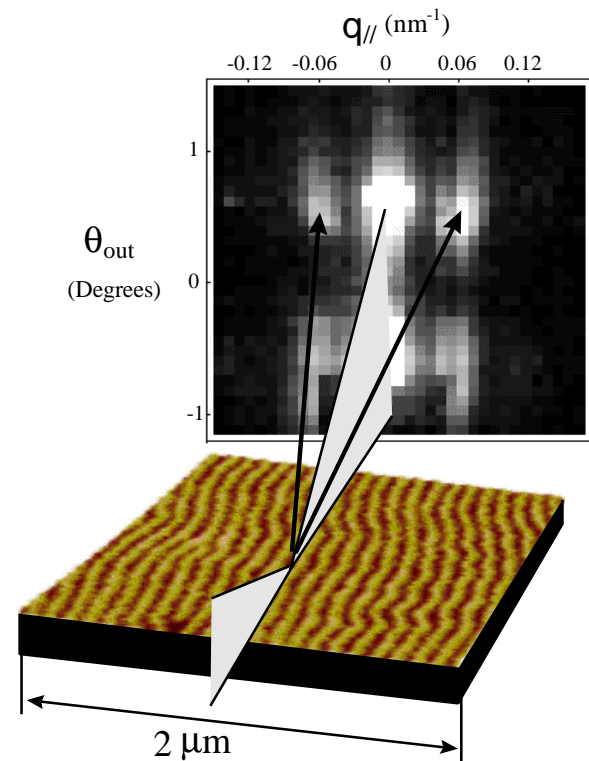


Figure 1 : diffraction geometry and off-specular scattering signal measured on a network of magnetic domains using a multidetector. The top peaks are the specular and off-specular peaks. The bottom signal is due to the refracted wave. The bottom picture is a Magnetic Force Microscopic image of magnetic domains observed in $\text{Fe}_{0.5}\text{Pd}_{0.5}$ thin films

The maximum intensity of the diffraction peaks is obtained when the incidence angle of the neutron beam on the sample is θ_c . These peaks have a behaviour similar to Yoneda peaks (or anomalous reflections) [4].

As a first approach, we have explained these observations by using a DWBA (Distorted Wave Born Approximation) approach. The considered « unperturbed » system is the flat FePd layer ; the perturbation is the magnetic structure created by the stripes. In this case, the diffuse cross-section can be written as [5] :

$$\left(\frac{d\sigma}{d\Omega} \right)_{\text{diff}} = (L_x L_y) \frac{|k_0^2 (1 - n^2)|^2}{16\pi^2} |T(\mathbf{k}_1)|^2 |T(\mathbf{k}_2)|^2 S(\mathbf{q}_t)$$

with

$$S(\mathbf{q}_t) = \iint_S dX dY C(X, Y) \exp(i(q_x X + q_y Y))$$

(in the case where q_z^t is small) where $C(X, Y)$ is the magnetic roughness correlation function, \mathbf{q} is the scattering vector $\mathbf{k}_2 - \mathbf{k}_1$ and \mathbf{q}_t is the wave-vector transfer in the medium. Maxima are obtained in the diffuse scattering when \mathbf{k}_1 or \mathbf{k}_2 makes an angle close to q_c since in these positions, the Fresnel coefficients \mathbf{T} reach a maximum.

$S(\mathbf{q}_t)$ is the Fourier transform of the magnetic roughness correlation.

In the case of our magnetic lines, we define the correlation function of the magnetic roughness as :

$$C(X, Y) = \frac{1}{S} \iint_S M(x, y) M(x + X, y + Y) dx dy$$

The surface diffraction signal measures the Fourier transform of the magnetic correlation function. The figure 2 shows the off-specular signal calculated for an incidence angle equal to the critical angle $\theta_i = \theta_c = 0.5^\circ$. The peak positions are unchanged whatever the incidence angle is. The maximum of

intensity is obtained when the incidence angle is equal to the critical angle θ_c .

The DWBA approach is however not well suited to this problem since the magnetic roughness extends over the full thickness of the magnetic layer so that the flat layer as a basis state is far from the real eigenstates of the system. We are presently working on a fully dynamical theory to be able to quantitatively analyse magnetic off-specular patterns.

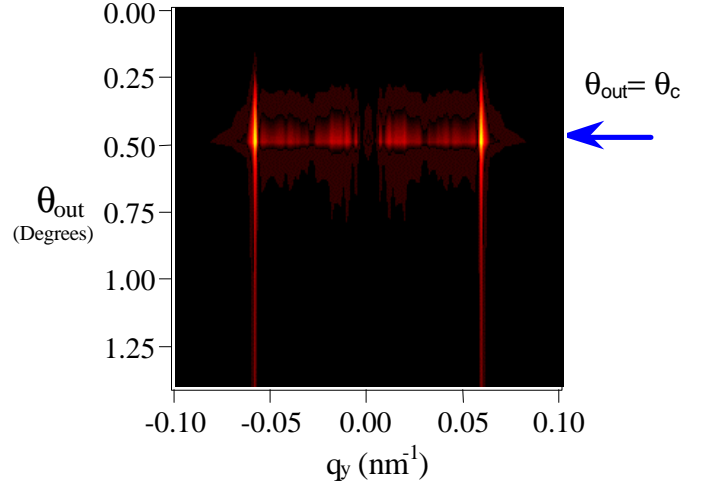


Figure 2 : calculated off-specular signal as measured on a multidetector for an incidence angle $q_{inc} = q_c = 0.5^\circ$. The peaks maximum position does not move when the incidence angle is varied but the intensity decreases as soon as the incidence angle is moved away from the critical angle θ_c .

We hope that this work will pave the way for a new technique of 3D magnetometry making it possible to measure quantitatively magnetic structures with an in-depth and in-plane resolution. The aim is to eventually be able to obtain magnetic information on the magnetic order in the plane of thin films through polarised neutron reflectometry. Off-specular and surface diffraction will then make it possible to probe in-plane magnetic structures of sizes ranging from 10 nm to 100 μm .

References

- [1] V. Gehanno, A. Marty, B. Gilles and Y. Samson, Phys. Rev. B **55** (1997) 12552.
- [2] A.L. Sukstanskii, K.I. Primak, J. Magn. Mater. **169** (1997) 31.
- [3] C. Fermon, F. Ott, B. Gilles, A. Marty, A. Menelle, Y. Samson, G. Legoff and G. Francinet, Physica B **267-268** (1999) 162-167.
- [4] Y. Yoneda, Phys. Rev. **131** (1963) 2010 ; O.J. Guentert, J. Appl. Phys. **30** (1965) 1361 ; A.N. Nigam, Phys. Rev. A **4** (1965) 1189.
- [5] S.K. Sinha, E.B. Sirota, S. Garoff and H.B. Stanley, Phys. Rev. B **38** (1988) 2297-2311.

NEW SCENARIO FOR HIGH- T_c CUPRATES : ELECTRONIC TOPOLOGICAL TRANSITION AS A MOTOR FOR ANOMALIES IN THE UNDERDOPED REGIME

F. Onufrieva , P. Pfeuty, M. Kisselev and F. Bouis

Laboratoire Léon Brillouin (CEA-CNRS)

This is a particularly exciting time for high- T_c . The experimental knowledge converges. Almost all experiments, nuclear magnetic resonance (NMR), angle resolved photoemission spectroscopy (ARPES), tunneling spectroscopy etc., provide an evidence for the existence of a characteristic energy scale $T^*(\delta)$ in the underdoped regime (δ is hole doping). Below and around the line $T^*(\delta)$ the "normal" state (i.e. above T_c) has properties fundamentally incompatible with the present understanding of metal physics. The field has reached the point when a consistent theory is needed to understand this experimentally well defined but theoretically exotic metallic behaviour and its relevance to high T_c superconductivity.

We show that these phenomena can be naturally understood within the concept of a proximity of the underdoped regime to an electronic topological transition (ETT). The concept of electronic topological transition due to the variation of the topology of the Fermi surface was introduced in the early 60's by I. Lifshitz and applied to 3D systems^[1]. It was shown that an ETT implies singularities in thermodynamic and transport properties at $T=0$ which are smoothed at finite temperature (this left Lifshitz in a difficult position concerning the classification of this transition as a phase transition). Due to (i) the weakness of the singularities in 3D case (the only dimension considered at Lifshitz's time) and (ii) the difficulty of classification, this phenomenon (which is as general as for example the phenomenon of phase transition) has been quite forgotten.

We analyse a 2D electron system on a square lattice (in direct application to the high- T_c cuprates) and show that it obligatory undergoes an ETT (the Fermi surface changes from open to closed) under change of electronic concentration n (or of hole doping $\delta=1-n$) and that the ETT occurs in the doping range where all anomalies in the high- T_c cuprates are observed. We show that the ETT point, $\delta = \delta_c$, $T = 0$, is a quantum critical point (QCP) (at Lifshitz's time the concept of QCP had not yet been introduced), which is very rich in the 2D case, and that its existence results in global anomalies of the system^[2-6]. Firstly, in the presence of interaction of necessary sign (such interaction does exist in the strongly correlated CuO_2 plane being of magnetic origin, see [7]), a d-wave superconducting state with high T_c develops

around the ETT QCP with maximum T_c at $\delta = \delta_c$; its symmetry and properties studied in [7] are in a good agreement with experiments. Secondly, the underdoped regime, $\delta < \delta_c$ above $T_{sc}(\delta)$ is a new type of metallic state: quantum spin-density wave (SDW) liquid re-entrant in temperature and frozen in doping [4,2]. The re-entrance means that the characteristics of the short range order behave in a re-entrant way: the system becomes more ordered with increasing T and it reaches a minimum disorder at some pseudocritical temperature $T^*(\delta)$ which increases with decreasing doping. Freezing means that the system keeps strong short range order (or strong quantum critical fluctuations) quite far in doping from the ETT QCP.

A detailed study of these phenomena allows to understand many effects observed in high- T_c cuprates by different experiments and unexplained until now. Below we present several examples of theoretical predictions of our theory. Notice that the different anomalies are explained within the same theory and that neither adjustable parameters nor phenomenological *ansatz* are used.

Nuclear magnetic resonance (NMR)

There are two glaring anomalies observed systematically in the underdoped high- T_c cuprates; (i) the nonmonotonical behaviour of the nuclear spin lattice relaxation rate $1/T_1T$ on copper with maximum at some T^* (see Fig.1b) instead of the Korringa law $1/T_1T=\text{const}$ for ordinary metals, (ii) qualitatively different behaviour of $1/T_1T$ measured on copper and oxygen (or for the wavevectors $\mathbf{q} \approx \mathbf{Q}_{AF}$ and $\mathbf{q} \approx 0$ from theoretical point of view), see Fig 1d. (The relaxation rate $1/T_1T$ is roughly proportional to the slope in the imaginary part of the spin dynamic susceptibility, $\lim_{\omega \rightarrow 0} \text{Im}\chi^0(\mathbf{q},\omega)/\omega$). The results of our theory are in a very good agreement with experiment, compare Fig.1a and 1b (there are no adjustable parameters). The shown dependences are a manifestation of the quantum SDW liquid : the nonmonotonic behaviour reflects the re-entrance in T . The difference in behaviour for $\mathbf{q} \approx \mathbf{Q}_{AF}$ and $\mathbf{q} \approx 0$ is related to the different aspects of criticality of the ETT QCP. The detailed analysis is done in [4].

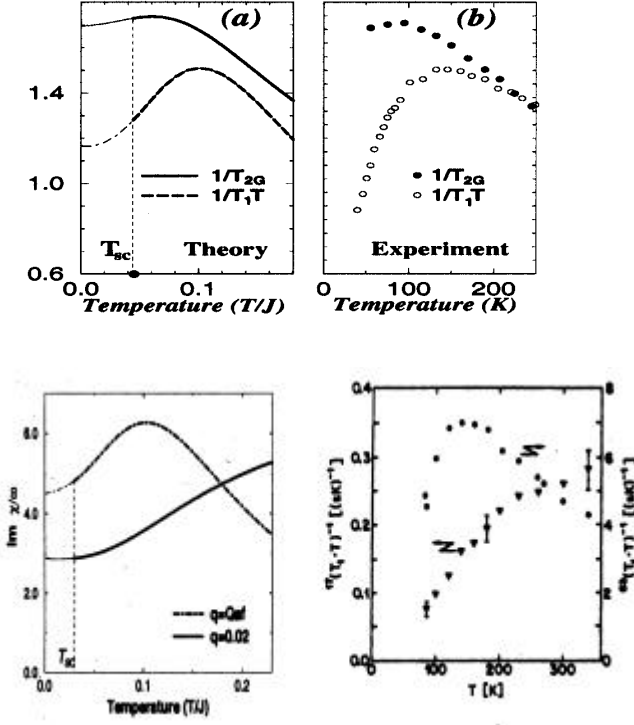


Figure 1. Comparison between theory and experiment for $1/T_1T$ on copper and oxygen. (a) and (b) show the $1/T_1T$ and $1/T_{2G}$ (nuclear transverse relaxation rate) on copper, (a) calculated [2,4] (should be considered only above T_{sc}) and (b) measured by NMR for $YBCO_{6.6}$ [8]; (c) and (d) demonstrate the qualitatively different temperature dependences for copper ($q \gg Q_{AF}$) and oxygen ($q \gg 0$): (c) shows the theoretical results nonintegrated in q (the function for $q = 0$ is multiplied by factor 20), (d) shows experimental data for $1/T_1T$ on copper (Cu^{63}) and on oxygen (O^{17}) in $YBa_2Cu_4O_8$ [9].

Angle resolved photoemission spectroscopy (ARPES)

There are numerous anomalies observed by photoemission in the underdoped regime (ARPES directly measures the electron spectral function as a function of energy and wavevector) which can be summarized as the so-called $(\pi,0)$ feature : the Fermi surface disappears in the normal state in the vicinity of $(\pi, 0)$ wavevector while in all ordinary metals it is well defined; the spectrum has a very unusual flat form as a function of wavevector; the electron spectral function $A(\mathbf{k}, \omega)$ is almost non-structured as a function of energy with a hump in the normal state and with the peak-dip-hump in the superconducting state instead of the usual almost δ -function form, etc. Within our theory all anomalies find a natural explanation. They are signatures of the quantum spin density wave (SDW) short range ordered liquid state, being a precursor of the ordered SDW phase. For example, the spectrum shown in Fig.2a, 2b is a result of a hybridization of the two parts of the bare spectrum in the vicinity of two

different saddle points $(0,\pi)$ and $(\pi,0)$. The bare spectrum (dashed line) splits into two branches, $\epsilon_1(\mathbf{k})$ and $\epsilon_2(\mathbf{k})$. The hybridization is static for the ordered SDW phase and is dynamic for the disordered (quantum SDW liquid) state. In the latter case the mode $\epsilon_2(\mathbf{k})$ is strongly damped and appears above an incoherent background. The spectrum is in excellent agreement with ARPES data, see Fig.2c (ARPES measures only the part corresponding to negative energies ω). The existence below Fermi level of the incoherent background and of the damped mode $\epsilon_2(\mathbf{k})$ explains the anomalous almost nonstructured ω dependence of the electron spectral function with the hump at energy $\approx \epsilon_2(\pi,0)$ observed experimentally above T_{sc} . The effect of splitting into two branches leads to the pseudogap opening. The behaviour as a whole is strikingly similar to that observed experimentally. It concerns the very existence of pseudogap below T_{gap}^* which grows with decreasing δ , its doping and temperature dependences, the gradual disappearance of the Fermi surface with T , the shape of the spectrum around $(0,\pi)$, etc. Details are given in [3].

These were the features existing at intermediate temperature (above T_{sc}). At low temperature, the general picture of the spectrum is the same except that the upper branch $\epsilon_1(\mathbf{k})$ (i) moves to lower energies and intersects the Fermi level [3], (ii) gets a gap, $E_1^\pm(\mathbf{k}) = \pm \sqrt{\epsilon_1^2(\mathbf{k}) + \Delta^2(\mathbf{k})}$ in the presence of superconductivity with $\Delta(\mathbf{k}) = \Delta(\cos(k_x) - \cos(k_y))$ for the d-wave symmetry. Therefore two modes exist below Fermi level: the well-defined $E_1^-(\mathbf{k})$ and

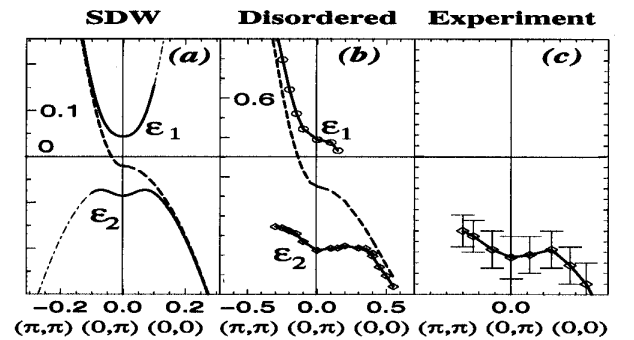


Figure 2. Electron spectrum $e(\mathbf{k})/t$ as a function of wavevector along $G - X$ symmetry lines in the Brillouin Zone, (a) in the ordered SDW phase, (b) in the quantum SDW liquid state above T_{sc} . (c) ARPES data^[10] for underdoped BSCO above T_{sc} . The dashed lines correspond to the bare spectrum, the thick lines to the two branches of the splitted spectrum, the dot-dashed line in (a) to the spectrum with the spectral weight less than 0.1.

the strongly damped $\varepsilon_2(\mathbf{k})$ which leads to the peak-dip-hump form of $A(\mathbf{k},\omega)$ as a function of ω observed experimentally in the superconducting (SC) state (E_1 corresponds to the peak and ε_2 to the hump).

Tunneling spectroscopy

The typical form of the tunneling function with peak-dip-hump features at negative energies, $\omega < 0$ as well as the asymmetry between $\omega < 0$ and $\omega > 0$ observed experimentally (see Fig.3b) and not understood until now are also explained well by our theory, compare Fig.3a and 3b. The effects are direct consequences of the discussed above form of the electron spectrum in the quantum SDW liquid state (tunneling spectroscopy measures the density of states, i.e. the electron spectral function integrated in \mathbf{k}). The peak-dip-hump structure seen in Fig.3 at negative ω results from the existence of two modes below the Fermi level (FL). So far, as it is not the case above FL, the picture in ω is quite asymmetrical.

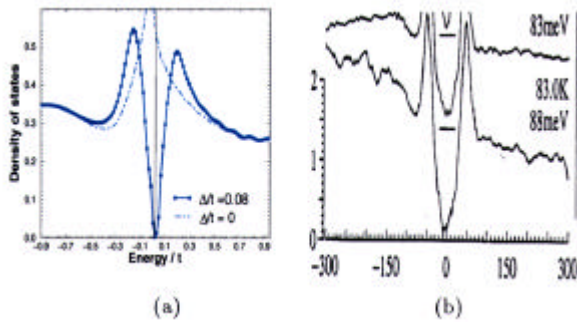


Figure 3. The density of states (a) calculated in the normal state (dotted line) and in the superconducting state (full line), (b) measured by tunneling^[11] at $T=4.2\text{K}$: the lowest curve corresponds to the underdoped Bi2212 ($T_c=83\text{K}$); the energy scale is given in meV.

Inelastic neutron scattering (INS)

The existence of the quantum SDW liquid state and of the corresponding quantum spin fluctuations have a direct consequence for the spin dynamics measured by INS. Firstly, it explains the very fact of magnetic response so strong that it can be measured by INS (in ordinary metals it is impossible). Secondly, it explains practically all details observed by INS. Most interesting among the theoretical predictions are maybe the existence in the SC state (i) of the resonance spin mode (with almost horizontal dispersion in the vicinity of \mathbf{Q}_{AF}) developing out of two particle electron-hole continuum and (ii) of the incommensurability at low energies^[5]. The former explains well the resonance peak at $\mathbf{q}=\mathbf{Q}_{AF}$ and $\omega \approx 40\text{ meV}$ with resolution-limited energy width and a finite q width observed systematically in the SC state from the beginning of high- T_c era^[12]. The latter explains recent results obtained with a high resolution spectrometer, see Fig.4b^[13]. The agreement with experiment is remarkable, compare Fig.4a and 4b.

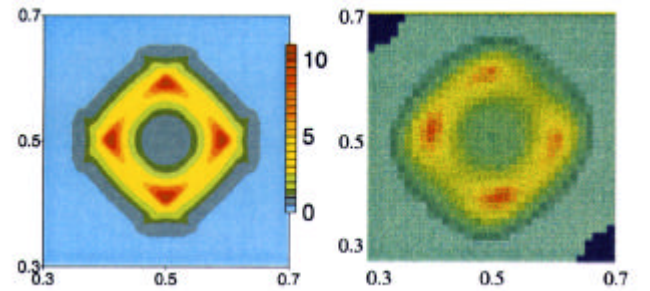


Figure 4. \mathbf{q} dependence of $\text{Im}C(\mathbf{q},\omega)$ (a) theoretical for $w/J = 0.25$, (b) experimental [13] ($\text{YBCO}_{6.6}$ for $w = 25\text{ meV}$). The point $(0.5, 0.5)$ corresponds to $(\pi/a, \pi/a)$. Note that $J \gg 120\text{ meV}$ for the cuprates.

References

- [1] I.M. Lifshitz, Sov.Phys.JETP. **11**, 1130 (1960)
- [2] F.Onufrieva, P.Pfeuty, M. Kisselev, Phys.Rev.Lett. **82**, 2370 (1999)
- [3] F.Onufrieva, P.Pfeuty, Phys.Rev.Lett. **82**, 3136 (1999)
- [4] F.Onufrieva, P.Pfeuty, Phys.Rev. B, (1999), to appear
- [5] F.Onufrieva, P.Pfeuty, cond-mat/9903097
- [6] F.Bouis, M.Kisselev, F.Onufrieva and P.Pfeuty, cond-mat/9906369
- [7] F.Onufrieva, S.Petit, Y.Sidis, Phys.Rev.B, **54**, 12464 (1996)
- [8] M. Takigawa, Phys.Rev.B, **49**, 4158 (1994)
- [9] C.Berthier et al, J. de Phys I France, **6**, 2205, (1997)
- [10] D.S. Marshall et al, Phys.Rev.Lett., **76**, 4841 (1996)
- [11] Ch. Renner et al, Phys.Rev.Lett., **80**, 149 (1998)
- [12] J.Rossat-Mignod et al, Physica C, **185-189**, 86 (1991); H.F. Fong et al, Phys.Rev.Lett. **78**, 713 (1997); P. Bourges et al, Europhys.Lett. **38**, 313 (1997)
- [13] H.A. Mook et al. Nature, **395**, 580 (1998)

STRUCTURES AND PHASE TRANSITIONS

The study of both crystallographic and magnetic structural phase transitions is an important activity of the Laboratoire Léon Brillouin. It makes use of several neutron scattering techniques, such as diffraction or inelastic scattering; the samples are either powders or single crystals. Most of the time, such studies are performed as a function of a unique parameter, namely the temperature, but pressure has recently become another important variable. Many different physical problems are related to these activities and the present summary intends to show the main goals of the research in the field. Magnetic phase transitions are treated in a different chapter.

FULLERENES AND CARBON NANOTUBES

Among the materials studied at LLB, fullerenes and carbon nanotubes are fashionable materials. The study of the former is older and the recent achievement of growing single crystals of C_{60} of sufficiently large size allowed the precise characterisation of the intramolecular dynamics of the molecule [L. Pintschovius et al, Kernforschungszentrum, Karlsruhe; see “*highlight*”]. Comparison with theory is particularly rich and yields the unambiguous identification of each of the internal modes of vibration. This comparison between experimental results and theory has been done, not only at the level of the frequencies, but also at the level of the intensities, in order to access the eigenvectors. The next step of this study will concern the intermolecular modes as a function of applied pressure. The problem of the nature of these interactions (which are weaker as compared with intramolecular interactions) is still not solved. It is currently assumed that they depend on the relative orientation of two neighbouring molecules and that the orientation is modified under pressure. Preliminary results show that pressure actually does not affect the vibrational frequencies as much as predicted by the theory.

More recently obtained (1991), **carbon nanotubes** are prepared by evaporation of graphite in the presence of metallic catalysts (Co, Ni, Fe...). The study of both the structure and vibrational dynamics of single wall carbon nanotubes (SWCN) has several interests. Firstly, SWCN are a model of one dimensional molecular systems that organise themselves as two dimensional crystalline bundles with a finite size. Also, their mechanical, optical and electronic properties are totally specific and dependent on the structure, which has been studied in real space by means of electronic and atomic force microscopies. However, even if they give useful information about the structure of the tubes and of the bundles, these techniques provide only a purely local picture. Studies in reciprocal space by neutron or X-ray scattering, are complementary and furnish the structure averaged over very large volumes. Comparison between experiment and theory yields the distribution of the diameters of the tubes and of the diameters of the bundles, and a relation to the processes of preparation of the SWCN is possible. The present activity in this domain concerns the pressure and temperature dependencies of the structural organisation of the tubes, by neutron scattering.

Concerning dynamic aspects, the low energy excitations (molecular and intermolecular) are very sensitive to the structure of the tubes. Raman scattering is widely used in studies of SWCN essentially because of the small amount of material requested by the technique and of the relatively high intensity of the signal. These experiments succeeded in obtaining the distribution of diameters from the analysis of the breathing modes of the tubes, in perfect agreement with former neutron scattering results. The first results obtained by inelastic neutron scattering showed clearly the breathing modes of the tubes in the domain $50\text{-}200\text{ cm}^{-1}$, but also other low frequency excitations ($< 50\text{ cm}^{-1}$), such as librations, interactions between tubes and a peculiar vibrational density of states [S. Rols, E. Anglaret, J.L. Sauvajol, Groupe de Dynamique des Phases Condensées, Université de Montpellier].

CHARGE ORDERING IN MANGANESE OXIDES

Concerning the study of perovskites of manganese with a giant magnetoresistance, an important problem is at present the eventual existence of ordering of the charges Mn^{3+} and Mn^{4+} at low temperature, according to the nature of the cations and the stoichiometry of the structure. The crystallographic order of Mn^{3+} and Mn^{4+} is relatively difficult to observe for these perovskites, due to the presence on the powder diffraction diagram of only one superstructure peak, which is very weak and within the wing of a structural line. However, such order has been

clearly observed in the defined compound LiMn_2O_4 which has a spinel structure at high temperature. Previous measurements of the electrical resistivity and experiments performed by thermal differential analysis, showed the existence of a first order transition just above room temperature, which can be due to a cooperative Jahn-Teller effect. Combination of electronic and neutron scattering data on powders allowed the classification of the transition as an order/disorder of the charges Mn^{3+} , Mn^{4+} (octahedral site of the spinel structure). The analysis of the data at $T = 230 \text{ K}$ demonstrates that this ordering is only partial [Collaboration Laboratoire de Chimie des Solides, Université Paris-Sud - LLB; see “*highlight*”; current PhD: G. Rousse, LCS, Orsay].

PEROVSKITES RELAXORS

Another problem extensively studied at LLB by the Laboratoire “Structure, Propriétés et Modélisation du Solide” of Ecole Centrale de Paris [J.M. Kiat et al; PhD: C. Malibert, B. Dkhil, ECP], is that of relaxor materials such as the perovskites $\text{Pb}(\text{B},\text{B}')\text{O}_3$, for which one observes a large dielectric constant, very soft in temperature and dependent upon the measuring frequency. Some of these materials have industrial applications, namely as capacitances. As far as structure is concerned, they are characterised by some disorder of the cations B and B' and one can actually observe ordered or disordered perovskites depending on the size and charge of the cations B and B'. The combination of X-ray and neutron diffraction allows the precise characterisation of the cationic order and its relation to the dielectric properties.

PHASE TRANSITIONS : STRUCTURAL STUDIES

Another example of structural determination using both X-rays and neutron diffraction concerns ErFe_4Ge_2 . This compound is magnetically ordered at low temperature and characterised by the existence of a strong magnetoelastic coupling, which is at the origin of a crystalline phase transition. Below the temperature of magnetic ordering, two different crystalline structures are present in ErFe_4Ge_2 and the relative volume of each domain depends on temperature [Collaboration Laboratorium für Kristallographie, ETHZ, Zürich - LLB].

One can also mention the following structural determinations by neutron diffraction:

- localisation of hydrogen atoms in strontium nitroprussiate, $4\text{H}_2\text{O}$ [Collaboration Laboratoire de Physique, Centre Pharmaceutique, Chatenay-Malabry - LLB];
- study of phase transitions of Co-0.85\% at Fe as a function of temperature or of time at fixed temperature (characteristic time of the order of hour, accessible to real time in situ neutron diffraction experiments) [Collaboration Institut für Experimental Physik, University of Vienna, Austria - LLB];
- study of tridimensional structures, such as iron phosphates or arseniates, of interest as possible anode materials in lithium batteries. The first members of the series were $\text{Li}_3\text{Fe}_2(\text{PO}_4)_3$ and $\text{Li}_3\text{Fe}_2(\text{AsO}_4)_3$, for which the order/disorder of alkaline cations in the structure has been followed as a function of temperature [Collaboration Laboratoire de Chimie des Solides, Université Paris-Sud - LLB; current PhD: C. Würm, LCS, Orsay].

MOLECULAR CRYSTALS

The determination of the structure of molecular crystals is an important problem for which neutron diffraction is particularly suitable because the neutron scattering amplitudes of the different constituents (light and heavy atoms) are of the same order of magnitude, in contrast with the situation of X-ray scattering. Moreover, in the particular case of hydrogen, the isotopes hydrogen and deuterium have very different coherent scattering lengths, one being positive and the other negative. This property has been used to study the structure of partially deuterated aspirin, $\text{C}_8\text{H}_6\text{O}_4\text{-CH}_2\text{D}$, a molecule where the methyl group is distinct from CH_3 or CD_3 , i.e. non-symmetric. Earlier studies by NMR had shown that the protons of this group remain relatively mobile down to 15 K . Consequently, the diffraction experiment should give an averaged image of the position of the H/D atoms, in a “superposition” of three methyl groups shifted by 120° , D-H-H, H-D-H and H-H-D. The crystalline structure of $\text{C}_8\text{H}_6\text{O}_4\text{-CH}_2\text{D}$ (monoclinic) has been determined first at room temperature (diffraction by a single crystal, data treatment using the maximum entropy method) and indeed, at this temperature, the nuclei H and D are not distinguishable, and an average scattering amplitude equal to $2/3 b_{\text{H}} + 1/3 b_{\text{D}}$ is obtained for each of the three sites H/D of the methyl group. However, at low temperature ($T = 15 \text{ K}$), such analysis is no more adequate. Actually, one of the positions among D-H-H, H-D-H or H-H-D is more likely than the other two, i.e. the deuterium occupies preferentially one of the three possible H/D sites of the methyl group [Collaboration Institut für Kristallographie, Tübingen - LLB; see “*highlight*”].

Potassium hydrogenomaleate [$\text{KH}(\text{OOC-CH=CH-COO})$] is a typical example of an intramolecular hydrogen bond, very strong and symmetric. The nature of the potential that explains the dynamics of the hydrogen bond has been the object of several discussions, because of the absence of a well defined crystalline structure at different

temperatures, of the complexity of the vibrational spectra and of the natural limitations of the quantum chemistry calculations. The structure determined by neutron diffraction shows that the hydrogen bond is rigorously centred at all temperatures. Following this experimental result, a new form of interaction potential has been proposed in order to take into account the inelastic neutron scattering spectra. This function is symmetric about the centre of the bond and has three wells. As far as we know, this is the first example of such form of potential. This study illustrates the complementarity of structural and dynamic studies. It is also a contribution toward a better knowledge of the mechanisms of proton transfer and of the elementary steps of chemical reactivity in solutions [Laboratoire de Dynamique, Interactions et Réactivité, CNRS, Thiais].

PHASE TRANSITIONS : LATTICE DYNAMICS

The study of phonons is one of the main domains accessible to inelastic neutron scattering. In this domain, the main results obtained at LLB, by the Karlsruhe research group, concern fullerenes (see above) and iridium. In both cases, comparisons between experiment and ab initio theory have been carefully established.

In the case of solid solutions $(\text{BaF}_2)_{1-x}(\text{RF}_3)_x$, where R represents a rare earth, the modifications of the phonon spectrum have been followed as a function of the temperature (from room temperature to 1000°C) and of the thermal history of the sample. These compounds are ionic conductors. Two main results have been obtained: first, the lattice vibrations are hardly observed at room temperature and appear more clearly at higher temperatures ($\text{R}=\text{Nd}$, $T \geq 400^\circ\text{C}$), as a consequence of the coupling between phonons and the mobility of the fluorine ions. One also observes low frequency components that correspond to localised vibrations of clusters formed by the ions R^{3+} and the ions F^- at neighbouring interstitial sites (compensation of charge). Such modes depend strongly on the geometry of the clusters, thus on the thermal history of the sample [PhD: P. Kadlec, Institute of Physics, Praha and CRMHT, Orléans].

The University Pierre et Marie Curie in Paris [S. Klotz et al, Laboratoire de Physique des Milieux Condensés], in collaboration with the LLB, has developed a common programme with the objective of measuring **phonon spectra under pressure** (cell “Paris-Edinburgh”, see the chapter on Technical and Instrumental Developments). Measurements on iron oxide, Fe_{1-x}O , one of the most studied compounds in Geophysics, have been performed intending to study more in detail the origin of the cubic-rhomboedric phase transition, observed around 15 GPa. Other authors, using different techniques (ultrasound, $P < 5$ GPa) have shown that the frequency of acoustical modes was reduced under pressure, suggesting that a soft mode could be at the origin of the observed phase transition. The results obtained by inelastic neutron scattering contradict this hypothesis: even if the frequency does decrease linearly as pressure increases, no soft mode is observed up to 12 GPa. It is worth noting that this pressure is the highest one at which a phonon has been observed so far.

The “**neutral-to-ionic**” transition is an unusual type of transition because it is associated to a change of electronic structure between two solid states. This transition is a consequence of the condensation and ordering (crystallisation) of charge transfer excitations. It has been observed in molecular materials of peculiar structures, when donor (D) and acceptor (A) molecules alternate in a linear chain. It is characterised by a cooperative modification of the electronic states of the molecules, accompanied by a significant increase of the level of charge transfer between the neutral and ionic states and by a dimerisation process taking place in the ionic state with formation of ionic pairs D^+A^- along the stacking axis. The prototype of such compounds is TTF-CA (TetraThiaFulvalene-ChlorAnile), which has been studied at LLB by the Groupe Matière Condensée et Matériaux of the University of Rennes [Current PhD: E. Collet, GMCM, Rennes]. Complementary measurements of Quadrupole Nuclear Resonance of ^{35}Cl and of inelastic neutron scattering under pressure, allowed the establishment of a phase diagram containing the neutral-to-ionic transition on TTF-CA. Actually this phase diagram “pressure, temperature” (for $P \leq 1.2$ GPa) is similar to a 3-phase (solid-liquid-gas) diagram, but concerns only the solid.

INCOMMENSURATE MATERIALS AND QUASICRYSTALS

Another important domain of research at LLB concerns incommensurate materials both in their structural and dynamical aspects. Here, incommensurate must be understood both in its strict meaning and in relation to the physics of quasi-crystals and composites.

Experimental studies on **BCCD** (Betaine and Calcium Chloride di-hydrated) are numerous and performed as a function of several external parameters: temperature, pressure, electrical field. The preceding activity report of LLB described most of this activity [PhD: O. Hernandez, LLB]. In a more recent experiment, chlorine has been partly replaced by bromine, introducing a “negative” pressure of chemical origin. The subsequent modification of the phase diagram has been followed as a function of temperature.

$(\text{ClC}_6\text{D}_4)_2\text{SO}_2$ (**BCPS**) is a molecular compound for which a displacive phase transition is observed, from a high temperature phase to an incommensurate phase at low temperature. Inelastic neutron scattering allowed the

evolution of collective excitations below the transition temperature (phasons) to be followed. It is worth noting that the observation of phasons is not usual because of their overdamped character at the neighbourhood of other satellite reflections: BCPS is one of the rare cases where phasons have been observed [Groupe Matière Condensée et Matériaux, Université de Rennes; PhD: J. Ollivier, GMCM, Rennes].

Incommensurate composite crystals are built with at least two interpenetrating lattices with periodicities that are mutually incommensurate at least in one direction. Such aperiodic systems are intermediate between incommensurate modulated systems (e.g. BCCD and BCPS) and quasi-crystals. The aim of the study performed by the Groupe Matière Condensée et Matériaux (Université de Rennes) was to use neutron scattering as a tool for the characterisation of structural and dynamic aspects of these little known materials. The study has been done on urea inclusion compounds. The determination of the structure is complementary to that performed by X-rays and has been done with a single crystal: the structure can be described in a 4-dimension space. The first observations of phonons associated with the host lattice have been done and show the presence of an anomalous high damping of the longitudinal acoustical mode propagating along the direction of incommensurability [PhD: R. Lefort, GMCM, Rennes].

A fundamental problem of the physics of **quasi-crystals** is the nature of the dynamic phasons. In contrast with the case of crystalline incommensurate materials, phasons in quasi-crystals are not propagative modes but, instead, atomic jumps. Experiments of inelastic neutron scattering on a large single domain sample of icosahedral Al-Mn-Pd demonstrated that indeed a correlation between simultaneous jumps is present. This surprising result represents an important contribution to the understanding of dynamic phasons in quasi-crystals [G. Coddens et al; see “*highlight*”; PhD: S. Lyonnard, LLB]. Atomic jumps have been studied also in the decagonal system Al-Co-Ni as a function of temperature, wave-vector and isotopic composition.

Many other aspects of the physics of quasi-crystals will be the objects of further studies. One can mention the study of the dynamics of hydrogen and deuterium atoms in Ni-Ti-Zr, the structural study of Al-Cu-Fe which will be approached by different techniques, namely quasielastic neutron scattering (isotopic substitution), inelastic neutron scattering, anomalous X-ray scattering and Mössbauer spectroscopy (for the correlations iron-iron).

THEORY : « DISCRETE BREATHERS »

Finally, one of the important activities of LLB is the theoretical studies of S. Aubry and co-workers [Current PhD: A.M. Morgante, LLB; PhD: J.L. Marin, Zaragoza, Spain; T. Cretigny, ENS-Lyon] about “discrete breathers”, periodic excitations in time that are localised in space. Their existence has been proved in non-linear systems whatever their dimensionality. One knows that spatial localisation can also be obtained by linear modes in a random medium. Consequently, the theoretical study of excitations in non linear systems has been extended to random media. Several one dimensional physical systems have been studied, such as the case of a periodic chain of atoms [see “*highlight*”] using an hamiltonian with harmonic frequencies randomly distributed at each site and a quadratic coupling of neighbouring sites. One of the interests of these models relates to new possible interpretations of relaxation in glasses and amorphous materials.

CONCLUSION

It is clear that neutron scattering is quite often a complementary technique of X-ray scattering, particularly in the case of molecular compounds. The isotopic substitution H/D, for example, is one of the major tools in structural determinations. We have seen that, for the first time, the positions of H and D in a crystalline structure have been clearly separated. In dynamic studies, the access to the whole Brillouin zone and the absence of selection rules complement the information obtained by optical spectroscopic techniques.

The very large variety of problems treated at LLB, such as $\text{Mn}^{3+}/\text{Mn}^{4+}$ charge ordering, incommensurate systems, quasi-crystals (observation of phasons), fullerenes and carbon nanotubes, studies under pressure (up to 12 GPa) and neutral-to-ionic transition, exemplifies the amplitude of the domain of research performed by neutron scattering and the role played by LLB in collaboration with several French and European groups.

VERWEY-LIKE TRANSITION IN A LITHIUM BATTERY MATERIAL: THE SPINEL LiMn_2O_4

J. Rodríguez-Carvajal¹, G. Rousse², C. Masquelier², M. Hervieu³

¹Laboratoire Léon Brillouin (CEA-CNRS)

²Laboratoire de Chimie des Solides, Université Paris-Sud, 91405 Orsay Cedex, France.

³CRISMAT, ISMRA, 6 Bld du Maréchal Juin, 14050 Caen Cedex, France.

An increasing interest has developed around Li-Mn-O spinels due to their potential use as positive electrode materials in lithium rechargeable batteries. A vast majority of the studies devoted to these compounds deals with their electrochemical characteristics in lithium cells^[1]; only very recently, their structural and physical properties have also been studied^[2-4]. The stoichiometric compound LiMn_2O_4 presents a first order structural transition close to room temperature (RT) that was attributed to a Jahn-Teller distortion^[4]. In the case of Mn-perovskites close to the composition $(\text{R}_{1/2}\text{D}_{1/2})\text{MnO}_3$ (R: trivalent rare earth, D: divalent ion), structural phase transitions accompanied by sharp modifications of electronic and magnetic properties have been attributed to charge-ordering^[5]. This phenomenon is supposed to be due to the Coulomb interaction that overcomes the kinetic energy of carriers below a certain temperature (Wigner crystallization) producing an alternating Mn^{3+} - Mn^{4+} NaCl-like lattice. This mechanism was first invoked by Verwey in 1941 to explain the low temperature transition in magnetite Fe_3O_4 as a Fe^{2+} - Fe^{3+} ordering within the B-sites of the spinel structure^[6]. In spite of a different lattice organization of Mn ions in the spinel as compared to Mn-perovskites, it is reasonable to expect some kind of similar electronic behaviors in both families.

To date, the structural details of charge-ordered Mn-perovskites are quite limited, since the superstructure reflections in neutron powder diffraction patterns are barely visible and single crystals show complicated twinning effects. It is extremely important to know whether the ionic picture usually invoked to describe the charge ordering in these materials is supported by structural experimental evidence. For instance, the simple NaCl-like ordering picture of Mn^{3+} and Mn^{4+} ions in $\text{La}_{1/2}\text{Ca}_{1/2}\text{MnO}_3$ has not yet been confirmed definitively even if experimental data are not in contradiction with such a picture^[7]. We have recently shown that the ionic picture is well supported in the case of LiMn_2O_4 spinel and we have demonstrated that the charge-ordered state is not complete at 230K^[8,9].

DSC (Differential Scanning Calorimetry) experiments confirmed the presence of a first order transition

around RT. With a cooling rate of 5 K/mn, the cubic \rightarrow orthorhombic transformation starts at 290K with a hysteresis of 10K (fig.1). An increase of resistivity is observed upon cooling to the low temperature phase (fig.1). The activation energy of the low temperature form is slightly higher but similar to that of the high temperature. The charge carriers are very probably Jahn-Teller small polarons.

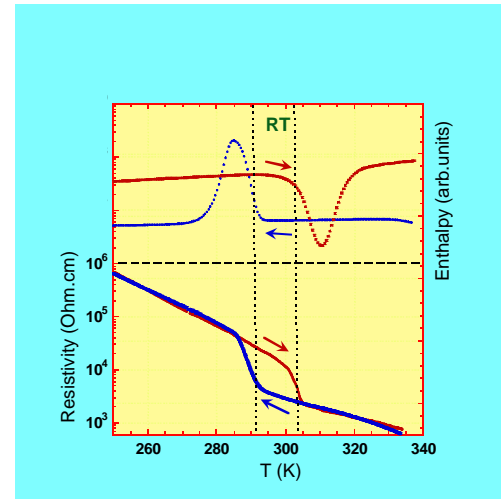


Figure 1: DSC and resistivity of LiMn_2O_4

Neutron diffraction experiments were performed using the high-resolution powder diffractometer 3T2. The high temperature form was carefully studied at 350K ($a=8.2495(2)\text{\AA}$) to confirm the crystalline quality and the stoichiometry of the sample (fig.2). The refined value of the oxygen occupation was the nominal value within the experimental error. The unique Mn-O distance is $1.9609(3)\text{\AA}$, which is intermediate between what is expected for Mn^{3+} -O and Mn^{4+} -O bond lengths. Neutron powder diffraction at low temperature showed many small superstructure reflections (fig.2). The indexing of the pattern using solely the neutron data was ambiguous and gave several reasonable solutions due to the strong overlap between neighboring reflections. The information provided by electron diffraction at different temperatures was of capital importance for finding a " $3a \times 3a \times a$ " supercell and extinction conditions compatible with the space group $Fddd$.

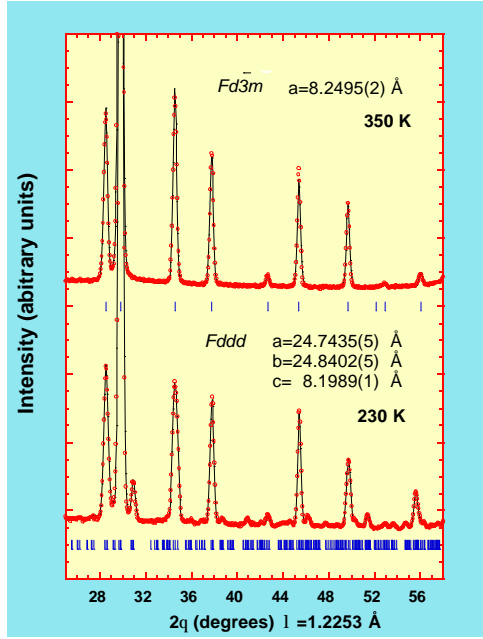


Figure 2: Details of the observed and calculated neutron diffraction patterns ($\lambda=1.2253$ Å) of the high temperature charge-disordered phase (350K), and of the low temperature partially charge-ordered phase (230K) of LiMn_2O_4 . Additional tick marks in the low temperature pattern correspond to the superstructure reflections.

The final atom positions can be found in reference [8]. The analysis of the structure obtained from the Rietveld refinement of our neutron data clearly shows the electron ordering nature of the phase transition and allows us to interpret the resistivity measurements. Two Mn-sites correspond to well-defined Mn^{4+} ions (the average Mn-O distance is 1.91 Å). The other three sites are not pure Mn^{3+} ions. This is revealed by the average Mn-O distance for the three Mn-sites (2.00 Å) which is slightly smaller than what is expected for pure Mn^{3+} (2.02 Å). To simplify the visualization of the crystal structure we have represented in Fig. 3 an idealized projection along [001] of the Mn and Li sites within a unit cell. Neglecting the z-position of the atoms, it is apparent that octagonal cylinders surfaces (hole-rich regions), containing all the Mn^{4+} , wrap two types of Mn^{3+} columns (electron-rich regions) which are distinguished by the presence, or lack therein, of Li ions. The space between the octagonal cylinders is occupied by columns containing the Mn(1) site in the special position (16d).

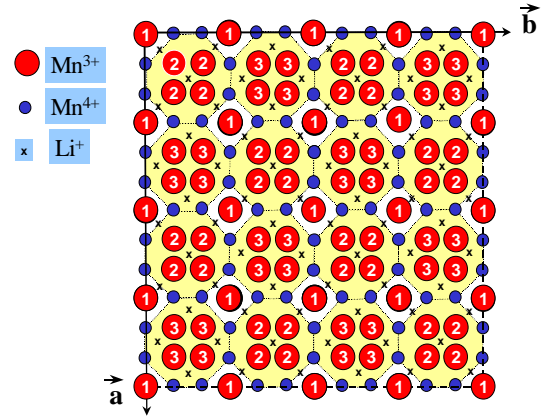


Figure 3. Simplified projection of the charge-partially-ordered structure. Oxygen atoms have been removed from the drawing. Static holes (Mn^{4+} , blue circles) wrap columns of nearly pure Mn^{3+} ions along the c -axis. $8/72=1/9$ of the total number of holes are mobile within the Mn^{3+} sublattices.

The average valence of Mn ions, obtained from chemical analysis and structure refinement at high temperature, indicates that the number of holes (Mn^{4+}) in the e_g -band is equal to the number of electrons (Mn^{3+}) available for hopping. The crystal structure indicates that there are 64 localized holes per unit cell, so there are eight remaining holes per cell distributed within the remaining 80 Mn positions. Thus, a certain electron hopping should persist at low temperature as revealed by the previous analysis. This is consistent with the semiconducting characteristics of the compound below the transition temperature. The static distortion of the three Mn^{3+}O_6 octahedra is consistent with a slightly attenuated Jahn-Teller effect^[9] due to the remaining electron hopping towards the 8 holes per cell. The charge ordering process is, consequently, accompanied by the presence of an orbital ordering which is the manifestation of the Jahn-Teller polaronic nature of the mobile charges above and below the transition temperature.

To our knowledge this is the first time that a partial charge ordering transition is clearly observed in a Mn oxide. The electronic crystallization observed in this compound must be due to a combination of Coulomb interaction and another mechanism implying electron-lattice coupling as is the Jahn-Teller effect. The analysis of the crystal structure shows that the ionic model seems to be adequate and the usual Mn^{3+} - Mn^{4+} picture is well justified in LiMn_2O_4 .

References

- [1] M.M. Thackeray, *Prog. Solid St. Chem.* **25**, 1 (1997), and references therein.
- [2] C. Masquelier *et al.*, *J. Solid State Chem.* **123**, 255 (1996).
- [3] V. Massarotti *et al.*, *J. Solid State Chem.* **131**, 94 (1997).
- [4] H. Yamaguchi, A. Yamada, and H. Uwe, *Phys. Rev.* **B58**, 8 (1998).
- [5] Y. Tomioka *et al.*, *Phys Rev Lett* **74**, 5108 (1995)
- [6] E.J.W. Verwey, and P.W. Haaymann, *Physica* **8**, 979 (1941).
- [7] P. Radaelli, D.E. Cox, M. Marezio, and S.-W Cheong, *Phys Rev B* **55**, 3015 (1997)
- [8] J. Rodriguez-Carvajal *et al.*, *Phys Rev Lett* **81**, 4660-4663 (1998)
- [9] J. Rodriguez-Carvajal *et al.*, *Phys. Rev.* **B57**, R3189 (1998)

L. Pintschovius^{1,2}, R. Heid¹, J.M. Godard³, and G. Krexner⁴

¹Forschungszentrum Karlsruhe - ²Laboratoire Léon Brillouin (CEA-CNRS)

³Laboratoire de Physique des Solides, Université Paris-Sud - ⁴Université de Vienne, Autriche

Solid C₆₀ is a prototypical example of a molecular solid with very strong *intramolecular* and very weak *intermolecular* bonds. The high symmetry of the C₆₀ molecule is certainly a major reason that it has attracted considerable interest. Moreover, it also greatly facilitates theoretical computations of its properties, and so C₆₀ has become the best studied member of the fullerene family. For this reason, C₆₀ can be considered as an ideal testing ground of theories for strong (covalent) forces as well for weak (van der Waals-like) forces. The most detailed information for a check of the theoretical predictions can be obtained by inelastic neutron scattering, and so we have undertaken a series of experiments to explore the vibrational properties of C₆₀. In the beginning, only the external vibrations could be studied because of the small size of the available single crystals (V~5 mm³)^[1,2]. With the advent of fairly large single crystals (V~100 mm³) we were able to investigate the internal vibrations, too, with energies up to E=70 meV. Moreover, we were able to study the pressure dependence of the external vibrations. In the following, we summarize the results of the most recent experiments.

An isolated C₆₀ molecule has 46 distinct vibrational modes. When the molecules are packed into a lattice, the intermolecular interactions give rise to mode splittings and to some dispersion. However, these effects are rather small due to the weakness of the intermolecular forces and can therefore be neglected. So, the problem of verifying the results of a certain theory reduces to verify the predicted *frequencies and displacement patterns* of the eigenmodes of the C₆₀ molecule. We emphasize that a good agreement between calculated and experimental frequencies is of little value unless it has been checked that the observed mode has the same character as the calculated one. A minimum requirement is that the symmetry of the displacement pattern of the observed mode is the same as predicted for this frequency. However, as most symmetry classes contain more than one member, their displacement pattern is not determined by symmetry alone, but by the force field as well. This is demonstrated in Fig. 1, where we plotted the displacement patterns of a number of C₆₀ eigenmodes, including those of the three lowest modes of H_g symmetry. Inelastic neutron scattering has the particular advantage that it allows one not only to unambiguously assign an observed frequency to a mode of a certain symmetry but, moreover, to check in detail whether the predicted displacement pattern

is correct or not. To this end, energy scans have to be made at many different points in reciprocal space. As can be seen from Fig. 2, the calculated scattering cross section versus momentum transfer differs widely for modes of the same symmetry but having different frequencies.

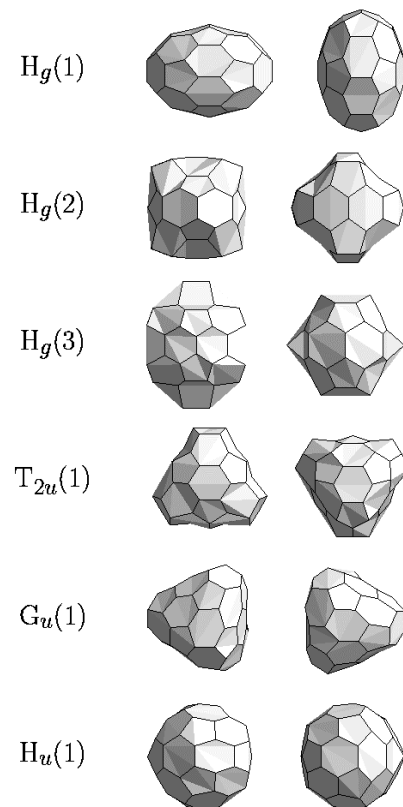


Figure 1: Displacement patterns for five different eigenmodes of the C₆₀ molecule. The elongations are strongly exaggerated for the sake of clarity. The left-hand and the right-hand figures correspond to extremal distortions following each other at time intervals 1/2 π . Eigenvectors are taken from the *ab initio* calculations of Bohnen et al. (Ref. 4).

Our results revealed that several modes had been assigned incorrectly in the literature. Furthermore, we were able to show that *ab-initio* theory based on the local density approximation^[4] describes not only the mode frequencies with high accuracy (~ 2%), but also the eigenvectors in a very satisfactory way. We note that the agreement between calculated and observed eigenvectors was significantly worse for a sophisticated model fitted to the experimental frequencies^[5], which shows that a good agreement between calculated and observed displacement patterns

is by no means granted even if the frequencies are reproduced correctly.

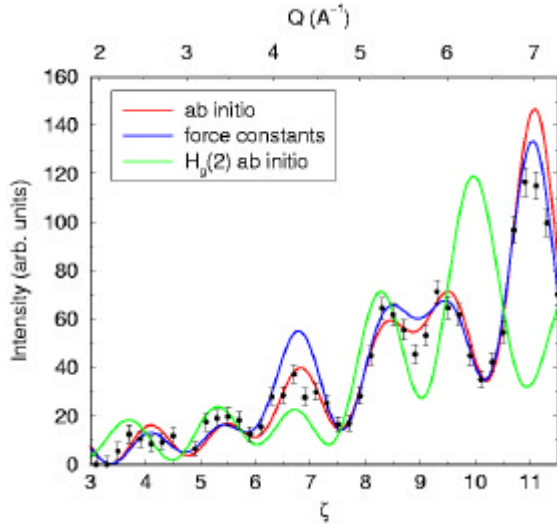


Figure 2: Intensity of the 33 meV peak versus momentum transfer ($z, z, 0$) observed on a single-crystal sample at $T=12$ K. The red and blue lines denote the predictions of an *ab initio* theory (Ref. 4) and of a force-constant model (Ref. 5) for the $H_g(1)$ mode, respectively, and the green line shows the prediction of the *ab initio* theory for the $H_g(2)$ mode using the same scaling.

The good understanding of the covalent intramolecular forces contrasts with our rather poor understanding of the weak intermolecular forces. From the large distance between atoms on different molecules (≥ 3 Å) it was assumed that these forces are of van der Waals (vdW) type. However, it is known for long that the vdW potential taken from graphite gives a poor account of many properties depending on the intermolecular potential. In particular, the frequencies of the hindered rotations (librations) calculated from the vdW are too low by more than a factor of two^[1,2].

In the absence of *ab-initio* calculations for the intermolecular forces, many empirical potentials have been proposed in the literature which were designed to improve the simple vdW ansatz by taking secondary interactions into account. For instance, several models have been developed which include Coulomb forces between charges placed on various locations on the C_{60} molecule. These models reproduce the dispersion of the external vibrations quite satisfactorily^[2]. However, a recent experiment of us has shown

that this is true only for the usual phase of C_{60} , where double bonds of one molecule face pentagonal faces of neighbouring molecules. By applying pressure, the C_{60} molecules can be switched to a different orientation, so that double bonds face hexagons. When the pressure is released at low temperatures, the 'hexagon' structure is frozen in. Measurements on this metastable phase have shown that there are surprisingly small differences between the frequencies of the external vibrations in the two phases (see Fig.3), whereas the empirical models predict very large frequency changes ($\approx 50\%$ for the librational modes, upwards or downwards, depending on the model).

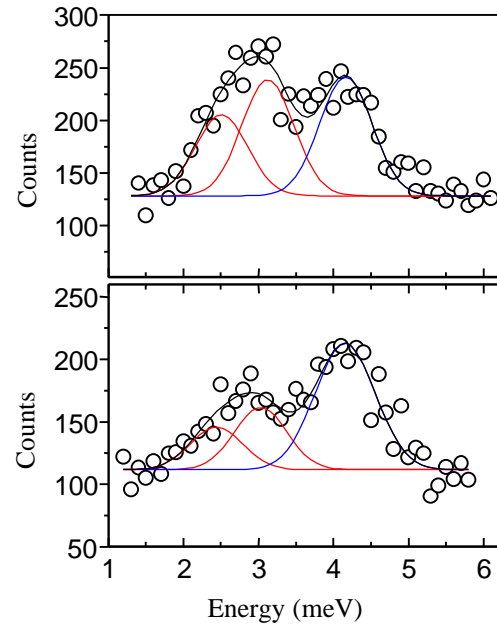


Figure 3: Energy scans taken at $Q=(7.5, 7.5, 0)$ at $T=70$ K. The data were fitted with three Gaussians with a width corresponding to the experimental resolution. From model calculations we know that the two low energy peaks correspond to librational excitations and the high energy peak to a translational excitation, respectively. The upper and lower graph refer to measurements on the "pentagon" and the "hexagon" phase, respectively.

Measurements of the external vibrations at pressures up to 7 kbars are planned in the near future. The results are hoped to advance further our understanding of the intermolecular potential in C_{60} .

References

- [1] L. Pintschovius et al., Phys. Rev. Lett. **69**, 2662 (1992)
- [2] L. Pintschovius and S.L. Chaplot, Z. Phys. B **98**, 527 (1995)
- [3] R. Heid, L. Pintschovius and J.M. Godard, Phys. Rev. B **56**, 6925 (1997)
- [4] K.-P. Bohnen, R. Heid, K.-M. Ho, and C.T. Chan, Phys. Rev. B **51**, 5805 (1995)
- [5] R.A. Jishi et al., Phys. Rev. B **45**, 13685 (1992)

CRYSTALLOGRAPHIC IMAGING OF A MOLECULAR CRYSTAL : Aspirin $C_8H_5O_4-CH_2D$

R.J. Papoular¹, W. Paulus¹, P. Schiebel², W. Prandl², H. Zimmerman³, A. Detken³, U. Haeberlen³

¹Laboratoire Léon Brillouin (CEA-CNRS)

²Institut für Kristallographie, Universität Tübingen, Charlottenstr. 33, D-72070 Tübingen

³Max-Planck Institut für medizinische Forschung, D-69120 Heidelberg

The nuclear density distribution of partially deuterated aspirin at 300 K and at 15 K has been determined by single-crystal neutron diffraction coupled with Maximum Entropy image reconstruction (MEM). While fully protonated and deuterated methyl groups in aspirin (acetylsalicylic acid) have been shown to be delocalized at low temperature due to quantum mechanical tunnelling, we provide here direct experimental evidence that in partially deuterated aspirin- CH_2D the methyl groups are orientationally ordered at 15 K whilst randomly distributed over three sites at 300 K. This is the first observation of low temperature isotopic ordering in condensed matter by diffraction methods.

PHYSICAL BACKGROUND

The quantum mechanical behavior of ever larger and heavier molecules and molecular subunits in condensed matter is a subject of considerable interest. The onset of quantum behavior is usually observed at low temperature. Substitution of hydrogen with deuterium leads to large isotopic effects, in fact the largest ones known in chemical physics. Spectroscopic methods such as NMR and QENS are the prevalent tools to investigate these phenomena.

The rotational dynamics of molecules or side groups such as methyl groups is a very sensitive probe of the interatomic forces in crystals. Rotating a methyl group about the bond connecting it to the rest of the molecule makes it experience a rotational hindering potential which arises from the interactions of the methyl hydrogens with their surroundings.

This potential has at least three wells due to the molecular symmetry. At moderately high temperatures, the methyl groups undergo thermally activated reorientations between all three wells, whereas at low temperature, say below 30 K, the dynamics of the methyl groups is usually dominated by rotational quantum tunnelling^[1].

While the dynamics of isotopically uniform methyl groups is by now well understood, little attention has been paid so far to the isotopically mixed CHD_2 and CH_2D groups. Due to the loss of the three fold permutation symmetry in the latter, dramatic differences in the dynamical behavior are expected.

WHY ASPIRIN ?

A well-studied case of the dynamics of the CH_3 and CD_3 groups is that of aspirin $C_8H_5O_4-CH_3$ and $C_8H_5O_4-CD_3$. The observation of rotational tunnelling in this compound by NMR triggered a whole series of studies concerned with the potential and with the dynamics of these methyl groups. These studies show that from room temperature down to about 35 K the per-protonated, the per-deuterated as well as the

isotopically mixed methyl groups perform thermally activated stochastic reorientations between the three potential wells. Upon cooling, the rate of the reorientations naturally slows down. What happens at low temperature depends crucially on the isotopic composition of the methyl group. For CH_3 and CD_3 , coherent rotational tunnelling was inferred from NMR experiments. This implies that the wavefunction describing the methyl group is such that the three protons, respectively deuterons, are completely delocalized over three sites. By contrast, partial ordering, which implies localization as well as a rapid incoherent process between the almost degenerate upper two of the three wells were suggested for CH_2D , again on the basis of NMR results.

As shown below, Neutron Diffraction provides a direct check of the indirect NMR hints^[2-4].

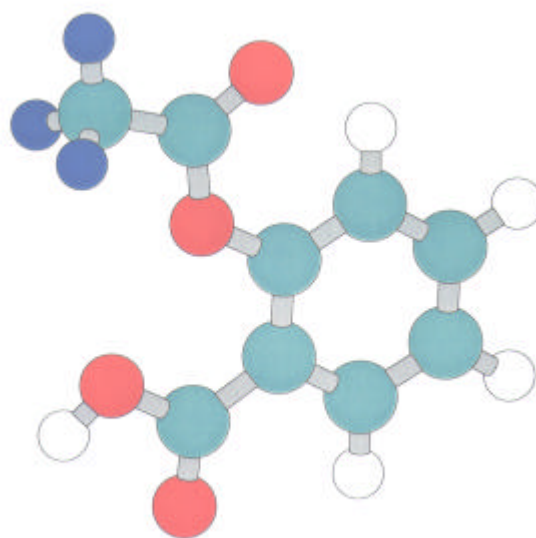


Figure 1. The aspirin molecule. Carbon and oxygen atoms are shown in blue-green and red. The hydrogen atoms from the methyl group are shown in blue and the

remaining protons attached to the backbone are shown in white.

SINGLE-CRYSTAL NEUTRON DIFFRACTION

This technique allows us to measure the nuclear density distribution within the crystallographic unit cell. This distribution is given by the probability density function of finding a nucleus at a given position, multiplied by the coherent neutron scattering length b of that nucleus. The probability density function relates to an average over space and time, *i.e.* over the volume of the sample and over the duration of the measurement. In case dynamic processes are involved, then neutron diffraction yields a direct long time exposure of those processes. Due to the opposite signs of the neutron scattering length of protons and deuterons ($b_H = -3.74$ fm, $b_D = 6.67$ fm), the former yield a negative contribution to the nuclear scattering density, in contrast to the latter. Thus neutron diffraction is an excellent tool for distinguishing protons from deuterons, and hence for studying isotopic ordering processes such as those proposed for aspirin-CH₂D.

A ZERO AVERAGE CONTRAST SAMPLE

In order to improve the visibility of the alleged H/D orientational order of the methyl groups at low temperature, we aimed at an aspirin-CX₃ sample with an average scattering length $\langle b_X \rangle$ of zero. Consequently the single-site nuclear scattering length is expected to be close to zero for a random orientational distribution, for which there will hardly be any coherent scattering from the methyl hydrogens. On the other hand, if ordering occurs, it will then be revealed by positive bumps and negative holes in the nuclear density distribution.

OUR EXPERIMENT

To test the above-mentioned ideas, we collected data sets from our crystal at 300 K and at 15 K on the four-circle 5C2 diffractometer ($\lambda = 0.8302$ Å) at LLB. At both temperatures the crystal was found to be isomorphous to normal protonated aspirin, which had been examined much earlier by X-ray diffraction [5]. The crystal is monoclinic, of space-group $P2_1/c$ with 4 molecular units per unit cell.

We used a crystal from a previous NMR study^[3], and for which the requirement $\langle b_X \rangle = 0$ is nearly met. In fact, $\langle b_X \rangle \approx -0.6$ fm, about 11 times smaller than $\langle b_D \rangle$. A further complication arises from the fact that our sample comprises approximately 70% CH₂D, 19% CH₃, 10% CHD₂ and 1% CD₃.

LEAST-SQUARES RESULTS

The program SHELXL97 was used for refinements. As expected, neither could methyl hydrogen positions be found, nor did the calculated difference Fourier

map reveal any contribution from either the methyl protons or deuterons. Any information about these latter hydrogens (which is definitely present in our data) is swamped by the inherent residual noise due to series termination effects.

Taking this model which does not include methyl hydrogens as the starting point for the LT structure refinement, two proton positions and one deuterium position are easily located by their negative and positive contributions in the difference Fourier map calculated by SHELXL97. Including these in the structural model without any bond length or bond angle constraint yields a good final agreement factor $R_1 = 0.0465$.

MAXIMUM ENTROPY IMAGING

We are specifically interested in the nuclear density distribution arising from the methyl hydrogens. Since conventional Fourier syntheses would not reveal the latter when used on our room temperature data, we therefore applied the Maximum Entropy reconstruction method (MEM) to both our LT and RT data sets. We use our program GIFT (Generalized Inverse Fourier Transforms) which makes use of the Cambridge MemSys algorithm.

A projection of the 3D MEM-reconstructed nuclear density distribution along the monoclinic b -axis based on our 15 K data set is shown in Fig.2.

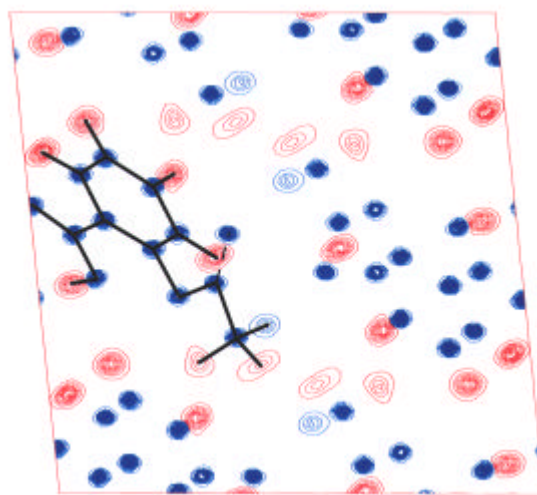


Figure 2. : Experimental nuclear density distribution of partially deuterated aspirin (acetylsalicylic acid) at 15 K projected along the monoclinic b -axis. Red contours pertain to protons, which have a negative scattering length, in contrast to deuterium, carbon and oxygen atoms shown here in blue. The solid line delineates a single aspirin molecule.

Similarly, the two sections shown below in Fig.3a,b are obtained from 3D scattering density reconstructions of the asymmetric unit of the aspirin

crystal by making use of MEM rather than conventional Fourier syntheses. Three dramatic improvements arise : (a) noise suppression, (b) flexibility to use non-uniform prior densities and (c) possibility to tackle partially phased data sets. In the present case, there is no phase problem : the phases of the structure factors are perfectly determined by the well-behaved atoms known from the X-ray study by Wheatley^[5]. The decisive point is that MEM enables us to locate the methyl hydrogen even at room temperature. This is demonstrated in Fig.3a, in which a section of the nuclear density distribution function through the plane of the methyl hydrogens is displayed. Three holes, all negative as they should be since $\langle b_X \rangle < 0$, are clearly seen. Despite being very shallow, the three minima are robustly reconstructed by MEM. No matter how the reconstruction is carried out, with or without non-uniform prior scattering length densities, the three minima are consistently reproduced. No prior knowledge about the hydrogen positions, available in principle from the 15 K data, was used in reconstructing this density distribution. It demonstrates the superior power of MEM over both standard Fourier and least-square techniques and provides clear evidence of the random distribution of the methyl protons and deuterons at 300 K over three geometrically well-defined sites.

In Fig.3b, we finally show the nuclear density distribution at 15 K for the same section as in Fig.3a, again reconstructed by MEM. The clear message of this figure is that the methyl protons and deuteron in aspirin-CH₂D are well-ordered at 15 K. The deuteron obviously occupies with high preference the site associated with the large positive bump whereas the protons occupy almost exclusively the sites related to the negative holes. Truly, the localization of the methyl hydrogens at 15 K is also detectable in standard Fourier maps, albeit with a sizable background noise.

COPING WITH THE ISOTOPIC MIXTURE

Quantitatively, the density distribution displayed in Fig.3b corresponds to the [70%-19%-10%-1%] superposition of the four isotopic species mentioned earlier. This results in **effective** occupancies for both H and D different from unity when an assumed unique species CH₂D is refined using SHELXL97. We find 0.7, 0.7 and 0.53 for the two protons and the deuterium respectively. It can then be deduced that the probability of finding a deuteron from the CH₂D isotopic species at the position evidenced by the positive bump seen in Fig.3b is at least equal to 0.86.

References

- [1] M.Prager, A.Heidemann, Chem.Rev. **97**, 2933 (1997)
 [2] A.Detken *et al*, Z. Naturforsch. **50a**, 95 (1995)
 [3,4] A.Detken, J.Chem.Phys.**108**, 5845,**109**,6791(1998)

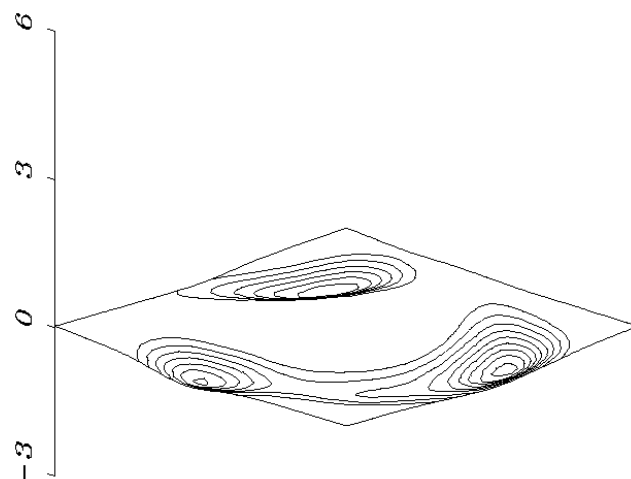


FIG.3a. MEM section of the nuclear density distribution through the methyl hydrogens of aspirin obtained from the 300 K data set. Note the three shallow minima of almost equal depth. They evidence the random occupation of the three methyl hydrogen sites by the protons and deuterons with weights corresponding to the isotopic composition of the crystal (see text). The residual (positive) contribution due to the thermal motion of the carbon atom of the CX₃ group has been removed numerically. (density unit : fm/A³)

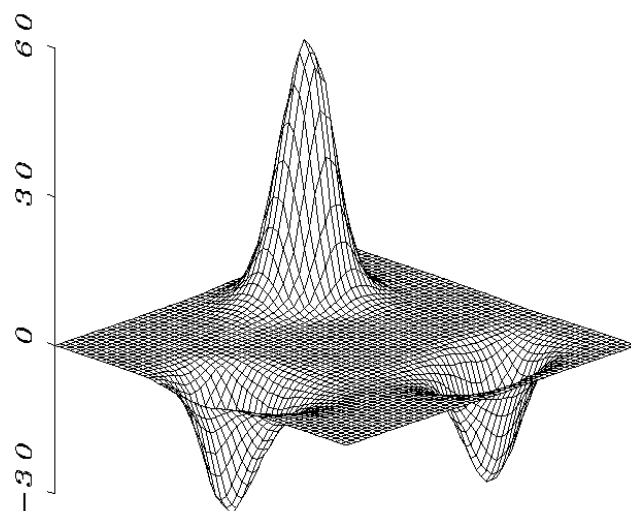


FIG.3b. MEM section of the nuclear density distribution through the methyl hydrogens of aspirin from the 15 K data set. Note that the vertical scale has been changed by a factor of 10 in comparison with that in Fig.3a. The graph demonstrates the orientational ordering at 15 K of the most abundant methyl isotopomer, CH₂D in our crystal sample. The deuteron occupies almost exclusively the site related to the (positive) bump while the protons preferentially occupy the two sites associated with (negative) holes. (density unit : fm/A³)

[5] P.J.Wheatley, J.Chem.Soc.,6036(1964)

CORRELATED SIMULTANEOUS PHASON JUMPS IN AN ICOSAHERAL Al-Mn-Pd QUASICRYSTAL

G. Coddens¹, S. Lyonnard¹, B. Hennion¹ and Y. Calvayrac²

Ph.D. thesis of S. Lyonnard

¹ Laboratoire Léon Brillouin (CEA-CNRS)

² C.E.C.M./C.N.R.S., 15, rue G. Urbain, F-94407 Vitry Cedex, France

The relationships between quasicrystals and other incommensurately modulated crystals (IC) have many interesting theoretical aspects. An obvious link is that both can be derived from a common description based on an embedding in a higher-dimensional superspace that contains a periodic lattice of so-called atomic surfaces. The superspace cut-and-projection algorithm permits a group-theoretical classification of all possible structures. Hyperspace crystallography leads also to the possibility of an attractive analogy within the realm of lattice dynamics based on the introduction of the notion of " phasons " in addition to the usual phonons. Here we stumble onto a first real difficulty. Once we go beyond one-dimensional structures, there are very important differences in the topology of the atomic surfaces between QC and IC. This has been pointed out by many authors, and turns the subject into a really subtle issue. Generally spoken, the atomic surfaces in QC are not continuous^[1].

Based on these studies it was anticipated that "phasons" in QC would not be *collective propagating modes* as in IC but rather atomic jumps^[2], that can be visualized by configuration flips within Penrose-like tiling models. Ensuing experimental studies confirmed this picture. In our current understanding an atomic jump is a stochastic single-particle process. The phonon heat bath produces a fluctuating environment that from time to time will open a low-energy gateway that is prosperous for a jump. Starting from this conceptual image that thrives on disorder, it is hard to imagine an orderly concerted choreography of simultaneous jumps of two or more atoms. This only stresses the fact that, although they are both materialized by a sliding of the cut in superspace, phasons in QC and IC should correspond to very different, antipodal types of dynamics. Nevertheless, this poses a number of small problems in QC. First of all, the (anomalous) temperature dependence of the (quasielastic) neutron-scattering signal that reveals the existence of the hopping does not tally with the description we gave above of the jump process in terms of a phonon bath^[3]. Secondly, tile flips in real, *i.e.* not *mono-atomic* structural models entail in general

several simultaneous atomic jumps. It was therefore inferred that the elementary phason building brick would rather be the atomic jump than the tile flip. In triple-axis neutron-scattering experiments on a large single-grain sample of the icosahedral phase Al-Mn-Pd, we came across some evidence that seems to challenge this common-sense based paradigm. In fact, we found a Q -dependence of the quasielastic signal that we are only able to explain by assuming that two (or more) atoms jump simultaneously keeping their separation vector fixed.

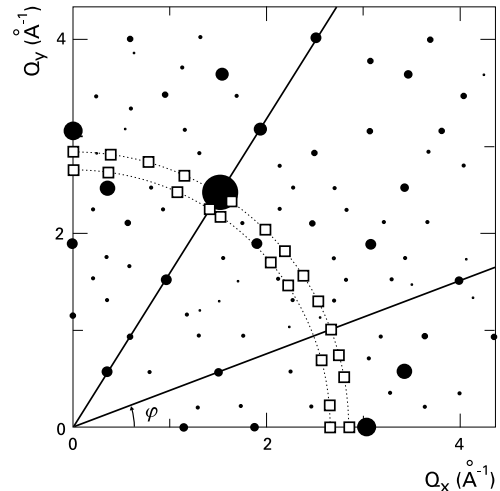


Figure 1. Binary scattering plane. The sizes of the full circles represent the intensity of the Bragg peaks. The locations of the various constant- Q scans have been drawn: they were all made in the $k_f = 1.64 \text{ \AA}^{-1}$ configuration. The angle φ is defined with respect to Q_x .

These experiments were performed with the cold-neutron double-monochromator triple-axis spectrometer 4F2 of the LLB in the fixed $k_f = 1.64 \text{ \AA}^{-1}$ and $k_f = 1.96 \text{ \AA}^{-1}$ configurations. The loci of some of the constant- Q energy scans in the binary scattering plane of the QC are indicated in Fig. 1, which also shows the intensities of the most prominent Bragg peaks. The choice of the binary plane allows to explore all types of symmetry axes (2-, 3-, and 5-fold) of the QC in one set-up. The 3 cm^3 -sized single-grain sample has been grown by the Czochralsky method.

A typical data set is featured in Fig. 2 together with a fit based on a Lorentzian quasielastic signal convoluted with the Gaussian resolution function. Also included in this fit are the elastic peak and a linear incoherent phonon background. The Q -dependence of the quasielastic intensity for $Q = 2.85 \text{ \AA}^{-1}$ is displayed in Fig. 3. It is strongly anisotropic. In a simple single-particle model in the white-noise approximation for atomic jumps between two sites separated by jump vectors \mathbf{d}_j along a m -fold axis of the QC, the quasielastic intensity should follow an (incoherent) structure factor:

$$S_{q.el}(\mathbf{Q}) = \sum_{j=1}^{30/m} \frac{1}{2} [1 - \cos(\mathbf{Q} \cdot \mathbf{d}_j)] \quad (1)$$

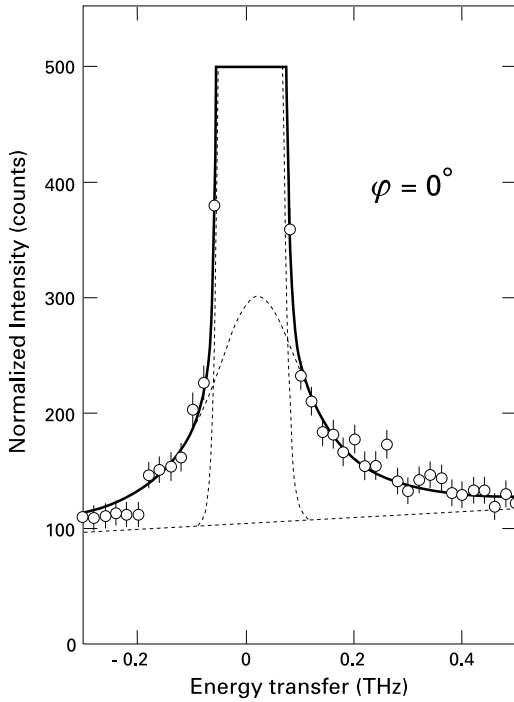


Figure 2. Typical constant- Q scan with fit. The data shown here correspond to $|Q| = 2.85 \text{ \AA}^{-1}$ and $\phi = 0^\circ$.

The sum allows for the fact that for jumps along m -fold directions there are $30/m$ symmetry-related jump vectors. If the direction of the jump is not along a symmetry axis, then the sums will have to extend over the whole icosahedral group. (This corresponds to the case $m=1$). The quasielastic and elastic intensities obey a sum rule such that the incoherent elastic structure factor is obtained from Eq.(1) by changing the sign in front of the cosine term:

$$S_{el}(\mathbf{Q}) = \sum_{j=1}^{30/m} \frac{1}{2} [1 + \cos(\mathbf{Q} \cdot \mathbf{d}_j)] \quad (2)$$

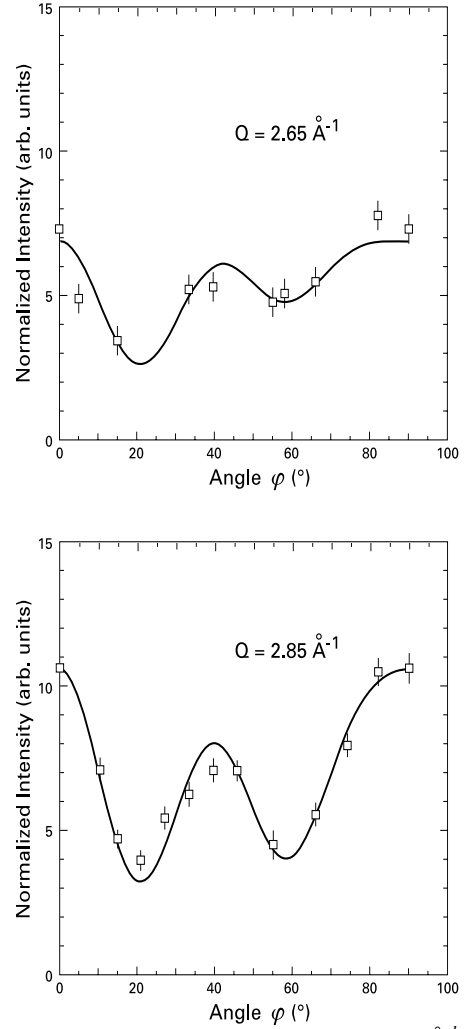


Figure 3. Quasielastic intensities for $|Q| = 2.65 \text{ \AA}^{-1}$ and $|Q| = 2.85 \text{ \AA}^{-1}$. A fit with model function (2) is also shown. (Data collected with a second sample, both in $k_f = 1.64 \text{ \AA}^{-1}$ and $k_f = 1.97 \text{ \AA}^{-1}$ set-ups, bear out the reproducibility of these results).

The quasielastic structure factors embodied by equation (1) all exhibit an isotropic first local maximum in Q , as can be appreciated from Fig.4 for two-fold jumps. This remains true if the direction of the jump is not a symmetry axis. This is quite at variance with the experimentally observed data which do not display such a spherical shell of maximum intensity and on the contrary exhibit their strongest anisotropy at low Q . We should point out that none of the three models ($m=2$; $m=3$; $m=5$) expressed by equation (1) can reproduce the peak/valley-ratios that occur in Figure 3. This means that one needs another type of model. By some serendipity we found out that the data shown in Fig. 3 are perfectly described by equation (2) for $m=3$ and $d = 3.85 \text{ \AA}$. Among the (idle) lines of thought we followed in our attempts to come to grips with this alienating finding, we can mention models as proposed

by Katz and Gratias^[4] and down-sized versions of Elser's escapement model^[4]. The failure to represent our data by such models helped us to realize where the minus signs in front of the cosines in equation (1) come from. Each time an atom jumps from A to an empty site B, the neutron-scattering contrast between A and B is inverted, which amounts to a π -flip of its phase. Therefore, the only way to obtain a plus sign is by designing a model that preserves the contrast despite the occurrence of the jump. This can only be achieved by admitting that two atoms in A and B are jumping simultaneously to A' and B' respectively, whereby the vectors AB and A'B' are equipollent. This leads to expressions of the type

$$S_{q,el}(\mathbf{Q}) = \sum_{j=1}^{30/m} \frac{1}{m} [1 - \cos(\mathbf{Q} \cdot \mathbf{d}_j)] [1 + \cos(\mathbf{Q} \cdot \mathbf{s}_j)], \text{ where}$$

the correlation vector \mathbf{s}_j is analogous to the separation vector AB. The $[1 - \cos(\mathbf{Q} \cdot \mathbf{d}_j)]$ parts are responsible for the first radial maximum, while $[1 + \cos(\mathbf{Q} \cdot \mathbf{s}_j)]$ terms entail a modulation of this local maximum that otherwise would have been an isotropic spherical

shell. In our data we thus have $s_j = 3.85 \text{ \AA}$, while d_j cannot be determined. At once, this means that phasons in QC could nevertheless share some collective character with propagating phason modes that are typical of IC. We must admit that such collective motion clashes with our *Weltanschauung*, as we were strong believers of the heat-bath-driven scenario outlined above. We must signal that the description of the data by Equation (2) breaks down at higher Q -values, where we are unable to explain the observed intensities. At 2.65 and at 2.85 \AA^{-1} we are so lucky to find ourselves in the small- Q limit, where the largest characteristic distance within the dynamics can be discerned in an isolated fashion, free from the obfuscating presence of signals corresponding to shorter length scales. We think that this novel result constitutes an important step towards the elucidation of the physical nature of phasons in QC.

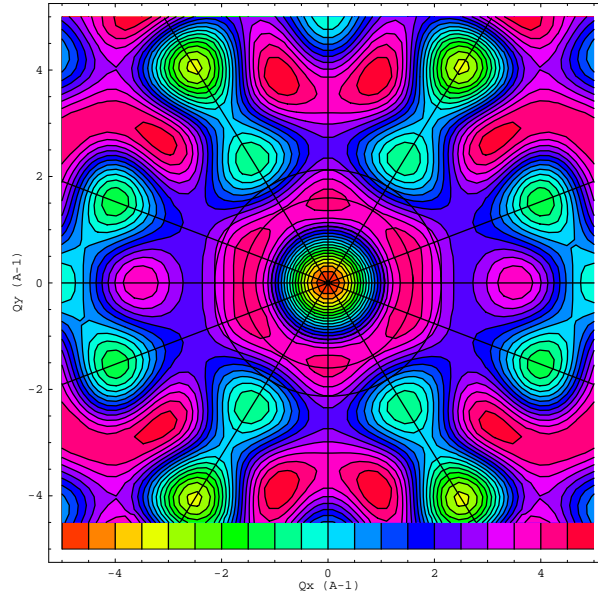


Figure 4. Contour plots for the quasielastic intensity, calculated in a model with two-fold jumps according to Equation (1), $m=2$. Note the almost isotropic first maximum of the intensity around $Q = 1.5 \text{ \AA}^{-1}$. The color code is shown at the bottom of the Figure, going from left to right, e.g. the first color on the left codes numerical values between 0 and 1.

References

- [1] L. S. Levitov, Quasicrystals, The State of the Art, ed. D. P. DiVincenzo and P. J. Steinhardt, Directions in Condensed Matter Physics, Vol. 11, (World Scientific, Singapore, 1991) p. 239.
- [2] G. Coddens, S. Lyonnard, and Y. Calvayrac, Phys. Rev. Lett. **78**, 4209 (1997).
- [3] A. Katz and D. Gratias, J. Non-Cryst. Solids **153 & 154**, 187 (1993)
- [4] V. Elser, Phil. Mag. A **73**, 641 (1996)

DELOCALIZATION INDUCED BY NONLINEARITIES OF ANDERSON LOCALIZED LINEAR MODES IN A RANDOM MEDIUM

G. Kopidakis et S. Aubry

Laboratoire Léon Brillouin (CEA-CNRS)

It is known for many decades that in some very particular models, there are exact solutions which correspond to spatially localized time periodic vibrations ("breathers"). About a decade ago, it has been realized that in classical systems which are both *nonlinear* and *discrete*, such solutions generically exist, that is no special potential forms are required^[1]. In principle, *discrete breathers* may exist in any periodic nonlinear model at any dimension taking into account the whole complexity of real systems, and moreover they are robust against model perturbations.

The existence of these *discrete breathers* is a consequence of the facts that on one hand the vibration frequency of an oscillation in a nonlinear system depends on its amplitude and on the other hand, the linear phonon spectrum is bounded in frequency because the system is discrete. Then, when the frequency and the harmonics of the *discrete breathers* are in the phonon gaps, no energy radiation is possible so that this localized vibration persists forever as an exact solution^[2].

These discrete breather solutions are often linearly stable, that is the small fluctuations do not grow exponentially^[3]. This result implies physically that in the presence of moderate fluctuations, for example the thermal fluctuations at low temperature, their life time will be much longer than those predicted by standard models of relaxation. Thus, it is not by chance that these classical excitations were first found numerically by molecular dynamics in a series of model with increasing complexity. It has been found that they appear spontaneously in some conditions out of thermodynamical equilibrium, for example under the effect of a thermal shock.

Otherwise, it is well-known since the pioneering works of Anderson^[4] in the fifties that the linear modes of a random medium may be spatially localized. In that case, disorder detunes in some sense, all the resonances which would exist between the vibrations which are localized at different spots of the system, which forbids any propagation of vibrational energy over long distance. This theory was also very successful for explaining the insulating properties of some random metallic alloys (e.g. $\text{Nb}_{1-x}\text{V}_x$) or of semiconductors.

Thus, it seems natural to expect that when both nonlinearity and disorder are involved in the same system, the localization effect of vibrational excitations will be enhanced. Indeed, since the

localized phonons of the linearized system cannot propagate any energy, the energy of a localized excitation cannot be dissipated through the system even if its frequency belongs to the phonon spectrum, and then it should persist indefinitely.

Actually, the phenomenon is more complex than one could believe, because nonlinearities play a "double-game". On one hand, disorder and nonlinearity may cooperate for generating discrete breathers which then are exact well localized solutions. On the other hand, for other time periodic solutions, disorder and nonlinearity conflict. Nonlinearity may restore resonances between sites which are far apart, and then generate unexpectedly spatially extended modes which can propagate some flux of energy.

We analysed in detail this effect on a very simple model which consists into a one dimensional chain of quartic oscillators coupled by harmonic springs. For that purpose, we improved and developed several original and reliable techniques for calculating very accurately both localized and the extended modes in large systems (which could become possibly very complex such as macromolecules)^[5].

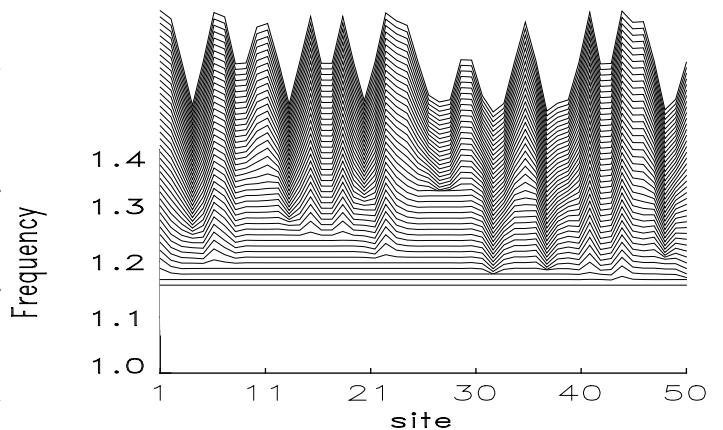


Figure: Profile of the initial positions for an exact time periodic and time reversible solution at different amplitudes which is initially a localized linear mode (on site 44) at zero amplitude for the hamiltonian

$$H = \sum_i \left(\frac{1}{2} u_i^2 + \frac{1}{2} \omega_{i,0}^2 u_i^2 + \frac{1}{4} u_i^4 + \frac{C}{2} (u_{i+1} - u_i)^2 \right)$$

$\omega_{i,0}^2$ is uniformly random in the interval $[0.5, 1.5]$ in a finite system with 50 sites. Each line corresponds to a given frequency and amplitude of the initial localized mode, increasing from lower to upper line.

With these methods, we can follow continuously the evolution of a time periodic solution as a function of its frequency (or amplitude of the initially localized linear mode) when model nonlinearities are present. The figure shows an example of such an evolution, for a solution which is initially a localized linear mode (on site 44) at amplitude zero. It is first observed as expected that the frequency of this solution increases as a function of its amplitude because of nonlinearities. However, it is clear that extra oscillations grow at spots which are possibly very far from the initial excited spot. These new oscillations start to develop precisely at the location of linear localized modes the frequency of which becomes resonant with those of the solution. Thus for an infinite system with a dense phonon spectrum, an infinite number of resonant frequencies are crossed for any small variation of the amplitude (or equivalently the frequency). As a result, the initial solution immediately delocalizes with small peaks at the corresponding resonant spots. However, while the solution is still small, the distribution of these spots is sparse which only allows a tiny transport of energy which nevertheless is not zero. When the amplitude becomes larger, the amount of energy which can be propagated by such a solution increases and becomes comparable to those of a nonlinear phonon in a similar but non random system.

We are also able to calculate accurately localized discrete breathers in the same systems, but with other methods^[6]. Our numerical results agree with a theorem of Albanèse and Fröhlich^[7] proven on a similar model, which states that there is a "quasicontinuum" of solutions with frequency in a fat

Cantor set (that is with a finite measure). The gaps in this Cantor set are the consequences of the resonances with the linear modes which destroy the localized character of the solution and must be avoided. Since there are infinitely many possible resonances, there are infinitely many gaps but however the widths of these gaps, decay as an exponential function of the distance between the breather to the resonant localized linear mode. Because of that, the frequency Cantor set is not void and keeps a finite measure.

These original results open new perspectives for a better understanding of glasses and other amorphous materials, which is non phenomenologic. On one hand, we predict that nonlinearities even very small imply that a nonvanishing residual thermal conductivity persists at low temperature but drops very fast to zero at zero K. On the other hand, a substantial part of the vibrational energy of the system may be spontaneously trapped as localized discrete breathers for very long times, which become macroscopic at very low temperature. This effect, which can be easily checked by molecular dynamics test, provides an alternative interpretation for the slow relaxation processes in glasses usually described by the old phenomenological two-level model of Anderson. Our interpretation only requires some nonlinearity in the model, which may be very weak and thus which should always exist. On contrary, the Anderson model requires the existence of double wells which actually has never been confirmed by direct structural observations (at least in most materials).

References

- [1] A.J. Sievers and S. Takeno, *Phys.Rev.Letts.* **61** (1988) 970.
- [2] R.S. MacKay and S.Aubry, *Nonlinearity* **7** (1994) 1623–1643.
- [3] S. Aubry, *Physica* **103D** (1997) 201–250.
- [4] P.W. Anderson, *Phys. Rev.***109** (1958) 1492.
- [5] G. Kopidakis and S. Aubry, *Intraband Discrete Breathers in Disordered Nonlinear Systems . I: Delocalization* , *Physica D* **130** (1999) 155-186.
- [6] G. Kopidakis and S. Aubry, *Intraband Discrete Breathers in Disordered Nonlinear Systems II: Localization*, submitted to *Physica D*.
- [7] C. Albanèse and J. Fröhlich, *Commun.Math.Phys.* **138** (1991) 193-205

DISORDERED SYSTEMS AND MATERIALS SCIENCE

The Laboratoire Léon Brillouin is progressively putting in place a pole of research in the field of materials science, in strong relationship with external laboratories. Indeed, it is the role of a national research infrastructure such as LLB to train the scientists working in french applied research and industrial laboratories, and to give them access to its characterization facilities.

The research at LLB in materials science covers two main domains : soft matter and metallurgy (in the broad sense, i.e. including ceramics, metal matrix composites, etc...). The results concerning soft matter are included in the chapter "Chemical Physics and Biology" of this report.

In the domain of metallurgy and ceramics, the properties of technological interest depend on the defect properties and on the defect structure of the material at the atomic (vacancies, impurities,...) or at the mesoscopic (dislocations, porosities,...) level. This is why materials science requires a fundamental corpus of knowledge on defects and disorder. In particular, the fundamental study of atomically disordered systems allows to develop theoretical models, and to validate numerical simulations (Monte-Carlo, molecular dynamics, etc...) which are then applied to understand "real" materials. Particularly important is the extrapolation of their properties at long time in operating conditions, and the prediction of their behaviour under thermal or irradiation-induced ageing.

At the interface between the study of disordered systems and materials science is physical metallurgy, working on model systems (e.g. phase transformations in binary alloys, etc...).

1. DISORDERED SYSTEMS

1.1. Introduction

The scientific activity of LLB in the field of disordered systems is mainly concentrated on the study of local atomic arrangements in topologically or chemically disordered solids or liquids, by elastic diffuse neutron scattering. Two instruments are entirely devoted to these studies :

- the 7C2 diffractometer, installed on the "hot" source, with short wavelength (generally $\sim 0.7 \text{ \AA}$) neutrons, and equipped with a 640 cell position sensitive linear multidetector, for liquid and amorphous systems;
- the G4.4 diffractometer, installed on a "cold" neutron guide, managed by ONERA and CEA/LSI, with time-of-flight analysis, devoted to the "in situ" high temperature study of local order in single crystals.

In the case of systems presenting a tendency towards phase separation, complementary studies by Small-Angle Neutron Scattering (SANS) are necessary.

Some studies of dynamics, mainly on glass transition, are also performed at LLB by external users, in particular with the time-of-flight inelastic spectrometer MIBEMOL.

1.2. Metallic alloys : local order, kinetics

This thematics is mainly developed at LLB by the team of LEM (ONERA-CNRS, R. Caudron et al).

A systematic "in situ" high temperature study of elastic diffuse neutron scattering in a series of f.c.c. binary transition metal alloys, performed on G4.4, has allowed a detailed understanding of their chemical order-disorder properties, and a fruitful dialogue with the statistical physics theory of alloys. This 10-years programme was concluded in 1997 by the PhD thesis of D. Le Bolloch on $\text{Pt}_{1-x}\text{V}_x$ alloys. In the frame of this work, it was in particular shown that, although $\text{Pt}_{0.75}\text{V}_{0.25}$ long-range orders below $T_c = 500^\circ\text{C}$ with superstructure diffraction peaks at $(1 \ 1/2 \ 0)$, the maxima of the diffuse intensity above T_c are at the (100) positions. Moreover, the diffuse intensity for another concentration, $x=1/9$, displays a splitting around (100) with maxima at incommensurate positions. It was found that, despite this strong concentration dependence of the diffuse intensity shape, the Effective Pair Interactions deduced of the experimental data by a reverse Monte-Carlo method, are nearly concentration independent, in contradiction with *ab initio* theories. A high temperature expansion of the mean-field theory was developed, and explained successfully the origin of this splitting, and its dependence with concentration and temperature.

This work is now being extended to kinetic phenomena (PhD thesis of X. Flament). Mean-field theory suggests for Pd_3V two different spinodal (instability) temperatures for the two ordering wave-vectors, e.g. (100) and $(1\ 1/2\ 0)$. Monte-Carlo simulations and preliminary synchrotron X-ray experiments are in agreement with these predictions. Several studies of local order and concentration fluctuations in various crystalline (Ni_2Cr , Ni-based superalloys) or amorphous (Fe_2Zr , $\text{Ti}_{84}\text{Si}_{16}$, selenite glasses) systems have also been performed by other groups (LSI/Palaiseau, CEMES/Toulouse, LLB, MPI/Stuttgart, Bulgarian Academy of Sciences (Sofia)).

1.3. Local order in quasi-crystals and their liquid precursors

If the indexation of diffraction peaks in quasi-crystals can be made with success, the problem of positions of specific types of atoms is far from being resolved. Is there or not chemical disorder? This has an important impact on our understanding of the origin of the stability of these materials at room temperature: i.e. are they stabilized by defects when cooling from high temperature? If such a disorder exists, it should manifest itself by an elastic diffuse scattering in the neutron or X-ray diffraction spectra. Scarce information existing up to now led to conflicting results. The advantage of neutrons over X-rays is the easiness to obtain absolute cross-sections and the possibility to separate experimentally the inelastic thermal diffuse scattering due to phonons. The difficulty with neutrons is their sensitivity to hydrogen contamination, and the lower q-resolution to well separate the Bragg peaks. We have therefore undertaken a study at LLB on this subject (PhD thesis of N. Schramchenko) in collaboration with LEM (ONERA-CNRS) and CECM-Vitry, where the samples are made.

First experiments performed on G4.4 at LLB on a single grain of Al-Pd-Mn, allowed to observe at room temperature a diffuse scattering far from the Bragg peaks. Normalized, it is in agreement with the theoretical disorder term from an approximant phase ξ' of similar composition. The data treatment is delicate, because one has to correct for a very large number of very small Bragg peaks.

The preliminary work presented in the previous LLB report (1995-96) on liquid precursors of Al-Pd-Mn, has been extended and completed in the frame of a multi-laboratory collaboration (LPS-Orsay, LTPCM-Grenoble, LLB-Saclay, PhD thesis of V. Simonet, Orsay, 1998, see highlight). The set of diffuse neutron scattering measurements performed at LLB on 7C2, and subsequently extended at ILL on D4B, confirmed the presence of a local order reminiscent from the solid, and could be fitted by a cluster-based (Al_{12}Mn icosahedron) numerical simulation.

Polarized neutron scattering experiments performed at D7, ILL, have confirmed the appearance of a magnetic signal in the liquid state, deduced previously from coupled 7C2 neutron scattering and magnetic susceptibility measurements.

1.4. II-VI and IV-VI liquid compounds

The classical semi-conductors of group IV (Si, Ge) as well as the III-V compounds (GaAs, GaSb) undergo at the melting point a semi-conductor \rightarrow metal transition, associated to a change of coordination number ($4 \rightarrow 6$). On the contrary, some II-VI compounds (CdTe , ZnTe) remain semi-conducting and tetrahedrally coordinated in the liquid state. To understand the origin of this behaviour, we have undertaken, in collaboration with the University of Liège, an experimental and theoretical study of $\text{Cd}_x\text{Te}_{1-x}$ in all the concentration range (PhD thesis of G. Prigent).

Monte-Carlo simulations in the frame of a tight binding model, have shown that the local order in these systems is mainly governed by the competition between the $s \rightarrow p$ promotion and the gain in binding energy (resonance between sp^3 orbitals). The charge transfer plays only a small role. CdTe remains semi-conductor, because the s level of Cd and the p level of Te are close in energy.

A double metal \leftrightarrow semi-conductor \leftrightarrow metal transition versus composition in the liquid state was observed experimentally from electrical measurements performed at the University of Metz. A fine analysis of neutron scattering (obtained on 7C2) and EXAFS data suggests a coexistence of metal Cd-rich and semi-conducting CdTe-rich domains of nanometric size for $x > 0.5$.

On the same subject, the team of University de Liège observed on 7C2 an astonishing re-entrant Peierls distortion in several IV-VI compounds: SnS , SnSe , GeSe and GeTe (PhD thesis of D. Raty): the Peierls distortion, observed at low temperature and which disappears when heating in the crystalline state, is recovered in the liquid state.

1.5. Fundamental structural studies of simple fluids

Very precise Small-Angle Neutron Scattering experiments, performed on noble gas (e.g. krypton) by an Italian group of the University of Firenze (R. Magli et al.), succeeded to show, for the first time, the role of irreducible three-body forces in the interatomic potential. Density fluctuations in these fluids have been measured in function of temperature and pressure and near the critical point.

1.6. Critical and supercritical fluids

Water is always an important and "hot" topic and gave rise to many studies where the structure and H-bond dynamics have been explored in various states, including metastable states under pressure and water in confined geometries (see the chapter "Chemical Physics and Biology" of this report). In particular, recent modelisation of LLB neutron diffraction experiments suggest strongly that two forms of liquid water may coexist at very low temperatures, possibly shedding light on why water has such unusual properties compared to other liquids. These structural and dynamic studies have been extended to water in supercritical state.

Supercritical water presents physical and chemical properties, e.g. viscosity and dielectric constant, which differ greatly from those of the liquid water. In particular, it is possible to dissolve in supercritical water organic or mineral substances, which are hardly soluble in normal liquid water. This is of great interest, in particular for depollution applications.

In view of developing these techniques, a "Club of Supercritical Fluids applied to Nuclear Industry" has been created in 1994. M.C. Bellissent-Funel chairs this group since 1998. It was decided to study at LLB by neutron scattering the local structure and dynamics of critical and supercritical fluids (water, CO₂, aqueous solutions), in order to validate Molecular Dynamics simulations (LPTL, University of Paris VI).

The partial pair correlation functions $g_{OD}(r)$, $g_{DD}(r)$ and $g_{OO}(r)$ in supercritical heavy water (T=380°C, pressure : 600 bar, density : 0.73 g/cm³) were determined by a reverse Monte-Carlo method from the 7C2 neutron data obtained on D₂O and two isotopic H₂O/D₂O mixtures, and from X-ray data (which gives the O-O partial structure factor). The structure of supercritical water is very different from that of water in ambient conditions. Nevertheless, modelisation of these data by Molecular Dynamics simulations show clearly that in dense supercritical water, although the tetrahedral arrangement of water molecules is lost, some hydrogen bonding is still present, contrary to previous statements of other authors.

SANS study of supercritical heavy water showed a large increase at small q (0.07 to 0.36 Å⁻¹) due to the divergence of density fluctuations at the critical point, and allowed the first measurement of the critical correlation length ξ_0 for water; the value, 1.36 ± 0.06 Å, is in fair agreement with theoretical predictions.

A first study of the (picosecond range) dynamics of supercritical H₂O by incoherent inelastic and quasielastic neutron scattering, performed by LLB researchers on IN6 at ILL, allowed to determine the evolution of D (translational diffusion coefficient of the water molecules), L (jump distance) and τ_0 (residence time) as a function of the density of the medium. D and L increase strongly as the density decreases. τ_0 is ten times shorter than that measured in liquid water at room temperature.

Simple fluids (CO₂, SO₂) or fluid mixtures (H₂O-benzene, CS₂-benzene, CS₂-C₆F₆,) are also the object of structural studies in the critical and supercritical states (LASIR, Lille, LPCM, Bordeaux, Universities of Lisboa and of Roma III).

1.7. Phase separation

Several studies performed by external laboratories approached the problem of phase separation in solids and liquids.

Isotope ordering of hydrogen and deuterium, predicted theoretically by Prigogine in 1954, was proved for the first time at LLB by an international team led by M. Bienfait (CRMC2, Marseille) (see highlight) : a clustering process of isotopic hydrogen mixtures H₂-D₂, adsorbed in order to form one monolayer on graphite (0001), was observed from 8 K downwards, at and above monolayer completion, by SANS and neutron diffraction measurements. This trend towards phase separation depends strongly on coverage and isotopic concentration.

A remarkable closed-loop miscibility gap has been found in the liquid tellurium-sulfur (Te_{1-x}S_x) binary diagram around $x = 0.4$, which is a unique observation in an inorganic system. Neutron diffraction measurements performed on 7C2, showed that this is directly related to a sudden change of the tellurium coordination at high temperature, from nearly 3 for $x < 0.4$ (as in pure Te), to around 2 for $x > 0.4$ (PhD thesis of M.V. Coulet, CTM Marseille).

A systematic study by neutron scattering of the local order of several liquid alloys (Mn-Sb, Mn-Ge, Ga-Pb), presenting a miscibility gap at lower temperature, has been undertaken on 7C2 by a team of the University of Metz (J.F. Gasser et al). It allowed to test interatomic potentials obtained by electronic structure calculations, and to explain the anomalous behaviour of electronic conductivity and thermal expansion in these alloys.

The understanding of the role of an uniaxial elastic strain on the phase separation in binary metallic alloys presenting a large size effect between the two atomic constituents, is object of a detailed small-angle neutron scattering work by the austrian team of University of Vienna associated to LLB (O. Blaschko[†], M. Prem). In particular, they could show that such strain applied during thermal treatment induces an anisotropy in the shape of the precipitates formed in CuRh, which can be explained by a misfit compensation mechanism.

1.8. Dynamics. Glass Transition

The study of relaxation processes in liquids near the glass transition has been the object of several studies performed by C. Alba-Simionesco (CPMA, Orsay). Combination of quasi-elastic spectra obtained in a wide frequency range show the existence of two relaxation processes. Several studies were performed under pressure, in order to separate the respective roles of volume reduction due either to pressure increase or to temperature decrease in the structural arrest near the glass transition.

Several other studies of the dynamics of disordered systems were performed by external laboratories at the LLB, mostly on the time-of-flight inelastic instrument MIBEMOL. These include :

- the first study of the vibrational density of states of carbon nanotubes (University of Montpellier);
- measurement of the mobility of HD molecules adsorbed on incommensurate Kr plated graphite, which confirmed the existence of a reentrant fluid phase, squeezed in between the commensurate and incommensurate phases (collaboration between Universities of Mainz, Germany, and of Marseille, France);
- study of the vibrational dynamics in plastic crystals (where a periodic lattice coexists with translational disorder) (Universities of Augsburg and Munich, Germany);
- dynamical behaviour of molecules confined in the pores of SiO₂, which allowed to distinguish non-rotating molecules adsorbed on the pore walls, and rotating molecules within the pores (University of Kiel, Germany);
- influence of the cross-linking ratio on the dynamics of the glass transition (University of Montpellier).

1.9. Evolution and Perspectives

The specificity of neutron-matter interaction leads to develop its use on samples held in extreme conditions (e.g. high temperatures, high pressures,...), as exemplified by the LLB studies on supercritical fluids. In this aim, an important upgrade of the 7C2 diffractometer for liquids is planned, in collaboration with several external french laboratories. It consists in :

- developing high temperature devices, in particular contactless heating methods : gas levitation technique for insulating liquids, and electromagnetic levitation for conducting liquids;
- increasing the counting rate (new more efficient multidetectors, improved neutron optics), in particular to improve the signal-to-noise ratio in the case of the small samples required by the above techniques.

This instrument upgrade will allow new applications in several important fields :

- materials processing : local structure of the liquid formers of metallic or oxide materials prepared by solidification;
- geophysics : "in situ" study of the high density forms of silicate glasses.

2. MATERIALS SCIENCE

2.1. Introduction

Materials Science aims to understand the properties of solid systems in their full complexity, and to optimize these properties by acting on the composition, atomic structure, and microstructure. This is a different approach to that of condensed matter physics, which focuses on model systems to study a given property or phenomenon. Obviously, materials science has an immediate bearing on industry and applications.

Neutrons are an ideal probe for studying the structure of materials, particularly because of their low absorption, which makes it possible to work on centimetre-thick parts, and the relative ease with which experiments can be carried out under complex or extreme conditions, such as high temperatures or applied stress.

Research currently under way at LLB includes studies in :

- Residual stress evaluation in complex systems,
- Evolution of textures with thermal or mechanical processing,
- Structure heterogeneity, precipitation, ageing of materials,
- Properties of coated glasses and gratings.

Studies on industrial materials are usefully complemented by studies of model materials that are easier to interpret. Methods for analysing the reciprocal lattice (neutron and X-ray scattering) and the real lattice (electron microscopy, atomic probe, near-field microscopy) are complementary, and always used together, especially for complex industrial materials.

2.2. Residual stresses

In the last decade, the use of neutron diffraction for stress analysis in components of technological interest has strongly developed. In fact, the unique properties of neutrons, in particular their high penetration depth, mean that neutron diffraction is the only non-destructive technique which enables the stress field evaluation within a defined volume in a bulk sample. Diffraction of hard X-rays, such as those available at the ESRF (Grenoble), open new possibilities, but also present technical difficulties and limitations (e.g. shape of the gauge volume).

In the last years, a new diffractometer entirely dedicated to stress analysis, DIANE (G5.2), was built up at the LLB in Saclay, in collaboration with the Italian INFM (Istituto Nazionale di Fisica della Materia). It has been designed in order to meet engineering requirements : good spatial resolution (of the order of 1 mm^3), accurate positioning of the specimen in three orthogonal directions, an adequate space for manipulation of heavy and cumbersome samples on the diffractometer, good instrumental resolution (high monochromator take-off angle), and fast data collection (Position Sensitive Detector).

A widely spread activity has been developed in the last two years at the LLB in the field of residual stress analysis, partly in collaboration with the University of Reims-Champagne-Ardenne (Prof. A. Lodini).

The main fundamental studies performed at the LLB in the field of residual stress analysis are summarized below :

Microstrain evaluation. Measurements of the diffraction line profile on DIANE at LLB allowed for the first time to characterize non-destructively the plastic region (i.e. its size and the maximum strain) at the tip of a crack in a stainless steel fatigue test specimen (PhD thesis of K. Hirschi, see highlight).

Residual stresses in metal matrix composites (MMC). We have studied and modeled the effect of plasticity on the thermally induced residual stresses in an Al matrix MMC reinforced with SiC particles (PhD thesis of R. Levy-Tubiana, in collaboration with M. Fitzpatrick, The Open University, U.K., and A. Baczmanski, University of Krakow, Poland).

Strains in geological materials. Elastic residual strains, required by the natural continuity of solids, originate in the rocks during the fold of the upper crust. Neutron diffraction is the only technique which allows to determine the internal strain tensor in polycrystalline rocks. For the first time, residual elastic strains have been determined in polycrystalline samples of geological interest (quartzites). The components of the strain tensor, determined on DIANE at LLB, are weak in absolute value, but significant. These residual elastic strains were found to disappear in recrystallized samples. An hydrostatic compressive state was also found in one sample, and is probably due to the presence of secondary phase inclusions (J.C. Guezou et al, University of Cergy-Pontoise).

Parallel to this fundamental activity, great effort is made to **open the neutron diffraction technique for stress analysis to industrial users**. To this end, we are involved in several international programs and industrial collaborations.

a) **VAMAS TWA 20** is an international programme, the objective of which is to establish accurate and reliable procedures for making reproducible and standardized non-destructive neutron diffraction residual stress measurements. It includes representatives from industry, universities and 13 neutron sources, in Canada, Europe, Japan and the USA. Different types of samples, in which residual stresses have been introduced by various procedures, are examined by the participating neutron sources, according to a common protocol. In the last two years, an aluminium alloy shrink-fit and plug has been examined for "round robin" inter-laboratory comparison. The results obtained on DIANE allow to classify this instrument as one of the most performants.

b) **TRAINSS** is a 4-years (1998-2001) european network, of the Brite-Euram III programme, aimed to train european industrial laboratories to the use of neutron diffraction for determination of internal stresses. The TRAINSS network groups 4 neutron sources (among which LLB), 6 university laboratories (among which ENSAM, Paris), and 10 industrials which bring specific problems (among which SNCF and PSA-Peugeot-Citroen). Two weeks per year of neutron beam time are devoted to this programme on the DIANE diffractometer. SNCF is interested in the influence of residual stresses on the propagation of cracks in the wheel axles of railway engines and carriages. The PSA problem is the determination of residual stresses in the discs of motor-car brakes.

c) Two other contracts with french industry have been initiated recently : with SNECMA (residual stresses in a Ti matrix-SiC fiber MMC, for compressor discs and blades of airplane motors), and with Aerospatiale (residual stresses in a welding between aluminium alloy plates for Airbus).

EDF financed a PhD thesis, submitted in 1997 (E. Pluyette), which allowed to realize a numerical modelization of the DIANE diffractometer, aiming to improve the measurement of residual stresses across interfaces (e.g. a bimetallic welding).

d) Various studies of residual stresses in technological components were made by external laboratories, in particular :

- the stress profile was measured along the throat of automotive gears, which had undergone a surface treatment (R. Magli et al, University of Firenze and LLB);
- the stress gradient could be resolved in a ceramic (AlN) plate as thin as 0.6 mm, which is well below what is commonly achieved in neutron stress analysis, and proves the excellent performance of DIANE (L. Pintschovius, Kf Karlsruhe);
- residual strains and stresses in MMC's, weldings and brazings for nuclear fusion technology (NET / ITER programme), coated materials, etc... (University of Reims, University of Ancona, ENEA (Italy), The Open University (UK)).

2.3. Textures

Crystallographic texture (preferred orientation of grains) is one of the parameters describing the microstructure of a polycrystalline material, which controls partly its mechanical properties. In metallic alloys, the texture appears during the solidification, then transforms during rolling or wire drawing, and ultimately during recrystallization. The understanding and the mastering of its texture during thermomechanical and/or annealing treatments are necessary in order to optimize the mechanical behaviour of a material.

Neutron diffraction is the best technique for obtaining precise texture of bulk specimens ($\sim 1 \text{ cm}^3$), under the form of a distribution function of crystalline orientations. Its use is in particular necessary in the case of coarse-grained materials (= a few mm^3), where conventional X-rays are inapplicable.

LLB has a diffractometer specially devoted to the determination of crystallographic textures : 6T1, equipped with an Euler cradle. The study of textures at LLB is made in strong collaboration with the Laboratoire de Métallurgie Structurale (LMS) of the Orsay University (T. Baudin, R. Penelle), where are performed complementary studies by EBSD (Electron BackScattered Diffraction) and numerical simulations of the evolution of the microstructure.

An important number of experiments was made to determine the texture in two-phase materials of technological interest, and to study the relation between texture components of each phase. Let us mention two of them :

- In the two-phase Ti-based high strength alloy β CEZ, developed for use in the compressor of jet engines, it was found that the sharpness of the crystallographic texture (but not its components which follow the usual orientation relationship) is strongly dependent on the morphology of the α -phase. This has important implications on the optimization of the thermomechanical treatments (LLB and University of Orsay).
- In a welded joint of 316L stainless steel containing coarse grains of f.c.c. austenite and a very small content (5%) of b.c.c. δ ferrite, the neutron diffraction analysis showed that on a macroscopic scale, both phases are in a cube-cube relationship, with a fiber texture [010] along the solidification direction. This unusual result shows that solidification has been duplex itself, with a solidification front and the growth of both ferrite and austenite primary phases; it is introduced in the numerical codes predicting the mechanical behaviour of the welding (J.L. Béchade et al, SRMA, Saclay, and Ecole des Mines de Paris).

Furthermore, the recrystallization process has been more specially investigated in different materials :

- The texture of Ti-Al based intermetallic alloys, considered for aerospace industry, influences their ductility and creep behaviour. A study of the dependence of texture on forging and (dynamic and static) recrystallization conditions has been undertaken, in order to suppress or reduce this texture and optimize the mechanical properties of the material (PhD thesis of Y. Hersart, University of Orsay).
- In a $\text{Fe}_{0.5}\text{Ni}_{0.5}$ alloy, neutron diffraction, associated to Transmission Electron Microscopy and EBSD experiments, allowed to follow the growth kinetics of the cube texture (which is interesting for magnetic applications) to the detriment of the deformation ones, after cold rolling and annealing. This study allows to improve the simulations of the recrystallization (LLB and LMS).

Since several years, a part of the texture activity at LLB is dedicated to the study of geological materials. In particular, neutron diffraction coupled to microstructural observations allowed, in quartzites coming from the betic zone of Spain, to identify two main components, $\{1-210\} \langle 10-10 \rangle$ and $\{1-101\} \langle 1-120 \rangle$, which have been associated respectively to the deformation and the recrystallization (University of Cergy-Pontoise).

2.4. Phase analysis

A research programme has been undertaken since 1997 at LLB by the Direction of Nuclear Reactors in CEA, Saclay, to characterize and study hydrogen-containing zircaloy-4 alloys, used as fuel cladding in Pressurized Water Nuclear Reactors (PWR) (see highlight). Because of its low thermal neutron absorption and incoherent cross-sections, Zr is a very favorable material for such studies. In a single experiment, it was possible to obtain the total

hydrogen content with high sensitivity and precision (< 20 ppm weight), the hydrogen content in hydride form, the crystallographic characterization of precipitates (hydrides and Laves phases), and to follow "in situ" up to 500°C the influence of H on the thermal expansion of zircaloy-4 and the thermal dissolution of hydrides. This last information allowed to determine the solubility of H in the material between room temperature and 500°C .

2.5. Nanopowders and sintering

The last two years have seen an important development of studies in this domain by neutron scattering (SANS and diffraction). Among these, two correspond to a more systematic and fundamental approach.

- The austrian group at LLB was one of the first to undertake an understanding of the sintering mechanisms. Their recent results concern nanocrystalline Y_2O_3 powders : the behaviour, summarized as variation of the total surface of pores (deduced from the Porod law in SANS) versus the volume fraction of porosity, was found very different from that of conventional micrometre-sized powders. Two successive stages are distinguished; in the first one, the surface of irregularly-shaped pores is reduced by surface diffusion, at nearly constant porosity; the second one corresponds to a reduction of total pore volume by transport of vacancies towards the external surface.

- Since 1997, a research programme was undertaken at LLB by the Section de Recherches en Métallurgie Physique of CEA/Saclay, on reactive milling and sintering. The first study concerns the composite material Ag-SnO₂, which is developed for electrical connections applications (PhD thesis of N. Lorrain). Neutron scattering allowed to follow separately the thermal evolution of different types of porosities (using wetting techniques), and the size of Ag and SnO₂ particles during the sintering process. This evolution could be correlated with the formation of small cavities filled with gas, and their subsequent connection in channels at higher temperature.

2.6. Ageing of materials

Nanometer-sized precipitates dispersed in ductile metallic alloys, generally increase the hardness of the materials. A major drawback is the reduction of fracture toughness : this embrittlement, which may appear during ageing in operating conditions, raises safety problems in nuclear industry.

In this context, within the last decade, the thermal or irradiation-induced ageing of materials of nuclear interest has been the object of several studies at LLB by SANS : in many cases, this is the technique which displays the largest scattering contrast between matrix and precipitates; moreover, in the case of (ferromagnetic) steels, supplementary information is obtained from the magnetic interaction with the neutron. We shall mention here the main results obtained in the last two years by CEA and by the german team of Forschungszentrum Rossendorf.

The CEA programme in this field is the object of a collaboration between LLB, the Service de Recherches Métallurgiques Appliquées (SRMA, CEA / Saclay) and the Laboratoire des Solides Irradiés (LSI, CEA / Ecole Polytechnique, Palaiseau).

A new research programme started in 1996 on the ageing of low activation martensitic steels for the fusion reactors (ITER programme). SANS measurements performed at LLB under magnetic field on thermally-aged samples, allowed to characterize the precipitation of carbides (undetected by Transmission Electron Microscopy), and showed a direct correlation between the observed number density of precipitates and the hardening of the material. Furthermore, the stability under neutron irradiation was found to be strongly dependent of the chromium content in the alloy, some of the samples showing an accelerated coherent phase separation of the b.c.c. ferrite into an iron-rich (α phase) and a chromium-rich (α' phase) components (see highlight).

Two austeno-ferritic samples taken on valves situated on the primary circuit of the PWR nuclear reactor of CHOOZ-A, which operated 140 000 hours respectively at 301°C (hot pipe) and 266°C (cold pipe), were studied by SANS, and showed α - α' phase separation in the ferrite responsible of a strong embrittlement; surprisingly, the cold pipe showed a larger phase separation than extrapolated from laboratory ageing tests (= 30 000 hours).

Neutron-irradiated surveillance specimens of Russian VVER-440 type nuclear power plants were investigated and carefully analyzed by SANS at LLB by a German team (Forschungszentrum Rossendorf). The volume fraction of the nanoscaled defects was shown to increase with the neutron fluence, whereas their size distribution (1 to 4 nm) does not change. After post-irradiation annealing, one observes both coarsening and dissolution of the nanoscaled defects. By comparing the ratio of magnetic and nuclear scattering with ASAXS (Anomalous Small-Angle X-ray Scattering) and APFIM (Atomic Probe - Field Ion Microscopy) results, it could be shown that the irradiation-induced defects are clusters consisting of vacancies and different alloying atoms like Mn, Cu and Si in the case of commercial heats, but mainly vanadium carbide in the case of laboratory heats.

2.7. Thin films and multilayers

The major use of neutron reflectivity is in the field of magnetism (with polarized neutrons) and in soft matter. For non-magnetic and non-organic materials, X-ray reflectometry is the usual technique. Nevertheless, neutrons are

useful in the case of favorable contrast : e.g. multilayers or thin films containing titanium, which has a negative scattering length.

This is the case of $\text{SiO}_y / \text{TiO}_x$ bilayers deposited on glass to optimize solar light transmission properties. A study performed with Stazione Sperimentale del Vetro (Murano, Italy) allowed to obtain much more information (i.e. thickness, roughness, composition) than spectrophotometry, and therefore to calculate the light transmission with improved precision.

The collaboration with Société CILAS on the behaviour of Ti-Ni supermirrors under neutron irradiation finished in 1997 (PhD thesis of K. Nguy). The neutron reflectivity data show that the supermirrors on boron glass cannot be guaranteed after a neutron dose of $3 \cdot 10^{19} \text{ n.cm}^{-2}$ (decrease of 30 % of the reflectivity), which corresponds to 8 years for the core side of the reactor beam holes of Orphée (which see a flux of $\sim 10^{11} \text{ n.cm}^{-2}.\text{s}^{-1}$), and 80 years at the outlet of the beam holes (i.e. beginning of the guides, flux : $\sim 10^{10} \text{ n.cm}^{-2}.\text{s}^{-1}$). For the HFR (ILL, Grenoble), because of the higher flux, these numbers are reduced respectively to 1 and 11 years.

Moreover, it was also shown that the boron glass substrate itself deteriorates, by formation of He bubbles.

In conclusion, for the installation of supermirrors at the entrance of the guides, a solution with a metallic substrate, which would offer also better thermal exchanges, should be tested.

In a more prospective direction, we could observe for the first time in non-specular reflectivity diffraction lines from micrometric periodic gratings realized on nickel films. This opens new perspectives for the study of magnetic nanostructures in the plane of thin films, through polarized neutron reflectometry.

2.8 Evolution and Perspectives

Applied research on materials using neutron scattering is expanding, driven by its non-destructive character and the technological needs of society. To meet these needs and promote the neutrons of Orphée by industry, LLB, with the help of its funding organisms (CEA and CNRS), is establishing a new strategy : marketing documents and web page, meetings and workshops, new internal organization. Two meetings have been recently organized in Saclay on the industrial applications of neutrons : a french-italian workshop (in january 1999), and an internal CEA workshop (in june 1999).

We intend also to put in place a new fast access procedure for testing and rapid characterization of samples (in particular in the field of powder diffraction); this is foreseen for the end of 1999.

It is of course important to upgrade the experimental facilities. With a financial participation of INFN (Italy), the stress spectrometer is being equipped with a testing machine that enables strain scanning under constant load (up to 25 kN), constant strain rate or fatigue cycles. The texture diffractometer will be improved with a furnace for in situ measurements and a multidetector to reduce the acquisition time.

From the fundamental point of view, we intend to develop the following subjects in the next years :

- in situ investigation by neutron diffraction (during thermal treatment and/or applied load) of the structure, microstructure and internal stresses in composite materials, with emphasis on line profile analysis (*University of Wien, LLB, University of Reims-Champagne Ardenne, and INFN*);
- fundamental understanding of the microstructure and texture evolutions of a model two-phase material (50-50 austeno-ferritic steel) during deformation and recrystallization (*International Programme involving LMS/Orsay, LLB, and the Institute of Metallurgy and Materials Science of Krakow*);
- correlation between milling conditions and microstructure of Giant MagnetoResistive nanocomposite materials (such as (Co, Fe) Cu) (*PhD thesis of S. Galdeano, LLB and CEA / SRMP, Saclay*);
- SANS study of the influence of irradiation on spinodal decomposition (i.e. α - α' phase separation in b.c.c. Fe-Cr solid solution) (*LSI / Palaiseau and LLB*).

Future trends in the field are the following :

- enlarged realization of "in situ" experiments;
- coupling with numerical simulations of the behaviour of materials, one major objective of the neutron experiments being the validation of models or codes;
- study of non-metallic materials : e.g. microstructure and ageing of cements;
- development of the study of materials of geological interest : the problems here are very similar to those encountered in metallurgy, with a predominant role of thermomechanical history on the microstructure.

ISOTOPIC ORDERING IN ADSORBED HYDROGEN MONOLAYERS

M. Bienfait¹, J.M. Gay¹, P. Zeppenfeld², O.E. Vilches³, R. Ramos³, I. Mirebeau⁴, G. Coddens⁴

¹CRMC2, Université de Luminy, Marseille, ²University of Linz, Linz, Austria

³University of Seattle, Seattle, USA; ⁴Laboratoire Léon Brillouin (CEA-CNRS)

The mass difference between the molecular isotopes hydrogen (H₂), deuterium hydride (HD) and deuterium (D₂) leads to very different liquid-vapor critical and liquid-vapor-solid triple points in both three and two dimensions. This effect is due to the importance of the zero point kinetic energy in these quantum systems. The zero point kinetic energy also manifests itself in the freezing of binary isotopic mixtures by the observation of bulk quantum fractionation, i.e. the separation at freezing of a liquid rich with the lower mass isotopic molecule, and a solid rich in the larger mass isotope.

The same quantum mass effect should also induce an isotopic ordering at low temperature in the bulk solid phase. Isotopic phase separation was predicted a long time ago by Prigogine^[1]. It was observed for ³He-⁴He mixtures but never for isotopic hydrogen solid solutions, although it has been predicted to occur at temperatures as high as ≈ 4 K.

Isotopic phase separation should be expected also in an adsorbed single layer of an isotopic hydrogen mixture. The reduced dimensionality and coordination number in a monolayer with respect to its three-dimensional counterpart makes the relative contribution of the zero-point kinetic energy to the total energy larger than in bulk. This is responsible, among other things, for a substantial difference in the molar areas of H₂ and D₂ at solidification and at monolayer completion. The difference in molar areas lifts the chemical equivalence of the isotopes and can be the driving force which may lead to phase separation.

This was the major motivation of our work on binary mixtures H_{2(x)}-D_{2(1-x)} or HD_(x)-D_{2(1-x)} of the hydrogen isotopic molecules H₂, D₂ and HD adsorbed on graphite, searching for the possible fractionation at solidification and for the expected isotopic phase separation in the solid phase at lower temperature^[2-4]. Neutron scattering is well suited for such investigations, taking advantage of the large difference in the coherent and incoherent cross sections of the various hydrogen isotopes. Indeed, the contribution to a diffraction process of all three isotopic molecules is large since the coherent scattering length of both H ($b_H = -3.742$ fm) and D ($b_D = +6.674$ fm) are comparable in magnitude. On the other hand, the large incoherent scattering length of H (especially in the HD molecule which does not undergo ortho-para conversion at low temperatures)

is particularly useful in quasielastic neutron scattering measurements.

We performed three kinds of neutron scattering experiments at various hydrogen surface densities (ρ), molar isotopic concentrations (x) and temperatures (T) :

-Diffraction experiments were performed on H₂-D₂ mixtures to identify long range ordering in the solid phases and its possible evolution with temperature.

-Small angle neutron scattering (SANS) investigations were carried out on monolayer H₂-D₂ mixtures. SANS is sensitive to the temperature dependence of the short and medium range structural and compositional order within the mixture. We were thus looking for small clusters of D₂ and H₂.

-Quasi-elastic neutron scattering (QENS) experiments were performed on HD-D₂ mixtures to determine the self-correlation function of the HD molecules in the fluid phase at high temperature (15...30K) and hence the corresponding diffusion coefficient.

The major part of the experiments was performed at the LLB on G6.1 and MIBEMOL ; it was complemented by measurements at the ILL on D1B and D16.

The diffraction measurements mapped portions of the ρ , T , x parameter space. The most meaningful results stem from intensity measurements of the (10) diffraction line at low temperature because they can distinguish between a compositionally disordered adlayer (random mixture) according to

$$I \propto [xb_H + (1 - x)b_D]^2 \quad (1)$$

and a fully phase-separated system, as given by

$$I \propto xb_H^2 + (1 - x)b_D^2 \quad (2)$$

The calculated intensity is represented in Fig. 1 (full line) for the random mixture ; it reaches zero for $x = 0.64$ as a result of the opposite signs of b_H and b_D , respectively. The dashed line represents eq. 2, i.e. the fully phase-separated system.

Two sets of experimental results are reported in Fig. 1, as well. One, for coverage $\rho = 1$, corresponds to the so-called commensurate $(\sqrt{3} \times \sqrt{3})R30^\circ$ structure. The intensities of the (10) lines fit very well the

calculated intensities of a compositionally disordered mixed crystal. The commensurate solid remains a random mixture down to 3K.

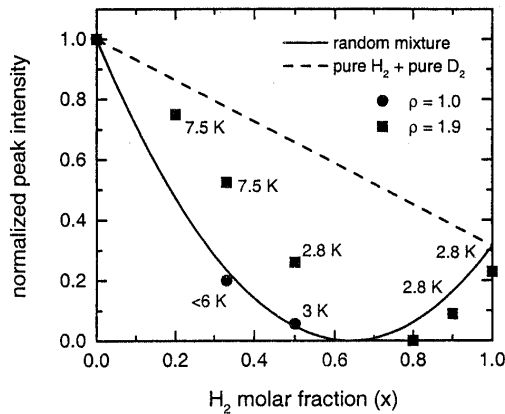


Figure 1. Behaviour of the (10) adlayer diffraction peak intensity

The other coverage $\rho = 1.9$ corresponds to a complete, very dense, incommensurate monolayer ($\rho \approx 1.5$) with, in addition, 30% of a second adsorbed layer (other experiments, not reported here, for $\rho \approx 1.5$, look qualitatively the same). In that case, the measured intensities for $0.2 < x < 0.5$ are intermediate between the calculated intensities of a random mixture and a fully phase-separated system. Hence, a partial phase separation is observed at monolayer completion for these isotopic molar concentrations.

The small clusters of D_2 or H_2 should be observed by SANS. We have measured the variation of the SANS intensity from 20 to about 3K by decreasing the temperature step by step for $x = 0.5$ and 4 coverages ($\rho = 1.92, 1.54, 1.2$ and 1.0). The results are represented in Fig. 2 as the difference of the recorded intensity at 3K, $I(3K)$ and at 20K, $I(20K)$, in order to eliminate the contribution of the beam adsorption due to the hydrogen condensation on the graphite surface.

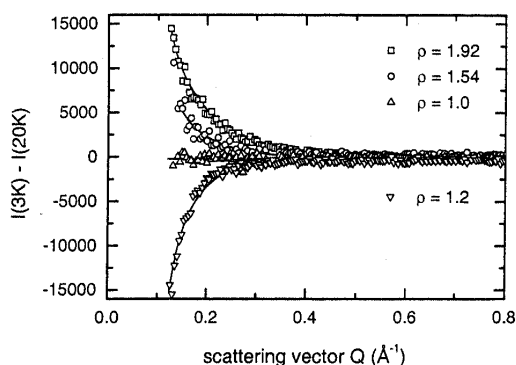


Figure 2 SANS results

At $\rho = 1.92$ and 1.54 , we measure at low temperature an increase of the intensity at small scattering vector which is readily interpreted as the signature of an isotopic clustering in the mixture. Hence, the trend towards phase separation observed by diffraction is confirmed by SANS for these coverages.

The interpretation of the decrease of the SANS intensity at low temperature, observed for $\rho = 1.2$, is not as straightforward. It suggests that more ordering occurs in the adsorbed layer at low temperature. This is also suggested by diffraction measurements because a superstructure peak is observed for this coverage at 3K.

In the vicinity of the commensurate solid ($\rho = 1$), the SANS intensity is essentially constant between 20 and 3K. No change in the ordering is detected between these temperatures ; this means that the adsorbed layer remains compositionally disordered down to 3K, as already seen by diffraction measurements.

At higher temperature, in the solid-liquid transition range, we looked, by QENS, for a possible ordering or phase separation at freezing in an isotopic hydrogen mixture adsorbed on graphite. We did not observe any indication of fractionation during the layer solidification but instead a rather unexpected effect : by substituting one half of HD by the heavier molecule D_2 in an adsorbed monolayer, we measured an enhancement of the hydrogen mobility with respect to the pure HD layer in the fluid phase just above the melting temperature. This effect is represented in Fig. 3. It can be interpreted in terms of a strengthening of the bonding of the lighter molecule, resulting from its larger quantum motion. Indeed, the lighter molecule has a larger vibrational amplitude and it tends to experience more strongly the repulsive part of the Van der Waals potential ; this effect stabilizes the lighter isotope adlayer.

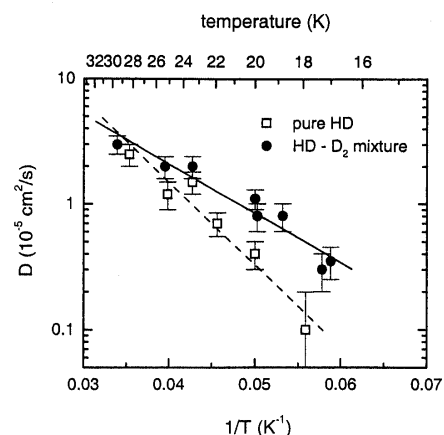


Figure 3. Diffusion coefficient of HD molecules deduced from QENS results

- [1] I. Prigogine et al., *Physica* **XX**, 383 (1954) ; ibid 516 ; ibid 633.
- [2] M. Bienfait, P. Zeppenfeld, L.J. Bovie, O.E. Vilches and H.J. Lauter, *Physica B* **234-236**, 159 (1997).
- [3] M. Bienfait, J.M. Gay, P. Zeppenfeld, O.E. Vilches, I. Mirebeau and H.J. Lauter, *J. Low Temp. Phys.* **111**, 555 (1998).
- [4] M. Bienfait, P. Zeppenfeld, R.C. Ramos, J.M. Gay, O.E. Vilches and G. Coddens, *Phys. Rev.B* (accepted)

ICOSAHDRAL CLUSTERS AND NON UNIFORM MAGNETISM IN LIQUID PRECURSORS OF AlPdMn QUASICRYSTALS

V. Simonet¹, F. Hippert¹, H. Klein², M. Audier², R. Bellissent³

¹Laboratoire de Physique des Solides , Université Paris-Sud, 91405 Orsay Cedex, France

²L.T.P.C.M, E.N.S.E.E.G., B.P.75, 38402 Saint Martin d'Hères, France

³Laboratoire Léon Brillouin (CEA-CNRS)

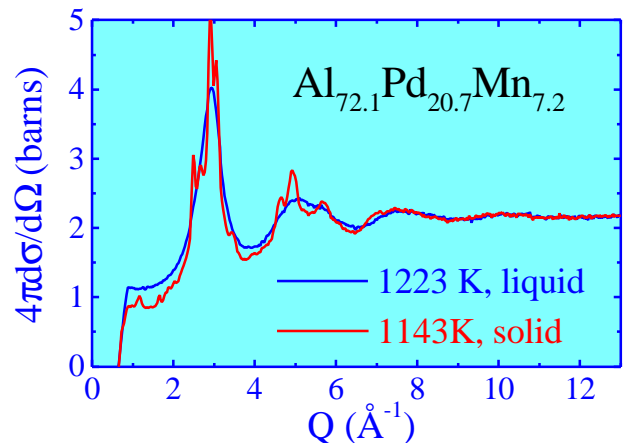
In a recent study of liquid AlPdMn alloys^[1] leading to quasicrystalline or approximant phases by primary crystallisation^[2], we put onto light a very strong local order. The close similarity between the intense Bragg peaks of the solid phase and the main peaks of the liquid structure factor suggests an icosahedral local order. On the other hand the liquid shows up a paramagnetic behaviour whereas the solid phases are non magnetic. The magnetic susceptibility of the liquid is proportional to the Mn content of the AlPdMn alloys ; it increases with increasing temperature, which could be associated to a decrease of the amount of icosahedral clusters^[3].

Most structural models for quasicrystals involve packings of various icosahedral clusters with a large number of atoms, such as Mackay clusters (54 atoms) in AlPdMn quasicrystals or Bergman clusters (104 atoms) in AlLiCu quasicrystals. The same clusters are also found in the approximants of quasicrystals, which are periodic phases with large unit cells whose structures are closely related to that of quasicrystals. Clusters are not only a convenient geometrical description of these complex phases, but can also play a role in their properties. In the case of a liquid - icosahedral solid phase equilibrium, it might be expected that the local order in liquids forming quasicrystals reflects the local organization of atoms in the solid. Therefore we have undertaken simultaneously a simulation of the liquid local order based on icosahedral clusters and an extension of our experimental work up to higher temperatures and with several Mn compositions. Polarised neutrons have been used to investigate the Mn magnetic form factor in the liquid.

Neutron diffraction

Neutron scattering spectra measured on 7C2 spectrometer on the $\text{Al}_{72.1}\text{Pd}_{20.7}\text{Mn}_{7.2}$ alloy at 1143 K where the eutectic was molten (and hence the solid icosahedral phase coexisted with a small fraction of liquid) and at 1223 K just above the melting point ($T_L=1160$ K) are shown in figure 1. The broad maxima of the differential scattering cross-section in

the liquid state correspond to the main Bragg peak groups of the icosahedral phase. At small Q values in the liquid state, a paramagnetic contribution is superimposed to the measured structure factor as



explained later.

Figure 1. Structure factor of AlPdMn alloys in the solid state (just below the melting point) and in the liquid state (just above the melting point), measured on 7C2, LLB.

The similarity between the liquid and solid spectra extends up to the largest Q values. The same kind of observation holds for other studied alloys : $\text{Al}_{77}\text{Pd}_{18}\text{Mn}_5$ and $\text{Al}_{76.5}\text{Pd}_{20}\text{Mn}_{3.5}$. Such an observation suggests the presence of strong local order in the liquid state above T_L , reminiscent of that in the solid. We have therefore searched for a possible evolution of the neutron scattered intensity with increasing temperature in the liquid state. This study was performed up to 1923 K, using the spectrometer D4B at ILL, on the $\text{Al}_{72.1}\text{Pd}_{20.7}\text{Mn}_{7.2}$ alloy whose primary crystallization gives rise to the largest proportion of icosahedral phase. Results are shown in figure 2. As expected in liquid metallic alloys, the oscillations of the structure factor are broadened and their amplitudes decrease with increasing temperature.

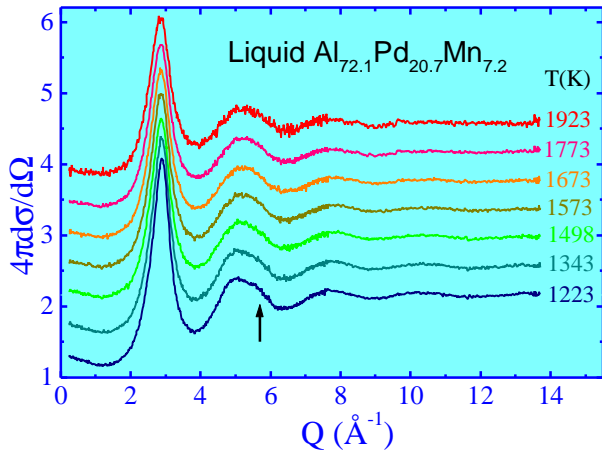


Figure 2. Differential neutron scattering cross-section versus temperature for the $\text{Al}_{72.1}\text{Pd}_{20.7}\text{Mn}_{7.2}$ in the liquid state (measured on D4, ILL). The vertical scale corresponds to the data measured at 1223 K. The curves at successive temperatures have been shifted by steps of 0.5 barns.

An evolution of the liquid structure is suggested by the fact that the second peak shoulder (shown by an arrow around 5.5 \AA^{-1}), well defined just above the melting point, is progressively damped with increasing temperature. Simultaneously the low Q limit of the intensity increases which indicates an increase of the magnetic moment. Finally it must be emphasized that the oscillations at larger Q remain well defined up to 1923 K and **their position is unchanged**, while the position of the first peak shifts towards small Q as expected from thermal expansion.

Polarized neutron scattering

Polarized neutron scattering experiments were performed on the D7 spectrometer at ILL (Grenoble) at room temperature and at 1170 K, just above the liquidus temperature^[4]. Incident neutrons were sequentially polarized along the three perpendicular directions. For each direction of polarization, the spin-flip and non-spin-flip scatterings were alternately measured. Paramagnetic and nuclear spin incoherent scatterings give rise to both spin-flip and non-spin-flip processes, while the nuclear coherent and incoherent (isotopic and chemical) scatterings are non-spin-flip. By suitable combinations of the measured spin-flip and non-spin-flip signals, the contributions of the nuclear spin incoherent scattering, the nuclear scattering and the paramagnetic scattering can be determined. The differential magnetic scattering cross-sections at 300 K and 1170 K (obtained by averaging spin-flip and non-spin-flip measurements) are shown in Figure 3. Very large error bars are due to small counting rates resulting from the significant attenuation of the incident and scattered beams within the neutron polarizer and analyzer devices.

Nevertheless, in agreement with previous results, a paramagnetic scattering is detected in the liquid state, while it is not measurable in the solid state. The differential nuclear scattering cross-section has been extracted as well it ascertains that the chemical incoherent scattering increases on melting and reaches its maximal value in the liquid state above T_L . Thus the increase of the differential scattering cross-section measured with unpolarized neutrons on melting is not only due to the onset of paramagnetic scattering in the liquid, but also to an increase of the chemical incoherent scattering.

Knowing the chemical incoherent scattering contribution, the differential paramagnetic scattering cross-section in the liquid can be calculated from the differential scattering cross-section measured using unpolarized neutrons. In the $\text{Al}_{72.1}\text{Pd}_{20.7}\text{Mn}_{7.2}$ alloy, at 1223 K, from $\sigma_0 = 1.2 \pm 0.06$ barns at $Q = 0.2 \text{ \AA}^{-1}$ one obtains $4\pi(d\sigma/d\Omega) = 0.49$ barns which is much larger than the signal measured using polarized neutrons ($\approx 0.075 \pm 0.015$ barns). This discrepancy is probably due to the quasi-elastic nature of the paramagnetic scattering. On D7 the integration on energy is limited, on the neutron energy loss side, by the low incident neutron energy ($E_i = 3.5$ meV) and, on the neutron energy gain side, by an effective cut-off (around 10 meV) due to the progressive decrease of the efficiency of the neutron spin analyzers with increasing energy.

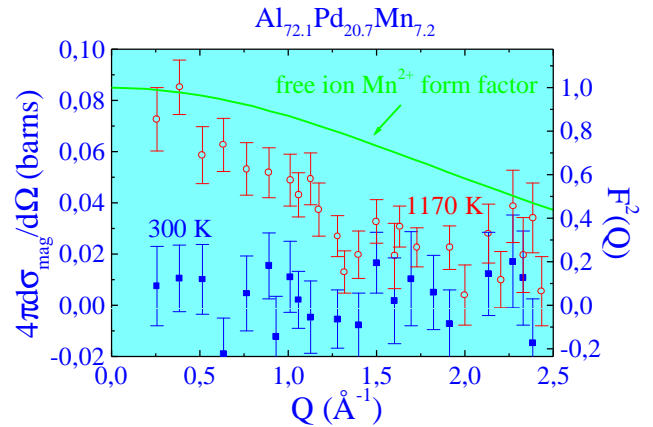


Figure 3 . Polarized neutron scattering measurements performed on D7, ILL : Q dependence of the differential paramagnetic scattering cross-section in $\text{Al}_{72.1}\text{Pd}_{20.7}\text{Mn}_{7.2}$ at 300 K (full blue squares) and at 1170 K in the liquid state (open red circles). There is a paramagnetic scattering in the liquid state and no such signal in the solid state. The data in the liquid state, normalized to 1 at $Q=0$ (right vertical scale), are compared to the form factor of a free Mn^{2+} ion (solid line).

On the contrary, the high incident energies used on the 7C2 and D4B spectrometers ($E_i \approx 170$ meV) permit an integration of a much larger fraction, or almost the whole, of the paramagnetic response.

Assuming the whole signal is integrated on 7C2 and D4B, then only 15% of the paramagnetic signal was detected on D7 at 1170 K. However, even with such a poor precision in the data, one can observe a narrowing of the form factor compared to that of the Mn^{++} ion, which suggests strong magnetic correlations in this liquid alloy.

Icosahedral local order of the liquid state

The great similarity found between the structure factor of the liquid AlPdMn alloys and the diffraction spectrum in the solid quasicrystalline phase led us to assume the presence of a strong local icosahedral order in the liquid. In order to ascertain this hypothesis, we analyze more quantitatively the liquid structure factor through numerical simulations based on icosahedral clusters.

Although simulations of the measured structure factors in the whole Q -range are a very complex task, an analysis of the structure factor at large Q is possible under several conditions and indeed brings very interesting information on the local order. The principle of the method, initially introduced to describe molecular solids, implies that a cluster can be defined in the liquid and that the atoms within the cluster are much more rigidly bound together than to other atoms in the system. The structure factor can be written as :

$$S(Q) = \frac{1}{N_{at}^c \langle b^2 \rangle} \sum_{i,j=1}^{N_{at}^c} b_i b_j \frac{\sin Q r_{ij}}{Q r_{ij}} e^{-W_{ij}}$$

It is compared to the experiment on figure 4a.

Because of the similarity between local order in the icosahedral solid and in the liquid, the choice of the cluster was guided by the structural description of several AlMn and AlPdMn approximant phases. We assumed therefore an icosahedral cluster of Al centered on a Mn Atom^[6]. The first icosahedron edge Al-Al distance $\langle r_1 \rangle$ was taken equal to 2.6 Å and the mean square variation $\langle \delta r_1^2 \rangle$ of this distance was 0.015 Å² as expected from the results of structure refinement of solid phases. $\langle r_0 \rangle$ is the Mn-Al distance (see insert of the figure 1b). The other icosahedron distances are then fixed. Their mean square variation

can be obtained assuming that :

$$\langle \delta r_i^2 \rangle = \langle \delta r_1^2 \rangle (\langle r_i \rangle / \langle r_1 \rangle)^2.$$

The Debye-Waller term is then defined with:

$$W_{ij} = \langle \delta r_i^2 \rangle / 3.$$

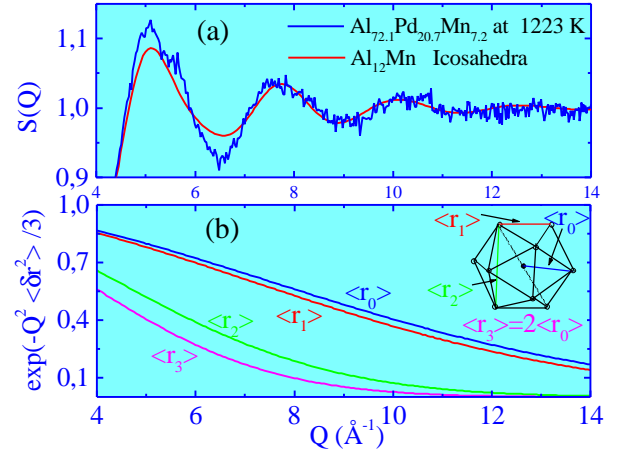


Figure 4.(a): Comparison for $Q > 4.5 \text{ Å}^{-1}$ of the measured structure factor at 1223 K in $Al_{72.1}Pd_{20.7}Mn_{7.2}$ (blue) with the calculated structure factor assuming $Al_{12}Mn$ icosahedra (red solid line)

(b) Q dependence of the Debye-Waller factors for the four pair distances within the $Al_{12}Mn$ icosahedron

Conclusion

In this work, by using a cluster based numerical simulation, we have proven the existence of **icosahedral clusters** with lifetime greater than the typical neutron interaction time with the cluster (i.e. 10^{-10} seconds).

The existence of such clusters with the same geometry up to very high temperatures, is the signature of a **molecular type** local order in a liquid **metallic alloy**.

Moreover this liquid is **non homogeneous** as far as no change occurs in intracuster distances, while bulk density strongly decreases.

We have shown that the unexpected behaviour of the magnetic properties of these alloys can be understood under the assumption than **Mn becomes magnetic outside of the $Al_{12}Mn$ clusters**.

References

- [1] D.Shechtman, I.Blech, D.Gratias, and J.W. Cahn, Phys. Rev. Lett. **53**, 1951 (1984).
- [2] M. Audier, M. Durand-Charre and M. de Boissieu, Phil. Mag. B **68**, 607 (1993).
- [3] F. Hippert, M. Audier, H. Klein, R. Bellissent, D. Boursier, Phys. Rev. Lett. **76**, 54 (1996).
- [4] O. Schärpf and H. Capellman, Phys. Stat. Sol. (a) **135**, 359 (1993).
- [5] H. Klein, L. Descotes, M. Audier, R. Bellissent, and F. Hippert, J. of non Cryst. Solids **205-207**, 6, (1997)
- [6] V.Simonet, F. Hippert, M. Audier, H. Klein, R. Bellissent, H.Fischer, A.P.Murani, D.Boursier, Phys. Rev. B **58**, 6273 (1998).

RESIDUAL STRESSES AND HARDENING NEAR CRACK TIP REGIONS OF AUSTENITIC STEEL FATIGUE SPECIMENS.

K. Hirschi¹, M. Ceretti¹, B. Marini², J.-M. Sprauel³

¹ Laboratoire Léon Brillouin (CEA-CNRS)

² CEREM/SRMA, CEA-Saclay, 91191 Gif sur Yvette Cedex

³ Laboratoire MécaSurf, ENSAM, 2 cours des Arts et Metiers, 13640 Aix en Provence

Austenitic stainless steel 316L is used extensively in the field of nuclear industry, and more specifically in the primary circuit of fast breeder reactors. As the normal operation temperature of the latter is about 650°C, it is very important to determine the role of residual stresses in the deformation and the fracture process in order to estimate the component's lifetimes. The plastic deformation is also an important parameter related to the residual stress relaxation and its redistribution after fatigue loading. The aim of this work was to determine the residual stress field in cracked fatigue specimens of austenitic stainless steel 316L by neutron diffraction techniques in order to use this data for quantifying the influence of the different loading parameters on the fatigue crack growth. On the other hand, some microstructural parameters, such as the average size of coherently diffracting blocks D and the mean-square microstrain $\langle \epsilon^2 \rangle^{1/2}$, were estimated by combining neutron and X-ray (synchrotron radiation) diffraction techniques. In fact, the shape and the broadening of diffraction profiles are directly correlated with the evolution and redistribution of microstructural defects.

Non-destructive neutron diffraction technique is nowadays extensively used for the determination of **internal elastic stresses** in polycrystalline materials due to the homogeneous distribution of strains across several grains, which result in a shift of the angular position of the Bragg peaks. However, the analysis of **plastic strains**, due to microstructural defects, by neutron scattering investigations still remains quite rare, in contrast to X-ray diffraction, widely used for this kind of analysis. Nevertheless, due to the high penetration of neutrons in most materials, the neutron diffraction is the only non-destructive technique, which enables to get information within a defined volume in a bulk sample and not only limited to the surface (as in the case of X-rays).

For the analysis of plastic strains by neutron scattering, experimental and theoretical methods for neutron diffraction line broadening analysis were developed [1]. These methods generally require a high instrumental resolution, which has been achieved by optimising the experimental conditions (large monochromator take-off angle and small incident beam divergence) [2]. Additionally, a new method of single peak analysis with indirect

deconvolution of instrumental profile was developed to relate the diffraction profile parameters with the microstructural parameters.

Measurements were performed on two Crack Test (CT) specimens of austenitic stainless steel 316L (Fig. 1) subjected to fatigue cycling with different load ratio (R) in order to modify the dimensions of the plastic region close to the crack tip ($R=0.1$ and $R=0.5$), called in the following CT_1 et CT_2, respectively. In particular, the first sample, with $R=0.1$, had been subjected to 25750 fatigue cycles, while the second one ($R=0.5$) has been submitted to 19530 cycles. A third specimen (CT_3) was deformed by tension up to 5 mm crack opening.

1. Internal elastic stresses

In the first part of the work, we have studied the macroscopic residual stresses by neutron diffraction. Three dimensional strain measurements (x , y , z directions) were performed in the middle of the sample, along the crack opening direction y , on the "strain dedicated" G5.2 diffractometer of the LLB.

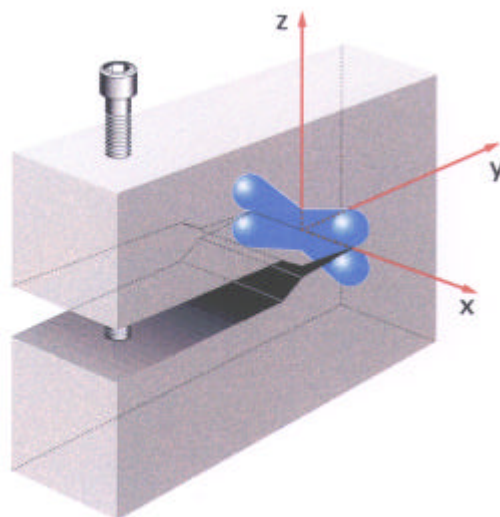


Figure 1: Geometry of the CT samples and measurements directions. The plastic zone near the crack tip is schematised in blue. The samples were 70 mm long in the direction of the crack growth, 45 mm high and 10 mm thick. Neutron measurements have been performed in the middle of the sample (at a depth of 5mm), along the crack opening direction y .

For all the investigated specimens, a three dimensional stress state was observed. In particular, the residual stresses obtained for the sample with a small R (CT_1) are rather weak and they increase in the second sample (CT_2) with higher R. Experimental residual stress distribution along the crack opening direction for the third sample (CT_3) is shown in figure 2, together with a finite element calculation. As seen from the figure, the maximum stress level was observed at 2 mm from the tip, where $\sigma_{xx} = 300$ MPa, $\sigma_{yy} = 500$ MPa and $\sigma_{zz} = 800$ MPa. At the distance of 8mm from the tip, the σ_{xx} and σ_{yy} components were found to be very low, whereas the σ_{zz} component becomes large and compressive. These measurements show a good agreement with a finite elements (3 dimensional) calculation performed using CASTEM2000 code, developed at DGMT (CEA). A small disagreement between the experimental and theoretical results was observed essentially in the region of some mm near the crack tip. This can be explained by the different spatial resolution used in the neutron measurements. In fact, the size of the finite elements selected in the calculations was 0.187 mm near the crack and 1.275 mm at the edge of the sample, while the spatial resolution ("gauge volume") of neutron measurements was $1 \times 1 \times 1 \text{ mm}^3$. We note as well that the calculated values of stresses are slightly higher than measured ones. This is probably due to relaxation effects due to the plastic deformation induced by the tensile test. Another possible reason for the deviation from the maximum value can be due to the fact that the calculation does not take into account the effect of the crack propagation.

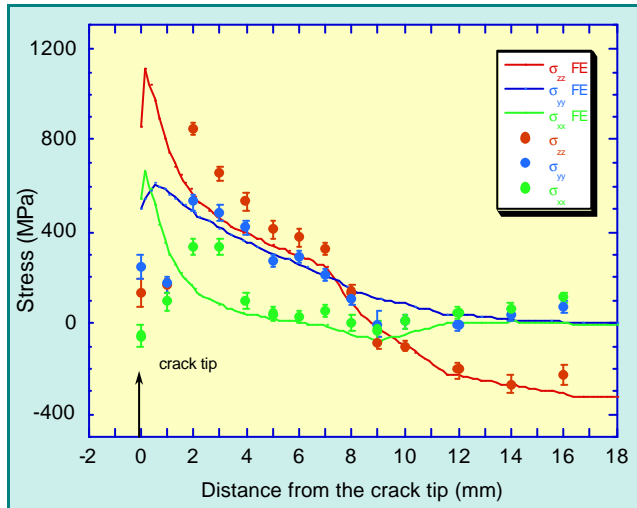


Figure 2 : Residual stress evolution as a function of the distance from the crack tip of the CT_3 sample. Comparison between the experimental results (dots) and the values obtained by Finite Element calculation (continuous lines).

2. Plastic strains : neutron measurements

In the second part of the work, the experimental study of microstructure and plastic deformation in the region close to the crack tip was performed by neutron and X-ray (synchrotron) diffraction. In fact, it is important to estimate the dimension of the plastic zone, created around the crack's tip, which is responsible for the stress redistribution affecting the crack propagation.

The microstrains evaluation by neutron diffraction have been performed in the middle of the sample (at a depth of 5mm) using the profile broadening analysis, based on the single-line Keijser's method [1]. The basic assumption of this approach is that the sample broadened profile can be described by the convolution of a Gauss function and a Cauchy function, depending on the strain and size, respectively. The indirect deconvolution method has been developed to extract the instrumental profile from the experimental data. The plastic zone was clearly distinguished for the CT_2 and CT_3 samples with the peak breadth considerably larger than that of reference sample. The dimension of the plastic zone (depending on the directions x, y, z) is about 2 to 3 mm for the CT_2 sample and about 4 mm for the CT_3 sample. The estimation of the plastic deformation and microstructural parameters (D and $\langle \epsilon^2 \rangle^{1/2}$) was done using a previous calibration on prestrained tensile specimens, by performing neutron single line broadening analysis. For the CT_3 sample it was found that the maximum plastic strain in the directions perpendicular (z) and parallel (y) to the crack propagation is localised at 1mm from the tip and it attains about 30% (Figure 3).

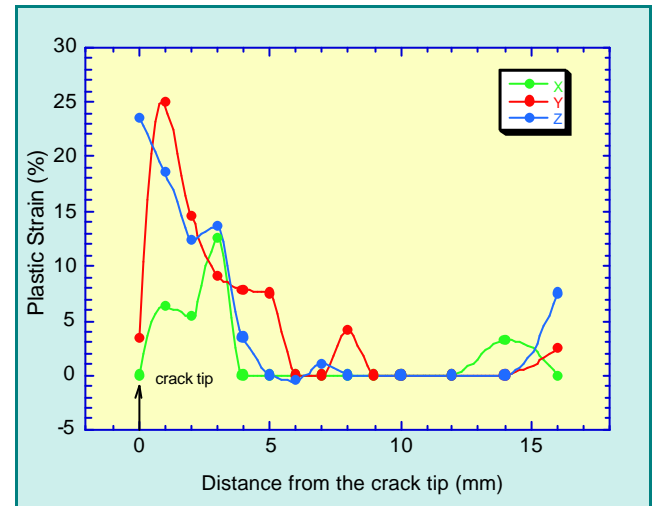


Figure 3 : Evolution of the plastic strain as a function of the distance from the crack tip, in the sample CT_3, determined by neutron diffraction.

3. Plastic strains : X-ray measurements

These results, obtained by a single peak broadening analysis, have been completed by a Warren-Averbach analysis using several X-ray (synchrotron radiation) Bragg reflections and higher orders. These complementary measurements were performed at the sample surface on the four circle diffractometer, WDIF4C, installed on the light guide DW22 at L.U.R.E. (Orsay). Plastic strains were determined using a recently developed theoretical model, based on the Warren-Averbach analysis and taking into account the contribution of Elastic Strain Heterogeneity (ESH) of the domains on the profiles broadening [3]. The values obtained for the mean size of the coherently diffracting blocks $\langle L \rangle$, the mean square of the 2nd kind micro-strains $\langle \epsilon_0^2 \rangle^{1/2}$ (related to the ESH effects) and the mean square of 3rd kind

micro-strains $\langle \epsilon_1^2 \rangle^{1/2}$ are reported in Figure 4 as a function of distance from the crack tip. As seen from the figure, the microstructural parameters obtained are quite scattered. This is probably due to the relatively large grain's size compared to the small X-rays beam dimensions and its weak divergence. In particular, the ESH and size effects are the most visible in the region close to the tip (2-3mm). In the region between 4 mm and 9 mm, we obtain very small (or zero) values of plastic deformation and negative values of $\langle L \rangle$. This is due to the imprecision of the deconvolution as the Bragg peak breadth is very close to the instrumental width. The calculated size of coherently diffracting blocks, which is about 255Å at the crack tip, corresponds to plastic strain of 30%. The increase of distortion values at the edge of the sample shows the presence of strong plastic strains in this region.

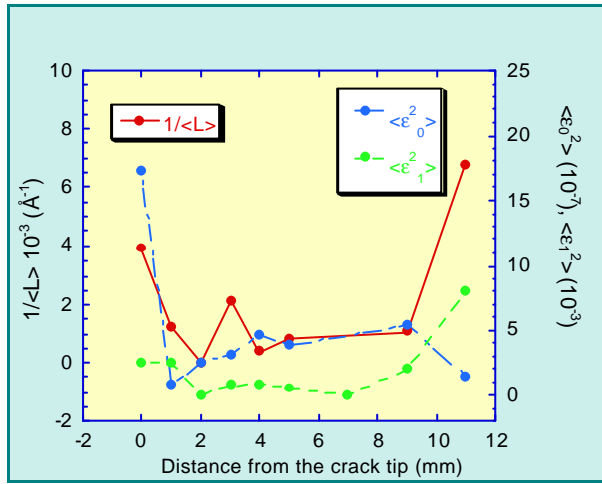


Figure 4 : Evolution of the diffraction coherent domains size $\langle L \rangle$, and of the microstrains $\langle \epsilon_0^2 \rangle$ (2nd order) and $\langle \epsilon_1^2 \rangle$ (3rd order) as a function of the distance from the crack trip in the CT_3 sample, determined by Warren-Averbach analysis using synchrotron radiation

References

- [1] de Keijser T. H, Mittemeijer E. J., Rozendaal H. C. F., *J. Appl. Cryst.* 16 (1983), 309-316
- [2] Hirschi K., Ceretti M., Lukas P., Ji N., Braham C., Lodini A., *Textures and Microstructures*, (1999), in print
- [3] Marbelly P., *Contribution à l'étude des pics de diffraction. Approche expérimentale et modélisation micromécanique*, Thèse de Doctorat, ENSAM, Aix en Provence, 1996.
- [4] Hirschi K., *Analyse des contraintes résiduelles et des paramètres microstructuraux par diffraction des neutrons dans un acier austénitique inoxydable*, Thèse de Doctorat, Université de Reims, 1999.

"IN SITU" NEUTRON SCATTERING STUDY OF HYDROGEN-CONTAINING ZIRCALOY-4 ALLOYS

F. Couvreur¹, G. André²

¹CEA, DRN/DMT/SEMI/LM2E, CEA-Saclay, 91191 Gif-sur-Yvette cedex

²Laboratoire Léon Brillouin (CEA-CNRS)

Aims of the study

The fuel cladding of Pressurized Water Nuclear Reactors (PWR), made in Zircaloy-4 (zirconium-based alloy, containing in weight typically 1.4% Sn, 0.2% Fe and 0.1% Cr), is sensitive to hydrogen absorption in the usual working conditions (i.e. under H₂O at 300°C). Hydride platelets may form, which are an important embrittlement factor of the cladding, and also which induce a swelling when they dissolve in the α -h.c.p. Zircaloy matrix. Moreover, recent studies suggest that these hydrides may be an accelerating factor of corrosion. This aspect will be all the more important as the new working PWR conditions will be more demanding.

It is therefore essential to characterize and understand the mechanisms of hydride formation and dissolution, in particular under neutron irradiation : this is the object of a research programme undertaken by the "Direction of Nuclear Reactors" of CEA, which includes a neutron scattering study at LLB.

The large coherent and incoherent cross-sections of hydrogen make this tool very powerful to determine the hydrogen content and characterize the hydrides ; indeed, the incoherent cross-section gives rise to a continuous background in diffraction spectra, which is **proportional** to the hydrogen content, and is (nearly) independent of scattering angle ; the coherent cross-section contributes significantly to the structure factor of the hydride phase, i.e. to the intensity of its diffraction peaks. Zirconium is a specially favorable element for this study, because its neutron absorption coefficient and incoherent scattering cross-sections are very weak : the diffraction spectra of H-free samples show very low background.

Results

In a first stage, we have shown, on the powder diffractometer G4.1 (equipped with a 800 cell linear multidetector), that the incoherent scattering contribution, obtained from the measurement of the background on samples originating from cladding tubes, allows to determine **non destructively** the total amount of incorporated hydrogen (Fig. 1), with very good sensitivity and precision (< 20 ppm weight). The principle of measurement consists to calibrate in absolute value the incoherent signal measured on a reference vanadium sample of cylindrical shape, after subtraction of the instrumental background ; this

allows to calibrate the signal difference between the hydrogenated sample and an hydrogen free sample.

On the other hand, the diffraction peaks of the hydride (f.c.c. δ -ZrH₂) and Laves phase precipitates (Zr(Fe,Cr)₂) can be easily detected and analysed, for very weak (< 1% atomic) H, Fe and Cr contents, which is not possible in conventional X-ray diffraction.

In a second stage, we have performed "in situ" measurements at various temperatures (between 20 and 500 °C) under secondary vacuum, on a section of Zircaloy-4 cladding tube containing 642 ppm weight hydrogen (length of the sample : 50 mm, diameter : 9.5 mm). The typical measuring time for a single spectrum was 2 hours. In a single experiment (total duration : 5 days), we have been able to obtain simultaneously from the analysis of diffraction spectra the following informations :

- total hydrogen content,
- hydrogen content in hydride form,
- crystallographic characterization of the Zr(Fe,Cr)₂ and ZrH₂ precipitates,
- solubility of H, dissolution of hydrides (Fig. 2),
- influence of H on the thermal expansion of Zircaloy-4 (Fig. 3).

Desorption of hydrogen out of the sample under secondary vacuum was observed above 450 °C, by a decrease of the incoherent background signal.

Conclusions and future prospects

Neutron scattering is the only experimental technique which allows to measure non-destructively the total hydrogen content in Zircaloy tubes. But, more than a simple hydrogen content determination at room temperature, the neutron scattering technique, when combined use is made of the incoherent background and of the diffraction peaks, is also a very rich technique, sensitive and reliable, and quite appropriate to follow "in situ" at high temperature the precipitation/dissolution phenomena of zirconium hydrides, even for very weak contents of precipitates. Future work will be the examination of neutron irradiated samples in PWR conditions (influence of irradiation on hydrogen solubility and on the structure of precipitates) and the study of the behaviour of the cladding in accidental situation (loss of primary cooling), which will require measurements at higher temperature (\approx 1000 °C).

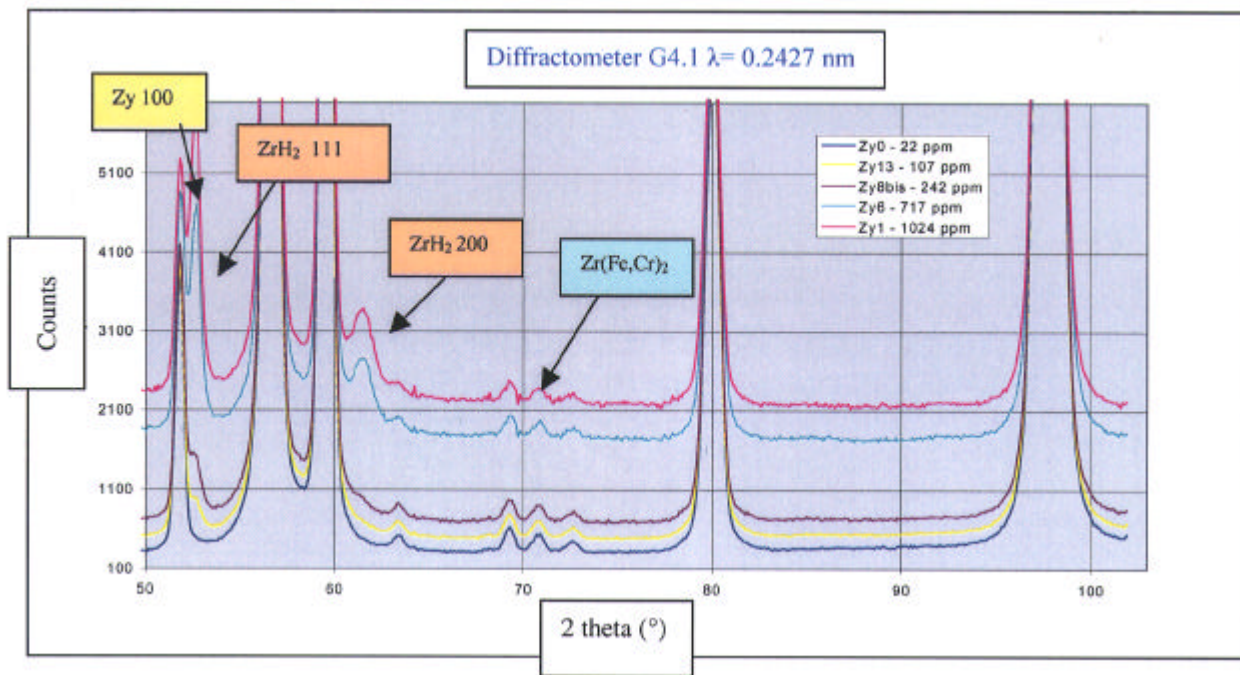


Figure 1 : Powder diffraction diagrams measured for several Zircaloy samples. One observes the increase of background with the hydrogen content, and the weak diffraction lines of δ -ZrH₂ hydride and Laves phase.

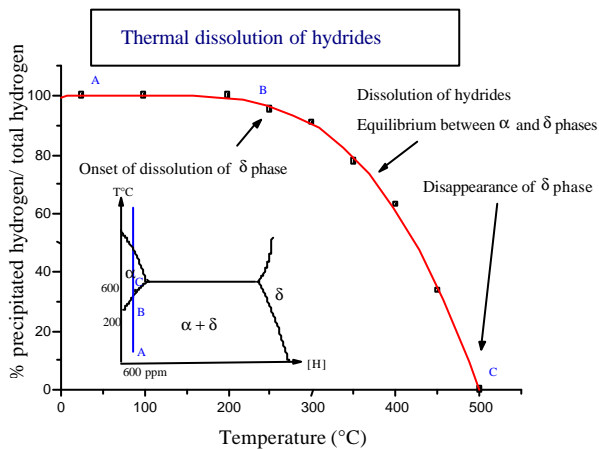


Figure 2 : Proportion of hydrogen content in hydride form (δ -phase) versus temperature, for a sample containing 642 ppm weight hydrogen. This quantity decreases with increasing temperature, according to the phase diagram shown in inset : above 500°C, dissolution of the hydrides is complete and the sample is a single-phase Zr-based (α) hexagonal solid solution. It allows to determine the hydrogen solubility curve in the studied material, between room temperature and 500°C, and to deduce a value for the enthalpy of dissolution of the δ hydrides in Zircaloy-4 : $\Delta H = 41.5 \text{ kJ/mol}$.

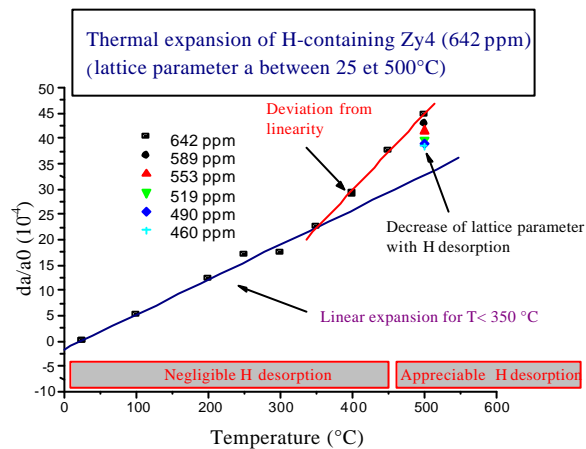


Figure 3 : Temperature dependence of the lattice parameter a of Zircaloy-4 (sample containing 642 ppm weight hydrogen). A similar curve is found for the lattice parameter c . We attribute the increase of slope above 350°C to the dissolution of hydrides, which introduces interstitial hydrogen atoms in the α -Zircaloy matrix and a supplementary swelling. This explanation is confirmed by the observed decrease of lattice parameter during an isothermal stay at 500°C, due to hydrogen desorption out of the sample.

References

- [1] P. Wille, D. Bunemann, H.J. Lahann, H. Mertins, « Hydrogen diffusion in metals measured by neutron scattering and adsorption », IAEA SM 219/36, pp.325-338.
- [2] J.H. Root, R.W.L. Fong « Neutron diffraction study of the precipitation and dissolution of hydrides in Zr-2.5Nb pressure tube material » Journal of Nuclear Materials 232 (1996) 75-85.

AGEING UNDER THERMAL TREATMENT OR NEUTRON IRRADIATION OF LOW ACTIVATION MARTENSITIC STEELS

M.H. Mathon¹, G. Geoffroy², Y. de Carlan³, A. Alamo³, C.H. de Novion¹

¹ Laboratoire Léon Brillouin (CEA-CNRS)

² Laboratoire des Solides Irradiés, Ecole Polytechnique, 91128 Palaiseau Cedex

³ CEA, DTA/DECM/SRMA, CEA Saclay, F-91191 Gif-sur-Yvette

Low Activation Martensitic (LAM) steels are candidates for internal structures of fusion reactors. The concept of Low Activation steels was introduced in nuclear industry for new materials that offer benefits on maintenance operations and waste management. For martensitic/ferritic steels, the main alloying elements such as molybdenum, niobium and nickel present in commercial steels are substituted by elements such as tungsten, vanadium, manganese and tantalum. These elements have a similar influence on the processing and the structure, but exhibit a lower radiological impact. The assessment of potential reduced activation martensitic steels requires a good understanding of the microstructural features in correlation with the mechanical behaviour. Consequently, much effort is underway to study the microstructural evolutions in these materials occurring under thermal ageing or neutron irradiation, and the effects of the substitution of W to Mo and Ta to Nb.

The microstructural investigations are focused on the following phenomena :

- precipitation of various carbides or nitrides : in particular of $M_2(C,N)$ particles responsible of a "secondary" hardening phenomenon (defined in §1),
- formation of the Laves phases $Fe_2(Mo,W)$ under long thermal ageing around 500°C,
- decomposition by a spinodal mechanism of the ferritic phase resulting in an ultra fine-scale interconnected network of Fe-rich α and Cr enriched α' phases or in very small α' particles around 400°C.

All these microstructural evolutions (which are at the origin of hardening phenomena and embrittlement) were studied in different martensitic steels with a chromium content between 7 and 12 at.%, using Small Angle Neutron Scattering (SANS). Indeed SANS allows, in this kind of materials, to characterise very small precipitates at early ageing time when they are not detected by Transmission Electron Microscopy. This is in particular the case for α - α' decomposition, which introduces very weak contrast for X-rays or electron scattering. Furthermore, the ferritic matrix being ferromagnetic, the $A(q)$ ratio of the magnetic and nuclear contrasts between the matrix and particles gives information about their chemical composition^[1].

1. Study of the secondary hardening phenomenon

In quenched (after 1h at 1050°C) and subsequently annealed at 450-550°C materials which simulate the thermally affected zone near a weld, one observes, at relatively short annealing time, an increase of the hardness which is called secondary hardening^[2]. It is related to the first steps of Cr-rich M_2X ($X = C$ or N) precipitation; the latter is detected by Transmission Electron Microscopy (TEM), but only after almost 100 annealing hours when the size of the particles is close to 10 - 20 nm. In order to describe the precipitation at the early stage of thermal ageing treatment, SANS experiments were performed on a conventional alloy "T0" (Fe-9%Cr-1%Mo) and on a LAM material "F82H" (Fe-7.5%Cr-2%W), previously aged for various durations at 500°C.

For the T0 alloy, an increase of the SANS intensity is observed at all annealing times. The mean diameter and number density N_p of the M_2X particles deduced from SANS are shown on figure 1. At short ageing time (<5h), the particles size remains small (1 to 2 nm) whereas N_p increases ("nucleation" stage). Around 5h ageing time, N_p and the hardness reach simultaneously their maximum value, corresponding to optimal pinning of the dislocations by the small precipitates. At long ageing time, N_p and the hardness decrease sharply whereas the average precipitate diameter increases by one order of magnitude ("coalescence" stage).

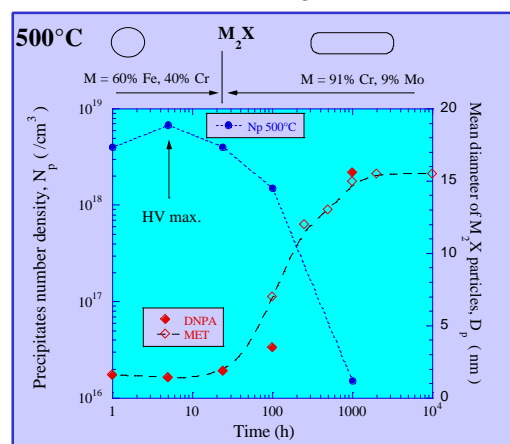


Figure 1 : Evolution with ageing time at 500°C of the mean size and the number density of the M_2X precipitates measured by TEM and SANS in the T0 alloy.

The form factor of the precipitates, obtained from the fit of the SANS curves, is spherical for the shorter

time ($t < 100$ h) and afterwards rod shaped ellipsoidal with a ratio between the big and the small axis of about 3. For large precipitates, the aspect ratio and the mean size measured after 1000 h, are in good agreement with TEM observations.

The A(q) ratio was found to decrease strongly with ageing time (i.e. from 6.6 to 2.4); this could be explained only by a progressive enrichment in Cr and by assuming that the interstitial element X is essentially carbon and not nitrogen. At long ageing time, the A ratio is in agreement with the presence of 9% Mo in the carbides measured by TEM.

For the low Cr content LAM alloy F82H, the maximum volume fraction of the carbides is noticeably smaller than for T0 (0.7% instead of 1.5%); this can explain the very weak increase of the hardness observed in the F82H alloy (figure 2). Besides, the chemical composition of the carbides at long ageing times, consistent with the A value, is 80%Cr-20%V (at. %) : contrary to the case of Mo in the T0 alloy, W does not enter in the composition of the M_2C carbides.

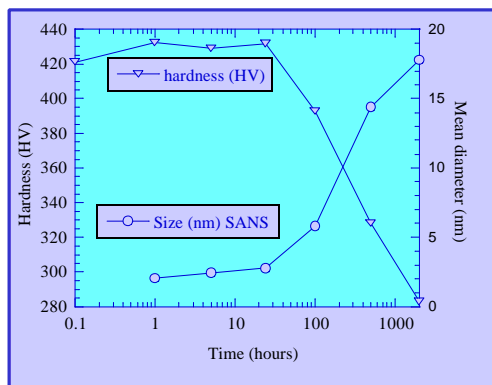


Figure 2 : Evolution with ageing time at 500°C of the hardness and of the mean size of the M_2X precipitates measured by SANS in the Low Activation F82H alloy.

2. Ageing under long thermal treatment or neutron irradiation

In austenitized (quenched from high temperature) and subsequently tempered (annealed 1 h at 750°C) materials, long thermal ageing performed at temperatures between 250 and 550°C up to 22000 h, can induce an important Ductile-to-Brittle Transition Temperature (DBTT) shift directly related to the formation of new phases^[3]. SANS measurements realised on several types of alloys (conventional and LAM) have shown different behaviours depending on the chemical composition. In particular, SANS was able to detect the formation of very small precipitates (nm size), not observed by TEM. For example, the formation of α' precipitates was observed by SANS in conventional and LAM alloys

containing initial Cr content above 9% under thermal ageing at 400°C.

Some of these alloys were studied after fast neutron irradiation up to a dose of 0.8 d.p.a. (displacement per atom) at 325°C. In a Low Activation ("La4Ta") alloy containing 11.2%Cr, neutron irradiation induces an increase of the scattered intensity (figure 3) which can be attributed to the α - α' spinodal decomposition not observed under thermal ageing at this temperature. **In this case, the neutron irradiation induces accelerated phase separation.** The "F82H" alloy presents no evolution under thermal ageing whatever the temperature as well as under irradiation up to 0.8 dpa. These behaviours are in qualitative agreement with the mechanical properties of the materials.

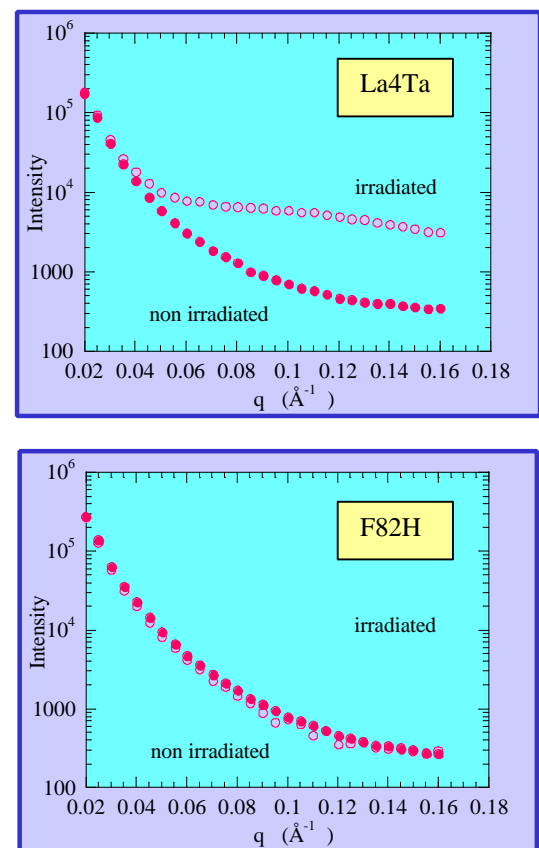


Figure 3 : SANS intensity scattered by two low activation alloys (F82H and La4Ta) before and after neutron irradiation.

In summary, the combined use of SANS and TEM allows to obtain a detailed description of precipitation. This study has put in evidence the role of the initial chemical composition on the alloys behaviour under thermal treatment or neutron irradiation. SANS measurements allowed a direct correlation of the microstructure evolution with the secondary hardening phenomenon.

1 Mathon M.H., Barbu A., Dunstetter F., Maury F., Lorenzelli N., de Novion C.H., J. Nucl. Mat., **245** (1997) 224-237

2 Brachet J.C., J. Phys. III, C3, 4 (1994) 83

3 Brachet J.C., Castaing A., Foucher A., Note Technique SRMA 95-2140, august 1995

CHEMICAL PHYSICS AND BIOLOGY

This very large chapter includes Soft Matter, and more precisely Polymers, and Biological Macromolecules. The latter part originates in previous studies of the structure and dynamics of water. It was realized some years ago that water has especially interesting properties when located in the vicinity of a hydrophilic or a hydrophobic surface. This led to a combined study of structural and dynamical properties of Proteins and of the water that is associated to them. It is interesting to note that a similar evolution occurred in Polymer Physics. There is a growing interest for water-soluble macromolecules, and/ or for copolymers with water-soluble sequences. This leads to conformations that are different from the structures that are usually considered. In some cases, the polymers are biological molecules that are studied in conditions very different from their normal working ones. Thus, there is a significant overlap between these apparently different topics. Among others, there is an interest in showing the strong similarity between the structure of a denaturated biological molecule and that of a synthetic polymer. Work in the second area focused on amorphous and mesomorphous Polymers in the bulk and at interfaces, on Gels, and on Polyelectrolytes. The first part was interested in the static and dynamic properties of soluble and membrane proteins and their associated water. It is indeed accepted that hydration water plays a central role in the stability and function of biological macromolecules. Therefore, it is important to look for the relation between structure, dynamics, and hydration water in proteins.

The neutron scattering experiments were performed essentially with the small angle spectrometers for the structures, by time-of-flight and spin-echo inelastic scattering techniques for the dynamics, and by reflectometry for interfaces.

1. BIOLOGY

1.1. Dynamics of proteins.

The dynamics of a photosynthetic protein, C-phyococyanin (CPC), was studied. This comprises the dynamics of the protein itself as well as of the water that is located at its immediate vicinity. Dynamical studies of the protein as a function of temperature and of the rate of hydration were made by time-of-flight technique, with the Mibemol spectrometer. They led to split the hydrogen atoms into motionless and mobile fractions. As temperature is varied, a dynamical transition is found at approximately 250 K ; it corresponds to the appearance of diffusive motions inside the protein. The radius of the diffusion sphere of the hydrogen atoms in the surface residues remains constant, at approximately 2 Å as temperature changes. But the fraction of motionless atoms decreases as temperature increases and reaches a limit that corresponds to the fraction that lies on the surface.

1.2. Dynamics of water.

A complementary study of the dynamics of the hydration water, in direct contact with CPC, was performed. In order to eliminate the contribution from bulk water, this was realized on powders at hydration rates such that the proteins are functional. Samples hydrated respectively with H₂O and D₂O were used for these experiments on Mibemol. The data may be interpreted with stretched exponentials, corresponding to a distribution of relaxation times for water. The average relaxation time varies as q^{-2} , where q is the momentum transfer. This leads to a diffusion constant equal to $1.5 \times 10^{-6} \text{ cm}^2/\text{s}$, smaller than the $2 \times 10^{-5} \text{ cm}^2/\text{s}$ of bulk water. Thus, the hydrophilic surface has a slowing down effect on hydration water.

These results were also compared with those of a "model" system, made of supercooled water in a porous Vycor silica glass with large specific surface- 116 m²/g. The latter is made of interconnected cylindrical pores of approximately 50 Å diameter, and is very hydrophilic. Two different hydration rates for Vycor were used. The quasi-elastic incoherent scattering experiments were made as a function of temperature. The data lead to a stretched exponential function, $\exp[-(t/\tau)^\beta]$. The relaxation time τ varies as q^{-2} . This leads to a diffusion coefficient equal to $1.1 \times 10^{-5} \text{ cm}^2/\text{s}$, again smaller than that of bulk water. The exponent β is interpreted by a distribution of relaxation times corresponding to motions inside cages with a distribution of sizes. These structural and dynamical studies show that at room temperature, interfacial water behaves as supercooled water.

The influence of water was also specified by looking at changes in the internal dynamics of two globular proteins as one goes from a hydrated powder to a solution. This was realized on lysozyme and myoglobin. It was made on the time-of-flight spectrometer IN6 at ILL. Various hydration rates in D₂O were used. It was shown that surface residues progressively get a local diffusive motion as the protein is hydrated until there is a water monolayer.

Further hydration increases the velocity of this diffusion, but does not involve more residues. Finally, the relaxation time in a solution is two times smaller than for a monolayer, with an amplitude of the motion three times larger. Finally, the dynamics of hydrogen bonds was studied on a water/ dimethylsulfoxide (DMSO) mixture. The latter interacts strongly with water by forming H bonds. The mixture that was used (1DMSO/2H₂O) is eutectic, and is characterized by a very large decrease in the crystallization point, located at -70°C. Quasi-elastic neutron scattering experiments with deuterated DMSO allows the observation of the motion of the protons of water. They show that the dynamics is slower : the diffusion coefficient is 4 times smaller in this mixture than in pure water. A more surprising result is that the H-bond lifetime is found to be unchanged, whereas a longer time might be expected. These results indicate that hydrogen bonds are stronger than in pure water.

I.3. Structure- dynamics- function relationship

A collaboration with the Service de Biophysique des Protéines et des Membranes of CEA/Saclay was set up in order to study the relation between structure, dynamics and function of membrane proteins. Its aim is to understand completely the energetics of protein folding, and to establish a precise relationship between the structure and the functionality of these macromolecules. To this end, it is necessary to know the three dimensional structure of these proteins. It is also important to characterize with the best possible precision their internal motions. The most interesting time scales are between pico- and nanoseconds (10^{-12} to 10^{-9} s). They are accessible by inelastic neutron scattering. This work is done with membrane proteins involved in the first stages of photosynthetic processes in purple bacteria. Reaction Centers (RC) and light harvesting proteins (LH1 and LH2) were used. They form an interconnected protein network in the membrane, are available in large amount, and their structure is known.

Two examples are discussed in the highlights. The first one deals with time-of-flight experiments, giving access to motions with times in the picosecond range in the protein. The second one allows for a comparison of the collective motions in RC and LH2 by neutron spin-echo technique, for times about nanoseconds (10^{-9} s). An example of structure determination by Small Angle Neutron Scattering (SANS) for LH1 is also discussed. A combination of inelastic neutron scattering techniques and more classical methods in Biophysics such as absorption of light and vibrational spectroscopies makes it possible to study the relation between structure, dynamics, and functionality. This is a part of the PhD thesis of S. Dellerue.

I.4. Denaturated proteins.

A second kind of studies is intermediate between polymers and Biology. It involves denaturated proteins, and the possible similarities between their behavior and that of synthetic polymers. Denaturation was made either by heating or by using a strong denaturing agent, guanidinium chloride (GdmCl). Small-angle neutron studies of yeast phosphoglycerate kinase PGK denaturated by GdmCl show an excluded volume behavior, very similar to what was observed on neutral synthetic polymers. The second virial coefficient was measured, and is in agreement with the theoretical predictions for polymers. Similar results were obtained with beta-casein and neocarzinostatin (NCS) denaturated by GdmCl (PhD thesis of V. Receveur).

NCS denaturation by heating was studied in detail by a combination of SANS with other techniques. This protein has a structure made of a single domain, is very analogous to that of immunoglobulins, and also is present in other proteins. Three stages were observed during the denaturation. In the first one, the size remains almost constant. This is reminiscent of the "molten globule". Then, the radius increases until a reversible endothermic transition. The latter corresponds probably to the breaking of hydrogen bonds. In the last regime, the molecule reaches a final state where NCS behaves as an ideal chain, without any interactions. This corresponds to the so-called "theta" regime in polymer Physics.

2. POLYMERS.

Polymer studies are an excellence area of L.L.B. They dealt essentially with mesomorphous polymers at rest and under shear and elongation stresses, gels, and interfaces. Some experiments were also made on polyelectrolytes and on the dynamics of chains in the vicinity of the theta point.

2.1. Mesomorphous polymers.

The Liquid Crystalline Polymers (LCP) that were considered have comb-like structures, with a mesogenous part grafted on the main chain through a flexible spacer. An important effort on the synthesis allowed us to get monodisperse mass fractions. This made possible the determination by Small Angle Neutron Scattering (SANS) of the variation of the radius of gyration with molecular weight. At rest, it has the same variation as for a gaussian chain in the isotropic phase. In the nematic phase, it has an exponent intermediate between the gaussian and the random self-avoiding walk values. In the smectic phase, the chains are confined between the mesogenic layers. In the direction parallel to the layers, they have a gaussian character. In the transverse direction, the exponent implies a stretching of the polymers, therefore validating the assumption of jumps between successive layers.

Two kinds of deformations were studied.

A work under shear showed the richness of the possible behaviors by a combination of large angle and SANS observations. The former gives the orientation of the director. The latter are made in the three planes defined by the velocity, velocity gradient, and neutral vectors. For a polymer having both a nematic and a smectic phase, a transition was found : in the high temperature nematic phase, the director is parallel to the velocity. For low temperatures, it orders along the neutral axis. This is coupled to a change in the orientation of the chains: for high temperatures, they are parallel to the mesogens, while at lower temperatures, they are normal to the director. This transition may be interpreted by assuming a coupling between smectic fluctuations and shear.

A work under uniaxial extension also combined SANS, X-rays, and rheological measurements. Introducing the parameter " duration of relaxation after stopping the deformation" allowed for a study of the dynamics of a chain for various values of the diffraction vector q . In order to extract the effect of the comb architecture from that of the nematic interactions, two isomers were prepared in similar thermal conditions. The first one was in the isotropic phase. The second one was in the nematic phase. The experiments in the isotropic phase show that the chain is as flexible as the corresponding amorphous polymer. But both the dynamics and the rheology are non classical: the relaxation time and the viscosity have molecular weight dependences that are more important than for linear polystyrene for instance. Under uniaxial applied strain, the rate of deformation of a single chain is constant, but smaller than for the macroscopic sample. This might be explained by assuming the existence of clusters. The latter are related to the existence of temporary junctions between the teeth of the combs. In the nematic phase, the deformation is also pseudo-affine. But it relaxes as a stretched exponential : the nematic interactions slow down the local relaxation of the chains (PhD thesis of V. Fourmaux-Demange).

2.2. Gels.

The work on gels dealt with their structure, in the various cases discussed below, as well as other phenomena occurring in these structures, because of their interfacial and confining properties. Therefore the study of liquid mixtures in Vycor is included in this part.

Studies concerning the structures concerned complexes made by the association of polymers, and model systems describing composite materials made of polymer and mineral charges.

Associative gels

The former gels were made in water by hydrogen bonding between polyacids and polybases. They may then be controlled by changing the pH for instance. Comparing the structures of free and of complexed chains in similar conditions allowed us to show by contrast variation that complexation is stoichiometric, and that complexed chains are tightly bound together and have compact structures.

Gels may also form, as for instance in methyl-cellulose, by associating chains with hydrophylic and hydrophobic sequences. Agregation in this case was considered in the dilute regime, where gelation is not possible, and where phase separation may eventually occur and be studied. This was done as a function of temperature by SANS and by elastic and quasi-elastic light scattering. The results indicate that there is a wide distribution of masses that decreases as a power law with increasing masses. However the aggregates are not self-similar because growth and local densification occur together.

Composites

Model composite materials are made with two types of spheres, respectively made of silica and of nanolatex. The degree of aggregation is also controlled by pH. The composites were studied by SANS and by rheological measurements for various sizes and stretching. The results are currently being interpreted with a computer simulation.

Confining effects

Two applications were considered. Both show the confining effects in gels. They show its influence on a first and a second order transition. SANS allows us to follow the processes in a confining medium because it is easy to eliminate its contribution to the scattering.

The confining effect of gels in crystalline nucleation of a protein - lysozyme- was studied. It may lead either to a promoting or to an inhibiting effect.

Agarose gel is in the first class. It was shown by SANS that the gel is an inert medium for the protein, and that aggregates with sizes larger than 500 Angström are present, as in solutions. But as one lowers temperature, their number becomes larger in a gel.

Silica gels belong to the second class. It was shown that a fraction of the molecules adsorb on the inner surface of the gel. It was possible to determine by SANS the effective fractal dimension of this adsorbed layer. When the solution is under saturated, the dimension is that of the gel. By increasing oversaturation, the dimension increases and goes to a limiting value on the order of 3.4. Because of this adsorption, the concentration in the solution decreases, and this may explain the decrease of the nucleation rate. Crystal growth seems to be related to desorption.

Vycor glass was used for its confining properties to study by SANS a critical mixture of alcane and perfluoroalcane. The temperatures that were considered were both above and below the critical temperature of the mixture. The latter has the interesting property that both components have very similar wetting properties. The results seem to indicate that the latter do not play a central role. The observed signal is interpreted as the sum of an Ornstein- Zernicke contribution, and another one related to the interactions between Vycor, a superficial layer rich in one of the components and a core rich in the other one. This allowed the observation of critical fluctuations the size of which may be significantly larger than the pore size.

2.3. Polymer solutions.

Dynamics at the Theta point.

A detailed study of the dynamics of a linear chain in the vicinity of the theta temperature was made by Spin Echo. It shows that the relevant length in the semi-dilute regime is the diameter of the tube rather than the screening length. It was also shown that the local viscosity η_{loc} depends on the concentration C of the solution :

$\eta_{loc} = \eta_0 (1+BC)$, where η_0 is the solvent viscosity, and B is a constant that vanishes when the solvent becomes good.

Shearing of polymer solutions.

This is the subject of a thesis made in collaboration with ILL (PhD thesis of I. Morfin). It analysed by SANS the concentration fluctuations induced by shear, and connected them with small-angle light scattering and rheological measurements. Two regimes are found. In the first one, the fluctuations are enhanced by shear. Then, fluctuations diverge and there is a phase separation into two regions respectively rich and poor in polymers. This transition occurs either by increasing the mechanical perturbation or by lowering temperature. The latter brings the mixture at rest closer to the coexistence curve.

Polyelectrolytes.

Studies of the form factor of polyelectrolytes were extended to Sodium sulfonate polystyrene in the presence of multivalent ions, Ca^{2+} and La^{3+} . For high concentrations, trivalent ions lead to a phase separation that is attributed to interchain linking. More precisely, it is observed on the form factor that this leads to the individual collapse of the chains. The effect of Calcium ions seems to be similar, and this is more surprising because there is no phase separation in this case. But there is probably a local thickening of the chains.

We chose to select a work that is external to our group in this area. This was realized by a team of Institut Charles Sadron (Strasbourg) both at LLB and ILL and deals with polyelectrolyte star-shaped polymers (see highlights). Two peaks are observed in the scattered intensity. The first one varies as $C^{-1/3}$, and corresponds to the average distance between centers of the stars. The second one corresponds, in semi-dilute solutions, to the average screening length of the solution. In the dilute regime, it becomes the average on a star of the screening length, that decreases as one goes from the periphery of the star towards its center.

2.4. Interfaces.

Proteins and polymers at interfaces.

The work on polymers at interfaces also considered macromolecules with biological origin, namely lipase and beta casein. The first one is an enzyme with an activity that increases significantly at the oil/ water interface. Neutron reflectivity experiments show that the enzyme is adsorbed, and that the superficial layer has the size of the molecule. In the presence of an anionic surfactant, SDS, the layer does not change, thus indicating that there are few interactions between species with same charge. In the presence of a cationic surfactant, TTAB, adsorption increases. In the vicinity of the bulk precipitation point, there appears a thick layer. This seems to imply the possible formation of complexes at the surface. For both cases, when the surfactant concentration reaches the critical micellar concentration (CMC), a small amount only of the enzyme is detected at the surface. The adsorbed layer becomes dilute, and its width becomes on the order of five times that of lipase alone. A possible interpretation is in terms of unfolding of lipase.

The adsorption of a thermosensitive polymer, poly(N-isopropylacrylamide) (PNIPAM), in the presence of SDS has also been studied at the air/ water interface (PhD thesis of B. Jean). The adsorbed layer density increases with temperature, an effect due to a decrease in the solvent quality. In the presence of SDS, adsorption of PNIPAM is modified above the critical aggregation concentration (CAC). The polymer is then progressively displaced from the surface at all temperatures studied. The concentration profiles suggest the presence of micellar- surfactant complexes in the adsorbed layer (see highlights).

Beta casein is a naturally unfolded protein, which adsorbs at the air/water interface. A simplified model was studied. Assuming a symmetrical structure of hydrophilic and hydrophobic sequences, it was possible to get a phase diagram in a temperature concentration plane. The various measurable quantities as well as the structure of the protein were determined in all the regimes of this diagram.

Polymers at the surface of vesicles.

Finally, polymers were grafted on vesicles in order to study their stability and their sizes as a function of the chains and of temperature. The radius increases as one heats the system, without changing noticeably the polydispersity. The characteristic time for growth decreases as membrane concentration increases. This implies a fusion of the latter. The temperature dependence may be explained by the existence of a potential barrier related to the existence of grafted chains. Addition of macromolecules leads to the formation of micelles, and to the destruction of vesicles. It seems that large masses have smaller perturbation effects on membranes. This might correspond to an effect predicted by Lipowsky, where isolated grafted chains create a tension effect in the membrane.

Polymer-polymer interfaces.

Finally, we studied the interface between a polymer melt, where the chains are free, and a network, where they are interconnected (PhD thesis of G. Bacri). The characteristics of the network (mesh size) and of the melt (length of the chains) are controlling the width of the interface. The aim of this work is to study the extent to which a modification of the width of the interface changes its mechanical properties, and more precisely its resistance to fracture (see highlights).

3. PERSPECTIVES.

In **Biology**, we intend to continue the following soaring activities :

i)-Denaturated states of proteins.

We will compare denaturation in various conditions:

- 1) by a chemical agent, namely guanidinium chloride,
- 2) by heating up or cooling down,
- 3) by pressure, which has hardly been studied.

Both the structure and the dynamics of the native and unfolded states will be studied by neutron and X-ray scattering techniques. Circular dichroism, static and time-resolved fluorescence, Differential Scanning Calorimetry and Fourier Transform Infra-Red techniques will be associated with the previous ones.

Kinetic studies will also be made in the presence of chemical denaturing agents, in order to characterise the intermediate states during denaturation and renaturation of a protein such as NCS, that we already studied.

ii)-Structure-dynamics- function relationship

This will be considered for soluble as well as for membrane proteins. The aim is the identification of those motions that are important for the function of the protein. We will use quasi-elastic and inelastic scattering of neutrons with selectively deuterated biological samples. This is a promising method for the identification of the motions in the pico- to nano-second time scale. NMR, Infra-Red (IR) spectroscopy and Raman will be associated. These perspectives depend crucially on the obtention of selectively deuterated biological samples. This is becoming easier with the growing interest of the biologists for the dynamics- function relation, that might explain some not so well understood properties of their systems.

For soluble proteins, we will take advantage of the possible studies of coupled effects hydration water/dynamics by coherent inelastic X-ray scattering.

The systems that will be studied are soluble photosynthetic proteins (C-phycocyanin) and membrane proteins, reaction centers and light harvesting proteins, hyperthermophilic and barophilic proteins (transcarbamylase aspartate), parvalbumin, and hemoglobin.

iii)-Molecular dynamics simulations.

Computer simulations by molecular dynamics will be continued, in collaboration with A. Petrescu (Romania) and J. Smith (Heidelberg). A project about the slow dynamics in the nanosecond scale within the Physics and Chemistry of Living Objects Programme (CNRS) is being set up in collaboration with G. Kneller (Orléans).

We will always work in physiological conditions, in close collaboration with various teams of biologists.

In the field of polymers, the following activities will be developed :

Collaboration with ICS (Strasbourg) for the study of the **dynamics of grafted fullerenes**, with various geometries (stars, dumb-bells, ..). The dynamical structure factors will be measured by Spin Echo technique. They exhibit a minimum for a scattering vector that corresponds approximatively to the cross-over between the global translation and the internal modes. This a new topic.

Study of [reinforced polymers](#). This is in a growth stage. It aims at mimicking reinforcement of polymers by solid mineral charges, and at studying model composite systems.

[Adhesion](#) between two polymer layers is studied by coupling mechanical measurements of the adhesion energy and interfacial profiles by neutron reflectivity and ion beam measurements. With the latter techniques, one may follow the penetration of the chains from one layer into the other one. The relation with the resistance of the interface should allow us to determine whether the interfacial chains play the role of connectors between both layers.

The experimental and theoretical studies of [multiblock copolymers](#) at interfaces will be continued. These will be made by local and outside LLB experimentalists for the studies about beta-casein. There should also be studies on synthetic copolymers manufactured by Elf-Atochem.

Studies of [polymers grafted on vesicles](#) will also be continued, in order to understand the consequences of grafting both on the structure of the polymers and of the vesicles.

INFLUENCE OF THE NEMATIC ORDER ON RHEOLOGY AND CONFORMATION OF STRETCHED COMB-LIKE LIQUID CRYSTALLINE POLYMERS.

V. Fourmaux-Demange¹, A. Brûlet¹, F. Boué¹, P. Davidson², P. Keller³, L. Hilliou⁴,
P. Martinoty⁴, J.P. Cotton¹

¹Laboratoire Léon Brillouin (CEA-CNRS) ²LPS, Université Paris XI, Orsay. ³Institut Curie, Paris. ⁴LUDFC, Strasbourg

Thermotropic liquid-crystalline polymers combine the long-range orientation phases with the mechanical properties of polymers. We study **melts of comb-like liquid-crystalline polymers** in which the mesogenic part is linked as a side-chain on each unit of a flexible polymer (see Fig.1). The understanding of **the dynamics of these materials** in the nematic phase raises fundamental questions: what is the influence of the **comb-like structure**? And what is the specific effect of the **nematic interaction** on the dynamics?

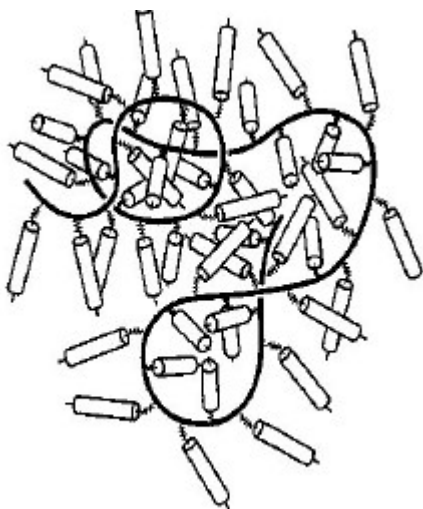


Figure 1. Schematic representation of a comb-like liquid crystalline polymer in an isotropic state.

For this purpose, we have synthesized **two isomers** of a comb-like polymetacrylate polymer (Fig.2). One polymer displays a **nematic phase** over a wide temperature range, between the glass transition temperature, $T_g=44^\circ\text{C}$, and the nematic to isotropic transition temperature, $T_{N-I}=83^\circ\text{C}$. Its isomeric form only has an **isotropic phase** above a glass transition temperature, $T_g=32^\circ\text{C}$. The comparison of the dynamics of the nematic polymer with that of its isotropic isomer and that of the linear amorphous polystyrene allows us to dissociate the contributions due to the comb-like structure and to the nematic interaction.

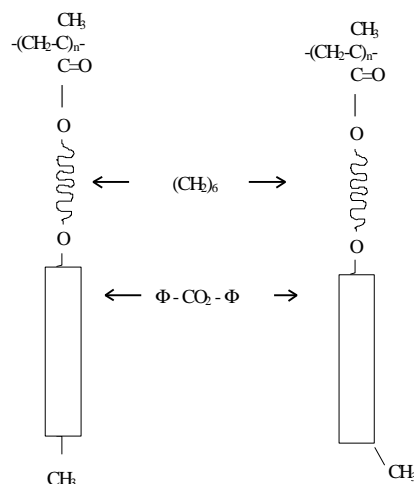


Figure 2. Chemical formula of the polymer and its isomeric form

For this study, we have associated :

- **classical rheology**, in order to obtain the characteristic times of the polymer chains both in the isotropic and nematic phases,
- **Small Angle Neutron Scattering (SANS)**, in order to measure the chain conformation relaxation after an uniaxial stretching,
- **X-Ray scattering**, in order to obtain the average orientation of the mesogenic moieties in the nematic deformed samples.

Due to an important work of synthesis and fractionation of the polymers, such a study has been performed, for the first time, on polymetacrylate chains of **well-defined molecular weights**.

In the isotropic phase, our SANS study ⁽¹⁾ shows that the conformation of the backbone of the comb-like polymers is similar to that of the linear polystyrene. Indeed, we have measured the variation of the radius of gyration, $R_g = 2.75N^{1/2}$, and the persistence length, $l_p \cong 10 \text{ \AA}$. Thus, despite the presence of a hanging group of about 23 \AA length every 2.5 \AA of monomer, the **conformation of the polymetacrylate backbone is that of polystyrene**. The local rigidity due to the mesogenic group is not transmitted to the

backbone, probably because of the flexibility of the spacer $-(CH_2)_6$.

For the dynamic study, our measurements⁽²⁾ by classical rheology (a shear of small amplitude) confirm previous results⁽³⁾ and show only little differences between the complex modulus curves (G' , G'') in the isotropic and nematic phases. A time/temperature superposition can be established across the isotropic to nematic transition leading to unique master curves for the complex moduli (see Fig.3). The absence of a rubber plateau on these curves for polymers with degrees of polymerization N in between 40 – 1000, shows that **these comb-like polymers are not entangled**. For linear polystyrene, the average number of monomers between two neighboring entanglements is 180. Nevertheless, the observed dynamics is different from the Rouse dynamics expected for free chains. Indeed, the terminal times varies as $\tau_{ter} \propto N^{2.6}$ instead of $\tau_{ter} \propto N^2$ for a Rouse dynamics, the viscosity $\eta_0 \propto N^{1.3}$ and not $\eta_0 \propto N^1$. These results suggest a **more collective dynamics for the comb-like polymers than for linear polystyrene**.

The SANS experiments⁽⁴⁾ allow us to describe the chain conformation of the deformed samples by two parameters: λ_p , the global chain deformation and p , the number of monomers of locally relaxed sub-chain. For a linear polymer in a Rouse regime, the chain deformation is affine (λ_p is equal to λ_s the deformation ratio of the sample) and p increases with the relaxation time t_R as $p \propto t_R^{1/2}$. For the isotropic comb-like polymer, the chain deformation λ_p remains constant, but is smaller than the sample deformation λ_s : **the chain deformation is pseudo-affine**. Meanwhile, the p values increases as $p \propto t_R$. To explain these results, we assume the existence of **living clusters made of temporary junctions between teeth of the comb**. The chain dynamics observed in the isotropic phase involves movements more rapid than a simple Brownian motion. If such effects probably come from specific interactions between teeth of the comb, their exact nature is still an open problem.

In the nematic phase, the chain deformation is also pseudo-affine as in the isotropic phase. But here, when the relaxation time increases, the chain deformation decreases as a stretched exponential function of the rheological terminal times (τ_{ter}) (see Fig.4).

The p values are small, and remain constant; they

only depend on the stretching temperature. We observe a slowing down of the chain dynamics. The **nematic interaction hindered the local relaxation of the chains**; the lifetime of the junctions is strongly prolonged. Therefore, the chain relaxation is the same at all scales.

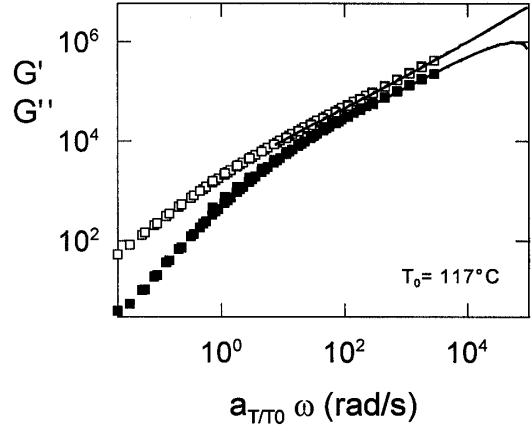


Figure 3. Master curves of the complex moduli G' G'' (unit : Pa) obtained from the time temperature superposition of the measurements obtained for the polymetacrylate polymer in the nematic phase (lines) and in the isotropic phase (G' (full symbols), G'' (open symbols)). a_T/T_0 are the shift factors. The reference temperature T_0 is 117°C.

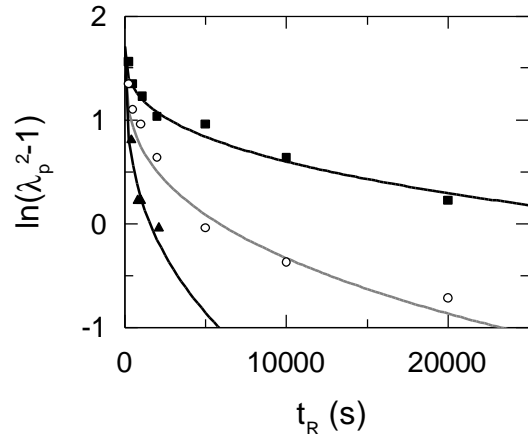


Figure 4. Relaxation of the global chain deformation of the nematic polymetacrylate of three different molecular weights. (square) $M_w=260\,000$; (o) $M_w=130\,000$; (triangle) $M_w=75\,000$. The full lines are the fits to a stretched exponential $\exp[(-t/\tau_{ter})^{0.35}]$. The exponent, 0.35, shows that the nematic interaction slows down the chain relaxation processes.

[1] Fourmaux-Demange, V.; Boué, F.; Brûlet, A.; Keller, P.; Cotton, J.P. *Macromolecules* **31** (1998) 801.

[2] Fourmaux-Demange, V.; Brûlet, A.; Cotton, J.P.; Hilliou, L.; Martinoty, P.; Keller, P.; Boué, F. *Macromolecules* **31** (1998) 7445.

[3] Colby, R.H.; Gillmor, J.R.; Galli, G.; Laus, M.; Ober, C.K.; Hall, E. *Liq. Cryst.*, **13** (1996) 233

[4] Fourmaux Demange V., Thèse, University Orsay.1998.

RELATION BETWEEN THE PROFILE AND THE MECHANICAL STRENGTH OF AN INTERFACE BETWEEN TWO POLYMERS.

G. Bacri¹, M. Geoghegan², A. Menelle¹, C. Creton³, F. Abel⁴, F. Boué¹

¹Laboratoire Léon Brillouin, CEA Saclay, 91191 Gif/Yvette

²Lehrstuhl für Physikalische Chemie II, Universität Bayreuth, D-95440 Bayreuth

³Laboratoire PCSM, ESPCI, 10 rue Vauquelin, 75231 Paris Cedex 05

⁴Groupe de Physique des Solides, UMR 75 88, 2 place Jussieu 75251 Paris Cedex 05

The understanding of the mechanical resistance of an interface between two polymers is very important for the control of adhesion, fracture and interfaces/interphases in composites polymer systems. Industrial applications are numerous. Here we focus on elastomers, which are often present in these systems. We are interested in the relation between :

- the profile of an interface created between two polymer layers. If one layer is made of perdeuterated polymer, and the second of non-perdeuterated polymer, neutron reflectivity gives access to this profile on the 10 Å to 100 Å scale ;
- and the mechanical strength of such an interface, measured using the razor blade test (from 2 to 300 J/m²).

We have considered the three cases where none of the layers, one or both are cross-linked. The chains are always polystyrene. In the absence of cross-linking, we have a polymer melt, which is liquid above the glass transition $T_g=100^\circ\text{C}$. With cross-linking we have a statistical network, where the cross-links are distributed at random. We characterize it by the average number of units between two successive cross-links, N , obtained from chemical titration.

Making the sample (Figure 1).

The samples for the two methods have been done in order to get interfaces as similar as possible.

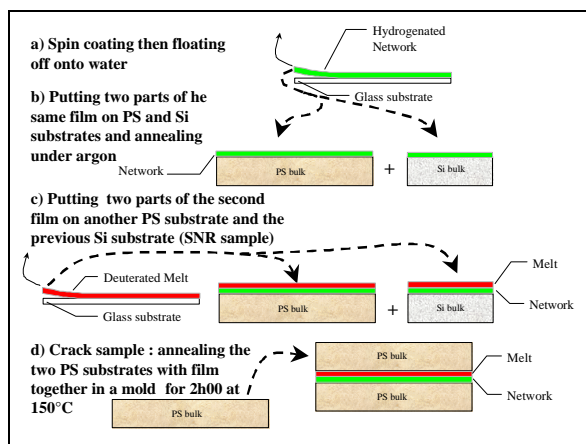


Figure 1. Making the sample

The layers, with thickness of several thousands Å, are made by spin coating on glass a polystyrene solution, or from aminomethylated polystyrene, which is

chemically cross-linked during and after the drying process (Figure 1a). Each layer is removed from the glass by immersion into water (floating). We divide it in two halves (Figure 1b).

For neutron reflectivity, one deuterated half is deposited onto a Silicon wafer, annealed, then a non perdeuterated half is floated on top (Figure 1c). The sample can be annealed for a time t_R .

For the razor blade test, each of the two halves is floated on a thick polystyrene plate (2mm). After a first annealing, the plates are pressed against each other in order to form a 4-fold sandwich, during a time t_R (Figure 1d).

In both cases the interface can be studied as a function of the annealing time t_R .

Neutron reflectivity data (Figure 2)

They are obtained on the time-of-flight spectrometer EROS of LLB, for two angles θ (1.3° and 1.5°) with wavelengths in the range 4 Å to 25 Å. We take advantage of the difference in effective index between perdeuterated and non perdeuterated polymers. We have simulated the reflectivity by a profile of concentration in deuterated polymer, which is close to symmetric, by the error function from the classical laws of inter-diffusion. We give in Figure 2 the equilibrium widths σ , when the profile does not spread anymore with increasing annealing time, for the diffusion of polystyrene chains into a polystyrene network for N around 250.

In a first regime of low molecular weight M , the chains diffuse inside the network by more than their own size: $\sigma > R_g$. In the corresponding intermediate stages, we can measure the diffusion coefficients directly from the widening of the interface with time. We observe that the chains are noticeably slower than in a melt.

In a second regime of larger molecular weight, σ is lower than the global size of the chain ($\sigma < R_g$). The large chains do not penetrate completely because their entropy of mixing becomes too low to balance the elastic deformation energy due to their presence in the network. The limit size of the interface is close to that of a polymer strand between two cross-links (i.e. a piece of chain of N units).

Thus, by varying N or the molecular weight, we have the possibility of tuning at will the interfacial width, and to see its effect on adhesion between the layers.

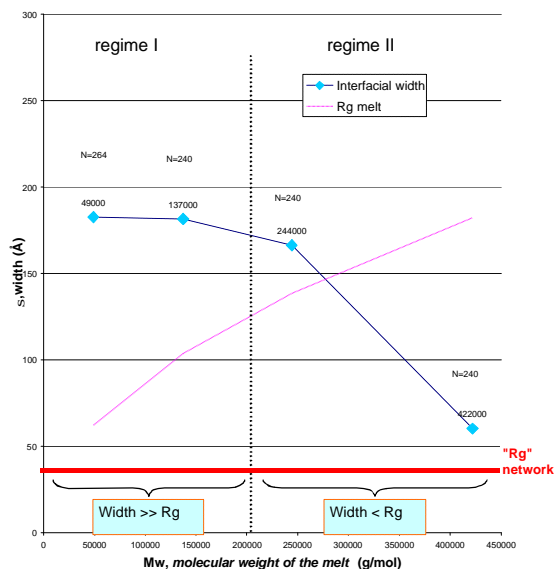


Figure 2. Neutron reflectivity data showing variation of the interfacial width s versus the molecular weight of the melt, M_w .

Razor blade test data (Figure 3, 4, 5).

In order to measure the adhesion energy, we insert a razor blade in the symmetry plane of the 4 fold sandwich, between the two polymer layers (Figure 3). The thick plates are here to store some elastic energy of bending, which will transfer into a plastic zone of deformation at the tip of the fracture. The distance a between the blade and the tip (measured after waiting 24 hours) gives the surface energy G (J/m^2).

Figure 3. Razor blade test

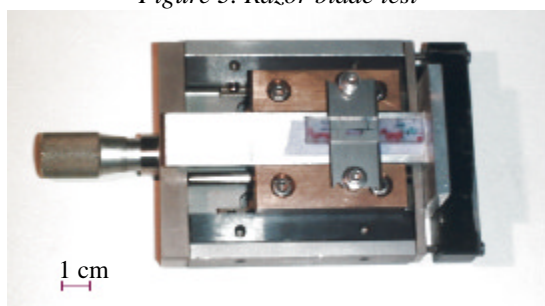


Figure 3a : picture of the experimental test

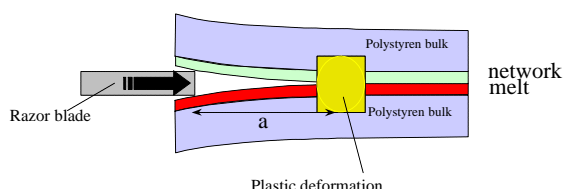


Figure 3b : diagram of test

After that the fracture has completely propagated, we can control by ion beam tests the amount of deuterium on both sides of the fracture. Thus we can check whether the fracture propagates between the perdeuterated and non-perdeuterated layers. We have also made microscopy observations of the tip zone (Figure 4): the usual propagation is by a stick slip process: one has deviation with respect to the symmetry plane (an asymmetric mode called 2), until

a new fracture restarts in the symmetry plane. One can also observe interference fringes ahead of the tip, in the craze region (polymer-specific cracks made of fibrils of chains).

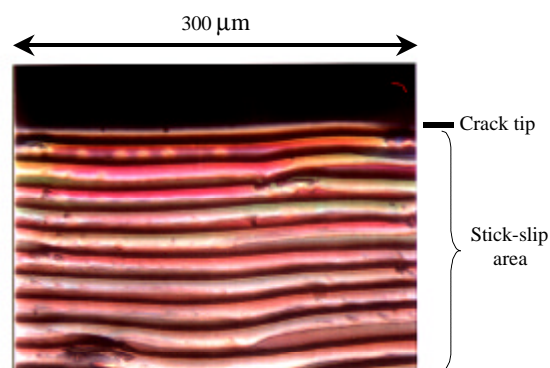


Figure 4. Top view of a crack sample made of a melt ($M_w = 40700$ g/mol) and a network ($N = 235$ units between cross-links).

Figure 5 shows that in the molecular weight range I of Figure 2, the toughness G increases. This could be explained by the increasing degree of entanglement of a longer chain inside the network (indeed it is observed for two uncross-linked layers that G increases with s). Conversely, in regime II ($R_g > \sigma$), this effect should stop since the width s stops increasing. However, we see in Figure 5 that G keeps increasing. As an explanation, we only see at the moment the viscoelastic dissipation, which increases with molecular weight, or a kind of “knotting” of the long chains at the interface (see below).

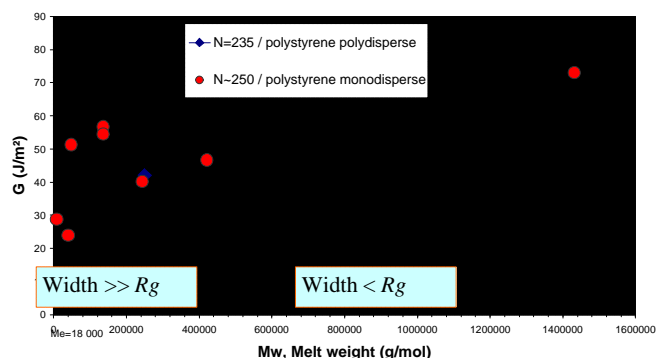


Figure 5. Plot of the toughness of the interface versus the molecular weight of the melt, M_w , static measurements

In summary, we are able to vary the interfacial width in some equilibrium conditions, which gives us a way to observe the influence of this width on the interfacial strength. It seems that the width is not the only driving parameter. Another one could be the configuration of the chains at the interface: a simplistic idea is the formation of loops by long chains in and back out of the network. We plan now to use different degrees of cross-linking in order to vary this configuration.

INTERACTION OF A THERMOSENSITIVE POLYMER WITH SURFACTANT AT THE AIR-WATER INTERFACE

B. Jean¹, L.T. Lee¹, B. Cabane²

¹Laboratoire Léon Brillouin (CEA-CNRS)

²PMMH, ESPCI, Paris

The ability to trigger a strong response with a low-level stimulus is one of the remarkable features in soft condensed matter. In colloidal systems, these responses may be expansion or collapse of a macromolecule, dispersion or self-assembly of small molecules and specific binding or unbinding between two components. The common external parameters that can generate these transitions in behavior are temperature, solvent quality, pH, specific ions and the action of a force field. For instance, there is a family of polymers which is soluble in water at low temperatures but phase-separates out of water when heated above a critical temperature, T_c . A particularly interesting example of this family of thermosensitive polymers is poly(N-isopropylacrylamide) (PNIPAM), that has an expansion-collapse "switching" temperature at 33 °C, near the body temperature. This makes it biologically important, with potential applications^[1] which include immunoassay technology and enzyme isolation where a two-phase partitioning technique is used to separate antigens and enzymes. Another important application which involves the coil-globule collapse is rate-controlled drug release. As a general viscosity modifier, its thermosensitivity provides an additional controlling parameter compared to other polymers.

Our interests lie in the applications of PNIPAM to systems that contain interfaces, such as emulsions, foams and dispersions, where the interfaces are frequently stabilized by adsorbed polymer layers. In such systems, surfactants are usually present. Therefore a relevant question is how the adsorbed polymer may be modified by other surface-active molecules. In this case, changes may occur directly at the interface where the polymer and surfactant may compete for adsorption sites or, they may mutually enhance their adsorption. Alternatively, changes may arise from interactions of the two species in the bulk phase, modifying the chemical potential of the adsorbing species and the equilibrium between the bulk and the surface. Indeed, it has been shown that PNIPAM interacts very strongly with an anionic surfactant, sodium dodecyl sulfate (SDS) in solution, resulting in a shift in the T_c to higher temperatures^[2].

In this work, we investigate the effects of such interactions at the air-water interface. There are two main points of interest: firstly, how will PNIPAM adsorption be affected by the presence of SDS? Secondly, are their interactions and their resulting structural properties in solution reflected by those at the interface? To address these questions, we have used neutron reflectivity to determine the properties of the adsorbed polymer layers. Neutron reflectivity, coupled with isotopic substitution where the index of refraction of a component can be adjusted to match that of the solvent, is the only technique which allows the study of individual components in a mixed surface layer.

Figure 1 shows the sensitivity of neutron reflectivity to the presence of adsorbed PNIPAM at the air-water interface. The figure shows the normalized reflectivity, R/R_f , versus the momentum transfer, Q . R_f is the Fresnel reflectivity of the pure solvent. In this representation, any deviation from $R/R_f=1$ is due only to the adsorbed polymer layer: the larger the deviation, the higher the amount of polymer adsorbed. These reflectivity curves also show the sensitivity of PNIPAM adsorption to temperature - an increase in temperature increases adsorption, a result due to a decrease in solvent quality. The continuous lines are the best-fits to the data using the concentration profiles shown in the inset. The profile consists of a thin monomer-rich zone near the surface followed by a central diffuse zone. As temperature increases, the monomer-rich zone becomes thicker and the central zone increases in density. Only a small increase in the overall thickness of the adsorbed layer is obtained.

The effect of surfactant on the adsorption of PNIPAM was investigated using SDS whose refractive index is matched to that of the solvent, allowing only the signal from the polymer to be registered. In Figure 2, the adsorption density of PNIPAM, Γ_p , obtained by integration of the concentration profile, is shown as a function of SDS concentration, C_s . At low C_s , PNIPAM adsorption is unaffected; at high C_s , it decreases progressively until very little polymer is left at the surface. Interestingly, the surfactant concentration at which Γ_p starts to

decrease corresponds to the critical aggregation fluorescence technique (2), where the surfactant interacts with the polymer in the bulk phase. This loss of polymer from the surface is observed even at high temperatures where the steep rise in adsorption is attenuated and pushed to higher temperatures (Figure 3).

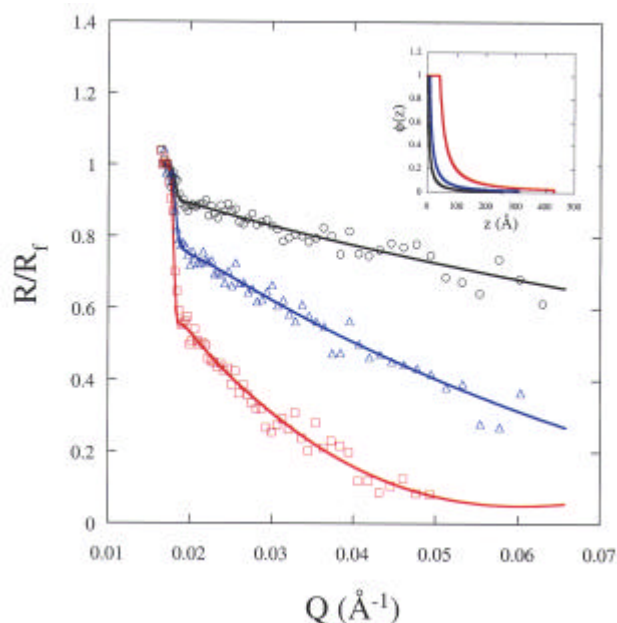


Figure 1. Normalized reflectivity of PNIPAM ($M_w = 165$ K) adsorbed at the air-water interface at $T=20.2$ °C (black circles), $T=28.2$ °C (blue triangles) and $T=31.2$ °C (red squares). The solid lines are best-fit curves using the concentration profiles shown in the inset.

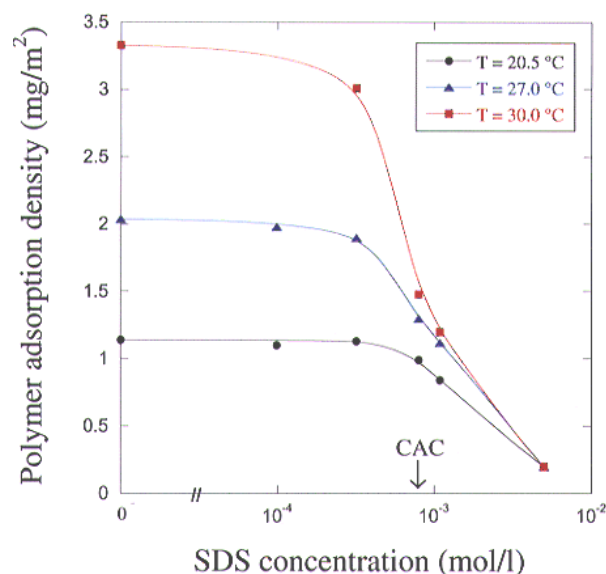
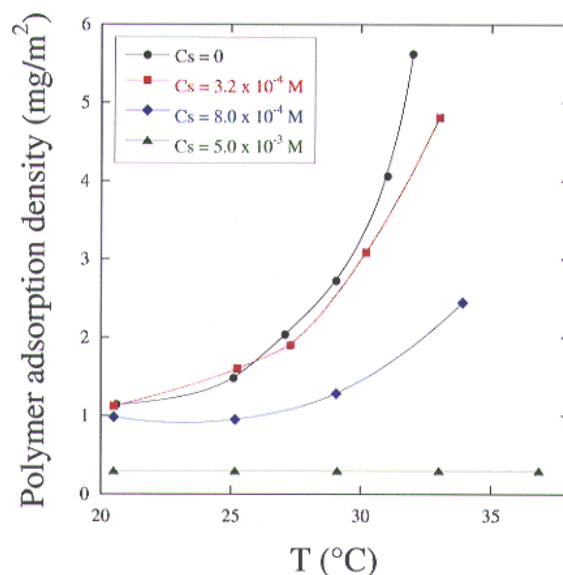


Figure 2. Effect of SDS on the adsorption density of PNIPAM.

Two possible reasons can account for the loss of polymer from the surface: it is displaced by an increasing surfactant pressure, or, it is depleted

concentration (CAC), as measured by

from the surface due to complexation with surfactants in the bulk solution. However, surface tension results show that in the range of C_s where the polymer is displaced, the surface pressure of the polymer layer is greater than that of the SDS. This fact strongly suggests that the loss of polymer from the surface is related to polymer-surfactant complexation in the bulk. Such complexes have been studied using small angle neutron scattering^[3]. It is found that above the CAC, the mixed aggregate has a "necklace" structure consisting of several micellar aggregates adsorbed on a polymer chain (Figure 4). Above T_c , the phase-separated PNIPAM is resolubilized by SDS in two steps: at low C_s , the precipitated polymer is dispersed into colloidal particles, and at high C_s , these particles are solubilized



into charged "necklaces".

Figure 3. Effect of temperature on the adsorption density of PNIPAM in the presence of SDS.

At the surface, the loss of polymer above the CAC can therefore be attributed to the formation of charged polymer-surfactant "necklaces" in the bulk phase. In this case, what is the structure of the polymer that is left at the surface? Is the charged "necklace" structure observed in the bulk conserved at the surface? The concentration profiles in Figure 5 show that in the absence of surfactant, an increase in temperature produces a dense adsorbed layer due to reduced excluded-volume interactions between monomers. At the same temperature in the presence of SDS, a diffuse layer is obtained. This result suggests strongly the presence of micellar aggregates, the repulsions of which decrease the monomer

packing density in the adsorbed layer even at raised temperature (Figure 6).

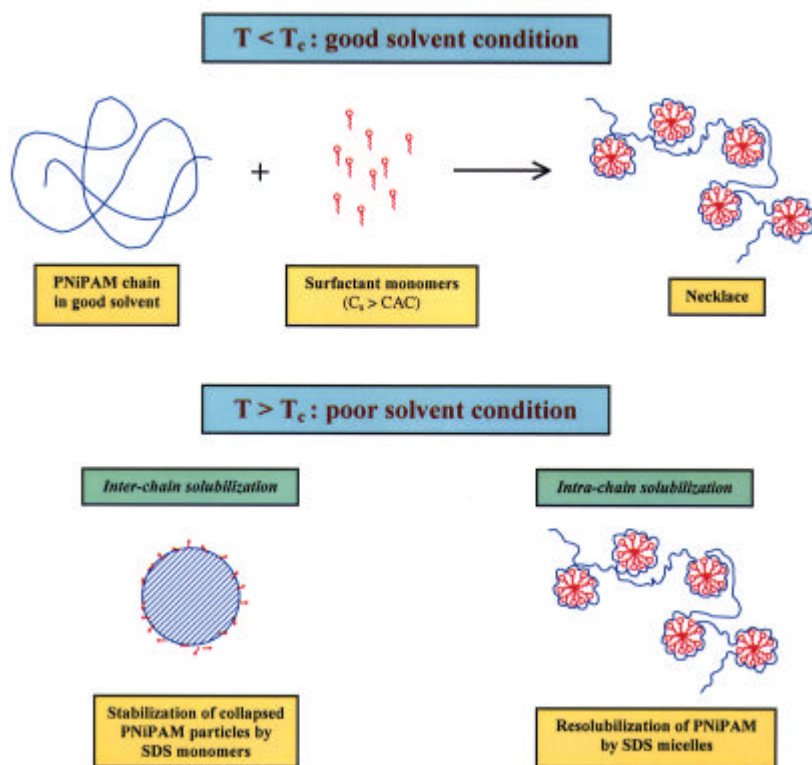


Figure 4. Interaction of PNIPAM with SDS in solution below and above the critical temperature T_c .

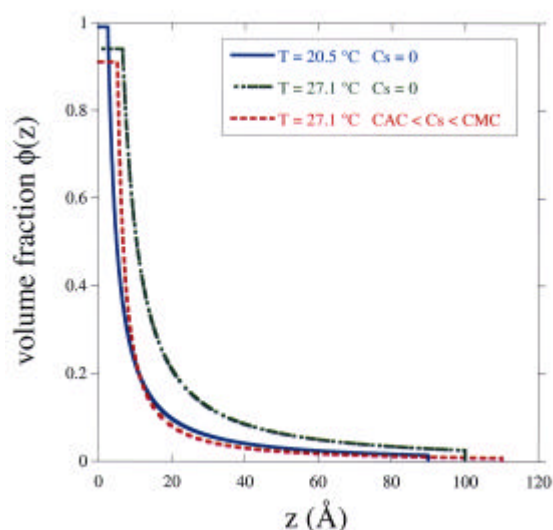


Figure 5. Concentration profiles of adsorbed PNIPAM: effects of temperature and surfactant (CMC = Critical Micelle Concentration).

In summary, PNIPAM adsorption at the air-water interface is very sensitive to small variations in temperature. In the presence of SDS, the polymer is progressively displaced from the surface due to formation of charged polymer-micelle "necklaces" in solution. Furthermore, the sensitivity of the polymer adsorption to temperature is attenuated and pushed to higher temperatures. This behavior parallels the solubilization of PNIPAM by SDS in the bulk phase and the resulting elevation in T_c . Therefore, PNIPAM-SDS interaction at the surface reflects that in the bulk solution. The concentration profiles of the adsorbed polymer show that diffuse or dense layers can be obtained, depending on the temperature and surfactant concentrations. Therefore, it is possible to modulate the T_c of PNIPAM by addition of SDS, and to control the molecular structures of the polymer both in solution and at the surface: swollen coil or collapsed globule in solution, and diffuse or dense adsorbed layers at the interface. This permits a great flexibility in tailoring the transition of the molecular structures of the thermosensitive polymer to specific uses both in solution and at interfaces.

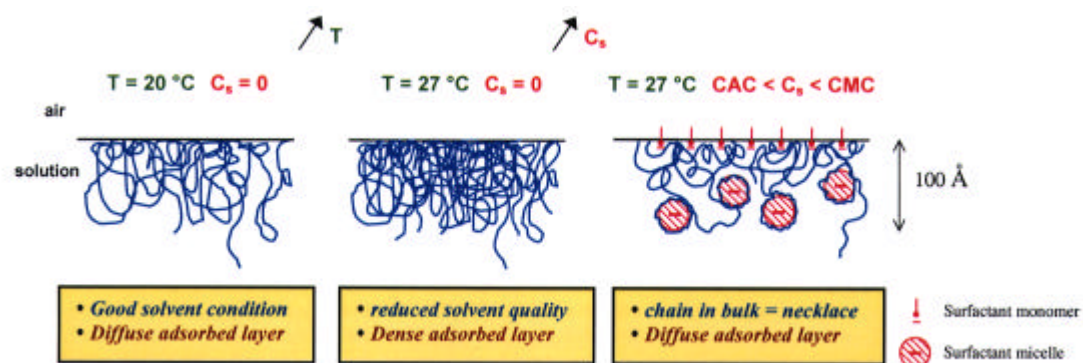


Figure 6. Structure of adsorbed layer of PNIPAM at the air-water interface: effects of temperature and surfactant.

References

- [1] H.G. Schild, Prog. Polym. Sci. **17** (1992) 163.
- [2] H.G. Schild and D.A. Tirrell, Langmuir **7** (1991) 665.
- [3] L.T. Lee and B. Cabane, Macromolecules **30** (1997) 6559.

STRUCTURE FUNCTIONS OF STAR-BRANCHED POLYELECTROLYTES

M. Heinrich, M. Rawiso, J.G. Zilliox

Institut Charles Sadron, CNRS-ULP, 6 rue Boussingault, 67087 Strasbourg cedex

Unusual structure functions have been measured for salt-free aqueous solutions of sodium sulfonated polystyrene (NaPSS) star-branched polyelectrolytes. Whatever the concentration, they display two kinds of maxima (figure 1). The first is related to a position order between star cores. It covers a main maximum at q_1^* and a further harmonic at $\sqrt{3}q_1^*$ for the lower concentrations in the dilute regime. The second comes into sight at higher q values. It involves one maximum at q_2^* , quite similar to the broad halo observed in the scattering pattern of a semidilute aqueous solution of NaPSS linear polyelectrolytes. It is therefore associated with a correlation hole of electrostatic character.

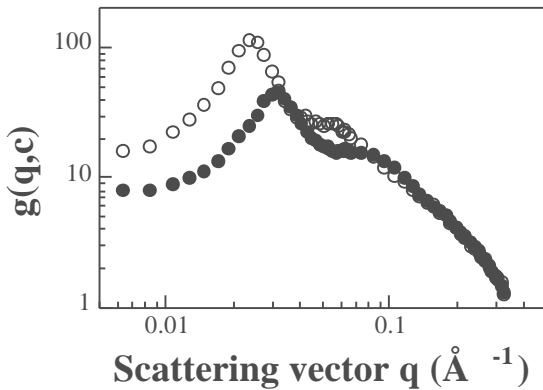


Figure 1 : Structure functions of NaPSS star solutions obtained on the spectrometer PACE at LLB

The NaPSS star sample corresponds to $f=12$, $N_a=100$ and $t_s=1$. Two concentrations are considered : $c=0.102 \text{ mol.l}^{-1}$ (open circles) ; 0.258 mol.l^{-1} (dark circles)

The variations of q_1^* and q_2^* with the monomer concentration c allow to stress the difference in nature of these maxima (Figure 2).

q_1^* almost scales as $c^{1/3}$ with prefactors depending on the star functionality f and the arm degree of polymerization N_a . No dependence upon the arm degree of sulfonation t_s , has been found in the t_s -range providing solubility of the NaPSS stars. Obviously, such results support the close relation between q_1^* and the mean distance between star cores ($d = 2\pi/q_1^*$), i.e.

the short or long range order character of the first maximum.

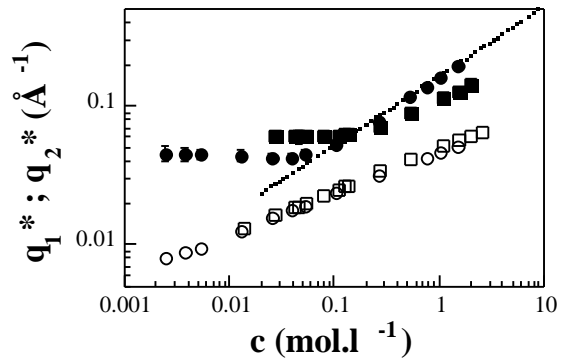


Figure 2 : Scattering vectors q_1^* and q_2^* associated with the main maxima of the NaPSS star structure functions

Two NaPSS star samples are considered. They have the same functionality ($f=12$) and arm degree of polymerization ($N_a=100$), but distinct t_s values. Open circles and squares correspond to q_1^* values measured for $t_s=1$ and 0.65 , respectively. Dark circles and squares correspond to q_2^* values measured for $t_s=1$ and 0.65 , respectively. The scaling law related to the electrostatic peak of NaPSS linear polyelectrolytes in semidilute aqueous solutions is also reported for $t_s=1$ (dotted line)

The c -dependence of q_2^* is quite different (q_1^* and q_2^* are therefore not commensurate). In the dilute regime ($c < c^*$), q_2^* is found to be constant, only depending on N_a and t_s . On the other hand, in the semidilute regime ($c > c^*$), q_2^* scales as c^α with α in between $1/3$ and $1/2$, according to the t_s value. Moreover, it is unaffected by any change in N_a . Such scaling laws fit those associated with the position q^* of the broad peak characterizing the structure functions of NaPSS linear polyelectrolytes in semidilute aqueous solutions. The second maximum of the NaPSS star structure functions is therefore primarily due to the existence of a correlation hole (or tube) surrounding each polyion, from which the others are expelled by the electrostatic repulsion. For $c > c^*$, it mainly corresponds to the semidilute solution formed by the interpenetration of stars and q_2^* yields its mean mesh size ξ or the Debye-Hückel screening length κ^{-1} (isotropic model). For $c < c^*$, it still represents the

electrostatic repulsion between arms. However, in that case, it is exclusively concerned with arms belonging to the same star. It is indeed a simple intramolecular feature, as demonstrated by using the zero average contrast method. Then q_2^* yields an effective screening length κ^{-1} , through the relation $q_2^* \propto \kappa$, which gives an information about the condensation of counterions inside each star. From this point of view, it is not really surprising that q_2^* is almost constant in the dilute regime. However, the results presented in figure 2 also

show that the counterion condensation inside each star increases as τ_s decreases. On the other hand, the variation of q_2^* with N_a is in agreement with the existence of an internal screening length distribution. Finally, the distinct behaviours of q_2^* in both the dilute and semidilute regimes provide a way to estimate the overlap concentration c^* .

A. Gall^{1,2}, S. Dellerue^{1,2}, B. Robert², M.-C. Bellissent-Funel¹

¹Laboratoire Léon Brillouin (CEA-CNRS)

²Section de Biophysique des Protéines et des Membranes and CNRS/URA 2096, CEA/DSV/Saclay, 91191 Gif-sur-Yvette

Introduction.

All cellular processes, whether in prokaryotes or eukaryotes, at some stage require proteins which may be located either in the cytosol or in membranes. As a result, many different laboratories now study the function and structure of proteins. This is mirrored in the Protein Databank (PDB) where over 8700 X-ray crystal structures of proteins have been deposited. It is currently agreed that about 30% of the total number of proteins in any organism are integrated into membranes. Unfortunately, less than 1% of all the PDB X-ray crystal structures are from membrane proteins. Therefore, any information pertaining to the function, dynamics and structure of a membrane protein is invaluable.

The aim of this project is to understand the detailed energetics of membrane protein folding, and to establish a precise relationship between the structure, function and dynamics of this class of biological macromolecule, including inter- and intra-protein interactions. Therefore, it is necessary not only to know their three-dimensional structures, but also to characterise, with the highest degree of accuracy possible, the internal motions of these proteins. Motions in proteins occur over a wide range of time scales from femtoseconds (10^{-15} s) to seconds or longer. Only a few experimental techniques permit one to study these motions. Among them, inelastic neutron scattering (INS) is capable of probing motions with characteristic times in the nanosecond (10^{-9} s) to picosecond (10^{-12} s) range. In fact neutrons interacting with molecular systems at normal temperature can exchange a significant proportion of their energy with thermal excitations and these energy changes can be readily measured by a variety of techniques. Moreover INS is a spectroscopic technique which allows to study internal motions on exactly the same time-scale that is now accessible by computer simulation.

Our membrane proteins: RC, LH1 and LH2.

We have chosen to study and compare the structural and dynamic properties of three membrane proteins involved in the primary steps of photosynthesis from purple bacteria. These proteins are called the photochemical reaction centre (RC), the core light-harvesting complex (LH1) and the peripheral light-harvesting complex (LH2). Solar energy is collected

by the bacteriochlorophyll (BChl) pigments in the LH proteins and the captured excitation energy is then transferred to the RC. Subsequent electron transfer within this protein yields a chemical potential gradient across the membrane that is used to drive many cellular processes. The proteins were chosen for study because: 1) The X-ray crystal structures of the LH2⁽¹⁾ and RC⁽²⁾ have been solved to resolutions better than 2.5 Å, and their accompanying detergent rings have been visualised using neutron diffraction experiments. 2) They are produced by the bacteria in large quantities making the biochemical purification and protein characterisation processes much easier. 3) The proteins contain BChl cofactors that serve as molecular markers which monitor protein structure and conformation. 4) Finally, they form a network of interconnecting proteins within the photosynthetic membrane (see figure 1). We can monitor the influence of inter-protein contacts on the structure-function-dynamics for each of our three proteins.

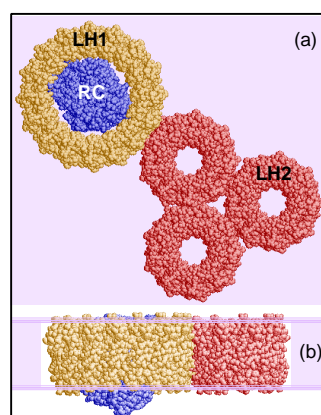


Figure 1 : A scheme of the photosynthetic integral membrane proteins from purple bacteria viewed (a) parallel and (b) perpendicular to the plane of the membrane which is coloured violet. Nearly all of the protein volumes are located within the lipid bilayer that makes up the membrane. Key to proteins : LH2, red; LH1, yellow; RC, Blue.

Principles of neutron scattering.

At this point we must remember that in INS experiment, the energy changes occurring when the incident neutrons interact with moving nuclei in the samples are measured such that an energy spectrum of scattered neutrons is obtained at each scattering angle. The fundamental quantity measured is the dynamic structure factor $S(Q, \omega)$ where Q is the momentum

transfer with $Q=(4\pi/\lambda)\sin\theta$ (λ is the neutron wavelength, 2θ the scattering angle) and ω is the energy transfer. Neutron spectroscopy takes advantage of the fact that hydrogen and deuterium have different coherent and incoherent scattering cross-sections. By varying the H/D contents between the sample of interest (e.g. a membrane protein) and its environment (e.g. the membrane) we can highlight or eliminate parts of the system. This method of *contrast variation* is one reason why neutron spectroscopy may have significant advantages over similar X-ray based techniques. The benefits of neutron techniques, which may provide information on dynamics (e.g. time-of-flight and neutron spin-echo) or give structural information (e.g. small angle neutron scattering), are illustrated by presenting three examples, one from each protein, from the wide selection of experimental results obtained at the LLB (and complementary data collected at the Institute Laue-Langevin, Grenoble).

Time-of-flight spectroscopy : LH2 in detergent micelles.

A rather unique tool used to gain experimental information on protein dynamics in the picosecond range (from 0.1 to a few hundred picosecond) is incoherent inelastic neutron scattering (IINS) which takes advantage of the large incoherent scattering cross-section of hydrogen atoms with respect to the relatively small cross-section of other constitutive atoms in proteins. A large fraction of the atoms (up to 50%) in globular proteins are hydrogen atoms, and since they are distributed nearly homogeneously within the protein molecule, IINS will thus allow protein dynamics to be characterized in a global manner by monitoring the individual dynamics (vibrations, translations, rotations) of hydrogen atoms. The fundamental quantity measured is the proton self dynamic structure factor $S_S^H(Q, \omega)$.

As an example, figure 2 shows the evolution of the $S_S^H(Q, \omega)$, as a function of ω for the LH2 protein in detergent micelles. The central part is analysed as a sum of elastic and quasi-elastic components⁽³⁾. The latter component is considered to be a Lorentzian line with a half-width at half-maximum Γ . In the top left insert, Γ is plotted as a function of Q^2 . It follows a plateau from 0.10 to 0.85 \AA^{-2} and is linearly dependent on Q^2 at higher Q^2 values. This evolution is characteristic of a diffusion in a confined volume⁽⁴⁾ whose shape is given by the elastic incoherent structure factor (EISF) (right top insert). From the high Q limit of the EISF, it appears that LH2 contains a large proportion of mobile protons (*ca.* 90%) compared to soluble proteins such as C-phycoerythrin.

This may be a consequence of the rather unique hollow ring-like structure of LH2 (see figure 1). The effect of different environments on the dynamics of the hydrophobic side chains is carried out by substituting deuterated detergent by deuterated lipids.

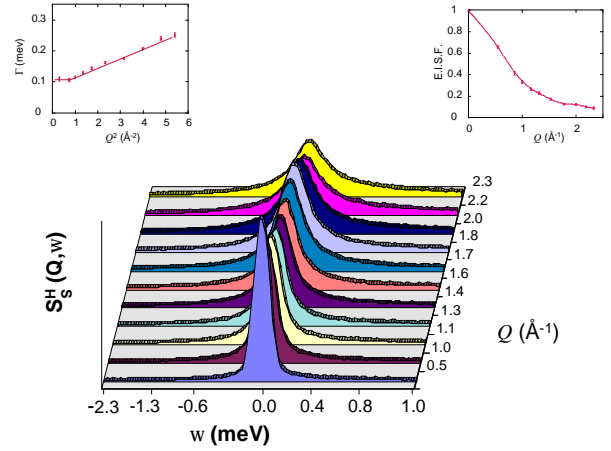


Figure 2 : $S_S^H(Q, \omega)$ of the LH2 protein in detergent micelles as a function of Q . $T=277 \text{ K}$, $\lambda=5 \text{ \AA}$. The spectra were collected with the time-of-flight spectrometer MIBEMOL. Top Left : Evolution of Γ as a function of Q^2 (see text). Top Right : Evolution of EISF as a function of Q .

Neutron spin-echo spectroscopy : Comparison between RC and LH2.

In order to study protein dynamics, *viz.* the nanosecond (10^{-9} s) time-scale, we use the neutron spin-echo⁽⁵⁾ (NSE) spectroscopy. NSE allows precise measurement of velocity changes of neutrons via Larmor precession of the neutron's spin. If several spin-echo measurements have been made on polymers, few attempts have been made to use it to probe biological samples. Here we make use of the separation in reciprocal space of the coherent and incoherent scattering to demonstrate the detection of a neutron spin-echo signal both in RC and LH2 proteins. A further advantage of the spin-echo technique is that it gives direct access to the dynamics of the sample in the time domain t by measuring the *intermediate scattering function*, $I(Q, t)$. Figure 3 gives examples of $I(Q, t)$ for the RC and LH2 proteins for two values of Q . It is evident that the coherent motions of these complexes are somewhat different. It may be observed that at $Q=0.197 \text{ \AA}^{-1}$ when time, t , approaches zero, the normalised $I(Q, t)$ for LH2 is only ≈ 0.6 indicating that the LH2 contains significantly higher levels of sub-nanosecond motions than the RC. Although having near identical numbers of amino acids (*ca.* 850), the RC and LH2 proteins have widely differing tertiary and quaternary structures. The LH2 consists of 18 independent transmembrane spanning α -helices located within 9

identical α/β -heterodimer subunits that form a hollow ring-like structure in the membrane (see figures 1 and 3). However, the RC has three much larger subunits with less overall symmetry (blue colour in figures 1 and 3). Therefore, we conclude that the overall protein motion is dependent on the quaternary structure of the protein.

The analysis of NSE data gave us access to the effective diffusion coefficient, D_{eff} of highly concentrated protein solutions which was not possible with dynamic light scattering (DLS) experiments. By comparing the results with those of dilute solutions of proteins we have demonstrated that in the case of RC the diffuse properties are invariant over a wide range of concentrations. $I(Q,t)$ is described by an exponential function, $\exp(-t/\tau)$, and $1/t = D_{eff}Q^2$. For our membrane proteins, DLS is limited to a maximum protein concentration of 0.8 mg ml^{-1} for which we have obtained a value of D_{eff} for the RC in detergent micelles of $3.7 \times 10^{-8} \text{ cm}^2 \text{ s}^{-1}$. Using the spin-echo spectrometer MESS we have measured $I(Q,t)$ over Q values between 0.055 \AA^{-1} and 0.197 \AA^{-1} and have obtained a very similar diffusion coefficient of $3.6 \times 10^{-8} \text{ cm}^2 \text{ s}^{-1}$ for higher concentrations of RC in the same detergent. We are presently investigating the role of the individual domains within these proteins by selectively deuterating different components. Other approaches include insertion within lipid bilayers and, in the case of the RC, selective subunit removal.

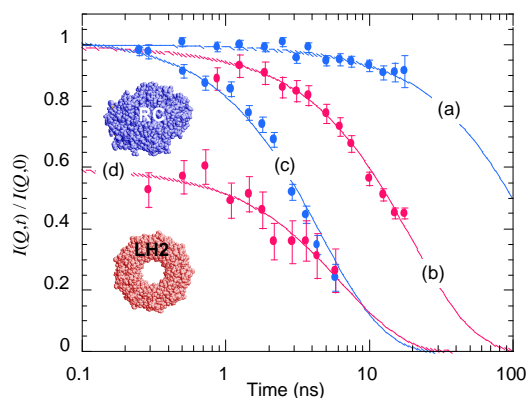


Figure 3 : The time dependence of normalised $I(Q,t)$ for the RC (shown in blue) and LH2 (shown in red) proteins at 0.055 \AA^{-1} (a,b) and 0.197 \AA^{-1} (c,d) measured at 288 K. The solid lines represent the best fits using an exponential function which may provide information on D_{eff} (see text). The spectra were collected with the spectrometer MESS. Key to proteins : LH2, red; RC, Blue.

Small angle neutron scattering : structural information on the B777 subform of LH1.

Unlike the previous two techniques which provide information on macromolecule dynamics, the *small angle neutron scattering* (SANS) technique allows us

to obtain structural information. Combining SANS techniques and H/D *contrast variation* on dilute solutions, or micro-emulsions, of biological macromolecules may provide information on the shape of the molecule *via* the *form factor* and on the interactions between the molecules *via* the *structure factor*. Although we have carried out a number of different SANS experiments on the RC and LH2 proteins in different sample environments, we have chosen to present some new structural results on our third protein, LH1.

The LH1 protein is similar in overall structure and function to the LH2. However, the number of α/β -dimers increases from 9 to 16 per ring. Let us notice that this closed ring structure may only be valid for an isolated protein. *In vivo*, it is possible that the ring may be open. An important property of the LH1 protein (also called B873) is that it is possible with detergents to progressively dissociate the ring of 16 α/β -dimers into its individual α - and β -subunits (B777), *via* an intermediate form (B820). This process is shown in figure 4 and has the added advantage of being fully reversible. Since it is possible to isolate individual RC proteins, co-purify RC-LH1 complexes and the different structural units (B777 and B820) that aggregate to form LH1, one can imagine that it is possible to attribute the influence of protein-protein contacts on individual secondary and tertiary structures.

Based on biophysical data, a theory on the thermodynamics of membrane polypeptide oligomerisation in light-harvesting complexes proposed that each B777 consists of a single polypeptide sequence with a single non-covalently attached BChl molecule ⁽⁶⁾. Recently, we decided to measure the SANS spectrum of the B777 complex in a fully deuterated detergent micro-emulsion. Figure 5 displays the data as compared with a fit using the *form factor* of an ellipsoid of length, L , of 60 \AA , with a diameter, D , of 28 \AA . The length of the ellipsoid is consistent with the distance required for the occupancy of a transmembrane-spanning α -helix. If the α -helix had unfolded it would not have given similar fitting parameters. Together with our Raman data ⁽⁷⁾, this is the first structural information that confirms the hypothesis that the B777 is made from one polypeptide containing a single membrane spanning α -helix with one bound BChl molecule. Further experiments with the B820 will allow to characterize the structural changes and the aggregation, that lead to the formation of the $(\alpha/\beta)_{16}$ membrane protein. This in turn will significantly help to improve our understanding of membrane protein thermodynamics and oligomerisation.

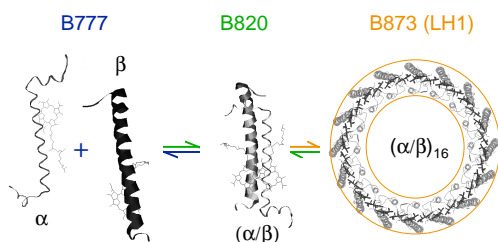


Figure 4 : The LH1 proteins are composed of a ring of 16 **a/b** dimers, each of which may be dissociated into individual **a**- and **b**-subunits. Each B777 polypeptide has a single non-covalently attached BChl that is responsible for capturing solar energy.

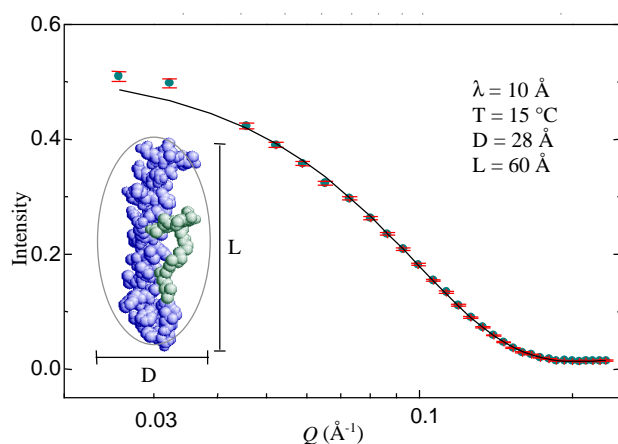


Figure 5 : SANS spectrum of the B777 complex in a deuterated detergent (D_{28} - n -octyl- β -D-glucopyranoside) micro-emulsion. The solid line results from the fit of data with an ellipsoid ($L=60$ Å, $D=28$ Å). Therefore, each B777 subunit consists of a single protein polypeptide with a non-covalently attached BChl. The scheme of the B777 is for guidance only and is based on the X-ray crystal structure of LH2 where the polypeptide is coloured blue and the BChl blue-green. The spectra were collected with the spectrometer PAXE. $T=15^{\circ}\text{C}$, $\lambda=10$ Å.

Summary and perspectives

In summary, the photosynthetic proteins from purple bacteria provide an unique opportunity to compare the influence of tertiary structures on internal protein dynamics. Our family of interconnecting membrane proteins also allows us to measure the effect of inter-protein interaction on protein dynamics and structure. Using SANS we can obtain novel information on protein structures, as shown by our approximation of the *form factor* of the B777. Furthermore, based on experimental data from time-of-flight and NSE spectroscopies, improved picosecond and new nanosecond molecular dynamics algorithms for membrane proteins are currently being developed.

Finally, our protein system provides an important contribution to the overall understanding of the inherent differences between integral membrane proteins and globular proteins, which are located in the cytosol. One such major physical difference is the pressure-sensitivity of proteins. In collaboration with the University of Tartu, Estonia, we have measured a series of electronic absorption and pre-resonance Fourier Transform - Raman spectra for the RC, LH1 and LH2 proteins which show that they are still intact at pressures where globular proteins, such as myoglobin, are denatured. In addition to our present series of experiments, we are presently planning Fourier Transform - Infra-Red and neutron measurements to establish the membrane protein structure-function-dynamic relationships as a function of applied hydrostatic pressure.

1. McDermott, G., Prince, S. M., Freer, A. A., Hawthornthwaite-Lawless, A. M., Papiz, M. Z., Cogdell, R. J., and Isaacs, N. W. (1995) *Nature (London)* 374, 517-21.
2. Roy, C., Lancaster, D., Ermler, U., and Michel, H. (1995) *Adv. Photosynth.* 2, 503-26.
3. Bee, M. (1988) *Quasielastic Neutron Scattering. Principles and Applications in Solid State Chemistry, Biology, and Materials Science*, Adam Hilger, Bristol, UK.
4. Volino, F., and Dianoux, A. J. (1980) *Mol. Phys.* 41, 271-9.
5. Mezei, F. (1980) *Lecture Notes in Physics, Vol. 128: Neutron Spin Echo*, Springer-Verlag, Berlin.
6. Sturgis, J. N., and Robert, B. (1994) *J. Mol. Biol.* 238, 445-54.

TECHNICAL AND INSTRUMENTAL DEVELOPMENTS

The study of the development of the neutron technique and the research of new methods are the two permanent goals of the instrumentation activity of the LLB. Due to the wide field of condensed matter physics, in which the neutron spectrometry is involved and often even unique, this domain of activity is very large. It ranges from the designs of new spectrometers, but also implies improvements of the existing spectrometers (neutron flux, versatility). Optimised neutron focussing and better polarising systems are now installed on the spectrometers. It also includes the developments of the sample environment facilities (high magnetic fields (12T), cryostats (down to 80mK), furnaces (1800°C), pressure systems (up to 40 GPa)...). The wide use of these devices also requires the development of raw data acquisition and data treatment systems, as simple as possible to use. All this specific neutron instrumentation generally results of collaborations between the researchers and the technical staffs (designs and drawings, “small” mechanics, electronics, computing) of the LLB and in some cases with external laboratories.

In summer 1997, the Zircaloy housing core has been replaced during the annual shut-down of the Orphée reactor. Three months were necessary for this essential operation, scheduled a long time ago. It has been successfully achieved with assiduous care by the staff of the Orphée reactor.

During the period 97-98, among the technical activity of the LLB, we find a few important technical realisations. Two of them are new instruments: the reconstruction of the reflectometer PADA (named now PRISM) and the neutron resonance spin-echo spectrometer (NRSE). These spectrometers were designed and built in collaboration with respectively “le Service de Physique de l’Etat Condensé (CEA-SPEC)” and the Technical University of München.

The experimental installations of LLB are continuously modernised. We wish to mention the realisation by the electronics staff of LLB, of a more rapid and powerful data acquisition and control system. Several important progresses have also been obtained in the sample environment facilities, as high-pressure devices specifically adapted to inelastic, diffraction or small angle experiments. Very important and due to improvements of the neutron technique, is the original 3-axis measurements of the spin-wave spectrum on very small samples grown by molecular beam epitaxy.

Besides these major developments, numerous other realisations in various domains have been carried out (new sample environments, new programs...), which render the domain of application of neutron scattering always larger.

DEVELOPMENT OF SPECTROMETERS.

A neutron resonance spin-echo spectrometer.

A *NRSE spectrometer*, which in contrast to a standard spin-echo relies on RF-coils rather than on static magnetic fields, had been built by the Technical University of München (Germany) and installed at the guide G1-bis, a polarised supermirrors guide. Both techniques can perform high-resolution energy measurements (neV) of condensed matter. The active part of NRSE acts over several centimetres, on the opposite to the traditional NSE, where the Larmor precessions occur over typical distances of several meters. A direct consequence of this peculiar point is a great flexibility of the instrument, especially for the large scattering angles from 5° up to 100°. This spectrometer is then complementary of the NSE spectrometer MESS at LLB, which is adapted to studies of long characteristic time processes at low angles. It has been designed with a wavelength range of 3Å to 12Å and a beam size at the sample position of 4*4 cm². The distance between the RF-coils has been set to 1.8m providing a maximum effective integral path of 1600G.m. Such characteristics give an access to a wide range of time (5ps to 15ns) at q values larger than 0.05Å⁻¹. In these q and time domains, the neutron flux on this instrument is comparable to that of IN11 at ILL. It is well suited for studying the complex dynamics of the liquid-glass transition. The NSRE spectrometer at LLB is, at the moment, the unique machine of this type operating in the world.

A Polarised Reflectometer for the Investigation of Surface Magnetism, PRISM.

The neutron reflectivity technique has emerged less than 15 years ago. It is devoted to the studies of solid and liquid surfaces and interfaces. At LLB, among its three reflectometers, one has been recently rebuilt as a new *polarised reflectometer with polarisation analysis*, named PRISM. As the neutron flux is a key point of the reflectometry experiments, several solutions have been operated to increase the flux. The focussing of 100mm high beam of the neutron guide to around 15mm high at the sample position and the multi-layers monochromator have required a huge modification of the spectrometer (the previous spectrometer was using a graphite monochromator). The wavelength resolution $\delta\lambda/\lambda$ has changed from 0.6% to 4%. These two improvements lead to increase the flux by a factor 15. A near future development will be the installation of a position sensitive detector based on the “microstrip” technique (realised in the frame of the European programme *XENNI*), which will allow off-specular studies on magnetic systems. The PRISM spectrometer is a good reflectometer, very well suited to magnetic studies; its new design renders it world leading.

TECHNICAL DEVELOPMENTS, SAMPLE ENVIRONMENT AND DATA TREATMENT.

A recurrent demand in neutron spectroscopy concerns *the increase of the neutron flux*. This goal can be now achieved due to important improvements either in multilayers guides or in the single crystal manufacture. With supermirrors guides (even polarizing), the maximum critical angle for neutron reflection (keeping a good reflectivity) is now around $3\theta_c$ (θ_c is the critical angle of the natural nickel). These improvements eventually combined with focussing methods are more and more applied to the instrumentation of LLB. The intensity gains thus obtained ranged in between 2 and 4-5 (even 15 mentioned above for PRISM, where the graphite monochromator was replaced by a multilayer monochromator).

Such upgrades can be “heavy” works, as the 2T operation, decided two years ago, to provide the best *3-axis spectrometer with polarised thermal neutrons* in the world. Several solutions have been adopted to increase the flux. Good single crystals of Heusler alloy (AlCu₂Mn) have been realized in collaboration with ILL. The size of both the monochromator and the analyser are increased; they are bent vertically as well as horizontally. In order to benefit from these technical improvements, an increase of the beam size of the 2T channel was required and thus a major modification of the 2T output and of its dense concrete shielding. The installation of the whole system is scheduled during the reactor shut-down, in April 99.

A new possibility is now proposed for inelastic neutron scattering measurements. It allows users to compare data obtained in the different neutron laboratories in the world, but also with other techniques, such as NMR. This method (recently settled at LLB) gives *absolute measurements of inelastic scattering on 3-axis spectrometer*. It will be useful in the understanding of the origin of the measured intensity. As example, it could be a step to relate the magnetic fluctuations observed in YBaCuO to the superconductivity mechanisms.

Optimising the neutron flux on the spectrometers may also offer new opportunities. As a matter of fact, recently, *3-axis inelastic scattering experiments on molecular beam epitaxy grown samples* have been tempted. They successfully led to the determination of the spin-wave spectrum of MnTe samples, of thickness of about 4-6 μ m and even of 1 μ m. Such a sample volume is well below that usually needed in neutron studies (typically a few cm³). Thus, such experiments on small samples are very encouraging and promise a new way for the development of the neutron scattering spectrometry.

Besides, since November'97, the powder diffractometer 3T2 is equipped with a new *focussing Ge monochromator*. The cut-off angle is still $2\theta_M \approx 90^\circ$, the wavelength 1.225Å, but due to the properties of the crystals (size and mosaic), the flux at the sample is four times higher than before. However, here, as the incident beam of 3T2 doesn't illuminate the whole monochromator, the focussing feature is then not fully used. An increase of the height of this beam, similarly to the 2T operation, is under consideration.

A focussing system has also been installed on the spin-echo spectrometer MESS. In order to balance the lack of intensity due to the high-resolution energy of this spectrometer, several *focussing guide elements coated with a non magnetic Cu⁶⁵ isotope* have been mounted in the first precession arm of the spectrometer. At the wavelengths commonly used on the spin-echo MESS, 6 and 8Å, the gain of intensity is in between 3 and 5. A specific *pneumatic system of positioning of the different guide elements* leads to flexibility in the choice of the energy resolution and the flux.

Developments of the sample environment facilities are also under progress. In particular, neutron scattering experiments under *pressure* are carried out at LLB since several years. On the one hand, in soft matter, even low pressure (<1GPa) may strongly change the inter-atomic distances and the physical properties. Depending on the

study involved, several pressure cells have been specifically designed. One made with an invisible alloy ($\text{Ti}_{0.34}\text{Zr}_{0.66}$) (coherent scattering length close to zero) allows to reach temperatures up to 800K under 1kbar; it has been used for studies of molecular liquids. Besides, a *high pressure cell for small angle neutron scattering* was realised to study supercritical fluids. It has sapphire windows and a great care of the temperature regulation allows a stability of $\pm 30\text{mK}$ at 400°C .

On the other hand, in solids, much higher pressures ($> 10\text{GPa}$) are generally required to induce a phase transition. Such an increase of pressure is generally obtained by an important decrease of the sample volume. During the last years, a Paris-Edinburgh high-pressure cell has been adapted to a 3-axis inelastic neutron scattering spectrometer, where focussing monochromator and analyser crystals had been previously settled. *Inelastic scattering experiments up to 12GPa* are now possible on samples of effective volume of 10mm^3 . This high-pressure equipment is now at the disposal of any user and several experiments have been carried out successfully for studying the phonon dispersion of different compounds.

In the domain of neutron diffraction, the magnetic studies under very high pressure require an important technical development both of the diffraction spectrometer (for the flux) and of the pressure cell. As a matter of fact, pressures higher than 10GPa are necessary for magnetic structure studies on powders or single crystals. During the last three years, several focussing systems (in the horizontal and vertical planes) made with Ni-Ti supermirrors ($3\theta_c$) have been developed on the powder diffractometer G6-1. The angle of focussing is variable in order to choose the optimal ratio of the intensity and resolution. The maximum gain of intensity achieved is about 7. Two pressure cells, with sapphire ($P < 10\text{GPa}$) and diamond ($P > 10\text{GPa}$) anvils, can rotate freely inside the cryostat, allowing to study textures or magnetic domains distributions. Recently, measurements on a GdAs sample of $\sim 1\text{ mg}$ weight have been done at a pressure of 43GPa ! The G6-1 *diffractometer for high-pressure studies, MICRO*, using special focussing devices to increase the neutron flux, is now operating half the year. This spectrometer is devoted to magnetic studies in the 50GPa pressure range. A new multidetector covering a high solid angle range is under construction at the EMBL (Grenoble); with the expected gain of counting rate, measurements at higher pressures could be tempted in the future.

Since several years, numerous physical-chemistry systems (lamellar phases, giant micelles, liquid-crystalline polymers) are studied under shear. The experiments consist in applying a shear deformation with a characteristic time $1/\dot{\gamma}$, where $\dot{\gamma}$ is the velocity gradient. When this time is about some specific times of the complex fluid, important structure changes can be observed. The Small Angle Neutron Scattering technique is especially well adapted to such studies. Several in-situ *shear devices* have been realised : couette or cone-plate shear cells. Recently, a very peculiar cone-plate cell has been realised: it allows the measurements of the scattering intensities in the three directions of the velocity with respect to the scattering vector q . The difficult observation of scattering in the plane (velocity, velocity gradient) could only be made owing to the huge penetration depth of neutrons in the materials. Another *cone-plate shear cell*, with quartz or sapphire windows, was designed with a velocity gradient range 10^{-3} to 200 s^{-1} , specially adapted to the study of viscous systems such as polymers.

The neutron scattering techniques are also very interesting to study materials. At LLB two diffractometers are specially devoted to *applied research in materials science and technology*, for *texture and strain-stress measurements*. Among the recent improvements in this field, the *DIANE diffractometer* (G5-2) has been recently equipped with a *mechanical test machine* for strain measurements under applied stress or during fatigue tests. With its detector installed two years ago, this spectrometer is very useful to industry, for the determination of residual stresses in materials. It gives to the LLB, the opportunity to participate to the European Brite-Euram program, *TRAINSS* (TRAIning Industry in Neutron Stress Scanning) and in the international *VAMAS* project, which aims at the definition of a standard method for the measurements of residual stress by neutron diffraction.

To the development of instrumentation, are added those of *programs for data analysis* suited to each method. As example, in some treatment programs of diffraction measurements, new fits to various functions (the Rietveld analysis, pseudo-Voigt decomposition method...) are always implemented. In this sense, *FullProf*, a program for the determination of complex crystalline structures from powder and single-crystal diffraction patterns, is extended to data treatments of X-rays (including from synchrotron sources). *WinPlotR* is a new tool working on Windows (95, 98, NT) systems, for data plot and fit of powder diffraction patterns. These programs, including a lot of examples and help, are at the disposal of the scientific community on Internet. In the same mind, the treatment program of SANS data, PASIDUR, has been adapted to the data file format of ILL. Furthermore, this program, used on the PACE spectrometer of LLB, allows fully automatic changes of the configuration (collimation, detector distance, wavelength, tuning, sample position, temperature...) and the data acquisition.

All the spectrometers at LLB and several spectrometers in other neutron laboratories in the world are equipped with the intelligent *control system for data acquisition*, named “LLB DAFFODIL System”. Its philosophy relies upon independent execution of three main functions (positioning, counting and position sensitive detector acquisition) together with versatility and simplicity of use for the physicists. In the past two years, a major upgrade of this control system has been studied by the electronic group of LLB. With the new counting module, a fully automatic acquisition mode for neutron polarisation and analysis is possible. Besides, the huge memory of the acquisition module allows all kinds of association of the multidetector cells, and the performance of the Time of Flight mode have been extended. A further expansion to kinetics experiments on multidetectors can now be considered.

The possibilities of the “DAFFODIL” system have been extended by the *electronic service* of LLB to manage different kinds of analogic signals (ADC, DAC, input-output voltage), to program logarithmic time scales for fast acquisition. All these facilities are used in several home made instruments: the rheometers, for the viscosimeters and the light scattering spectrometers. On its side, the *computing group* goes on the development of data acquisition programs; up to now about ten spectrometers of LLB are running with their recent programs. Besides, as only 5 persons are working in this group, they cannot solve all the problems encountered by the large number of PC users. They took the decision to spread a PC's administration system, Windows NT, to survey most of the PC machines.

The LLB has participated during the period 1996-1999, in two areas of the XENNI program (the 10-Member European Network for Neutron Instrumentation) : that of polarising multilayers and that of multidetectors. Several large surface etched transmission polarisers have been realised and tested on the reflectometers at LLB. It is now possible to produce polarisers with less than 10% of absorption (instead of 30% for the conventional ones). The technology of optical gratings is used to build a new type of position sensitive detector with a high spatial resolution, the microstrip detector. With UV lithography makes it possible to achieve large surface arrays with periods down to 200 nm. This type of detector has very large counting rates and very low noise.

PERSPECTIVES.

Among the improvements planned for the forthcoming years, one can mention:

- a new multidetector covering a high solid angle range, under construction at the EMBL (Grenoble). It will be installed in 1999 on the powder diffractometer for high-pressure, MICRO ;
- another multidetector for the new PRISM reflectometer, based on the microstrips technique, in the frame of the European program XENNI ;
- in autumn 1999, the final installation of the polarised neutron option on the thermal 3 axis spectrometer 2T ;
- a double chopper for the EROS reflectometer, which will give variable Δq values (between 1% and 4%), is under tests at LLB.

Furthermore, we are considering the replacements of the mechanical selectors of the SANS spectrometers. As a matter of fact, since they are partially coated with supermirrors, the guides where the SANS instruments are installed have a maximum flux of the wavelength distribution around 2 to 3 Å, which cannot be used with the present selectors. In order to meet a demand of users, i.e. to increase the available q range, a Dornier selector was ordered at the end of last year. It is planned to be installed on PACE. An intensity gain of about 20% (due to the transmission) and a possible choice of smaller wavelengths (due to the maximum velocity) are expected.

Finally, to end this summary of the technical developments at LLB, we would like to stress two projects of new instruments. A second *time of flight spectrometer*, with high flux, would allow to satisfy the important number of proposals for experiments, notably in biology. The time focussing technique studied allows an increase in flux of approximately one order of magnitude compared to choppers-designed spectrometers, as Mibémol, with a comparable energy resolution (40 to 200 μeV). This increase is mainly due to a monochromatisation of the incident beam using crystals operating in Bragg geometry. We will use vertically and horizontally focussing monochromators.

A *Small Angle Neutron spectrometer (TPA)*, at very low q , is under consideration in order to extend the existing possibilities in SANS. The scattering vector range aimed is 10^{-4} - 10^{-2}Å^{-1} . It would allow the studies of large scale objects (1000 Å) such as giant micelles, cell membranes, cavities, precipitation in alloys, biophysics gels... As the manufacture of large position sensitive detectors for neutrons with a good resolution ($\sim 1\text{mm}$) is a major problem, we plan to use an image plate. At the beginning, a pin hole collimation will be used; further possibilities in this direction will be studied later on.

As a conclusion, all these developments are very encouraging and render the neutron spectrometry more and more useful and determinant to any research at the microscopic level (structure and dynamics) in physics, chemistry, biology and materials science.

NEUTRON RESONANCE SPIN-ECHO SPECTROSCOPY AT LLB

M. Koeppe¹, P. Hank¹, U. Rauch¹, S. Longeville^{1,2}, R. Gaehler¹, J. Wuttke¹, W. Petry¹,
R. Kahn²

¹Technische Universität München, Physik Department, James Franck Strasse, D-85747 Garching

²Laboratoire Léon Brillouin (CEA-CNRS)

Neutron spin echo spectroscopy (NSE) has been discovered by F. Mezei in 1972^[1]. The basic principle of the technique is to use the neutron spin to monitor the neutron velocity changes induced by scattering processes. The measured signal $P(\mathbf{Q}, \tau)$, i.e. the polarisation of the scattered beam at the echo point, is proportional to the cosine transform of the scattering function $S(\mathbf{Q}, \omega)$. NSE provides the highest energy resolution nowadays achievable in neutron scattering and is consequently a very useful tool for the measurements of slow relaxation processes occurring in many fields of condensed matter physics.

In 1987, a new scheme for NSE spectroscopy was proposed by R. Gähler and R. Golub^[2]. In this technique, called Neutron Resonance Spin-Echo (NRSE), the two high magnetic field coils are replaced by four radiofrequency coils; it is directly inspired by the principle of Nuclear Magnetic Resonance. On the contrary to the traditional NSE, where the Larmor precession occurs over typical distances of several meters, the active part of NRSE acts over distances of several centimetres; the rest of the neutron path has to be magnetically shielded. As a consequence of the localisation of the fields, this technique allows an increased flexibility within the same covered Fourier time domain.

A spin echo spectrometer based on this principle has been constructed in collaboration between the TU München and the LLB and was installed at the neutron guide G1bis. This spectrometer has been designed for measurements over scattering angles ranging from 5 to 100 degrees. Complementary to the conventional NSE spectrometer of the LLB, which is specially adapted for low angle studies, it bridges a gap in the NSE spectroscopy at the LLB. Several innovations have been realised, such as a new design for the radiofrequency coils in order to minimise the stray fields and the consecutive decreases of the polarisation (see figure 1). A polarising section (FeCoTiN_x supermirrors) has been implemented into the curved guide^[3] providing a useful neutron wavelength range between 3 and 12 Å; the polarised neutron flux is of $0.9 \cdot 10^7 \text{ n.cm}^{-2}\text{s}^{-1}$ at the sample position ($\lambda=4.8\text{Å}$, $\Delta\lambda/\lambda=0.15$).^{*}

The distance between the NRSE coils has been set to 1.8 m providing an effective field integral path of ~1600 G.m whereas the sample to detector distance has been kept shorter than 3 meters. This leads to

intensity accessible Fourier time domain comparable to the classical NSE spectrometer IN11 of the High Flux Reactor of the ILL.

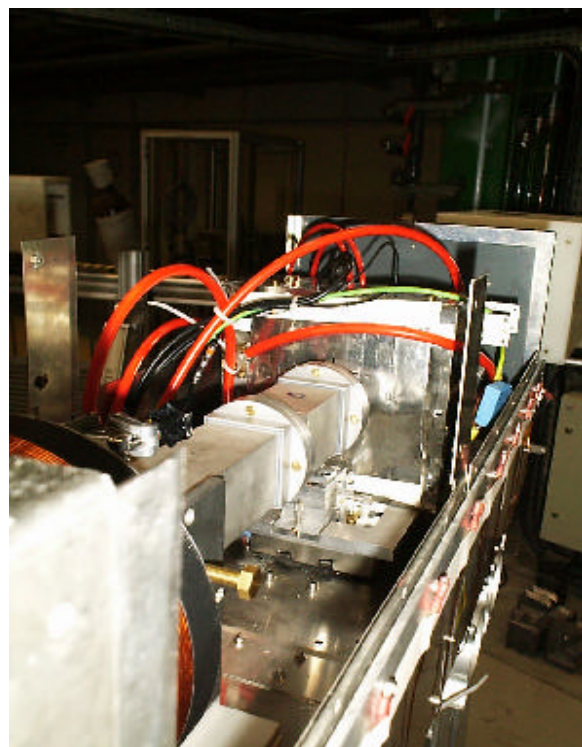


Figure 1. The NRSE instrument G1bis at Saclay

Tests measurements were performed late 1996 and during 1997, but real experiments only started after the commissioning of the new guide and were completed in 1998.

For example, measurements were performed to study the temperature-wave-vector dependence of the slow relaxation processes of a ionic mixture $\text{Ca}[(\text{NO}_3)_2]_{0.4}[\text{RbNO}_3]_{0.6}$. In such systems in which a liquid to glass transition is observed, complex dynamics occur over large time scales. These dynamics cannot be understood by a simple cross-over from vibrational excitations to structural relaxation.

Experimental data show additional intensity, which can be ascribed as rattling of particles in transient cages formed by their neighbours, as it has been quantitatively modelled in mode coupling theory^[4]. The predicted scaling laws have been verified in a couple of systems, the most prominent example being $\text{Ca}[(\text{NO}_3)_2]_{0.4}[\text{KNO}_3]_{0.6}$, which is believed to stand as a model for glass forming liquids^[5]. This believe has

^{*} From gold Activation measurement.

been challenged by recent dielectric measurements^[6] on a chemically homologous system $\text{Ca}[(\text{NO}_3)_2]_{0.4}[\text{RbNO}_3]_{0.6}$, which have shown a quite different evolution of the dynamic susceptibility.

NSE spectrometry is specially suited for the study of the slowest part of the relaxation, called α -relaxation. This process enters the time range of the spectrometer, for temperatures significantly above the calorimetric glass transition. Typical spectra obtained at $Q=1.7\text{\AA}^{-1}$ are shown in figure 2.

The count rate was nearly $60\text{ neutrons.s}^{-1}$, and the polarisation at $\tau=0$ was around 0.6. Measurements were performed at temperatures ranging between 395 and 496K. The continuous lines represent fits with

the Kohlrausch-Williams-Watts (KWW) function. The inset shows the same spectra, but now shifted in time according to the time-temperature shift principle. The relaxation times extracted from the individual KWW fits were taken as scaling times. Apparently the data obey the time-temperature shift principle.

In summary, the NRSE spectrometer is well suited for high-resolution studies involving slow dynamics within microscopic and mesoscopic length scales. These cover wide domains such as physics of glasses and liquids, biology, polymer science, critical phenomena.... Technical developments under progress should allow to perform studies on crystals within the very next future.

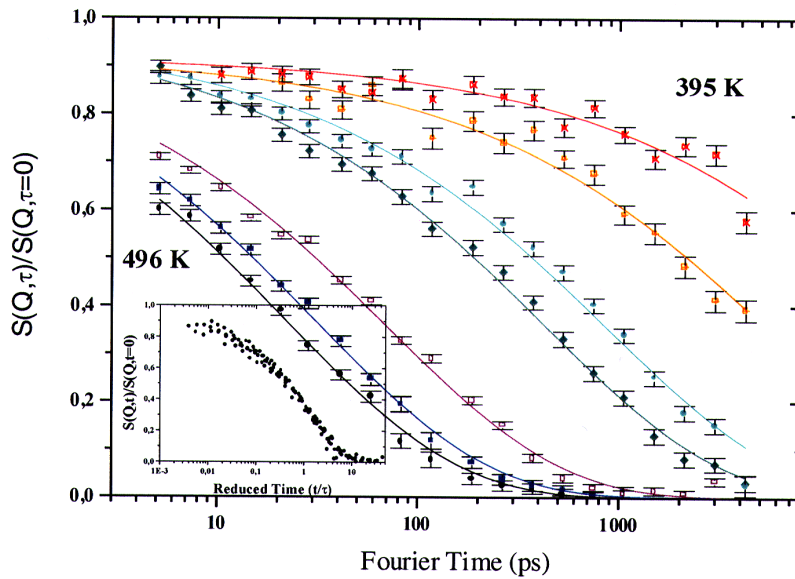


Figure 2 : Intermediate scattering function $S(Q,t)$ for $\text{Ca}[(\text{NO}_3)_2]_{0.4}[\text{KNO}_3]_{0.6}$ at $Q=1.7\text{\AA}^{-1}$ on the NRSE spectrometer G1bis.

References

- [1] F. Mezei, Z. Physik, **255** (1972) 146
- [2] R. Gähler and R. Golub, Z. Phys. B -Cond. Matt., **65** (1987) 289
- [3] K. Al Usta, R. Gähler, B. Böni, P. Hank, R. Kahn, M. Koppe, A. Menelle, W. Pétry, Physica B **241-243** (1998) 77.
- [4] W. Götze, in *Liquids, Freezing and the Glass Transition*, edited by J.P. Hansen, D. Levesque and D. Zinn-Justin. (Les Houches, session LI) North Holland : Amsterdam (1991).
- [5] F. Mezei, W. Knaak and B. Farago, Phys. Rev. Lett. **58** (1987) 571
- [6] P. Lunkenheimer, A. Pimenov and A. Loidl, Phys. Rev. Lett. **78** (1997) 2995.

NEW MONOCHROMATOR AND FOCUSING GUIDE ON THE POLARISED NEUTRON REFLECTOMETER PRISM : A POLARISED REFLECTOMETER FOR THE INVESTIGATION OF SURFACE MAGNETISM.

F. Ott¹, C. Fermon²

¹Laboratoire Léon Brillouin (CEA-CNRS)

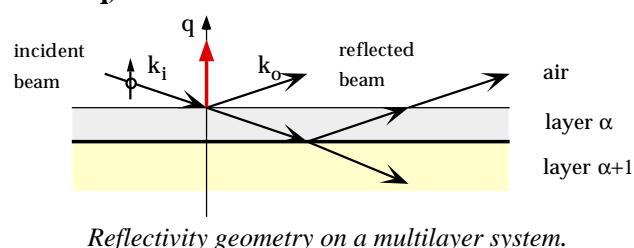
²Service de Physique de l'Etat Condensé, CEA-Saclay, 91191 Gif-sur-Yvette

The neutron reflectivity technique has emerged less than 15 years ago. It appeared as a key technique in the study of polymers and magnetic thin films. Topics such as polymer interdiffusion, di-block copolymers ordering have been addressed. Besides, especially after the discovery of the giant magnetoresistance (GMR) effect, neutron reflectivity has been successfully applied to the study of magnetic multilayers and ultrathin films. Problems such as the magnetic ordering in rare-earth multilayers, surface magnetism and anisotropy in ultrathin magnetic layers have been solved. However, in order to extend the possibilities of the neutron reflectivity, an increase of the flux was necessary. In that aim, we have recently rebuilt a polarised reflectometer with polarisation analysis, dedicated to the study of magnetic thin films.

Neutron reflectivity principle

The neutron reflectivity technique consists in measuring the reflection of a neutron beam on a thin film (liquid, polymer or solid) at grazing incidence. The measured reflectivity as a function of the scattering wave vector q gives information on the chemical composition, the thickness of the layers and the roughness of a multilayer system. Neutron reflectometry is especially interesting to study polymers because of the large scattering length of hydrogen, and of the possible labelling of polymer chains by selective deuteration.

Moreover, the neutron is a $\frac{1}{2}$ spin particle and the magnetic interaction with unpaired electrons is very large (as large as the nuclear scattering). By using polarised neutron reflectivity with polarisation analysis, it is possible to obtain information on magnetic systems: the type of magnetic ordering in multilayers systems (ferro, anti-ferro or helicoidal) or more generally the magnetisation profiles throughout the depth of magnetic thin films (along the scattering vector q).



To increase the available neutron flux, three different solutions are or will be put in place :

- increase of the wavelength spectrum width $d\lambda/\lambda$ by using a multilayer monochromator,
- focussing of a 100 mm high neutron beam onto a 15 mm high region at the sample position,
- use of a position sensitive detector.

The previous PADA reflectometer was a two axis spectrometer using a graphite monochromator which had an excellent wavelength resolution $\delta\lambda/\lambda$ ($\sim 0.6\%$). The new PRISM spectrometer is still located on the guide G2 of the reactor Orphée. Here is the description of this instrument, schematically represented in figure 2.

The incident beam is deviated and monochromatised by a 3 m guide (M) made of nickel-titanium multilayers. The direction of the monochromatised beam makes an angle of 2.4° with the direction of the main guide. This part of the guide has been built and mounted by the CILAS company. The angular deviation of 2.4° is however not enough to move away the output beam from the main guide at the sample position. Thus, we have mounted two 1.80 m long $2\theta_c$ -supermirror neutron guides (B) after the monochromator. The total beam deviation, from the main guide at the sample position is of 900 mm. This is enough for the shielding around the main guide (50mm lead, 250mm concrete) and the sample environment (cryostat, magnetic field). Since most of the studies on magnetic samples are realised on samples less than 20mm wide, we have focussed the beam vertically on the sample position. This vertical focussing is realised by a 8 m conical neutron guide (C) made of $2\theta_c$ -supermirrors, which is interrupted twice. These two interruptions allow the introduction of the polarising (P) and flipping systems. The transmission polariser is made of Fe/Si multilayers deposited on 50 mm high silicon substrates (these mirrors were provided by Th. Christ from the HMI in Berlin). The incidence angle on the polarisers is small, 0.3° , in order to reject long wavelength neutrons generated by the monochromator system. The polarisation efficiency is 0.97 and the transmission of this polariser is 70%. At the sample position, a 50 mT field allows to maintain a good polarisation efficiency. The analysis system (A) is similar to the polariser except that the height of the device is 80 mm. It enables a full analysis of the

reflected beam, which is highly divergent in the vertical direction.

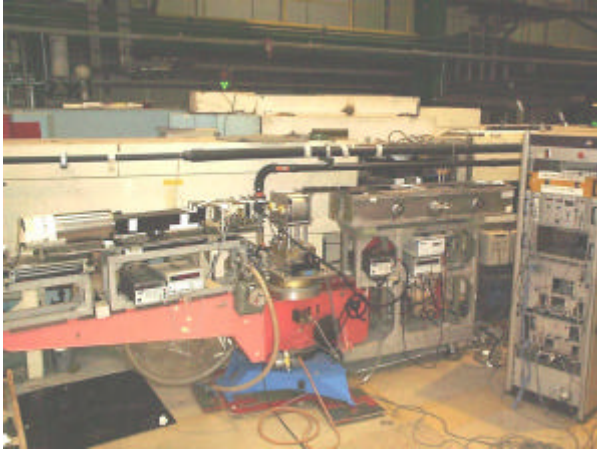


Figure 1. The Polarized reflectometer PRISM

With these two improvements (new monochromator and focussed beam), the available flux has been multiplied by a factor 15 and is presently of 5×10^5 neutrons/cm².s after analysis on the detector with a resolution $\delta\theta = 0.03^\circ$.

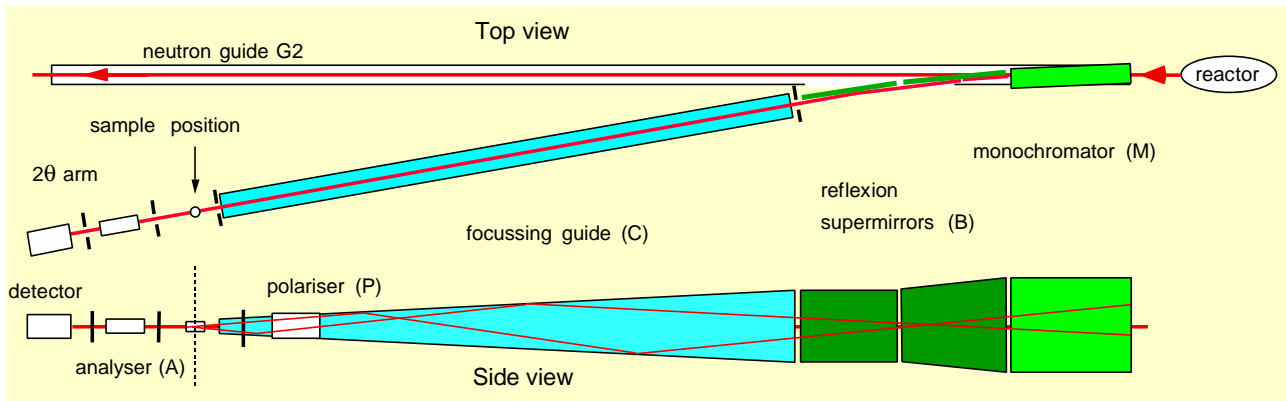


Figure 2. Scheme of the PRISM spectrometer and of its focussing guide, top view and side view

This high neutron flux will allow two main progresses in the reflectivity experiments. It will drastically reduce the measuring times of the reflectivity curves, and will permit measurements in various conditions of magnetic field and temperature. The second gain is the scattering vector range, twice as large as before. ($1.10^{-2} < q(\text{\AA}^{-1}) < 0.25$). The wavelength is now 4 Å with a resolution $\delta\lambda/\lambda$ of 4%. The angular resolution $\delta\theta$ can be varied from 0.01 to 0.06° . The intensity dynamic range of measurement is now typically between 10^5 to 10^6 neutrons/s on a 1 cm² sample for an 8 hours full analysis scan and a resolution $\delta\lambda/\lambda = 4\%$ and $\delta\theta = 0.05^\circ$ (see figure 3). During 1999, a position sensitive detector, based on the micro strip technology (currently developed in the frame of the European XENNI program) will be installed. It will allow off-specular studies on magnetic systems.

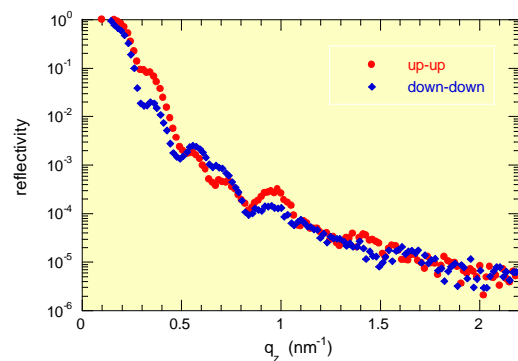


Figure 3. Reflectivity of a spin-valve system (Mn/Fe/Co/Ru/Co/NiFe) under a 0.3T field. The measurement time was 3 minutes per point on a 1 cm² sample

3-AXIS INELASTIC NEUTRON SCATTERING ON MOLECULAR BEAM EPITAXY GROWN SAMPLES

B. Hennion¹, W. Szuszkiewicz²

¹Laboratoire Léon Brillouin (CEA-CNRS)

²Institute of Physics, Warsaw, Poland

Optimizing the use of neutron beams on triple axis spectrometers implies focusing by **curved monochromators and analysers**, bent vertically as well as horizontally (Figure 1).

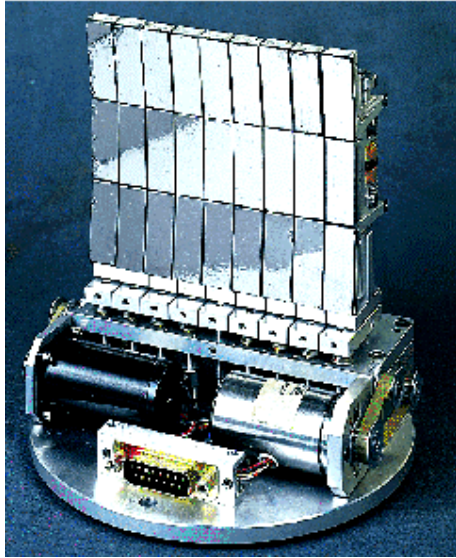


Figure 1. Focusing analyser of the 3-axis spectrometer 1T

The gain in intensity, keeping a low background level, offers new opportunities of **inelastic neutron scattering** measurements on small size samples (a few mm³).

Thus, **MBE grown samples** have been used to measure **spin waves on MnTe**. Such measurements are illustrated on Figure 2. MnTe is often used to obtain by substitution of Mn by non magnetic ions (e.g. Zn or Cd) diluted magnetic semiconductors. These compounds have the Zinc blende (ZnS) cubic structure and the evolution of their magnetic properties depends on exchange integrals, responsible of the magnetic order of the pure compound. But pure MnTe has not the blende structure, but that of hexagonal NiAs! **Only MBE grown samples of MnTe have the blende structure**, because of uniaxial constraint due to epitaxy. Such samples offer therefore the possibility to **determine exchange integrals** by measuring the **spin wave spectrum of MnTe**, with inelastic neutron scattering. Raw data measured on MBE grown samples are illustrated on figure 2.

They are obtained on samples of **4 and 6 mm width** grown at the Institute of Physics of the Polish Academy of Sciences in Warsaw, on an AsGa

substrate with a buffer of 2 or 4 μm of CdTe. With a surface of about 2 cm², **the sample volume was about 1 mm³**. The only known information was the value of the anisotropy gap of the spin wave spectrum, that previous Raman scattering measurements had determined as ≈ 1.05 THz.

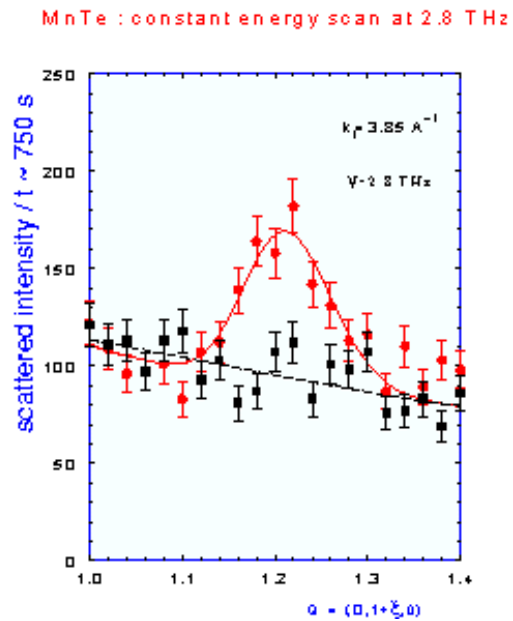


Figure 2: Raw data obtained at $T=13$ K. \bullet and 75 K \blacksquare Spin-waves only exist at low temperature.

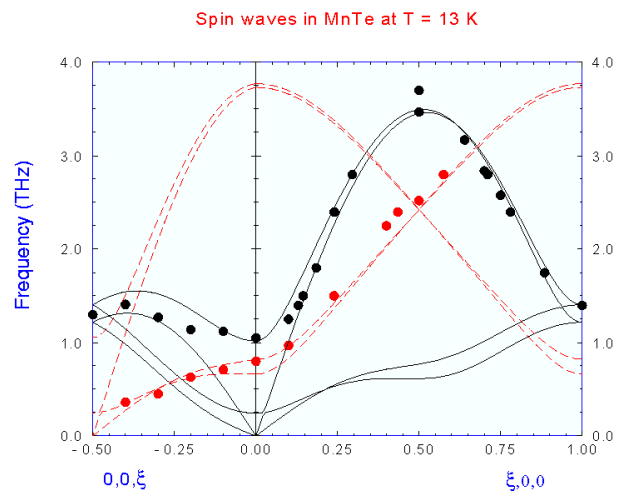


Figure 3. Black lines and symbols are respectively the measured and calculated spin-wave spectra at $T=13$ K for one magnetic domain in the sample. Red dashed lines and red symbols correspond to modes in the second magnetic domain of the MBE sample.

Study of the sample by elastic neutron scattering [1] confirmed its structural and magnetic characteristics. The magnetic transition takes place at $T_N \approx 65$ K and is associated to a structural transition (tetrahedral distortion). The low temperature magnetic structure is **antiferromagnetic of type III**. If $[1,0,0]$ is the crystallographic axis perpendicular to the layers, the doubling of the magnetic cell is along $[0,1,0]$ or $[0,0,1]$, due to the nature of the buffer. Therefore, in the MBE sample, 2 magnetic domains coexist and we have to account for the superimposition of 2 reciprocal lattices. This lowers the scattered intensity and hampers the analysis of the results. Anyhow, a pertinent set of data has been obtained with a counting time of about 15 minutes per step. On

Figure 3 are reported the experimental results and the theoretical dispersion curves, calculated with a Heisenberg hamiltonian

A test measurement has been done on a **MnTe/ZnTe multilayer**, made of alternating 20 MnTe and 3 ZnTe atomic layers. The sample width was 1 μm , but it was a single domain. The long range magnetic order is preserved and spin gap at $q=0$ as well as the zone boundary mode have been observed.

Even though such experiments benefit of the high value of the Mn moment (spin 5/2) [2], they are very encouraging as a first step towards the study of dynamical properties of magnetic multilayers.

References:

- [1] W. Szuszkiewicz, B. Hennion, M. Jouanne, J.F. Morhange, E. Dynowska, E. Janik, T. Wojtowicz, M. Zielinski and J.K. Furdyna, *Acta Physica Polonica*, Vol 93, No 3 (1998) 583-587
- [2] The inelastic results are not yet published.

NEUTRON DIFFRACTION UNDER VERY HIGH PRESSURES: EXPERIMENTS IN THE 40 GPa PRESSURE RANGE.

I.N. Goncharenko^{1,2}, I. Mirebeau¹ and J.-M. Mignot¹

¹Laboratoire Léon Brillouin (CEA-CNRS)

²Kurchatov Institute, Moscow, Russia

The role of high pressures in solid state physics is essentially twofold: 1) pressure varies interatomic distances in a controlled way and therefore could be used to verify theoretical models, 2) it induces new phases, which may exhibit unusual characteristics. In practice, the possibility of using pressure strongly depends on the range of pressure needed and on the technical tools required to reach it. In soft matter, even pressures of less than 1 GPa may strongly change the interatomic distances and the physical properties. In contrast, in most solids, much higher pressures (10 GPa or more) are needed to produce significant change of the sample volume ($\Delta V/V > 10\%$). In the recent years, crystal structures studies in the 100 GPa pressure range have strongly benefited from the development of third-generation synchrotron X-ray sources, whereas magnetic studies in the same pressure range are still much less developed. Anomalous magnetic X-ray scattering cannot be used because of the huge absorption of the pressure device, and Mössbauer studies do not provide any information about the long range magnetic order. Neutron diffraction is usually limited to much lower pressures (1–3 GPa). This is because pressures above 10 GPa could be reached only by a drastic decrease of the available sample volume (down to 10^{-4} to 10^{-6} mm³ in the 100 GPa pressure range). Such a sample volume is well below that usually needed in neutron studies (typically a few mm³ to a few cm³).

At the beginning of the 1990's, a project was initiated at the LLB to develop magnetic studies under very high pressure using high intensity neutron diffraction [1]. The steady state reactor with a cold source provides the most convenient q-range for such studies.

The project encompasses both single crystal and powder diffraction under pressure. Single-crystal diffraction yields very detailed information about spin arrangements. Numerous studies using single crystal diffraction under pressures were performed at the LLB during the last years [1,2], most of them on the lifting detector spectrometer 6T2. Very recently a new superconducting magnet and a dilution refrigerator, compatible with the high pressure setup, have become available. Implementing high magnetic fields (up to 8 T) and very low temperatures (down to 30 mK) together with

pressures up to 10 GPa opens new possibilities to single crystal studies.

On the other hand, powder diffraction is the most straightforward way to extend neutron studies well above 10 GPa. In this pressure range, single crystals could be easily destroyed by pressure inhomogeneities or by a first order structural transition.

The development of a specialized powder diffractometer, allowing neutron studies to be made at pressures up to 50 GPa, i. e. at higher pressures than in any other neutron facility, was the most ambitious part of the project. During the last three years the G6.1 diffractometer (equipped with a 400-cell multidetector) was transformed in a specialized spectrometer, optimized for the magnetic diffraction of small samples (less than 1 mm³) under very high pressures. In this high pressure version, G6.1 is equipped with a double-stage focusing system inserted between the monochromator and the sample position (fig 1).

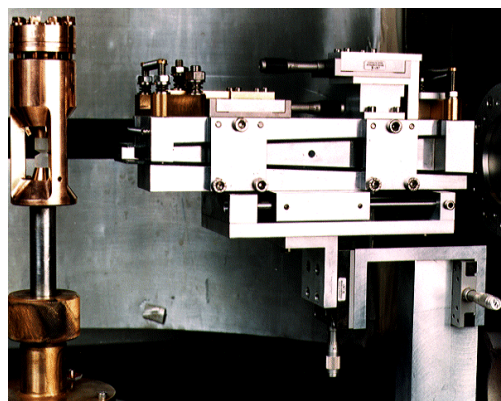


Figure 1. The pressure cell and the focusing device used in the high pressure version of the G6.1 spectrometer.

The focussing system, consisting of Ni-Ti supermirrors “compresses” the neutron beam both in horizontal and in vertical planes [3]. Using a double-stage system allows us to simulate a curved profile of the mirrors’ surface. This is the optimal profile to get both the highest gain in intensity for a given length of the system (limited by the free space between the monochromator and the sample) and a smooth angular distribution of neutrons in the focused beam. The variable angle of focussing makes it possible to

choose the optimal trade-off between intensity and resolution for each experiment. The maximal gain in intensity obtained by focusing is 7.

Together with a high intensity of the incident beam, a very low background is crucial to measure small samples. A sophisticated protection and an especially designed cryostat allow us to reduce the background to a very small value – only a few counts/per cell/per hour.

We use pressure cells with sapphire ($P < 10$ GPa) and diamond anvils ($P > 10$ GPa). The implementation of the sapphire anvil cells for neutron diffraction is based on over 10 years of experience gained for such experiments in Kurchatov Institute (Moscow). A number of such cells, adapted to low temperature measurements, were developed and implemented in the neutron experiments (single crystal or powder) at the LLB during the last years. One of the most compact cells with sapphire anvils is shown in fig. 2. This cell can be rotated freely inside the cryostat, allowing to study textures or magnetic domain distributions. The cell is compatible with the dilution refrigerator and the superconductive magnet, making possible to use high pressures, magnetic fields and mK-temperatures in the same experiment.



Figure 2. This small pressure cell can be rotated inside a cryostat

The power of the above technique is illustrated here by the study of magnetic interactions in two closely related systems, the europium monochalcogenides and the gadolinium monpnictides. Both families, having the same crystal structure and the same electronic structure ($4f^7$) for the cations (Eu^{2+} and Gd^{3+}) are usually considered as “model systems” to study magnetic interactions in semiconductors and semi-metals. The neutron diffraction patterns of EuTe and GdAs under pressure are shown in figs. 3 and 4.

The pressure strongly modifies the magnetic properties of EuTe, resulting in a sequence of magnetic transitions at pressures around 10 GPa [4]. As the lattice constant decreases, the ferromagnetic exchange interaction increases very rapidly, leading to a transformation of the initial antiferromagnetic

order to a ferromagnetic one, followed by an exponential increase of the Curie point [5].

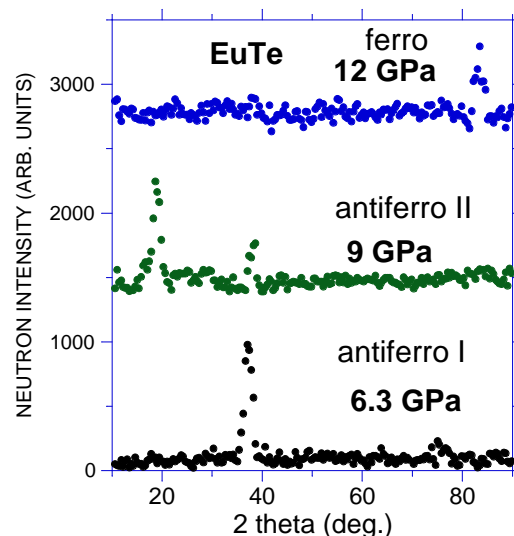


Figure 3. Magnetic neutron diffraction spectra under high pressure in EuTe.

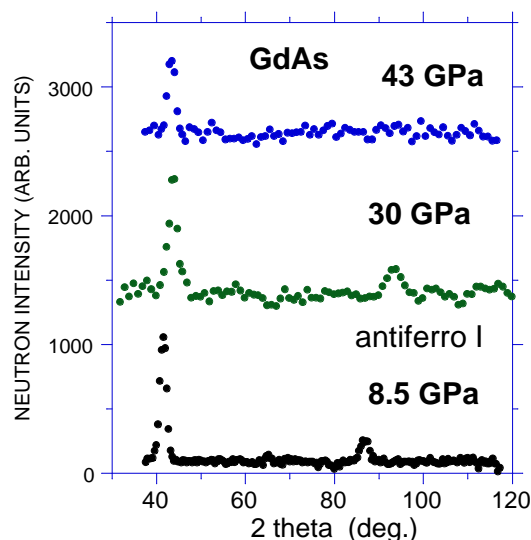


Figure 4. Magnetic neutron diffraction spectra under high pressure in GdAs. The GdAs sample was prepared by A.Ochiai (Univ. of Niigata, Japan).

The GdAs sample, having the same magnetic structure at ambient pressure, shows a very different behavior. Pressure only increases the Néel point. Even at 43 GPa, when the volume decrease reaches about 40%, the compound remains antiferromagnetic. In this measurement, the sample was as small as about 1 mg of weight (0.002 mm^3). This is likely the smallest sample under the highest pressure ever measured with neutrons.

Comparing the two systems (GdAs and EuTe) allows us to see the role of the band structure in the formation of the antiferro- and ferromagnetic exchange between the cations.

In the year 1999, we expect the next upgrade of the high pressure version of the G6.1 spectrometer ("MICRO" diffractometer). A new multidetector, optimized for small samples studies and covering a 7 times larger solid angle, is currently under construction in the European Molecular Biology Laboratory (Grenoble), in collaboration with A. Gabriel. The upgrade of the spectrometer will allow us to increase the available pressure range above 50

GPa and will also provide better possibilities to meet the needs of a growing number of experimental teams, suggesting various studies under pressure in many different fields of physics. Besides the traditional field of magnetism under pressure, new subjects appear, for instance the studies of mesoscopic structures such as the recently discovered carbon nanotubes.

References:

- [1] I. N. Goncharenko, J.-M. Mignot, I. Mirebeau, *Neutron News* **7** (1996) 29.
- [2] P. Link, I. N. Goncharenko, J.- M. Mignot, T. Matsumura and T. Suzuki, *Phys. Rev. Lett.* **80** (1998) 173.
- [3] I. N. Goncharenko, I. Mirebeau, P. Molina, P. Böni, *Physica B* **234-236** (1997) 1047.
- [4] I. N. Goncharenko, I. Mirebeau, *Europhys. Lett.* **37** (1997) 633.
- [5] I. N. Goncharenko and I. Mirebeau, *Phys. Rev Lett.* **80** (1998) 1082 .

DATA ACQUISITION & CONTROL SYSTEM FOR NEUTRON SPECTROMETERS AT THE LLB

G. Koskas, J. Drapeau, M. Antoniadès, M. Donois, P. Froment

Laboratoire Léon Brillouin (CEA-CNRS)

There are 24 neutron spectrometers installed around the ORPHEE research reactor, all equipped with an acquisition and control system known as « **DAFFODIL SYSTEM** ». This system has been developed by the electronic group of the laboratory. Its backbone is the IEEE 488 BUS. Up to 32 peripherals can communicate with the user host computer via this standard communication protocol. The DAFFODIL SYSTEM is composed of a few IEEE 488 devices, which are designed for independent execution of complete functions (see figure 1).

The past two years, three main functions (**positioning**, **counting** and **Position Sensitive Detector acquisition** including **Time Of**

Flight) have been particularly developed at the LLB for a maximum integration and simplicity of use. They form the core of the data acquisition equipment for any kind of neutron spectrometer.

For each function, an intelligent IEEE 488 microprocessor board has been designed. These boards constitute the Euro series (**EuroMove**, **EuroScale** and **EuroPsd**), which are at present installed on the experiments. This triple function subsystem comes in the form of a single (see figure 2) or double Europe crate. It contains the location for the Euro series modules, power supplies for the electronic system as well as for the motors and the peripherals boards for motor control, readout and display of encoded axis and diverse I/O.

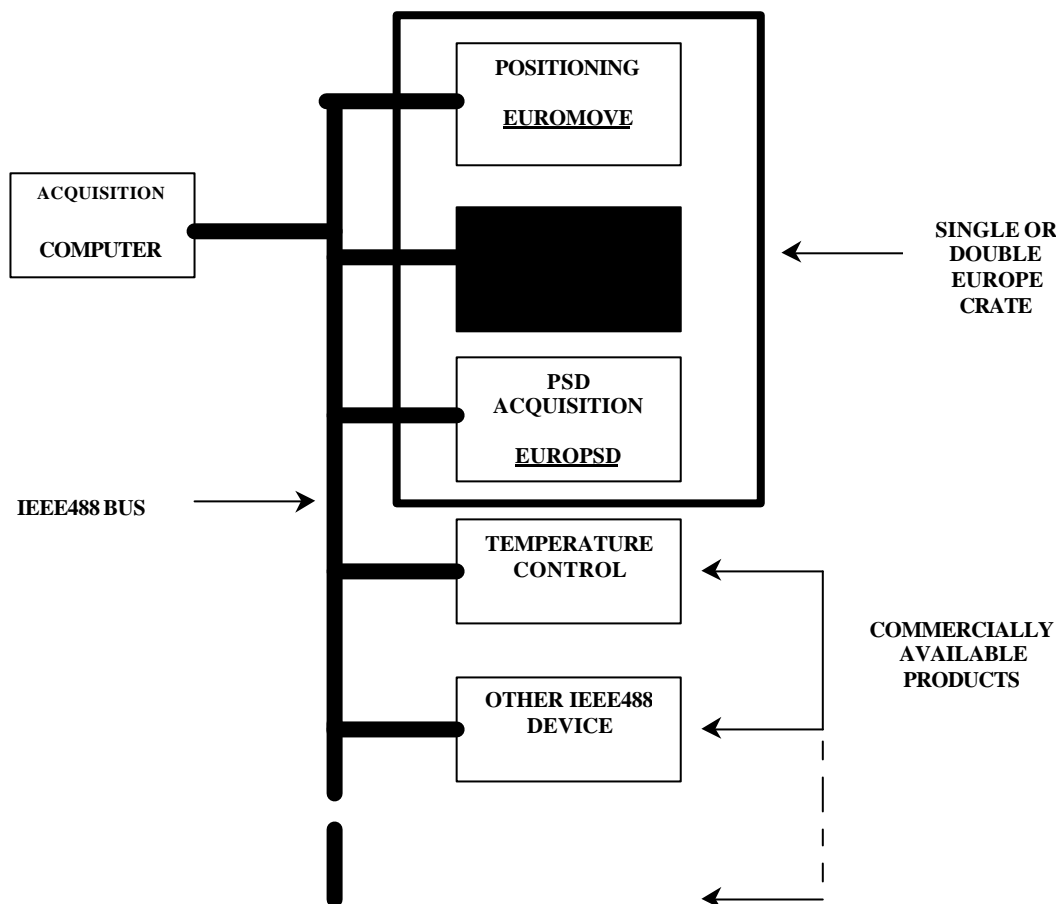


Figure 1. Outline description of the LLB Daffodil system.

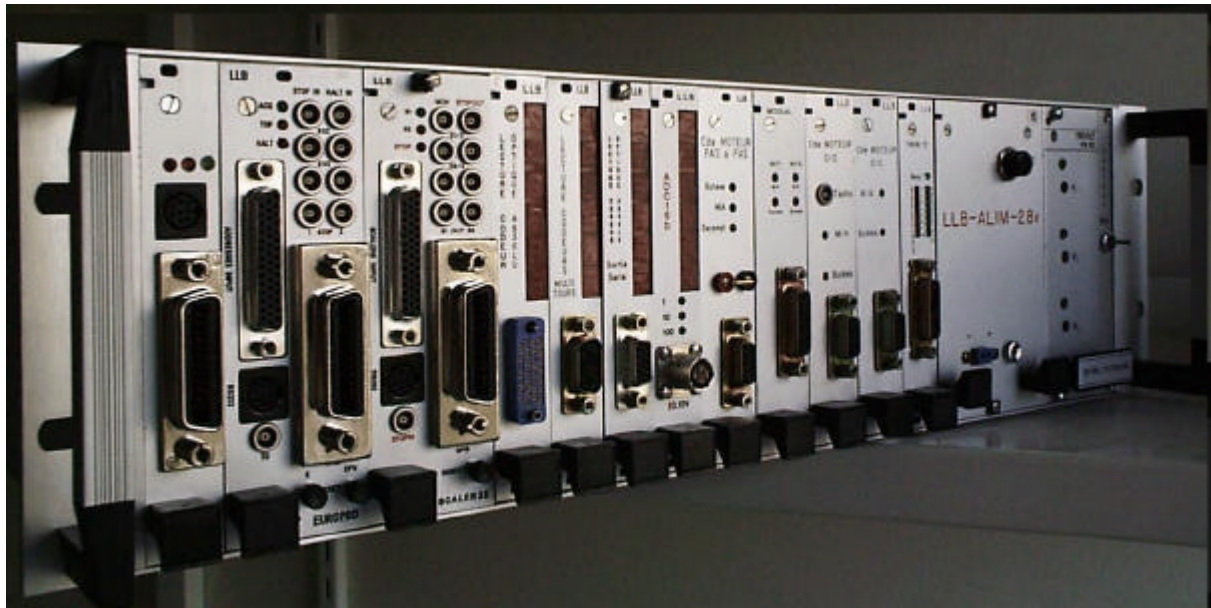


Figure 2 . Single Europe crate for the Daffodil System of LLB

THE EUROMOVE MODULE

The EuroMove module is a positioning controller.

It is a single Europe board (100 x 220 mm²), which can control **up to 10 axis simultaneously** through its own bus. This in-house design bus has been studied to allow on the one hand the mixing of power and logical signals and on the other, to provide a very simple and efficient interface to slave boards (encoder, motor, I/O boards etc.). Since the Europe crate contains the power supplies for the motors, **there is no need for another distinct power crate** nor additional connections.

The main role of the EuroMove module is to drive the motors through the motor boards, while monitoring the actual position of the mechanics via the encoder boards, to a position required by the computer. This module also provides a **real time display of the position** of each of the movements on the front panel of the encoder boards. The calculations are performed on 16 000 000 points, the displays showing 6 digits.

The onboard software embedded in the EuroMove module operates with different methods of positioning for each movement depending on its own encoder, motor and mechanic characteristics. In particular, it provides a **complete functional control of the pneumatic system** required by the « Tanzboden modules ».

Two types of boards, for D.C. and stepping motors as well as encoder boards for optical, magnetic and resistive sensor technologies have been designed. Thus, the user can choose the motorization and position encoding equipment that best fits his particular environment.

THE EUROSCALER MODULE

The EuroScaler module is basically a counting module for discrete detectors and monitors. Designed as a single Europe board, it is stand-alone and needs only the +5V to operate.

The EuroScaler module has an internal timer, a monitor counter and 32 scalars; it therefore can manage **a complete monitor preset or time preset operation on 32 detectors**. Moreover, it provides a **fully automatic acquisition mode for polarized neutrons** including up to 4 phases for polarized neutron analysis. The module outputs logical signals for driving the flippers. The duration for each of the phases and the dead time for the flipping of the magnetic field are programmable.

Input and output triggers for external synchronized systems like a EuroPsd module or another EuroScaler module are also available. For example, if there are more than 32 detectors on the experiment, several EuroScaler modules can be used, one of them will play the role of master and the others the role of slaves via their input triggers.

THE EUROPSD MODULE

For **data acquisition with fast Position Sensitive Detectors** (in particular those based on delay lines or microstrips), and to provide **Time Of Flight operation**, we have designed the **EuroPsd module** (see figure 3), which is stand-alone like the EuroScaler module.

The main function of the EuroPsd module is **histogramming memory**. It accepts a 18 bits to

accommodate a 512x512 cells PSD. Cells of the detector are associated **with 32 bits data counters**. One of the features of this module is the programming, through user friendly commands, of the allocation of the counters via a **routing memory**. This feature has many applications, for example, **converting a rectangular detector into a virtual circular detector**. Non adjacent cells can also be grouped together to form a multiparts « macrocell ». In the Time Of Flight mode, the delay, the number of time channels (up to 4096) and their **width (200 nsec**

up to 7 minutes by steps of 100 nsec) are programmable. Long duration time channels can be used in conjunction with another capability of the EuroPsd module, which is to follow and to distinguish several « frames » in a **kinetic experiment**.

With this EuroPsd module, the **maximum counting rate achievable is 5 MHz** with a null dead time, i.e. an address takes less than 200 nsec to be processed (routing, histogramming and T.O.F).



Figure 3. EuroPsd module for data acquisition and Time Of Flight

Several laboratories in the world are equipped with the LLB DAFFODIL system, among them K.F.K.I. (Hungary), I.T.N. (Portugal), Institute of Physics (China), Institute of Nuclear Technology (Greece), and more recently K.A.E.R.I. (Korea) in association with the CILAS company.

THE REPLACEMENT OF THE ORPHEE REACTOR'S HOUSING CORE

(SUMMER 1997)

The research reactor Orphée built by the CEA at Saclay in the late seventies went first critical in december 1980. Since then the reactor has provided the neutron beams used by physicists on the experimental spectrometers located around the reactor. During the summer 1997 the reactor was stopped for a major refurbishment : the remplacement of the housing core located in a heavy water tank.

This housing core, a square tube of $25 \times 25 \times 200 \text{ cm}^3$ is the backbone of the reactor as it contains the reactor core itself. It is the one barrier between the heavy water, from the tank, and the light water that cools the reactor core. The zircaloy 2 had been choosen for its characteristics both mechanical, close to those of the stainless steel, and physical (it does not interfere with the neutrons) to make the housing core and its 2 flanges. These two casted flanges are welded to both ends of the tube, and it is by them that the housing core is attached to the top and the bottom of the middle of the heavy water tank. The water tightness between the 2 types of water is done by two 0-ring metallic joints. The reactor core is supported by the grid core, located at the bottom of the housing core. The core is composed by eight fuel rods and one beryllium rod. So outside the tube there is the heavy water and inside it, there is the core itself cooldown by light water.

In reactor early life, year 1983, the metallic 0-ring upper joint, between the tank and the housing core, went to leak. So it has been replaced by a new one. This operation was done by removing the housing core from the heavy water tank and then the joint was changed by reputting it in its original place. The strain on the studs and nuts was increased to ensure the tighness of the system.

Meanwhile, it was obvious that the leak was due to the growth of the housing core that will, in the long run, lead to another leak. So it was decided to study the zircaloy growth by putting some samples inside the beryllium rod located in the middle of the reactor core itself. At the same time a new housing core was ordered.

The main difference between the two housing cores is that the new one is fitted at its top with a growth absorber made of a double stainless steel wall and flanges.

In the year 1995, it was foreseen, in the light of the study of the zircaloy, that the housing had to be changed by the turn of the century. It was then decided that it will be done in the summer 1997 to allow time to plan the operations. This planning was made by looking back in 1983 when the housing was first taken out to foresee the coming problems.

The main concerns were the four bottom studs and nuts as they had already given us troubles. It was decided to make some specific tools to destroy either the nut or, at worst possible case, the stud. The planning was done to start the refurbishment on the 15 july 1997.

The reactor was stopped on the 13, the core unloaded on the 14, and the heavy water replaced by light water on the 15. Before removing the housing core itself, several operations had to be done :

- i) Remove the bars that link the control rods and their mechanism,
- ii) Remove the rod trolley,
- iii) Remove the loading-unloading anti-fault grid,
- iv) Remove the core grid.

After that, it was possible to take out of the tank the housing core. The housing core was put in the canal to be disposed later. It was now possible to look inside the heavy water tank for an inspection done with a remote camera and also on the two 0-ring spans. It had shown that the two spans should be meticulously cleaned before we put back the new housing core.

Through out these tasks, the new housing core and all its parts were put together on a mock-up tank for a final check before it was put in its real location, the heavy water tank.

After all the checks, both on the span ring, on the tank and on the new housing with all its parts, it was then decided to put the new housing in place. When it was in place two tasks were done. First the three 0-ring joints were tested for water tightness. There is one more joint, the one between the zircaloy flange and the stainless steel of the growth absorber device. As the test gave us satisfaction, all the other parts were put back into place.

When all the operations have been completed a mock up core was loaded in the new housing core for hydraulic tests. When completed, we asked the French Safety Authorities for the green light to start the reactor. The reactor was then loaded with the fuel rods. We had the go ahead green light to start on the 27 october 1997.



Figure 1. Removal under water of the old housing core

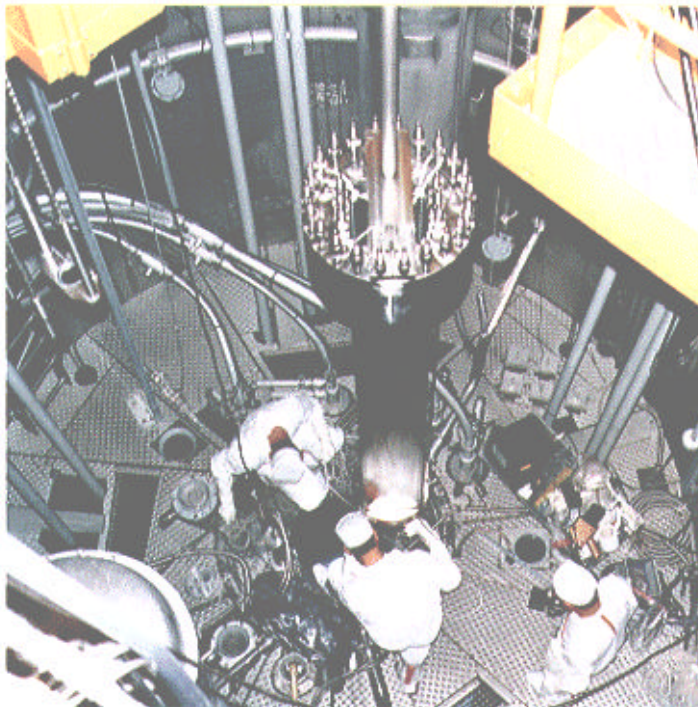
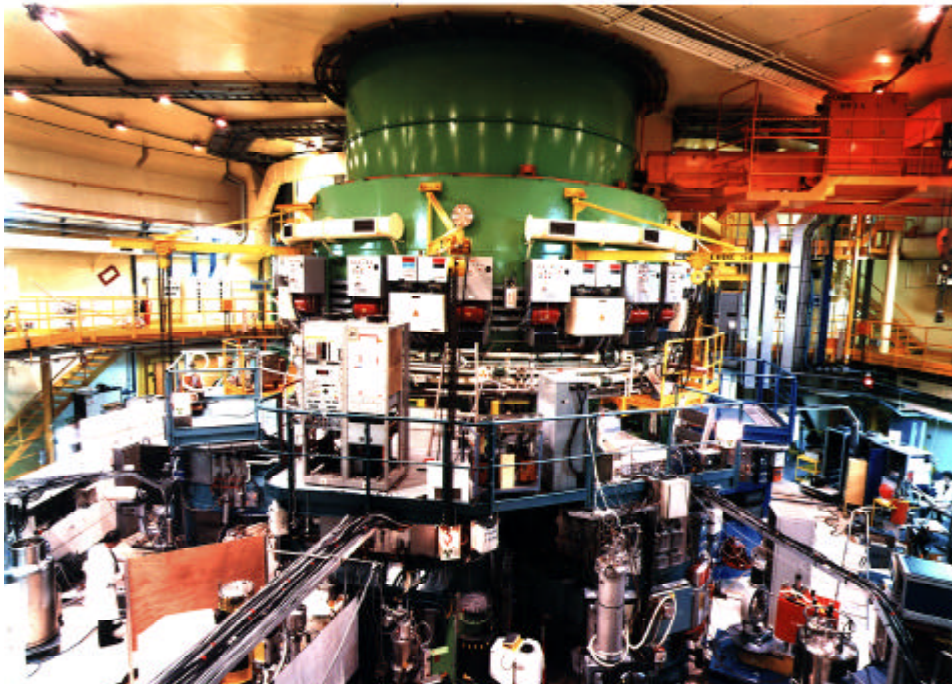


Figure 2. Installation of the new housing core

EXPERIMENTAL PROGRAMME AND USER ACTIVITIES



HALL OF REACTOR ORPHEE

EXPERIMENTAL PROGRAMME AND USER ACTIVITIES

1. SUMMARY OF THE USER ACTIVITIES IN 1997 AND 1998

1.1 Operation of Orphée reactor and LLB facility

The reactor Orphée operated 190 days in 1997 and 222 days in 1998. 3834 and 4518 experiment days were realized respectively in 1997 and in 1998 on the 24 scheduled instruments.

These values do not take into account the beam time given to the CRG teams on the following instruments : 2T (Kf Karlsruhe), G4.3 (University of Wien) and G5.2 (INFM, Italy, only for 1998). The CRG time is usually 1/3 of the Orphée operating time (25% for G5.2).

They include the full beam time for G4.4 (managed by ONERA), 5C2 (managed by University of Aachen) and G5.2 (INFM, for 1997).

Remark : The low operating time of the reactor in 1997 is of course due to the replacement of the zircaloy housing core (a square tube which contains the reactor core itself), which required a long shut-down from 13 july to 27 october 1997, i.e. 2 months more than the usual summer shut-down. Since 27 october 1997, the reactor operates with the new housing core very satisfactorily, and the scheduling of users activity could be made as previously planned.

At the Steering Committee of 13 january 1998, our funding agencies (CNRS and CEA) decided, for financial reasons, to decrease the operating time of Orphée from ~ 245 days (average value up to 1996) to 210 days per year, starting from 1998. Nevertheless, a specific authorization to pass this value was given for 1998 and 1999, in order to recover the 20 days shortage accumulated in 1997.

1.2. Instruments

The list and main characteristics of LLB instruments and a layout of their implantation are given in the introducing chapter « Presentation of LLB ».

In Table 1 are summarized the numbers of realized experiments and scheduled beam days, on the different instruments.

The new high resolution powder diffractometer, built in Gatchina, and installed in the guide hall in 1996, was progressively opened to users during the first semester of 1997.

Few instruments did not operate at full time, because of technical problems and/or refurbishment operations. In particular, new electronics and data acquisition programmes were installed on TV (Mibemol, G6.2). The mechanical parts of 5C1 were replaced by a-magnetic materials, necessary to operate the new 8 Teslas cryomagnet.

1.3 User statistics

Table 2 indicates the distribution of beam time per country (based on the location of the laboratory of the main applicant), for experiments realized in 1997 and 1998 respectively.

Around 70% of the total beam time was used by french users in 1997 and 1998, which is slightly more than in 1996. 29-30% was used by foreign users; this number includes 16% for European Union, 5% for CEI (Russia and Ukraina) and 5% for PECO (Eastern and Central Europe) countries.

Among the E.U. users, those involved in the TMR access programme received 332.5 beam days in 1997 and 359 in 1998 (8.7% and 8.0% of the total beam time respectively).

The distribution of total beam time per scientific domain (Round Table Sessions) was the following :

- 23% for Physical Chemistry and Biology (session A),
- 20% for Structural Studies and Phase Transitions (session B),
- 36% for Magnetism and Superconductivity (session C),
- 21% for Disordered Systems and Materials (session D).

2. BEAM TIME REQUEST AND ALLOCATION

2.1 The present organization

We have kept the new system of round tables and user selection panels put in place in 1996, which aimed to favour long-term projects.

To perform an experiment at LLB, the researcher must first submit a proposal written on a special form, where he explains his scientific interest and describes the proposed experiment. All the proposals submitted at LLB are examined by a peer review Selection Panel, which encounters once a year (at the end of november), and which is subdivided into 4 thematic sessions :

- Physical Chemistry and Biology,
- Structural Studies and Phase Transitions,
- Magnetism and Superconductivity,
- Disordered Systems and Materials Science.

Each session of the Selection Panel comprises typically 9 members (3 of LLB, 3 French non-LLB, 3 non-French). The list of members for the Selection Panel of december 1997 (which selected the experiments to be performed in 1998) is given in Table 3.

The Selection Panels classify the proposals in A, B,C, on the basis of scientific merit :

- A : accepted and to be performed,
- B : eventually performed if beam time available,
- C : rejected.

The applicant is informed by an official mail, of the classification of his proposal and, in case of success, of the allocated beam time. In case of classification C, the reasons are explained to the applicant.

The Selection Panels are preceded by user meetings, called "Tables Rondes du LLB". These meetings consisted of :

- invited talks (in each "Table Ronde", half a day was devoted to a specific theme, for example "magnetic thin films" in session C, and "fluids near the critical point" in session D);
- presentation of new long-term projects or programmes;
- presentation of recent scientific results obtained at the LLB ("poster" session);
- technical presentations;
- discussions with users.

30 to 40 people participated in the average to each of the four "Tables Rondes".

2.2 Beam time request

The evolution of beam time request since 1990 is presented in Table 4 and the associated figure.

The overall volume and proportion of french versus foreign request remains approximately constant since 1994 (end of ILL shut-down). Within the foreign request, the E.U. part slightly decreases; this is compensated by an increase from non-E.U. countries.

2.3 Analysis of the requests and allocations.

The beam time request and allocation for 1999 (evaluated by the User Selection Panel of november 1998) are summarized per country in Table 5, and per instrument and scientific session in Table 6.

Table 7 gives the overload factor for the LLB instruments, averaged on 3 years (Selection Panels of november 1995, 1996 and 1997) : this is defined as the ratio between the required beam time and the foreseen operating time of the instrument (80% of the operating time of Orphée, the 20% remaining being used for maintenance, repairs, tests, urgent experiments, etc...). The total overload factor is 1.5.

These numbers are practically constant since the refurbishment of the ILL reactor (1995).

2.4 Foreseen modifications of the beam time allocation.

Important modifications of the present system will be introduced at the end of 1999 :

- a) Submission of proposals and Selection Panels will be organized twice a year, in autumn and spring (in fact, a second session was already introduced in spring 1999 for the european TMR access programme).
- b) A fast access procedure by web for characterization experiments will be set-up on several instruments (in particular powder diffraction).
- c) A larger part of the total beam time will be reserved for long-term projects in the form of contractual programmes (with a typical duration of 3 or 4 years), for urgent or innovative proposals, and for industrial-type experiments. These types of proposals must be addressed to the LLB management, who will attribute beam time after external evaluation.

REALIZATION BY INSTRUMENT
FOR 1997 AND 1998

TABLE 1

INSTRUMENTS	1997		1998	
	Number of experiments performed	Beam time (days)	Number of experiments performed	Beam time (days)
TRIPLE-AXIS SPECTROMETERS				
1T	18	182	20	219
2T (german CRG)*	12	121	14	135
4F1	} 34	} 352	14	222
4F2			15	220
G4.3 (austrian CRG)*	8	81	14	135
POWDER DIFFRACTOMETERS				
3T2	33	182	43	211
G4.1	47	177.5	44	196
G4.2 (russian CRG)*	25	120.5	21	136
G6.1	19	158	29	190
MATERIALS DEDICATED DIFFRACTOMETERS				
6T1 (textures)	12	174	15	215
G52 (residual stresses) (1/2 Italian CRG)	20	174	21	222
SINGLE CRYSTAL DIFFRACTOMETERS				
5C1	8	122	12	168
5C2 (german CRG)*	18	191	20	224
6T2	14	172	12	164
REFLECTOMETERS				
Eros (G3 bis)	15	179	20	217
Desir (G5 bis)	16	169	13	177
Pada (G2.2)	19	187	22	222
DIFFRACTOMETERS FOR DISORDERED SYSTEMS				
7C2	20	160	21	155
G44 (ONERA CRG)	3	130	4	110
SMALL ANGLE NEUTRON SCATTERING				
PACE	} 95	} 493	43	221.5
PAXE			45	204
PAXY			42	205.5
QUASI-ELASTIC SCATTERING				
Spin Echo	10	153	10	155
TV (Mibemol)	23	156	23	194
TOTAL	469	3834	537	4518

* Not included CRG beam time given on 2T to germans, on G4.3 to austrians, on G4.2 to russians

REALIZATION BY COUNTRY FOR 1997 AND 1998

TABLE 2

COUNTRIES	1997			1998		
	Number of experiments performed	Beam time (days)	Total experiment beam time (%)	Number of experiments performed	Beam time (days)	Total experiment beam time (%)
TOTAL FOR FRANCE	315	2705	70,55%	365	3190	70.61%
AUSTRIA	5	23	0,6%	5	17.5	0.39%
BELGIUM	1	10	0,26%	2	14	0.31%
GERMANY	35	277	7,22%	39	312.5	6.92%
GREECE	3	9	0,23%	1	11	0.24%
IRELAND	2	14	0,37%	1	4	0.09%
ITALY	24	145.5	3,79%	33	179	3.96%
NETHERLANDS	2	5.5	0,14%	3	12	0.27%
PORTUGAL	4	35	0,91%	6	76	1.68%
SPAIN	2	11	0,29%	4	24	0.53%
SWEDEN	1	15	0,39%			
UNITED KINGDOM	10	77	2,01%	6	47	1.04%
TOTAL FOR E.U.	89	622	16,21%	100	697	15.43%
TOTAL FOR RUSSIA-CEI	17	209	5,45%	25	233	5.16%
BULGARIA	1	5	0,13%			
CZECH REPUBLIC	4	49	1,28%	2	14	0.31%
HUNGARY	10	48	1,25%	6	37.5	0.83%
POLAND	17	111.5	2,91%	20	172	3.81%
YUGOSLAVIA				2	11	0.24%
TOTAL FOR PECO	32	213.5	5,57%	30	234.5	5.19%
ALGERIA	1	3.5	0,09%			
AUSTRALIA	4	9	0,23%			
CUBA				1	10	0.22%
INDIA	1	6	0,16%			
JAPAN	2	28	0,73%	4	46	1.02%
KOREA	1	2	0,05%			
MOROCCO	1	10	0,26%	4	39	0.86%
SWITZERLAND	4	12	0,31%	3	18	0.40%
UNITED STATES	2	14	0,37%	5	50.5	1.12%
OTHERS	16	84.5	2,2%	17	163.5	3.62%
TOTAL	469	3834	100%	537	4518	100%

TABLE 3

USER SELECTION PANEL – « TABLES RONDES » 1997

SESSION A : Physical Chemistry, Biology		
LLB MEMBERS	FRENCH MEMBERS	NON-FRENCH MEMBERS
<i>Organizers :</i> A. Menelle J.M. Zanotti L. Auvray J.P. Cotton J. Teixeira	J.S. Candau (<i>président</i>), L.U.D.F.C.. Strasbourg F. Nallet, C.R.P.P. Bordeaux M. Roth, I.B.S. Grenoble	M. Corti, Univ. Milan B. Farago, I.L.L. Grenoble R.E. Lechner, Univ. Onasbruck

SESSION B : Structural Studies, Phase Transitions		
LLB MEMBERS	FRENCH MEMBERS	NON-FRENCH MEMBERS
<i>Organizers :</i> F. Moussa J.M. Kiat G. André B. Hennion R. Kahn M. Quilichini	A. Bulou, P.E.C. Le Mans R. Currat (<i>président</i>), I.L.L. Grenoble F. Denoyer, U.P.S. Orsay M.H. Lemée-Cailleau, G.M.C.M. Rennes	W.F. Kuhs, Univ. Goettingen E. Lorenzo-Diaz, Lab. Cristallo. Grenoble W. Prandl Univ. Tübingen

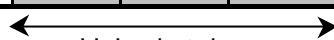
SESSION C : Magnetism, Superconductivity		
LLB MEMBERS	FRENCH MEMBERS	NON-FRENCH MEMBERS
<i>Organizers :</i> B. Hennion G. André C. de Novion C. Fermon A. Goukassov M. Hennion	M. Alba, SPEC B. Chevalier, L.C.S. Talence B. Fak, DRFMC. CEN G P. Mangin (<i>président</i>) LMPSM, Nancy	J.C. Gomez-Sal, Univ Cantabria P. Schweiss, K.F.K. Karlsruhe

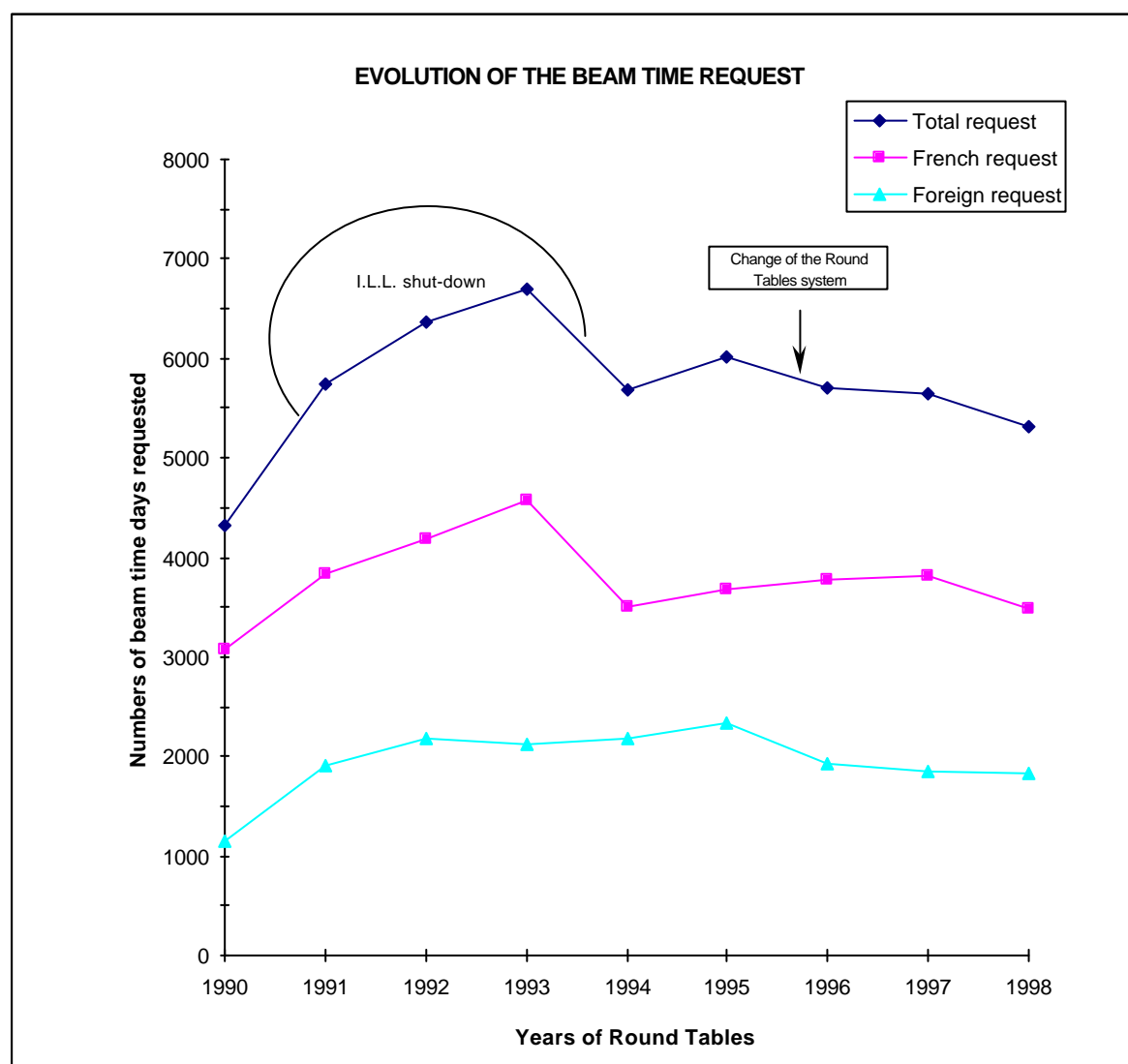
SESSION D : Disordered Systems, Materials		
LLB MEMBERS	FRENCH MEMBERS	NON-FRENCH MEMBERS
<i>Organizers :</i> M.H. Mathon M. Bonetti F. Bourée C.H. de Novion	B. Frick, ILL Grenoble J.M. Sprauel, ENSAM Aix en Provence P. Lagarde, LURE Orsay J.L. Bechade, SRMA CEA/Saclay	F. Barocchi, Univ. Florence J.P. Gaspard (<i>président</i>), Univ. Liège G. Krexner, Univ. Wien

TABLE 4

EVOLUTION OF THE BEAM TIME REQUEST
(Number of beam time days : annual request)

Years of Round Tables	1990	1991	1992	1993	1994	1995	1996	1997	1998
Total request	4322.5	5739	6363	6696	5690.5	6021	5698	5651.5	5304.5
French request	3080	3826	4182	4572.5	3509	3687.5	3767	3811	3478
Foreign request	1142.5	1913	2181	2123.5	2181.5	2333.5	1931	1840.5	1826.5


 I.L.L. shut-down



ROUND TABLES 1998 : REQUEST AND ALLOCATIONS (PRIORITY A) PER COUNTRY FOR 1999

TABLE 5

COUNTRIES	Number of proposals submitted	Beam time requested (days)	Allocated beam time (days) (as priority A)					% of total allocated beam time
			Session A	Session B	Session C	Session D	Total	
<i>TOTAL FOR FRANCE</i>	292	3478	516.5	430	760.5	685.5	2392.5	71.09%
AUSTRIA	6	49	3.5		21	7	31.5	0.94%
BELGIUM	4	34	3.5			14	17.5	0.52%
GERMANY	40	435.5	42	67	112	57	278	8.26%
GREECE	1	4	4				4	0.12%
IRELAND	1	8			7		7	0.21%
ITALY	15	136	22.5		31	29	82.5	2.45%
NETHERLANDS	3	50	14		7		21	0.62%
PORTUGAL	3	34		26			26	0.77%
SPAIN	4	69		7	41		48	1.43%
UNITED KINGDOM	13	104	4	13	26	5	48	1.43%
<i>TOTAL FOR E.U.</i>	90	923.5	93.5	113	245	112	563.5	16.74%
<i>TOTAL FOR RUSSIA-CEI</i>	28	359	3.5	13	98	0	114.5	3.40%
BULGARIA	1	6					0	0.00%
CZECH REPUBLIC	3	34			7	5	12	0.36%
HUNGARY	12	89	17.5			7	24.5	0.73%
POLAND	16	98			38	8	46	1.37%
RUMANIA	1	7				5	5	0.15%
<i>TOTAL FOR PECO</i>	33	234	17.5	0	45	25	87.5	2.60%
AUSTRALIA	1	15			10		10	0.30%
CUBA	1	5				5	5	0.15%
JAPAN	5	56			49		49	1.46%
MOROCCO	7	54		7	32	4	43	1.28%
MEXICO	1	10	7				7	0.21%
SWITZERLAND	4	42			31		31	0.92%
TUNISIA	1	8	3.5				3.5	0.10%
UNITED STATES	9	120	35	24			59	1.75%
<i>TOTAL FOR OTHER COUNTRIES</i>	29	310	45.5	31	122	9	207.5	6.17%
TOTAL	472	5304.5	676.5	587	1270.5	831.5	3365.5	100.00%

TABLE 6

ROUND TABLES 1998 - REQUEST AND ALLOCATIONS PER INSTRUMENT FOR 1999

INSTRUMENTS	Request		Allocated beam time (as priority A)				
	Number of proposals	Beam time (days)	Session A (days)	Session B (days)	Session C (days)	Session D (days)	TOTAL (days)
TRIPLE-AXIS SPECTROMETERS							
1T/2T	30	360		72	192	7	271
4F1/4F2	42	575	7	98	216	20	341
G4.3	7	93	21	49	21	28	119
POWDER DIFFRACTOMETERS							
3T1 (test instrument)	1	14				14	14
3T2	38	188.5		96	49	4	149
G41	36	222		24	93	37	154
G42	11	90		42	51	2	95
G61	19	232	4	7	128	14	153
MATERIALS DEDICATED DIFFRACTOMETERS							
6T1 (textures)	16	314				169	169
G52 (strains)	20	218				105	105
SINGLE CRYSTAL DIFFRACTOMETERS							
5C1	7	140			129		129
5C2	24	414		118	49		167
6T2	22	351		55	121		176
REFLECTOMETERS							
Desir/Eros	15	199	143		49	7	199
Pada	15	212			135		135
ELASTIC DIFFUSE SCATTERING							
7C2	19	243	7	3		146	156
G44	4	180				154	154
SMALL ANGLE NEUTRON SCATTERING							
Pace, Paxe, Paxy	118	852	347.5	2	17.5	73.5	440.5
QUASI-ELASTIC SCATTERING							
SPIN ECHO	9	159	91				91
TV	18	228	56	21		51	128
NRSE G1.bis (commissioning)	1	20			20		20
TOTAL	472	5304.5	676.5	587	1270.5	831.5	3365.5
			3365.5				

OVERLOAD FACTOR PER INSTRUMENT

TABLE 7

	Instrument	Overload factor (average)
Powder Diffractometers	3T2	1.25
	G4.1	1.75
	G4.2	0.9
	G6.1	1.15
Diffractometers for Materials Science Studies	6T1	1.8
	G5.2	2.7
Single Crystal Diffractometers	5C1	0.95
	5C2	2.7
	6T2	1.95
Diffuse Scattering Instruments	7C2	1.45
Small-Angle Scattering Instruments	all	1.75
Reflectometers	DESIR (G5 bis)	0.95
	EROS (G3 bis)	0.95
	PADA (G2.2)	1.4
Triple-axis Instruments	1T/2T	1.4
	4F1/4F2	1.35
	G4.3	0.9
Quasi-elastic Instruments	MIBEMOL (G6.2)	1.6
	MESS (G3.2)	1.2

PAPERS PUBLISHED IN SCIENTIFIC PERIODICALS AND CONFERENCE PROCEEDINGS

- ADAM M., LAIREZ D., RASPAUD E., FARAGO B. - *Dynamic properties of semidilute solutions at the theta point*.
Physical Review Letters **78** (1997) 1197
- ADAM M., LAIREZ D., KARPASAS M., GOTTLIEB M. - *Static and dynamic properties of crosslinked poly(dimethylsiloxane) pregel clusters*
Macromolecules **30** (1997) 5920-5929
- ADAM M., FARAGO B., SCHLEGER P., RASPAUD E. LAIREZ D. - *Binary contacts in semidilute solution : good and Θ solvents*
Macromolecules **31** (1998) 9213-9223
- AEBERSOLD M., GILLON B., PLANTEVIN O., PARDI L., KAHN O., BERGERAT P., VON SEGGERN I., TUCZEK F., OHRSTROM L., GRAND A., LELIEVRE-BERNA E. - *Spin density map in the triplet ground state of $[\text{Cu}_2(\text{t-BuPy})_4(\text{N}_3)_2]$ -(t-BuPy=para-ter-butylpyridine) : a polarized neutron diffraction study*
Journal American Chemical Society **120** (1998) 5238-5245
- AIN M., LORENZO J.E., REGNAULT L.P., DHALENNE G., REVCOLEVSCHI A., HENNION B., JOLICOEUR Th. - *Double gap and solitonic excitations in the spin-Peierls chain CuGeO_3*
Physical Review Letters **78** (1997) 1560-1563
- AIN M., REGNAULT L.P., DHALENNE G., REVCOLEVSCHI A., LORENZO J.E., JOLICOEUR Th. - *Double gap in the spin-Peierls compound CuGeO_3*
Journal of Applied Physics **81** (1997) 4393-4395
- AKSEL'RUD L.G., ANDRE G., KULIKOV L.M., TAKZEI G.A., SEMENOV-KOBZAR A.A., ROMAKA L.P. - *Tantalum and niobium disulfides intercalated with chromium and nickel*
Inorganic Materials **34** (1998) 395-400
- AKSENOV V.L., BALAGUROV A.M., SIKOLENKO V.V., SIMKIN V.G., ALYOSHIN V.A., ANTIPOV E.V., GIPPIUS A.A., MIKHAILOVA D.A., PUTILIN S.N., BOUREE F. - *Precision neutron diffraction study of the high- T_c superconductor $\text{HgBa}_2\text{CuO}_{4+\delta}$*
Physical Review B **55** (1997) 3966-3973
- ALBERTINI G., BRUGNAMI D., BRUNO G., CERETTI M., EDWARDS L., RUSTICHELLI F. - *Residual stresses in a ferritic steel welded pipe : an experimental comparison between reactor and pulsed neutron sources*
SPIE Proc. Vol. 2867 (1997) 123-128
- ALBERTINI G., CAGLIOTI G., CERETTI M., FIORI F., OGGIONI F., RUSTICHELLI F., VIVIANI L. - *Neutron diffraction measurements of residual stresses in a thermoelastically coupled AA6082 alloys system*
Radiat. Phys. Chem. **51** (1998) 525-526
- ALEKSEEV P.A., MIGNOT J.-M., LAZUKOV V.N., SADIKOV I.P., PADERNO YU.B., KONOVALOVA E.S. - *Influence of the mixed-valence state on the magnetic excitation spectrum of SmB_6 -based compounds*
Journal of Solid State Chemistry **133** (1997) 230-236
- ALEKSEEV P.A., MIGNOT J.-M., CLEMENTYEV E.S., LAZUROV V.N., SADIKOV I.P. - *Magnetic excitations and variation of valence in SmB_6 -based systems*
Physica B **234-236** (1997) 880-882
- ALEKSEEV P.A., FABI P., MIGNOT J.-M., NEFEODOVA E.V., OCHIAI A., RIAZANTSEV S.A. - *Intermultiplet transitions and crystal field in mixed valence Sm_2Te_4*
Physica B **234-236** (1997) 883-885
- ALLOUL H., BOBROFF J., MAHAJAN A., MENDELS P., YOSHINARI Y., COLLIN G., MARUCCO J.F. - *NMR studies of the original magnetic properties of the cuprates : influence of impurities and defects*
Physica C **282-287** (1997) 226
- ALMASY L., CSER L., DEZSI I., KALI G. - *Small angle neutron scattering (SANS) study of frozen solutions*
Physica B **234-236** (1997) 297-299
- ALMASY L., JAKLI A., ROSTA L., PEPY G. - *Structural memory effect in liquid crystal phases stabilised by silica particle aggregates*
Physica B **241-243** (1998) 996-998
- ALONSO J.A., BOUCHERLE J.X., GIVORD F., SCHWEIZER J., GILLON B., LEJAY P. - *Evidence for 5d anisotropic negative polarization along the Ce chains in CeRh_3B_2*
Journal of Magnetism and Magnetic Materials. **177-181** (1998) 1048-1049
- ALTOUNIAN Z., SAINI S., MAINVILLE J., BELLISSENT R. - *A neutron diffraction study of Al-rich glasses*
Physica B **241-243** (1998) 915-917
- AL USTA K., MENELLE A., N'GUY K. - *Large θ_c neutron supermirrors and stress evolution with irradiation*
Physica B **234-236** (1997) 1044-1046
- AL USTA K., GAEHLER R., BOENI P., HANK P., KAHN R., KOPPE M., MENELLE A., PETRY W. - *A new polarizing guide at LLB*
Physica B **241-243** (1997) 77-78
- ANDRE G., BOUREE F., OLES A., PENC B., SIKORA W., SZYTULA A., ZYGMUNT A. - *Magnetic ordering of RNiSb_2 ($R = \text{Pr}, \text{Nd}$ and Tb) compounds studied by neutron diffraction and magnetic measurements*
Journal of Alloys and Compounds **255** (1997) 31-42
- ANDRE G., BOUREE F., OLES A., SIKORA W., BARAN S., SZYTULA A. - *Magnetic structures of HoPdSb compound*
Solid State Communications **104** (1997) 531-534
- ANDRE G., BOUREE F., WOCHOWSKI K., SUSKI W. - *Magnetic structure of the $\text{UCu}_4\text{Ni}_8\text{Al}_8$ system*
Solid State Communications **104** (1997) 189-192
- ANDRE G., BOUREE F., OLES A., PENC B., SIKORA W., SZYTULA A., ZYGMUNT A. - *Magnetic structures of RNiSb_2 ($R = \text{Pr}, \text{Nd}$ and Tb) compounds*
Physica B **234-236** (1997) 650-651
- ANGLARET E., SAUVAJOL J.-L., ROLS, S., JOURNET C., GUILLARD T., ALVAREZ L., MUNOZ E., BENITO A.M., MASER W.K., MARTINEZ M.T., DE LA FUENTE G.F., LAPLAZE D., BERNIER P. - *Molecular dynamics of single wall nanotubes*
In « Electronic Properties of Novel Materials », edited by H. Kuzmany et al. (1998) pp. 318-321
- ARISTOV D.N., MALEYEV S.M - *RKKY interaction in the nearly-nested Fermi liquid*
Physical Review B **56** (1997) 8841-8848
- ARISTOV D.N. - *Bosonization for a Wigner-Jordan-like transformation : backscattering and umklapp processes on a fictitious lattice*
Physical Review B **57** (1998) 12825-12831
- ARISTOV D.N, YASHENKIN A.G. - *Comment on « Impurity states and the absence of quasiparticle localization in disorder d-wave superconductors »*
Physical Review Letters **80** (1998) 1116
- AUBRY S. - *Breathers in nonlinear lattices : existence, linear stability and quantization*
Physica D **103** (1997) 201-250
- AUBRY S., CRETEGNY T. - *Mobility and reactivity of discrete breathers*
Physica D **119** (1998) 34-46

- AUBRY S. - *Discrete Breathers in Anharmonic model with acoustic phonons*
«Annales de l'Institut Henri Poincaré Physique Théorique» **68** (1998) 381-420
- AUBRY S. - *Breathers in nonlinear lattices. Recent results from the concept of anticontinuity*
In «Progress in Statistical Physics», Eds. W. Sung, I. Chang, B. Kahng, C.S. Kim, S. Kim, J.-H. Oh, (1998) pp. 131-157, World Scientific, Singapore
- BACZMANSKI A., WIERZBANOWSKI K., TARASIUK J., LODINI A. - *Determination of residual stress by diffraction method in anisotropic materials*
Archives of Metallurgy **42** (1997) 172-188
- BACZMANSKI A., WIERZBANOWSKI K., TARASIUK J., BRAHAM C., LODINI A. - *Examination of internal stresses in two phases polycrystalline materials*
Archives of Metallurgy **42** (1997) 173-188
- BACZMANSKI A., WIERZBANOWSKI K., TARASIUK J., LODINI A., LEVY R., CERETTI M., FITZPATRICK M. - *Study of second order stresses for single and two phases polycrystalline materials*
Proceedings of UCRS5, Linköping (1997) 208-213
- BACZMANSKI A., WIERZBANOWSKI K., TARASIUK J., CERETTI M., LODINI A. - *Anisotropie des microcontraintes mesurées par diffraction*
La Revue de Métallurgie (1997) 1468-1474
- BACZMANSKI A., WIERZBANOWSKI K., TARASIUK J., CERETTI M., LODINI A. - *Anisotropy of micro-stress measured by diffraction*
La Revue de Métallurgie (1997) 1-8
- BACZMANSKI A., WIERZBANOWSKI K., TARASIUK J., LIPINSKI P., LEVY R., LODINI A. - *Internal stresses in metal matrix composite diffraction experiment and elasto-plastic model*
Proceedings of MAT-TEC 97, Reims, A. Lodini (ed.) (1997) 269-274
- BAGLIONI P., GAMBI C.M.C., GIORDANO R. - *SANS on fluorinated water in oil microemulsions*
Physica B **234-236** (1997) 295-296
- BAGLIONI P., GAMBI C.M.C., GIORDANO R., TEIXEIRA J. - *Complexation of counter-ions in ionic micellar solutions: a small-angle neutron scattering study*
Colloid and Surface Science **A121** (1997) 47-52
- BAGLIONI P., GAMBI C.M.C., GIORDANO R., LO NOSTRO P., TEIXEIRA J. - *SANS on micellar solutions of octyl-18-crown-6*
Physica B **234-236** (1997) 300-302
- BALAGUROV A.M., SIKOLENKO V.V., LYUBUTIN I.S., ANDRE G., BOUREE F. - *Magnetic structure of UPd₂Ge₂ doped with Fe*
ZhETP Letters **66** (1997) 615-619 [version russe], JETP Letters **66** (1997) 647-652 [American Institute of Physics]
- BALDINOZZI G., GREBILLE D., SCIAU PH., KIAT J.M., MORET J., BEBAR J.F. - *Rietveld refinement of the incommensurate structure of the elpasolite (ordered perovskite) Pb₂MgTe₆*
Journal of Physics : Condensed Matter **10** (1998) 6461-6472
- BARADEL N., BIANCHI L., BLEIN F., FRESLON A., JEANDIN M., CERETTI M., LU J. - *Evaluation of residual stresses within plasma-sprayed zirconia (ZrO₂-Y₂O₃ 8%wt) coatings*
In "Thermal Spray, Meeting the challenges of the 21st Century" Edited by C. Coddet (1998) pp.1623-1627
- BARBU A., MATHON M.H., MAURY F., BELLIARD J.F., BEUNEU B., DE NOVION C.H. - *A comparison of the effect of electron irradiation and of thermal ageing on the hardness of FeCu binary alloys*
Journal of Nuclear Materials **257** (1998) 206-211
- BARDEAU J.F., BULOUE A., SWANSON B.I., HENNION B. - *Inelastic neutron scattering studies of a quasi one-dimensional charge density-wave system : characterization of interchain interactions*
Physical Review B **58** (1998) 2614-2619
- BARON V., GILLON B., COUSSON A., MATHONIERE C., KAHN O., GRAND A., OHRSTROM L., DELLEY B., BONNET M., BOUCHERLE J. - *X - Spin density maps for ferrimagnetic chain compound MnCu(pba)(H₂O)₃.2H₂O (pba = 1,2-propylene-bis (oxamato)); polarized neutron diffraction and theoretical studies*
J. Am. Chem. Soc. **119** (1997) 3500-3506
- BARON V., GILLON B., KAHN O., RUNDLOF H., TELLGREN R. - *Low temperature and X-ray diffraction studies on Mn(cth)Cu(oxpn)(CF₃SO₃)*
Acta Chem. Scand. **51** (1997) 683-688
- BELIN-FERRE E., TRAMBLY DE LAISSARDIERE G., PECHEUR P., SADOE A., DUBOIS J.M. - *Electronic structure of orthorhombic Al₅Co₂*
Journal of Physics : Condensed Matter **9** (1997) 9585-9596
- BELLISSENT-FUNEL M.-C., FILABOZZI A., CHEN S.H. - *Measurement of coherent Debye-Waller factor in an in-vivo deuterated C-phycocyanin by inelastic neutron scattering*
Biophysical Journal **72** (1997) 1792-1799
- BELLISSENT-FUNEL M.-C., FILABOZZI A., CHEN S.H. - *Dynamics of a deuterated C-phycocyanin protein as studied by coherent inelastic neutron scattering*
In «Biological Macromolecular Dynamics» (Eds. S. Cusack, H. Buttner, M. Ferrand, P. Langan and P. Timmins) Adenine Press (1997) p.143
- BELLISSENT-FUNEL M.-C. - *Recent developments in biology at Laboratoire Léon Brillouin*
Proceedings of «The International Workshop on Cold Neutron Utilization» Kaeri, The Republic of Korea, (1997) p. 147-157
- BELLISSENT-FUNEL M.-C. - *Le rôle de l'eau dans la stabilité et la fonction des macromolécules biologiques*
"Interface Physique Biologie" dans les Lettres du Département SPM du CNRS - n°30 (1997) 7-9
- BELLISSENT-FUNEL M.-C. - *L'eau qui brûle*
Les Défis du CEA, n°61 (1997) 23-25
- BELLISSENT-FUNEL M.-C., NARS S., BOSIO L. - *X-ray and neutron scattering studies of the temperature and pressure dependence of the structure of liquid formamide*
Journal of Chemical Physics **106** (1997) 7913-7919
- BELLISSENT-FUNEL M.-C., TASSAING T., ZHAO H., BEYSENS D., GUILLOT B., GUISSANI Y. - *The structure of supercritical heavy water as studied by neutron diffraction*
Journal of Chemical Physics. **107** (1997) 2942-2949
- BELLISSENT-FUNEL M.-C. - *Coup de sonde dans l'eau*
Les Défis du CEA, n°69 (1998) 22
- BELLISSENT-FUNEL M.-C. - *Experimental evidence of a liquid-liquid phase transition in supercooled water*
Europhysics Letters **42** (1998) 161-166
- BELLISSENT-FUNEL M.-C. - *Two forms of liquid water*
Physics Today, Physics Update **51** (1998) 9
- BELLISSENT-FUNEL M.-C. - *Two forms of liquid water*
Physics News, Supplement to APS news (1998) 6
- BELLISSENT-FUNEL M.-C. - *H-bond networks in stability and function of biological macromolecules*
In «Dynamical Network in Physics and Biology» edited by D. Beyens and G. Forgacs, Springer and EDP Sciences (1998) 213-225
- BELLISSENT-FUNEL M.-C., DANIEL R., DURAND D., FERRAND M., FINNEY J.L., POUGET S., REAT V., SMITH J.C. - *Nanosecond protein dynamics : first detection of a neutron incoherent spin-echo signal*
Journal American Chemical Society . **120** (1998) 7347-7348
- BELLISSENT-FUNEL M.-C., TEIXEIRA J. - *Structural and dynamic properties of bulk and confined water*
In «Freeze-Drying/Lyophilization of Pharmaceutical and Biological Products» edited by L. Rey and J.C. May, Publishers Marcel Dekker, New York (1998) p.53-77

- BELLISSENT-FUNEL M.-C. - *Structure and dynamics of water near hydrophilic surfaces*
J. Mol. Liquids **78** (1998) 19-28
- BELLISSENT-FUNEL M.-C. - *Evidence of a possible liquid-liquid phase transition in supercooled water by neutron diffraction*
Il Nuovo Cimento D **20D**, n°12bis (1998) 2107-2122
- BENHAYOUNE M., SCHWAB D., LODINI A. - *Influence of the velocity and diameter of the shot on the state of stress induced by shot peening*
Proceedings of MAT-TEC 97, Reims, A. Lodini (ed.) (1997) 153-158
- BERGMAN C., SEIFERT-LORENZ K., COULET M.V., CEOLIN R., BELLISSENT R., HAFNER J. - *Local order in liquid potassium-antimony alloys studied by neutron scattering and ab initio molecular dynamics*
Europhysics Letters **43** (1998) 539-545
- BERRET J.F., GAMEZ-CORRALES R., OBERDISSE J., WALKER L.M., LINDNER P. - *Flow structure relationship of shear-thickening surfactant solutions*
European Physics Journal B **3** (1998) 463-469
- BESENBOCK W., GÄHLER R., HANK P., KAHN R., KOPPE M., DE NOVION C.H., PETRY W., WUTTKE J. - *First scattering experiment on MIEZE a Fourier transform time-of-flight spectrometer using resonance coils*
Journal of Neutron Research **7** (1998) 65-74
- BIENFAIT M., GAY J.M., ZEPPEFELD P., VILCHES O.E., MIREBEAU I., LAUTER H.J. - *Isotopic ordering in adsorbed hydrogen single layers*
Journal of Low Temperature Physics **111** (1998) 555-560
- BOBROFF J., ALLOUL H., YOSHINARI Y., MENDELS P., BLANCHARD N., COLLIN G., MARUCCO J.F. - *¹⁷O NMR comparison of zinc and nickel substituted YBa₂Cu₃O_{6.6}*
Physica C **282-287** (1997) 1389-1390
- BOBROFF J., ALLOUL H., YOSHINARI Y., KEREN A., MENDELS P., BLANCHARD N., COLLIN G., MARUCCO J.F. - *Using Ni substitution and ¹⁷O NMR to probe the susceptibility $\chi'(q)$ in cuprates*
Physica C **282-287** (1997) 2117-2120
- BODENAN F., CAJIPE V.B., DANOT M., OUVREARD G. - *Spin glass like behavior in the selenide Cr₂Sn₃Se₇*
Journal of Solid State Chemistry **137** (1998) 249-254
- BOGARD V., REVEL P., KIRCHER D., LODINI A. - *Modeling by finite elements method of thermomechanical behaviour of forming tools*
Proceedings of MAT-TEC 97, A. Lodini (editor), Reims, (1997) 183-188
- BONETTI M., CALMETTES P. - *Coherent neutron scattering from the ionic mixture of ethylammonium nitrate and deuterated n-octanol in the critical region*
Int. J. Thermophys. **19** (1998) 1555-1566
- BONETTI M., CALMETTES P. - *A very precisely regulated compact thermostat for small-angle neutron scattering*
Rev. Sci. Instrum. **68** (1997) 4163-4168
- BORDERE S., CHEVALIER B., LAFFARGUE D., ETOURNEAU J. - *Application of the anisotropic RKKY model on the composition dependence of the Néel temperature for U₅(Ni_{1-x}Pd_x)₂Sn system.*
Journal of Magnetism and Magnetic Materials **175** (1997) 263-271
- BOTTI S., CELESTE A., COPPOLA R. - *Particle size control and optical properties of laser synthesized silicon nanopowders*
Applied Organometallic Chemistry **12** (1998) 361-365
- BOULET P., DAOUDI A., POTEL M., NOËL H., GROSS G.M., ANDRE G., BOUREE F. - *Crystal and magnetic structure of the uranium digermanide UGe₂*
Journal of Alloys and Compounds **247** (1997) 104-108
- BOUREE F. - *Structures magnétiques et diffraction de neutrons sur poudre*
Ecole thématique « Cristallographie et neutrons », Journées Rossat-Mignod 1997, Cours - Tome I [18 pages]
- BOURGES P., REGNAULT L.P., SIDIS Y., BOSSY J., BURLET P., VETTIER C., HENRY J.Y., COUACH M. - *Shifting of the magnetic-resonance peak to lower energy in the superconducting state of underdoped YBa₂Cu₃O_{6.8}*
Europhysics Letters **38** (1997) 313-318
- BOURGES P., FONG H.F., REGNAULT L.P., BOSSY J., VETTIER C., MILIUS D.L., AKSAY I.A., KEIMER B. - *High energy spin excitations in YBa₂Cu₃O_{6.5}*
Physical Review B **56** (1997) 11439-11442
- BOURGES P., CASALTA H., REGNAULT L.P., BOSSY J., BURLET P., VETTIER C., BEAUGNON E., GAUTIER-PICARD P., TOURNIER R. - *High magnetic field dependence of spin fluctuations in YBa₂Cu₃O₇*
Physica B **234-236** (1997) 830-831
- BOURGES P., CASALTA H., IVANOV A.S., PETITGRAND D. - *Superexchange coupling and spin susceptibility spectral weight in undoped monolayer cuprates*
Physical Review Letters **79** (1998) 4906-4909
- BOURGES P., REGNAULT L.P., DAI P., YETHIRAJ M., MOOK H.A., LINDEMER T.B., DOGAN F. - *Comment on magnetic dynamics in underdoped YBa₂Cu₃O_{7-x}: direct observation of a superconducting gap*
Physical Review Letters **80** (1998) 1793-1794
- BOURGES P. - *From magnons to the resonance peak : spin dynamics in high T_c superconducting cuprates by inelastic neutron scattering*
In «The Gap Symmetry and Fluctuations in High Temperature Superconductors » Eds. J. Bok, G. Deutscher, D. Pavuna, S.A. Wolf - vol. 371 in NATO ASI series, Physics (1998) p. 349-371
- BRADEN M., ADELMANN P., SCHWEISS P. - *Structural aspects of the phase transition in (Nd_{1-x}Tb_x)_{1.85}Ce_{0.15}CuO₄*
Physica C **282-287** (1997) 1059-1060
- BRADEN M., REICHARDT W. - *Phonon dispersion in Ba(Pb_{0.75}Bi_{0.25})O₃*
Physica C **282-287** (1997) 1037-1038
- BRADEN M., MOUDDEN A.H., NISHIZAKI S., MAENO Y., FUJITA T. - *Structural analysis of Sr₂RuO₄*
Physica C **273** (1997) 248-254
- BRADEN M., REICHARDT W., NISHIZAKI S., MORI Y., MAENO Y. - *Structural stability of Sr₂RuO₄*
Physical Review B **57** (1998) 1236-1240
- BRADEN M., HENNION B., REICHARDT W., DHALENNE G., REVCOLEVSCHI A. - *Spin phonon coupling in CuGeO₃*
Physical Review Letters **16** (1998) 3634-3637
- BRADEN M., RESSOUCHE E., BÜCHNER B., KESSLER R., HEGER G. - *Anharmonic structural behavior in CuGeO₃*
Physical Review B **57** (1998) 11497-11503
- BRADEN M., ANDRE G., NAKATSUJI S., MIENO Y. - *Crystal and magnetic structure of Ca₂RuO₄ : magneto-elastic coupling and metal insulator transition*
Physical Review B **58** (1998) 847-861
- BRAHAM C., CERETTI M., COPPOLA R., LODINI A., NARDI C. - *X-ray and neutron diffraction study of residual stresses in electron beam welded F82H modified martensitic steel for fusion reactors*
Proceedings of MAT-TEC 97, Reims, A. Lodini (ed) (1997) 333-338
- BRAHAM C., CERETTI M., COPPOLA R., NARDI C., LODINI A. - *X-ray and neutron diffraction study of residual stresses in electron beam welded F82H modified martensitic steel for fusion reactors*
Proceedings of ICRS5, Linköping 1997, 244-249

- BRAITHWAITE D., DEMUER A., GONCHARENKO I.N., ICHAS V., MIGNOT J.-M., REBIZAN J., SPIRLET J.C., VOGT O., ZWIRNER S. - *Pressure effects on magnetism in the uranium and neptunium mononitrides*
Journal of Alloys and Compounds **271** (1998) 426-432
- BRANDO E., VINCENT H., RODRÍGUEZ-CARVAJAL J. - *Synthesis, X-Ray, Neutron and Magnetic Studies of New In-Plane Anisotropy M-Hexaferrites $BaFe_{12-2x}A_xMe_xO_{19}$ ($A=Ru, Ir$; $Me=Co, Zn$)*
Journal de Physique IV France, Coll C1, (1997) C303-C306
- BRIGANTI G., GIORDANO R., LONDEI P., PEDONE F. - *Small angle neutron scattering analysis of thermal stability of 23S rRNA and the intact 50S subunits of *Sulfolobus solfataricus**
Biochimica et Biophysica Acta **1379** (1998) 297-301
- BURGER K., COX D., PAPOULAR R., PRANDL W. - *The application of resonant scattering techniques to ab Initio structure solution from data using $SrSO_4$ as a test case*
J. Applied Crystallography **31** (1998) 789-797
- BUTTNER H.G., KEARLEY G.J., FILLAUX F., SCHIEBEL P., OULADDIAF B., LAUTIE M.F., KAHN R. - *Quantum free rotor transitions of partially deuterated NH_3 in a Hoffmann clathrate*
Physica B **241-243** (1998) 469-471
- CABACO M.I., DANTEN Y., BESNARD M., BELLISSENT-FUNEL M.-C., GUISSANI Y., GUILLOT B. - *Neutron diffraction and MD investigations of the temperature dependence of the local ordering in liquid cyclopropane*
Molecular Physics **90** (1997) 817-840
- CABACO M.I., DANTEN Y., BESNARD M., BELLISSENT-FUNEL M.-C., GUISSANI Y., GUILLOT B. - *Neutron diffraction and MD investigations of the structural evolution of liquid cyclopropane from the melting point up to supercritical domain*
IAEA Technical Committee Meeting on Neutron Beam Research (1997)
- CACCAVALE F., COPPOLA R., MENELLE A., MONTECCHI M., POLATO P., PRINCIPI G. - *Characterization of SnO_x films on architectural glass by neutron reflectometry, SIMS, CEMS and spectrophotometry*
J. of Non-Crystalline Solids **218** (1997) 291-295
- CALMETTES P. - *Le repliement des protéines : étude structurale de l'état complètement déplié par diffusion des neutrons*
dans "Des Phénomènes Critiques au Chaos ?" Actes du Colloque Scientifique à la Mémoire de Pierre Bergé, Ed. DSM-CEA (1998)
- CAMPO J.J., PALACIO F., PADUAN-FILHO A., BECERRA C.C., FERNÁNDEZ-DÍAZ M.T., RODRÍGUEZ-CARVAJAL J. - *Anomalous Antiferromagnetic-Spin Flop Boundary in the Phase Diagram of $Rb_2Fe_{1-x}In_xCl_3H_2O$ Solid Solutions*
Physica B **234-236** (1997) 622-624.
- CAPUZZI G., PINI F., GAMBI C.M.C., MONDUZZI M., BAGLIONI P., TEIXEIRA J. - *Small-Angle Neutron Scattering of $Ca(AOT)_2/D_2O/Decane$ Microemulsions*
Langmuir **13** (1997) 6927-6930
- CASALTA H., BOURGES P., PETITGRAND D., D'ASTUTO M., IVANOV A. - *2D magnetic behaviour of Nd in Nd_2CuO_4 below T_N*
Physica B **234-236** (1997) 803-805
- CASALTA H., BOURGES P., D'ASTUTO M., PETITGRAND D., IVANOV A. - *Magnetic behavior of Nd in Nd_2CuO_4 above 1.5 K*
Physical Review B **57** (1998) 471-475
- CASALTA H., SCHLEGER P., BELLOUARD C., HENNION M., MIREBEAU I., FARAGO B. - *Direct measurement of super paramagnetic fluctuations in monodomain Fe particles*
Physica B **241-243** (1998) 576-578
- CAUDRON R., FINEL A., CALVAYRAC Y., FRADKIN M., BELLISSENT R. - *Diffuse scattering of neutrons in $AlPdMn$ quasicrystals*
Physica B **241-243** (1998) 317-319
- CERETTI M. - *The new strain dedicated neutron diffractometer at the Laboratoire Léon Brillouin*
Proceedings of MAT-TEC 97, A. Lodini (editor), Reims, (1997) p. 45-53
- CERETTI M., HIPPSLEY C.A., HUTCHINGS M.T., LODINI A., WINSOR C.G. - *Neutron diffraction measurement of the triaxial stress field in a fatigued test specimen*
Physica B **234-236** (1997) 967-971
- CERETTI M., COPPOLA R., FIORI F., MAGNANI M. - *Microstructural evolution, under tempering at 700°C, in a steel for fusion reactors*
Physica B **234-236** (1997) 999-1002
- CERETTI M., HIRSCHI K., LODINI A., BRAHAM C. - *Microstrain investigation by neutron diffraction line broadening analysis*
in "Surface Modification Technologies XI" Edited by T.S. Sudarsham, M. Jeandin, K.A. Khor, The Institute of Materials, London, 1998, p.1031-1037
- CERETTI M., COPPOLA R., DI PIETRO E., NARDI C. - *High-temperature residual strain measurements, using neutron diffraction, in brazed Cu/CFC graphite divertor structures*
Journal of Nuclear Materials **258-263** (1998) 1005-1009
- CHEVALIER B., FOURGEOT F., LAFFARGUE D., ETOURNEAU J., BOUREE F., ROISNEL T. - *Magnetic phase transitions in the ternary stannides Ce_2T_2Sn , with $T = Ni, Pd$ or Pt*
Physica B **230-232** (1997) 195-197
- CHEVALIER B., FOURGEOT F., LAFFARGUE D., GRAVEREAU P., FOURNES L., ETOURNEAU J. - *Crystal chemistry and magnetic properties of ternary stannides R_2M_2Sn ($R =$ rare earth or uranium, $M = Ni, Pd$)*
Journal of Applied Chemistry **262-263** (1997) 114-117
- CHEVALIER B., FOURGEOT F., LAFFARGUE D., POTTGEN R., ETOURNEAU J. - *Magnetic ordering in the $RE_2Pd_{2+x}Sn_{1-x}$ ternary stannides ($RE = Gd, Tb, Dy, Ho, Er$)*
Journal of Applied Chemistry **275-277** (1998) 537-540
- CHEVRIER G., NAVAZA A., KIAT J.M. - *X-ray powder diffraction of the strontium nitroprusside tetrahydrate at different temperatures under 300K : Sample evolution to a mixed (Tetra, Di, Mono)-hydrate phase*
Materials Science Forum. **278-281** (1998) 648-653
- CHEVRIER G., NAVAZA A., KIAT J.M., GUIDA J.A. - *Neutron structure of strontium pentacyanonitrosilferrate(II) tetrahydrate below the 153 K phase transition*
Eur. J. Solid State Inorg. Chem. **35** (1998) 667-678
- CHIKINA I., DAOUD M., - *Slow relaxation in interpenetrating networks*
Journal of Chemical Physics **107** (1997) 5948-5951
- CHIKINA I., DAOUD M., - *Structure of interpenetrating polymers networks*
Journal of Polymer Science B **36** (1998) 1507-1512
- CHTOUN E., HANEBAI L., GARNIER P., KIAT J.M. - *X-ray and neutron Rietveld analysis of the solid solution $(1-x)A_2Ti_2O_7-xMgTiO_3$*
Eur. J. Solid State Inorg. Chem. **34** (1997) 553-561
- CLEMENTYEV E.S., KOEHLER R., BRADEN M., MIGNOT J.-M., VETTER C., MATSUMURA T., SUZUJI T. - *Neutron scattering study of crystal field excitation in $TmTe$*
Physica B **230-232** (1997) 735-737
- CLEMENTYEV E.S., ALEKSEEV P.A., BRADEN M., MIGNOT J.-M., LAPERTOT G., LAZUROV V.N., SADIKOV I.P. - *Anomalous lattice dynamics in intermediate-valence $CeNi$*
Physical Review B Rapid Communication **57** (1998) R8099-8102
- CODDENS G., LYONNARD S. - *A Method to calculate coherent quasi-elastic neutron scattering signals : illustration on the case of atomic hopping in quasi-crystals*
Physica B **233** (1997) 93 (erratum)
- CODDENS G. - *Models for assisted phason hopping and phason elasticity in icosahedral quasicrystals*
Int. J. Mod. Phys. **B 7** (1997) 1679-1716.

- CODDENS G., VIANO A.M., GIBBONS P.C., KELTON K.F., KRAMER M.J. - *Time-of-flight Neutron Scattering Study of Hydrogen Dynamics in Icosahedral $Ti_{45}Zr_{38}Ni_{17}H_{150}$ Quasicrystals* Solid State Communications **104** (1997) 179-182.
- CODDENS G., LYONNARD S., CALVAYRAC Y. - *Time scales and atomic species in the phason dynamics of AlCuFe quasicrystals*; Physical Review Letters **78** (1997) 4209-4212.
- CODDENS G., VIANO A.M., GIBBONS P.C., KELTON K.F., KRAMER M. - *Time-of-flight Neutron Scattering Study of Hydrogen Dynamics in Icosahedral $Ti_{45}Zr_{38}Ni_{17}H_{150}$ Quasicrystals* Proceedings of the 6th International Conference on Quasicrystals, Yamada Conference XLVII, World Scientific, Singapore, (1998) pp. 285-288.
- CODDENS G., LYONNARD S., HENNION B., CALVAYRAC Y. - *Phason dynamics in perfect icosahedral quasicrystals* Aperiodic'97, Proc. Int. Conf. Aperiodic Cryst., editors : M. De Boissieu, Verger-Gaudry J.L., Currat R., (Publ. World Scientific) ; Also in Festschrift for Prof. Dr. Hans-Ude Nissen on the occasion of his 65th birthday.
- COLMENERO J., ARBE A., CODDENS G., FRICK B., MIJANGOS C., REINECKE H. - *Transition from independent to cooperative segmental dynamics in polymers: Experimental realisation in poly(vinyl chloride)* Physical Review Letters **78** (1997) 1928-1931.
- COPPOLA R., FIORI F., LITTLE E.A., MAGNANI M. - *A microstructural comparison of two nuclear-grade martensitic steels using small angle neutron scattering* Journal of Nuclear Materials **245** (1997) 131-137
- COPPOLA R., EHRLICH K., MAGNANI M., MATERNA-MORRIS E., VALLI M. - *Microstructural characterization of materials for nuclear applications using small-angle neutron scattering* Journal of Applied Crystallography **30** (1997) 607-612
- COULOMB J.P., MARTIN C., GRILLET Y., LLEWELLYN P.L., ANDRE G. - *Structural properties of methane (CD_4) and hydrogen (D_2) sorbed phases on MCM-4 ($F=40 \text{ \AA}$)* Studies in Surface Sciences and Catalysis **117** (1998) 309-316
- COULOMB J.P., MARTIN C., GRILLET Y., LLEWELLYN P.L., ANDRE G. - *Structural properties of simple sorbed gases (N_2, Kr, D_2O) ($F=25 \text{ \AA}$)* Studies in Surface Sciences and Catalysis **105** (1997) 1827
- COUSSON A., COUSTARD J.M. - *X-ray structure determination of products resulting from trapping of hydroxynitrilium ion* Tetrahedron **54** (1998) 6523-6528
- COTTON J.P., HARDOUIN F. - *Chain conformation of liquid crystalline polymers studied by small angle neutron scattering* Progress in Polymer Sciences **22** (1997) 795-828
- COUVREUR F., GIBERT C., ANDRE G. - *Mesure quantitative de l'hydrogène dans le Zircaloy 4-D par diffraction neutronique* Rapport DMT, SEM/LECM **97-379**, LECM **97/062**, (1997) 1-20
- COUVREUR F., GATTY R., ANDRE G. - *Etude par diffusion et diffraction neutronique de l'influence de l'hydrogène sur le comportement du Zircaloy en température* Rapport DMT, SEM/LECM **98-67** (1998) 1-30
- CRETEGNY T., AUBRY S. - *Spatially inhomogeneous time-periodic propagating waves in anharmonic systems* Physical Review B Rapid Communications **55** (1997) 11929-11932
- CRETEGNY T., AUBRY S. - *Patterns of energy flux in periodic solutions of Klein-Gordon lattices* Physica D **113** (1998) 162-165
- CRETEGNY T., AUBRY S., FLACH S. - *1D phonon scattering by discrete breathers* Physica D **119** (1998) 73-87
- CSER L., GROSZ T., JANCZO G., KALI G. - *The nature of the interaction of tetramethylurea in various solvents* Physica B **234-236** (1997) 279-280
- DAMAY F., MARTIN C., HERVIEU M., MAIGNAN A., RAVEAU B., ANDRE G., BOUREE F. - *Structural transitions in the manganite $Pr_{0.5}Sr_{0.5}MnO_3$* Journal of Magnetism and Magnetic Materials. **184** (1998) 71-82
- DAMAY F., JIRAK Z., HERVIEU M., MARTIN C., MAIGNAN A., RAVEAU B., ANDRE G., BOUREE F. - *Charge ordering and structural transitions in $Pr_{0.5}Sr_{0.41}Ca_{0.09}MnO_3$* Journal of Magnetism and Magnetic Materials **190** (1998) 221-232
- DAMAY F., MARTIN C., MAIGNAN A., HERVIEU M., RAVEAU B., BOUREE F., ANDRE G. - *Neutron diffraction evidence for a new ferromagnetic phase in Cr doped $Pr_{0.5}Ca_{0.5}MnO_3$* Applied Physics Letters **73** (1998) 3772-3774
- DAMAY P., LECLERC F., MAGLI R., FORMISANO F., LINDNER P. - *Universal critical-scattering function : an experimental approach* Physical Review B **58** (1998) 12038-12043
- DANIEL C., MENELLE A., BRULET A., GUENET J.M. - *Thermoreversible gelation of syndiotactic polystyrene in toluene and chloroform* Polymer **38** (1997) 4193-4199
- DANIEL C., MENELLE A., BRULET A., GUENET J.M. - *Thermoreversible gelation of syndiotactic polystyrene: Effect of solvent type* Macromolecular Symposia **114** (1997) 159-164
- DAOUD M. - *Branched Polymers and gels* in Dynamical Networks in Physics and Biology, D. Beysens and G. Forgacs Eds., EDP Sciences 1998
- DAOUD M. - *Structure des polymères linéaires et branchés* Revue Marocaine des Sciences Physiques **1** (1998) 5-46
- d'ARRIGO G., GIORDANO R., TEIXEIRA J. - *Small angle neutron scattering study of binary and ternary aqueous solutions of 2-butoxyethanol and nonionic surfactant triethylene glycol monoethyl ether* J. Mol. Structure **404** (1997) 319-334
- DE BERNABE A., BERMEJO F.J., CRIADO A., PRIETO C., DUNSTETTER F., RODRIGUEZ-CARVAJAL J., CODDENS G., KAHN R. - *Low-energy magnetic neutron scattering from α -oxygen* Physical Review B **55** (1997) 11060-11063.
- DECAP G., RODRÍGUEZ-CARVAJAL J., GRENECHE J.M., CALAGE Y. - *Magnetic behaviour of the $Pb_xM_3F_{12} \cdot 3H_2O$ phases ($M = Mn^{2+}, Fe^{2+}, Fe^{3+}$)* Journal of Physics : Condensed Matter **9** (1997) 7643-7665
- DELAMARE M.P., POUILLAIN G., SIMON CH., SANFILIPPO S., CHAUD X., BRULET A. - *Vortex lattice accommodation on twin boundaries in $YBa_2Cu_3O_7$* European Physical Journal B **6** (1998) 33-38
- DE NOVION C.H. - *Neutrons in materials science and technology* Proceedings of MAT-TEC 97, A. Lodini (ed.) Reims (1997) 3-17
- DE NOVION C.H. - *Summary of conference presentations : Instrumentation and sources* Physica B **234-236** (1997) 1242-1243
- DE NOVION C.H. - *Studies of irradiated materials by scattering of cold neutrons* Proceedings of «The International Workshop on Cold Neutron Utilization» Kaeri, The Republic of Korea, (1997) p. 129-140
- DE NOVION C.H. - *Recent advances of neutron scattering in materials science and technology* Proceedings of the Conference ISRP-7, Jaipur, Inde, 24-28 février 1997 Radiation Physics and Chemistry **51** (1998) 637-643
- DEME B., LEE L.T. - *Adsorption of a hydrophobically modified polysaccharide at the air-water interface : kinetics and structure* The Journal of Physical Chemistry B **101** (1997) 8250-8258
- DERVENAGAS P., PAOLASINI L., HIESS A., LANDER G.H., PANCHULA A., CANFIELD P. - *Competing exchange interactions in ferromagnetic $CeFe_2$* Physica B **241-243** (1998) 649-650

- DJEMIA P., GANOT F., DUGAUTIER C., QUILICHINI M. - *Brillouin scattering from the icosahedral quasicrystal $Al_{70.4}Mn_{8.4}Pd_{21.2}$*
Solid State Communications **106** (1998) 459-461
- DORNER B., BAEHR M., PETITGRAND P., TOPERVERG B. - *Identification of magnetic energies in $CsFeCl_3$ with polarised neutrons*
Physica B **234-236** (1997) 549-551
- DUBENKO I.S., GOLOSOVSKY I.V., MARKOSYAN A.S., MIREBEAU I. - *Neutron diffraction study of the magnetic ordering in the $Ho(Mn_{1-x}Al_x)_2$ system.*
J. Phys. : Condens. Matter **19** (1998) 11755-11764
- DUBOIS E., CABUIL F., BACRI J.C., PERZYNSKI R., - *Phase transition in magnetic fluids.*
Prog. Colloid Polym. Sci. **104** (1997) 173-176
- DUBOS O., PETRY W., NEUHAUS J., HENNION B. - *Anharmonic dynamical behaviour in bcc Zirconium*
European Physical Journal B **3** (1998) 447-454
- DUFOUR C., DUMESNIL K., MOUGIN A., MANGIN Ph. MARCHAL G., HENNION M., - *Stabilization of the helicoidal phase in Tb and in Dy_xTb_{1-x} alloys films epitaxed on Y.*
J. Phys. Condens. Matter **9** (1997) L131-L136
- DUFOUR E., ROBERT P., RENARD D., LLAMAS G. - *Investigation of b-Lactoglobulin gelation in water/ethanol solutions*
International Dairy Journal **8** (1998) 87-93
- EHRENBERG H., WITSCHKE G., RODRIGUEZ-CARVAJAL J., VOGT T. - *Magnetic structures of the tri-rutiles $NiTa_2O_6$ and $NiSb_2O_6$.*
Journal of Magnetism and Magnetic Materials **184** (1998) 111-115
- EIJT S.W.H., CURRAT R., LORENZO J.E., SAINT-GREGOIRE P., HENNION B., VYSOCHANSKII YU.M. - *Soft mode behaviour of incommensurate Sn_2Se_6 : an inelastic neutron scattering study*
Ferroelectrics **202** (1997) 121-129
- EIJT S.W.H., CURRAT R., LORENZO J.E., SAINT-GREGOIRE P., HENNION B., VYSOCHANSKII YU.M. - *Soft modes and phonon interactions in $Sn_2P_2S_6$ studied by neutron scattering*
European Physical Journal B **5** (1998) 169-178
- EIJT S.W.H., CURRAT R., LORENZO J.E., SAINT-GREGOIRE P., HENNION B., VYSOCHANSKII YU.M. *Soft modes and phonon interactions in $Sn_2P_2S_6$ studied by means of neutron scattering*
J. Phys. : Condens. Matter **10** (1998) 4811-4844
- ELBADRAOUI E., BAUDOUR J.L., BOUREE F., TAILLADES P., ROUSSET A. - *Cationic distribution in defect Co-Mn ferrites from neutron diffraction*
Journal de Physique IV **7** (1997) C1-525-C1-526
- ELBADRAOUI E., BAUDOUR J.L., BOUREE F., GILLOT B., FRITSCH S., ROUSSET A. - *Cation distribution and mechanism of electrical conduction in nickel-copper manganites spinels*
Solid State Ionics **93** (1997) 219-225
- ELHAMDI B., LU J., LODINI A. - *Measurement of residual stresses in alumina coating deposited by plasma torch, using the neutron diffraction and the encremenntal hole drilling method*
Fourth European Conference on Residual Stresses, edited by S. Denis et al., vol. 1, pp 193-202, 1997.
- ERUKHIMOVICH I.Ya., KHOKHLOV A.R., VILGIS T.A.V., RAMZI A., BOUE F. - *Static structure factor and chain dimensions in polymer blends with nonlocal mixing*
Comput. Theor. Polym. Sci. **8** (1998) 133-142
- FAK B., BOSSY J. - *Temperature dependence of $S(Q,E)$ in liquid 4He beyond the roton*
Journal of Low Temperature Physics **112** (1998) 1-19
- FAK B., BOSSY J. - *Excitations and their temperature dependence of $S(Q,E)$ in superfluid 4He beyond the roton*
Journal of Low Temperature Physics **112** (1998) 531-536
- FAUCHER M.D., SCIAU P., KIAT J.M., ALVES M.G., BOUREE F. - *Refinement of the monoclinic and tetragonal structures of Eu^{3+} doped $LiYO_2$ by neutron diffraction at 77 and 383 K, differential scanning calorimetry and crystal field analysis*
Journal of Solid State Chemistry **137** (1998) 242-248
- FEDOROV V. I., GUKASOV A. G., KOZLOV V., MALEYEV S. V., PLAKHTY V. P., ZOBKALO. I. A. - *Interaction between the spin chirality and elastic torsion.*
Phys. Lett. A **224** (1997) 372-378.
- FERMON C., GRAY S., LEGOFF G., MATHET V., MATHIEU S., OTT F., VIRET M., WARIN P. - *Vector magnetometry with polarized neutron reflectometry with spin analysis*
Physica B **241-243** (1998) 1055-1059
- FERNÁNDEZ BARQUÍN L., GORRIA P., BARANDIARÁN J.M., GÓMEZ SAL J.C., RODRÍGUEZ-CARVAJAL J. - *In situ study of the crystallisation process and magnetism in some FeNbSiBCu amorphous alloys*
Physica B **234-236** (1997) 418-420
- FITZPATRICK M.E., EDWARDS L., WANE D.Q., WRIGHT J.S., CERETTI M., LODINI A. - *Neutron diffraction measurement of strains in AISI316 welded steel structures*
Proceedings of MAT-TEC 97, A. Lodini (editor), Reims, (1997) 327-332
- FITZPATRICK M.E., WITHERS P.J., BACZMANSKI A., HUTCHINGS M.T., LEVY R., CERETTI M., LODINI A. - *Effect of plastic flow on the thermal mismatch stress in an Al/SiC_p metal matrix composite*
Fourth European Conference on Residual Stresses, edited by S. Denis et al. vol. 1 (1997) pp 961-970
- FLORIA L.M., MARIN J.L., AUBRY S., MARTINEZ, FALO F., MAZO J.J. - *Josephson-junction ladder. A benchmark for nonlinear concepts*
Physica D **113** (1998) 387-396
- FOMPEYRINE J., DARRIET J., MAGUER J.-J., GRENECHE J.M., COURBION G., ROISNEL T., RODRÍGUEZ-CARVAJAL J. - *Magnetic Properties and Neutron Diffraction Study of the Chlorofluoride Series $Ba_2MM'F_7Cl$ ($M,M' = Mn, Fe, Co, Ni, Zn$)*
Journal of Solid State Chemistry **131** (1997) 198-214
- FORMISANO F., BAROCCHI F., MAGLI R. - *Long range interactions in Xenon*
Physical Review E **58** (1998) 2648-2651
- FOURET R., DEROLLEZ P., LAAMYEM A., HENNION B., GONZALEZ J. - *Phonons in silver gallium diselenide*
J. Phys. : Condens. Matter **9** (1997) 6579-6589
- FOURGEOT F., CHEVALIER B., LAFFARGUE D., ETOURNEAU J. - *Field-temperature magnetic phase diagram of the antiferromagnet ternary stannides $Nd_2Pd_{2-x}Sn_{1-x}$ ($x = 0.02, 0.06$ and 0.12).*
Journal of Magnetism and Magnetic Materials **182** (1998) 124-130
- FOURMAUX V., BOUE F., BRULET A., DAVIDSON P., KELLER P., COTTON J.P. - *Effect of the molecular weight on the whole conformation of a liquid crystalline comb like polymer in its melt*
Macromolecules **31** (1998) 801-806
- FOURMAUX V., BRULET A., COTTON J.P., HILLIOU P., MARTINOTY P., KELLER P., BOUE F. - *Rheology of a comb like liquid crystalline polymer as a function of its molecular weight.*
Macromolecules **31** (1998) 7445-7452
- FOURNEE V., BELIN-FERRE E., TRAMBLY DE LAISSARDIERE G., SADOE A., VOLKOV P., POON S.J. - *The Electronic structure of orthorhombic Al_2Ru*
J. Phys. Condensed Matter **9** (1997) 7999-8010
- FUJISHIRO K., UESE Y., YAMADA Y., DKHIL B., KIAT J.M., YAMASHITA Y. - *Optical and nonlinear optical studies of the relaxor PMN*
J. of the Korean Phys. Soc. **32** (1998) S964-S966

- FUJISHIRO K., VLOKH R., UESE Y., YAMADA Y., KIAT J.M., DKHIL B., YAMASHITA Y. - *Optical observation of heterophase and domain structures in relaxor ferroelectrics PZN/PT*
Japan Journal Apl. Phys. **32** (1998) S9640
- GALL A., FOWLER G.J.S., HUNTER C.N., ROBERT B. - *Influence of the protein binding site on the absorption properties of the monomeric bacteriochlorophyll in rhodobacter sphaeroides LH2 complex*
Biochemistry **36** (1997) 16282-16287
- GARCÍA-MATRES E., MARTÍNEZ J.L., RODRÍGUEZ-CARVAJAL J. - *Temperature evolution of the magnetic structures in $R_2\text{BaNiO}_5$ oxides*
Physica B **234-236** (1997) 567-568
- GARCIA-MUÑOZ J.L., SUAIDI M., FONTCUBERTA J., RODRIGUEZ-CARVAJAL J. - *Reduction of the Jahn-Teller Distortion at the Insulator-to-Metal Transition in Mixed Valence Perovskites*
Physical Review B **55** (1997) 34-37
- GARCÍA SOLDEVILLA J., ESPESO J.I., BLANCO J.A., GÓMEZ SAL J.C., GALEZ P., PACCARD D., RODRÍGUEZ-CARVAJAL J., OULADDIAF B. - *Elastic and Inelastic Neutron Scattering on $\text{NdNi}_{1-x}\text{Cu}_x$*
Physica B **234-236** (1997) 758-759
- GAVOILLE G., HUBSCH J., MIREBEAU I. - *A magnetization study of the frustrated spinel compounds $\text{Mg}_{1.55}\text{Fe}_{0.09}\text{Ti}_{0.55}\text{O}_4$*
Journal of Magnetism and Magnetic Materials **171** (1997) 291-299
- GAZEAU F., DUBOIS E., HENNION M., PERZYNSKI R., RAIKHER YU. - *Quasi-elastic neutron scattering on $\gamma\text{-Fe}_2\text{O}_3$ nanoparticles*
Europhysics Letters **40** (1997) 575-580
- GEBEL G., LAMBARD J. - *Small angle scattering study of water-swollen perfluorinated ionomer membranes*
Macromolecules **30** (1997) 7914-7920
- GEBEL G., LOPPINET B., HARA H., HIRADAWA E. - *Small angle neutron scattering study of polyethylene-Co-methacrylate ionomer aqueous solutions*
Journal of Physical Chemistry **101** (1998) 3980-3987
- GEOGHEGAN M., ABEL F. - *High resolution elastic recoil detection analysis of polystyrene depth profiles using carbon ions*
Nuclear Instruments and Methods in Physics Research B **143** (1998) 371-380
- GEOGHEGAN M., BOUE F., BACRI G., MENELLE A., BUCKNALL D.G. - *A neutron reflectometry of polystyrene network interfaces*
European Physical Journal B **3** (1998) 83-96
- GEOGHEGAN M., JANNINK G. - *On the reflectivity discontinuity generated by critical adsorption at the liquid-vapour interface*
Proceedings of the Royal Society of London Series A **454** (1998) 659-669
- GIORDANO R., MAISANO G., TEIXEIRA J. - *SANS studies of octyl-B-glucoside and glycine micellar solutions*
J. Appl. Cryst. **30** (1997) 761-764
- GIRARDIN E., LODINI A., RUSTICHELLI F., BRAHAM C., LEMAGNAN G. - *Study of crystallinity in plasma sprayed hydroxyapatite deposits for HIP prosthesis*
Proceedings of MAT-TEC 97, A. Lodini (ed.), Reims (1997) 219-224
- GOBEL A., WANG D.T., CARDONA M., PINTSCHOVIVUS L., REICHARDT W., KULDA J., PYKA N.M., ITOH K., HALLER E.E. - *Effect of isotope disorder on energies and lifetimes of phonon in germanium*
Physical Review B **58** (1998) 10510-10522
- GOLOSOSOVSKY I.V., KVIATKOVSKY B.E., SHARIGIN S.V., DUBENKO I.S., LEVITIN R.Z., MARKOSIAN A.S., GRATZ E., MIREBEAU I., GONCHARENKO I.N., BOUREE F. - *Neutron diffraction study of magnetic ordering and phase transitions in TmCo_2 : instability of 4f-magnetism*
Journal of Magnetism and Magnetic Materials **169** (1997) 123-129
- GONCHARENKO I.N., MIREBEAU I., IRODOVA A.V., SUARD E. - *Interplay of magnetic and hydrogen orders in the Laves hydride $\text{Ym}_2\text{H}_{4.3}$*
Physical Review B Rapid Communications **56** (1997) R2580-2584
- GONCHARENKO I.N., MIREBEAU I., MOLINA P., BÖNI P. - *Focusing neutrons to study small samples*
Physica B **234-236** (1997) 1047-1048
- GONCHARENKO I.N., MIREBEAU I. - *Magnetic order in EuTe under pressures up to 17 GPa. A neutron study*
Europhysics Letters **37** (1997) 633-638
- GONCHARENKO I.N., MIREBEAU I. - *Ferromagnetic interactions in EuS and EuSe , studied by neutron diffraction at pressure up to 20.5 GPa*
Physical Review Letters **80** (1998) 1082-1085
- GONCHARENKO I.N., MIREBEAU I. - *Magnetic neutron diffraction at very high pressures. Study of europium monochalcogenides*
Review of High Pressure Science Technology **7** (1998) 475-480
- GORDELIY V. I., KISELEV M. A., LESIEUR P., POLE A.V., TEIXEIRA J. - *Lipid membrane structure and interactions in dimethyl sulfoxide/water mixtures*
Biophysical Journal **75** (1998) 2343-2351
- GORDEYEV G., OKOROKOV A., RUNOV V., RUNOVA M., TOPPERVERG B., BRULET A., KAHN R., PAPOULAR R., ROSSAT-MIGNOD J., GLATTLI H., ECKERLEBE H., KAMPMANN R., WAGNER R. - *Small Angle scattering of polarized neutrons in HTSC ceramics.*
Physica B, **234-236** (1997) 837-838
- GRADZIELSKI M., LANGEVIN D., SOTTMANN T., STREY R. - *Droplet microemulsions at the emulsification boundary: the influence of the surfactant structure on the elastic constants of the amphiphilic film*
Journal of Chemical Physics **106** (1997) 8232-8238
- GRADZIELSKI M. - *Effect of the cosurfactant structure of the bending elasticity in nonionic oil in water microemulsions*
Langmuir **14** (1998) 6037-6044
- GREVIN B., BERTHIER Y., COLLIN G., MENDELS P. - *Evidence from charge instability in the CuO_3 chains of $\text{PrBa}_2\text{Cu}_3\text{O}_7$ from $^{63,65}\text{Cu}$ NMR*
Physical Review Letters **80** (1998) 2405-2408
- GRIPON C., LEGRAND L., ROSENMAN I., VIDAL O., ROBERT M.C., BOUE F. - *Lysozyme solubility in H_2O and D_2O solutions: a simple relationship*
J. Cryst. Growth **178** (1997) 238-247
- GRIPON C., LEGRAND L., ROSENMAN I., VIDAL O., ROBERT M.C., BOUE F. - *Lysozyme-lysozyme interactions in under- and super-saturated solutions: a simple relation between the second virial coefficients in H_2O and D_2O*
J. Cryst. Growth **178** (1997) 575-584
- GRIPON C., LEGRAND L., ROSENMAN I., BOUE F., REGNAUT C. - *Relation between the solubility and the effective solute-solute interaction for C_{60} solution and lysozyme solutions: a comparison using the sticky hard-sphere potential*
J. Cryst. Growth **183** (1998) 258-268
- GROS V., AL. TAWHEEL B., CERETTI M., PRIOUL C., LODINI A. - *Residual stresses in notches resulting from impacts*
Fourth European Conference on Residual Stresses, edited by S. Denis et al., vol. 1 (1997) pp 567-576
- GUENET J.M., JEON H.S., KHATRI C., JHA S.K., BALSARA N.P., GREEN M.M., BRULET A., THIERRY A. - *Thermoreversible Aggregation and Gelation of poly(n-hexylisocyanate)*
Macromolecules **30** (1997) 4590-4596
- GUENOUN P., DELSANTI M., DAVIS H.T., MALDONANDO A., MAYS J.W., TIRRELL M., URBACH W., AUVRAY L., GAZEAU D. - *Structural properties of charged diblock copolymer solutions,*
Rev. Inst. Fr. du Petr. **52** (1997) 274-277

- GUENOUN P., DELSANTI M., GAZEAU D., MAYS J.W., COOKS D., TIRRELL M., AUVRAY L. - *Structural properties of charged diblock copolymer solutions*
European Physical Journal B **1** (1998) 77-86
- GUENOUN P., MULLER F., DELSANTI M., AUVRAY L., MAYS J.W., TIRRELL M. - *Rodlike behaviour of polyelectrolyte brushes*
Physical Review Letters **81** (1998) 3872-3875
- GUKASOV A., WISNIEWSKI P., HENKIE Z. - *Neutron Diffraction Study of Magnetic Structure of U_3Bi_4 and U_3Sb_4*
Physica B: **234-236** (1997) 694-695
- GUKASOV A., STEIGENBERGER U., BARILO S. N., GURETSKII S.A. - *Neutron Scattering Study of Spin Waves in $TbFeO_3$*
Physica B **234-236** (1997) 760-761
- HELLWEG T., LANGEVIN D. - *Bending elasticity of the surfactant monolayer in droplet microemulsions : determination by a combination of dynamic light scattering and neutron spin-echo spectroscopy*
Physical Review E **57** (1998) 6825-6834
- HENKIE Z., CICHOREK T., FABROWSKI R., KUZHEL B. S., PIETRASZKO A., KEPINSKI L., KRAJCZYK L., GUKASOV A., WISNIEWSKI P. - *On the origin of the impurity Kondo-like resistivity component of $UAsSe$ ferromagnets.*
J. Phys. Chem. Solids **59** (1998) 385-393
- HENKIE Z., WISNIEWSKI P., GUKASOV A. - *U_3Bi_4 single crystal growth by the molten metal solution evaporation method*
Journal of Crystal Growth **172** (1997) 459-465
- HENNION M., PARDI L., MIREBEAU I., SUARD E., SESSOLI R., CANESHI A. - *A neutron study of mesoscopic magnetic clusters : $Mn_{12}O_{12}$*
Physical Review B **56** (1997) 8819-8827
- HENNION M., MOUSSA F., RODRÍGUEZ-CARVAJAL J., PINSARD L., REVCOLEVSKI A. - *New dynamical features in $La_{0.95}Ca_{0.05}MnO_3$ perovskite*
Physica B **234-236** (1997) 851-853
- HENNION M., MOUSSA F., RODRÍGUEZ-CARVAJAL J., PINSARD L., REVCOLEVSKI A. - *Coherent Waves of Magnetic Polarons Propagating in $La_{0.95}Ca_{0.05}MnO_3$*
Physical Review B **56** Rapid Communications (1997) R497-R500
- HENNION M., MOUSSA F., RODRÍGUEZ-CARVAJAL J., PINSARD L., REVCOLEVSKI A. - *New spin-wave branch induced by the hole doping in $La_{1-x}Ca_xMnO_3$*
Journal of Magnetism and Magnetic Materials **177-181** (1998) 858-859
- HENNION M., MOUSSA F., BIOTTEAU G., RODRÍGUEZ-CARVAJAL J., PINSARD L., REVCOLEVSKI A. - *Liquidlike Spatial Distribution of Magnetic Droplets Revealed by Neutron Scattering in $La_{1-x}Ca_xMnO_3$*
Physical Review Letters **81** (1998) 1957-1960
- HERNÁNDEZ-VELASCO J., SÁEZ-PUCHE R., RODRÍGUEZ-CARVAJAL J. - *Magnetic structure of Nd_2BaCoO_5*
Physica B **234-236** (1997) 569-571
- HERNANDEZ-VELASCO J., SAEZ-PUCHE R., RODRÍGUEZ-CARVAJAL J. - *Yb_2BaCoO_5 : magnetic and crystal structure determination from neutron scattering*
Journal of Alloys and Compounds **275-277** (1998) 651-656
- HERNANDEZ O., QUILICHINI M., COUSSON A., PAULUS W., KIAT J.M., GOUKASSOV A. - *Structural study of D-BCCD by neutron diffraction*
Aperiodic'97, Proc. Int. Conf. Aperiodic Cryst., editors : M. De Boissieu, Verger-Gaudry J.L., Currat R., (Publ. World Scientific) (1997) 365-369
- HIESS A., BOUCHERLE J.X., GIVORD F., SCHWEIZER J., LELIEVRE-BERNA E., TASSET F., GILLON B., CANFIELD P.C. - *Magnetization density in the intermediate valence compound $YbAl_3$*
Physica B **234-236** (1997) 886-887
- HIRCHI K., CERETTI M., BRAHAM C., LODINI A. - *Microstrain investigation by neutron diffraction line broadening analysis*
Proceedings of SMT11, Paris 1997, 1031-1037
- HIRCHI K., CERETTI M., BRAHAM C., LODINI A. - *Microstrain investigation by neutron diffraction line broadening analysis*
Proceedings of MAT-TEC 97, A. Lodini (ed.) Reims (1997) 95-100
- HIRCHI K., MILLET P., LODINI A. - *Stress evaluation in prosthesis fixed structures supported by teeth or implants*
Proceedings of MAT-TEC 97, A. Lodini (ed.) Reims (1997) 247-252
- HLINKA J., QUILICHINI M., CURRAT R., LEGRAND J.F. - *Phason dispersion in the incommensurate phase of betaine calcium chloride dihydrate*
J. Physics : Condensed Matter **9** (1997) 1469-1475
- HOLLAND-MORRITZ E., MÜLLER R., CODDENS G., LECHNER R.E., LONGEVILLE S., FITTER J. - *Spin dynamics in the high T_c superconductor $La_{2-x-y}Sr_xRE_yCuO_4$*
J. Phys. Chem. Solids **59** (1998) 2233-2236
- HOUREDET D., L'ALLORET F., DURAND A., LAFUMA F., AUDEBERT R., COTTON J.P. - *Small angle neutron scattering study of microphase separation in thermoassociative copolymers*
Macromolecules **31** (1998) 5323-5335
- HUXLEY A., BOUCHERLE J.X., BONNET M., BOURDAROT F., SCHUSTLER I., CAPLAN D., LELIEVRE E., BERNHOEFT N., LEJAY P., GILLON B. - *The magnetic and crystalline structure of the Laves phase superconductor $CeRu_2$*
J. Phys. : Condens. Matter **9** (1997) 4185-4195
- IRODOVA A.V., PARSHING P.P., SHILOV A.L., BELLISSENT R. - *Hydrogen-induced amorphization of the Laves phase $PrNi_2$. Neutron and X-ray study*
Poverkhnost **12** (1997) 36-44
- IVANOV A., PETITGRAND D., BOURGES P., ALEKSEEV P. - *Dispersion of crystal field excitations in Nd_2CuO_4 and Pr_2CuO_4*
Physica B **234-236** (1997) 717-718
- JAKLI A., KALI G., ROSTA L. - *Silica particle aggregates in LC-matrix*
Physica B **234-236** (1997) 297-299
- JANKOWSKA-KISIELINSKA J., MIKKE K., MILCZAREK J.J., HENNION B., UDOVENKO V.A. - *Temperature dependence of magnetic inelastic neutron scattering in $Mn(12\%Ge)$ alloy*
Acta Physica Polonica A **91** (1997) 483-486
- JOANNIC R., AUVRAY L., LASIC D.D. - *Monodisperse vesicles stabilized by grafted polymer*
Physical Review Letters **78** (1997) 3402-3405
- JOHANSSON M., AUBRY S. - *Existence and stability of quasiperiodic breathers in the discrete nonlinear Schrödinger equation*
Nonlinearity **10** (1997) 1151-1178
- JOHANSSON M., AUBRY S., GAIDIDEI Y.B., CHRISTIANSEN P.L., RASMUSSEN K.O. - *Dynamics of breathers in discrete nonlinear Schrödinger models*
Physica D **119** (1998) 115-124
- JOUBERT J.M., LATROCHE M., PERCHERON-GUEGAN A., BOUREE-VIGNERON F. - *Thermodynamic and structural comparison between two potential metal-hydride battery materials $LaNi_{3.55}Mn_{0.40}Al_{0.30}Co_{0.75}$ and $CeNi_{3.55}Mn_{0.40}Al_{0.30}Co_{0.75}$*
Journal of Alloys and Compounds **275-277** (1998) 118-122
- KAISER E., PAULUS W., COUSSON A. - *Crystal Structure of 2,6-dimethylpyrazine, $C_4H_2N_2(CH_3)_2$*
Zeitschrift für Kristallographie - New Crystal Structures **213** (1998) 79
- KAISER E., PAULUS W., COUSSON A. - *Crystal Structure of 4-methylpyridine N-oxide, C_6H_7NO*
Zeitschrift für Kristallographie - New Crystal Structures **213** (1998) 80

- KAISER MORRIS E., PAULUS W., COUSSON A., HEGER H., FILLAUX F.- *Disorder of Methyl Groups with Temperature in Two Molecular Crystals by Neutron Diffraction* Physica B **234-236** (1997) 74-75
- KAHN O., MATHONIERE C., SRINIVASAN B., GILLON B., BARON V., GRAND A., OHRSTROM L., RAMASESHA S. - *Spin distributions in antiferromagnetically coupled $Mn^{2+}Cu^{2+}$ systems : from the pair to the infinite chain* New. J. Chem. **21** (1997) 1031-1045
- KAKZMARSKA K., PIERRE J., SCHMITT D., LAMBERT-ANDRON B., BELLISSENT R., GUZIK A. - *Specific heat and magnetic structure of GdT_2X_2 compounds ($T=Cu, Ni, X=Sn, Sb$)* Acta Phys. Pol. **92** (1997) 347-350
- KALOSAKAS G., AUBRY S. - *Polarobreathers in a generalized Holstein model* Physica D **113** (1998) 228-232
- KALOSAKAS G., AUBRY S., TSIRONIS G. - *Polaron solution of the semiclassical Holstein model in one, two and three dimensions* Physical Review B **58** (1998) 3094-3104
- KALOSAKAS G., AUBRY S., TSIRONIS G. - *Possibility of observation of polaron normal modes at the far-infrared spectrum of acetanilide and related organics* Physics Letters A **247** (1998) 413-416
- KASSAPIDOU K., JESSE W., KUIL M.E., LAPP A., EGELHAAF S., VAN DER MAAREL J.R.C. - *Structure and charge distribution in DNA and poly(styrenesulfonate) aqueous solutions* Macromolecules **30** (1997) 2671-2684
- KEIMER B., AKSAY L.A., BOSSY J., BOURGES P., FONG H.F., MILIUS D.L., REGNAULT L.P., REZNIK D., VETTIER C. - *Spin excitations and phonons in $YBa_2Cu_3O_{6+x}$: a status report* Physica B **234-236** (1997) 821-829
- KEIMER B., AKSAY L.A., BOSSY J., BOURGES P., FONG H.F., MILIUS D.L., REGNAULT L.P., VETTIER C. - *Bilayer spin dynamics in underdoped $YBa_2Cu_3O_{6+x}$* J. Phys. Chem. Solids **59** (1998) 2135-2139
- KENT M.S., MAJEWSKI J., SMITH G.S., LEE L.T., SATIJA S. - *Tethered chains in theta solvent conditions : an experimental study involving Langmuir diblock copolymer monolayers* Journal of Chemical Physics **108** (1998) 5635-5645
- KIAT J.M., BOEMARE G., RIEU B., AYMES D. - *Structural evolution of $LiOH$: evidence of a solid-solid transformation toward Li_2O close to the melting temperature* Solid State Communications **108** (1998) 241-246
- KLEIN H., SIMONET V., AUDIER M., HIPPERT F., BELLISSENT R. - *Icosahedral order in a liquid metallic alloy : Molten $AlPdMn$ quasicrystal* Physica B **241-243** (1998) 964-966
- KLOTZ S., BESSON J.M., BRADEN B., KARCH K., PAVON P., STRAUUCH D., MARSHALL W.G. - *Pressure induced frequency shifts of transverse acoustic phonons in Germanium up to 9.7 GPa* Physical Review Letters **79** (1997) 1313-1316
- KLOTZ S., BRADEN B., BESSON J.M. - *Is there an electronic topological transition in zinc ?* Physical Review Letters **81** (1998) 1239-1242
- KLOTZ S., BESSON J.M., HAMEL G., NEMES R.J., MARSHALL W.G., LOVEDAY J.S., BRADEN B. - *High pressure neutron studies to 25 GPa : some recent results* Review of High Pressure Science and Technology **7** (1998) 217-220
- KLOTZ S., BESSON J.M., BRADEN B., KARCH K. - *Pressure induced mode softening in Ge* Review of High Pressure Science and Technology **7** (1998) 718-720
- KNORR K., MÄDLER F., PAPOULAR R.J. - *Model free density reconstruction of host/guest compounds from high-resolution powder diffraction data* Microporous and Mesoporous Materials **21** (1998) 353-363
- KOHGI M., IWASA K., OCHIAI A., SUZUKI T., MIGNOT J.-M., GILLON B., GUKASOV A., SCHWEIZER J., KAKURAI K., NISHI M., DONNI A., OSAKABE T. - *Charge order and one dimensional properties of Yb_4As_3* Physica B **230-232** (1997) 638-640
- KOHGI M., IWASA K., MIGNOT J.-M., OCHIAI A., SUZUKI T. - *One dimensionality in the low-carrier heavy electron system Yb_4As_3 : a role of charge ordering* Physical Review B, Rapid Communication **56** (1997) R11388-R11391
- KOHGI M., OSAKABE T., IWASA K., MIGNOT J.-M., GONCHARENKO I.N., LINK P., OKAYAMA Y., TAKAHASHI H., MORI N., HAGA T., SUZUKI T. - *Magnetic phase diagram of CeP under high pressure* Review of High Pressure Science and Technology **7** (1998) 221
- KOKEL B., BACHET B., COUSSON A. - *Synthesis and crystal structure of the 2-dimethylamino-4-phenyl-7,9-dimethyl-1,3,7,9-spiro [4,5] decane (7H-9H)-6,8,10-trione-ium chloride* Bull. Soc. Chim. Belg. Short Commun. **106** (1997) 293-294
- KOKEL B., BACHET B., COUSSON A. - *Crystal structure of the 1,3 dimethyl-5-(dimethylaminochloromethylene) barbituric acid, $C_6H_{12}ClN_3O_3$* Zeitschrift für Kristallographie. **213** (1998) 81-82
- KOUZELI K., CERETTI M., MICHAUD V., PRIOUL C., PANTEUS D., LODINI A.- *Determination of residual stresses distribution of silicon nitride-nodular cast iron in the interior brazed joints by neutron diffraction* Proceedings of MATTEC 97, Reims (1997) 313-320
- KRATZ K., HELLWEG T., EIMER W. - *Effect of connectivity and charge density on the swelling and local structural and dynamics properties of colloidal PNIPAM Microgels* Ber. Bunsenges. Phys. Chem. **102** (1998) 1603-1608
- KUZNIETZ M., PINTO H., CASPI E., MELAMUD M., ANDRE G., BOUREE F. - *Incommensurate and ferrimagnetic phases in $U(Ni,M)_2Si_2$ with minor $M = Co$ or Cu* Journal of Alloys and Compounds **271-273** (1998) 474-478
- KVARDAKOV V.V., PEPY G., SOMENKOV V.A. - *Neutron nonlinear magnetoacoustics* Physica B **241-243** (1998) 736-738
- LAIREZ D., CARTON J.P., ADAM M., RASPAUD E. - *Aggregation of telechelic triblock copolymers : from animals to flowers* Macromolecules **30** (1997) 6798-6809
- LAL J., SINHA S.H., AUVRAY L. - *Structure of polymer chains confined in Vycor* J. Phys. II, **7** (1997) 1597-1615
- LAL J., SINHA S.H., AUVRAY L. - *Structure of polymer chains confined in Vycor* M. R. S. Symposium Proceedings, **464** (1997) 363-370
- LAL J., AUVRAY L. - *The structural changes induced by anchored polymers on droplets and bicontinuous microemulsions* MRS Symposium Proceedings **463** (1997) 87-96
- LAFFARGUE D., BOUREE F., CHEVALIER B., ROISNEL T., GRAVEREAU P., ETOURNEAU J. - *Crystal and magnetic structures of the ternary stannides $U_2Pd_{2+y}Sn_{1-y}$* Journal of Magnetism and Magnetic Materials **170** (1997) 155-167
- LAFFARGUE D., ROISNEL T., CHEVALIER B., BOUREE F. - *Neutron powder diffraction study of the antiferromagnetic compound $Tb_2Pd_{2.05}Sn_{0.95}$* Journal of Alloys and Compounds **262-263** (1997) 219-224
- LAFFARGUE D., BOUREE F., CHEVALIER B., ROISNEL T., BORDERE S. - *Magnetic structures of the ternary stannide $U_2(Ni_{0.70}Pd_{0.30})_2Sn$* Journal of Alloys and Compounds **271-273** (1998) 444-447
- LAMPARTER P., NUDING MA., STEEB S., BELLISSENT R. - *Direct measurement of the hydrogen-hydrogen correlation in hydrogenated amorphous $Ni_{56}Dy_{44}$ by neutron diffraction* Z. Naturforsch. **53a** (1998) 766-770

- LATROCHE M., PAUL-BONCOUR V., PERCHERON-GUEGAN A., BOUREE-VIGNERON F., ANDRE G. - *Neutron diffraction study of YMn_2D_2*
Physica B **234-236** (1997) 599-601
- LATROCHE M., PAUL-BONCOUR V., PERCHERON-GUEGAN A., BOUREE-VIGNERON F. - *Crystallographic study of $YFe_2D_{3.5}$ by X-Ray and Neutron Powder Diffraction*
Journal of Solid State Chemistry **133** (1997) 568-571
- LATROCHE M., PAUL-BONCOUR V., PERCHERON-GUEGAN A., BOUREE-VIGNERON F. - *Temperature dependance study of $YMn_2D_{4.5}$ by means of neutron powder diffraction*
Journal of Alloys and Compounds **274** (1998) 59-64
- LATROCHE M., PERCHERON-GUEGAN A., BOUREE-VIGNERON F. - *Investigation of the crystallographic structures of $LaNi_4CoD_{4.4}$ and $LaNi_{3.55}Mn_{0.40}Al_{0.30}Co_{0.75}D_x$ ($x=2.0$ and 4.6 D/f.u.) by neutron powder diffraction*
Journal of Alloys and Compounds **265** (1998) 209-214
- LAZUKOV V.N., ALEKSEEV P.A., KLEMENTIEV E.S., NEFEDOVA E.V., SADIKOV I.P., MIGNOT J.-M., KOL'CHUGINA N.B., CHISTYAKOV O.D. - *Influence of unstable valence of cerium ions on the crystal field in $ReNi$ compounds*
Journal of Experimental and Theoretical Physics **86** (1998) 943-952
- LE BOLLOCH D., CAUDRON R., FINEL A. - *Experimental and theoretical study of the temperature and concentration dependence of the short-range order in Pt-V alloys*
Physical Review B **57** (1998) 2801-2811
- LECLERC E., CALMETTES P. - *Interactions in micellar solutions of β -casein*
Phys. Rev. Lett. **78** (1997) 150-153
- LECLERC E., CALMETTES P. - *Interactions in micellar solutions of β -casein*
Physica B **234-236** (1997) 207-209
- LECLERC E., DAOUD M.. - *Multiblock copolymers at interfaces : concentration and selectivity effects*
Macromolecules **30** (1997) 293-300
- LECLERC E., CALMETTES P. - *Structure of β -casein micelles*
Physica B **241-243** (1998) 1141-1143
- LECOMMANDOUX S., NOIREZ L., ACHARD M.F., HARDOUIN F. - *What about the backbone conformation in nematic and smectic C phases of a side-on fixed liquid crystal polymers ? A SANS study*
J. Phys. II France **7** (1997) 1417-1424
- LECOMMANDOUX S., NOIREZ L., ACHARD M.F., BRULET A., COTTON J.P., HARDOUIN F. - *Backbone conformation study on « side-on fixed » liquid crystal polymers*
Physica B **234-236** (1997) 250-251
- LECOMMANDOUX S., ACHARD M.F., HARDOUIN F., BRULET A., COTTON J.P. - *Are nematic side-on polymers totally extended ? A SANS study.*
Liquid Crystal **22** (1997) 549-555
- LEDUC F.X., HEDOUX A., KIAT J.M. - *Description of the $ZnCl_4$ ordering process in K_2ZnCl_4 from X-ray scattering investigation*
Physical Review B **57** (1998) 11023-11026
- LEE L.T., KENT M.S. - *Direct measurements of the penetration of free chains into a tethered chain layer*
Physical Review Letters **79** (1997) 2899-2902
- LEE L.T., CABANE B. - *Effets of surfactants on thermally collapsed poly(N-isopropylacrylamide) macromolecules*
Macromolecules **30** (1997) 6559-6566
- LEFEBVRE J., RENARD D., SANCHEZ-GIMENO A.C. - *Structure and rheology of heat-set gels of globular proteins*
Rheology Acta **37** (1998) 345-347
- LEFORT R., ETRILLARD J., TOUDIC B., GUILLAUME F., BRECZEWSKI T., BOURGES P. - *Aperiodic features of urea/alkane intergrowth organic compounds*
Aperiodic'97, Proc. Int. Conf. Aperiodic Cryst., editors : M. De Boissieu, Verger-Gaudry J.L., Currat R., (Publ. World Scientific) (1997) 679-683
- LEGUAY R., DUNLOP A., DUNSTETTER F., LORENZELLI N., BRASLAU A., BRIDOU F., CORNO J., PARDO B., CHEVALLIER J., COLLIEUX C., MENELLE A., ROUVIERE J.L., THOME L. - *Evidence of atomic mixing induced in metallic bilayers by electronic energy deposition*
Nuclear Instruments & Methods in Physics Research B **122** (1997) 481-502
- LEMEE-CAILLEAU M.H., LE COINTE M., CAILLEAU H., LUTY T., MOUSSA F., ROOS J., BRINKMANN D., AYACHE C., KARL N. - *Thermodynamics of the neutral-to-ionic transition as condensation and crystallization of charge-transfer excitations*
Physical Review Letters **78** (1997) 1690-1693
- LI M.H., BRULET A., KELLER P., COTTON J.P. - *Conformation of main chain liquid crystal polymers*
Neutron News, **8**, n°2 (1997) 16.
- LINK P., GONCHARENKO I.N., MIGNOT J.-M., MATSUMURA T., SUZUKI T. - *Ferromagnetic mixed-valence and Kondo lattice state in $TmTe$ at high pressure*
Physical Review Letters **80** (1998) 173-176
- LINK P., GUKASOV A., MIGNOT J.-M., MATSUMURA T., SUZUKI T. - *Neutron-diffraction study of quadrupolar order in $TmTe$: first evidence for a field-induced magnetic superstructure*
Physical Review Letters **80** (1998) 4779-4782
- LONGEVILLE S., EVEN J., BERTAULT M., MOUSSA F. - *Experimental evidence on the influence of extended defects on a structural phase transition : polymer chains in a monomer matrix*
J. Physique I **7** (1997) 1245-1248
- LOPPINET B., GEBEL G., WILLIAMS C. - *Small angle scattering study of perfluorosulfonated ionomer solutions*
Journal of Physical Chemistry **101** (1998) 1884-1892
- LOPPINET B., GEBEL G. - *Rodlike colloidal structure of short pendant chain perfluorinated ionomer solutions*
Langmuir **14** (1998) 1977-1983
- LORENZO J.P., AUBRY S. - *Insulator-metal transition versus temperature for the CDW of the 1d adiabatic Holstein model*
Physica D **113** (1998) 276-282
- LORENZO J.E., REGNAULT L.P., HENNION B., HENNION M., AIN M., BOURDAROT F., KULDA J., DHALENNE G., REVCOLEVSCHI A. - *Spin dynamics in the spin-Peierls compound $CuGeO_3$*
J. Phys. Condens. Matter. Letter to the Editor **9** (1997) 211-217
- LORENZO J.E., CURRAT R., MONCEAU P., HENNION B., BERGER H., LEVY F. - *A neutron study of the quasi-one-dimensional conductor $(TaSe_4)_2I$*
J. Phys. Condens. Matter. **10** (1998) 5039-5068
- LORENZO J.E., REGNAULT L.P., AIN M., HENNION B., KULDA J., DHALENNE G., REVCOLEVSCHI A. - *Neutron scattering studies on the continuum of excitations and double gap in the spin-Peierls compound $CuGeO_3$*
Physica B **241-243** (1998) 531-533
- LOTTERMOSER W., REDHAMMER G., FORCHER K., AMTHAUER G., PAULUS W., ANDRE G., TREUTMANN W. - *Single crystal Mössbauer and neutron powder diffraction measurements on the synthetic clinopyroxene Li-acmite $LiFeSi_2O_6$*
Zeitschrift für Kristallographie, **213** (1998) 101-107
- LYONNARD S., CODDENS G., HENNION B., CALVAYRAC Y. - *Dynamics of phason hopping in $AlFeCu$ and $AlMnPd$ quasicrystals*
Physica B **234-236** (1997) 28-29

- LYONNARD S., CODDENS G., HENNION B., CALVAYRAC Y. - *Triple-axis neutron scattering study of phason hopping in icosahedral AlMnPd quasicrystal*
Proceedings of the 6th International Conference on Quasicrystals, Yamada Conference XLVII, World Scientific, Singapore, (1998) pp. 463-466.
- MAAZA M., PARDO B., CHAUVINEAU J.P., MENELLE A., RAYNAL A., BRIDOU F., CORNO J. - *Zeeman neutron tunneling in Ni-Co-Ni thin film resonators*
Physics Letters A **235** (1997) 19-23
- MAIER CH., BLASCHKO O., PICHL W. - *The influence of uniaxial deformation on the martensitic phase transformation in Li and LiMg*
Physica B **234-236** (1997) 126-128
- MALIBERT C., DKHIL B., KIAT J.M., DURAND D., BERAR J.F., SPASOJEVIC A. - *Order and disorder in the relaxor ferroelectric perovskites PSN, comparison with BaTiO₃ and TbTiO₃*
Journal of Physics : Condensed Matter **9** (1997) 7485-7500
- MANIFACIER L., COLLIN G., BLANCHARD N. - *Correlations between physical and crystallographic parameters in the (Bi,Pb)₃Sr₂(Ca,Y)Cu₂O_{8+δ}*
International Journal of Modern Physics B **12** (1998) 3306-3312
- MARGACA F. M. A., MIRANDA SALVADO I. M., TEIXEIRA J. - *A SANS study of ZrO₂.SiO₂ gels*
J. Non-Cryst. Solids **209** (1997) 143-148
- MARGACA F. M. A., MIRANDA SALVADO I. M., TEIXEIRA J. - *Microstructure of Silicate Gels by SANS*
Proceedings of the IAEA Technical Committee Meeting on Neutron Beam Research, ed. by Nuclear and Technological Institute, Lisbon, Portugal (1998)
- MARIANI P., CASADIO R., CARSUGHI F., CERETTI M., RUSTICHELLI F. - *Structural analysis of membranes from photosynthetic bacteria by SANS*
Europhysics Letters **37** (1997) 433-438
- MARIN J.L., AUBRY S., FLORIA L.M. - *Intrinsic localized modes : discrete breathers. Existence and linear stability*
Physica D **113** (1998) 283-292
- MARIN J.L., AUBRY S. - *Finite size effects on instabilities of discrete breathers*
Physica D **119** (1998) 163-174
- MARTINEZ P.J., FLORIA L.M., MARIN J.L., AUBRY S., MAZO J.J. - *Floquet stability of discrete beathers in anisotropic Josephson junction ladders*
Physica D **119** (1998) 175-184
- MATTAUCH S., PAULUS W., GLINNEMANN J., HEGER G. - *Polymorphism of RbH₂PO₄ (RDP)*
Physica B **234-236** (1997) 40-42
- MATHON M.H., BARBU A., DUNSTETTER F., MAURY F., LORENZELLI N., DE NOVION C.H. - *Experimental study and modelling of copper precipitation under electron irradiation in dilute FeCu binary alloys*
J. Nuclear Materials **245** (1997) 224-237
- MAYOU D., ROCHE S., TRAMBLY DE LAISSARDIERE G., BERGER C., GIGNOUX C. - *Band structure and conductivity of quasicrystals*
In « 6th International Conference on Quasicrystals » edited by S. Takeuti, F. Fujiwara, World Scientific, 1998, pp.555-562
- MEDARDE M., RODRÍGUEZ-CARVAJAL J. - *Oxygen Vacancy Ordering in La_{2-x}Sr_xNiO_{4-δ} (0≤x≤0.5): Crystal Structure and Microstructure Investigated by Neutron Powder Diffraction*
Zeitschrift für Physik B-Condensed Matter **102** (1997) 307-315
- MEDARDE M., LACORRE P., CONDER K., RODRÍGUEZ-CARVAJAL J., ROSENKRANZ S., FAUTH F., FURRER A. - *Evidence for electron-lattice coupling in RNiO₃ perovskites*
Physica B **241-243** (1998) 751-757
- MEILLON S., DUNSTETTER F., PASCARD H., RODRIGUEZ-CARVAJAL J. - *Fast neutron irradiated magnetite and haematite investigated by neutron diffraction*
Journal de Physique IV **7** (1997) 607-608
- MENELLE A., POGOSSIAN S.P., LE GALL H., DESVIGNES J.M., BEN YOUSSEF J. - *Observation of magnetic thin films neutron waveguides*
Physica B **234-236** (1997) 510-512
- MEZEI R., SINKO K., CZER L., KALI G., FRATZL P. - *Small angle scattering experiments on inorganic gel*
Physica B **234-236** (1997) 279-280
- MEZIANI A., ZRADBA A., TOURAUD D., CLAUSSE M., KUNZ W. - *Can aldehydes participate in the nanostructuration of liquids containing charged micelles ?*
Journal of Molecular Liquids **73** (1997) 107-118
- MEZIANI A., TOURAUD D., ZRADBA A., PULVIN S., PEZRON I., CLAUSSE M., KUNZ W. - *Comparison of enzymatic activity and nanostructures in water/ethanol/brij 35 and Water/1-pentanol/brij 35 systems*
Journal of Physical Chemistry B **101** (1997) 3620-3625
- MICHOR H., HILSCHER G., KRENDELSBERGER R., ROGL P., BOUREE F. - *Effect of Ni-site substitutions in superconducting La₃Ni₂B₂N₃*
Physical Review B **58** (1998) 15045-15052
- MIKKE K., JANKOWSKA-KISIELINSKA J., HENNION B. - *Inelastic neutron scattering in some g-Mn alloys below and above T_N*
Physica B **241-243** (1998) 609-612
- MILCZAREK J.J., JANKOWSKA-KISIELINSKA J., MIKKE K., HENNION B. - *Anisotropy of the generalized susceptibility in Mn(38%Ni) alloy in the magnetic phase transition region*
In : Itinerant Magnetism : Fluctuation Effects, D. Wagner et al. (Eds) Kluwer Academic Publishers, 1998, pp.61-65
- MILLET P., LODINI A. - *Influence des colorants alimentaires sur le comportement de deux composites dentaires*
Journal de Biomateriaux **12** (1997) 125-133
- MIREBEAU I., GAVOILLE G., IANCU G., BOUREE F., HENNION M., HUBSCH J. - *Neutron study of the spinel compounds Fe_{2-2x}Mg_{1+4x}Ti₄O₄ across the percolation threshold of the dominant interaction*
Journal of Magnetism and Magnetic Materials **169** (1997) 279-288
- MIREBEAU I., SUARD E., HENNION M., FERNANDEZ-DIAZ M.T., DAOUD-ALADDINE A., NATEPROV A. - *Chemical and magnetic order in ZnMn₂As₂, as studied by neutron diffraction*
Journal of Magnetism and Magnetic Materials **175** (1997) 290-298
- MIREBEAU I., GONCHARENKO I.N., IRODOVA A.V., SUARD E. - *Pressure decoupling of a magneto-structural transition in YMn₂D_{4.3}*
Physica B **241-243** (1998) 672-674
- MIREBEAU I., HENNION M., GINGRAS M.J.P., KEREN A., KOJIMA K., LARKIN M., LUKE G.M., NACHUMI B., WU W.D., UEMURA Y.J., CAMPBELL I.A., MORRIS G.D. - *Depolarisation in reentrant spin glasses : a comparison between neutron and muon probes*
Hyperfine Interactions **104** (1997) 343-348
- MODEC B., PAPOULAR R., BRENCIC J.V. - *Bis(Pyridinium) pentachloro(pyridine-N)-molybdate(III)*
Acta Crystallographica **C54** (1998) 736-738
- MONTEITH A.R., PETITGRAND D., VISSER D. - *Magnetic ordering and magnetic excitations in the induced moment distorted triangular antiferromagnet TlFeCl₃ under hydrostatic pressure*
J. of Applied Physics **81** (1997) 5292
- MORINEAU D., DOSSEH G., PELLENQ R.J.M., BELLISSENT-FUNEL M.-C., ALBA-SIMIONESCU C. - *Thermodynamic and structural properties of fragile glass-forming toluene and meta-xylene : experiments and Monte-Carlo simulations*
Mol. Simul. **20** (1997) 95-113

- MORINEAU D., ALBA-SIMIONESCU C., BELLISSENT-FUNEL M.-C., LAUTHIE M.-F. - *Experimental indication of structural heterogeneities in fragile and hydrogen-bonded liquids*
Europhysics Letters **43** (1998) 195-200
- MORR D.K., SCHMALIAN J., SLICHTER C.P., BOBROFF J., ALLOUL H., YOSHINARI Y., KEREN A., MENDELS P., BLANCHARD N., COLLIN G., MARUCCO J.F. - *Comment on Using Ni substitution and ^{17}O NMR to probe the susceptibility $\chi(q)$ in cuprates*
Physical Review Letters **80** (1998) 3662-3663
- MOUALLEM-BAHOUT M., CALAGE Y., BOUREE F., ANDRE G., CAREL C. - *Magnetic and structural characterisation of new alkaline copper iron sulfide $\text{Rb}_2\text{Cu}_3\text{FeS}_4$*
Materials Letters **34** (1998) 294-298
- MOUDDEN A. H., VASILIU-DOLOC L., GOUKASSOV A., DE LEON-GUEVARA A. M., PINSARD L., REVCOLEVSCHI A. - *Spin Waves of Lightly-Doped $\text{La}_{1-x}\text{Sr}_x\text{MnO}_3$*
Physica B **234-236** (1997) 859-860
- MOUDDEN A.H., VASILIU-DOLOC L., PINSARD L., REVCOLEVSCHI A. - *Spin dynamics in $\text{La}_{1-x}\text{Sr}_x\text{MnO}_3$*
Physica B **241-243** (1997) 276-280
- MOUSSA F., HENNION M., RODRIGUEZ-CARVAJAL J., PINSARD L., REVCOLEVSCHI A. - *New spin dynamics in GMR Ca doped manganites*
Physica B **241-243** (1997) 445-447
- NADAUD N., LEQUEUX N., NANOT M., JOVE J., ROISNEL T. - *Structural studies of Tin-doped (ITO), Iron-doped (IIO) oxides and behavior of $\text{In}_4\text{Sn}_3\text{O}_{12}$*
Journal of Solid State Chemistry **135** (1998) 140-148
- NATEPROV A., TOMAK I., HEIMANN J., CISOWSKI J., MIREBEAU I. - *Ferrimagnetic-like behavior of ZnMn_2As_2*
Journal of Magnetism Magnetic Materials **172** (1997) 193-197
- NATEPROV A., CISOWSKI J., MIREBEAU I. - *Magnetic semiconductors with anti- La_2O_3 crystal structure*
Balkan Physics Letters, Proc. Suppl. BPL **5** (1997) 772
- N'GUY-MARECHAL K., MENELLE A., GERGAUD P., AL-USTA K. - *Stress evolution under neutron irradiation of NiC/Ti supermirrors*
Microscopy, Microanalysis, Microstructures **8** (1997) 239-249
- NICOLAI B., KAISER E., FILLAUX F., KEARLEY G.J., COUSSON A., PAULUS W. - *Inelastic Neutron Scattering Study of Methyl Tunneling in an Oriented Single-Crystal of 2,6-Dimethylpyrazine at Low Temperature and Rotational-Potential Calculations*
Chemical Physics **226** (1998) 1-13
- NIPKO J.C., LOONG C.K., LOEWENHAUPT M., BRADEN M., REICHARDT W., BOATNER L. - *Lattice dynamics of Xenotime : the phonon dispersion relations and density of states in LuPO_4*
Physical Review B **56** (1997) 11584-11592
- NIPKO J.C., LOONG C.K., LOEWENHAUPT M., REICHARDT W., BRADEN M., BOATNER L. - *Lattice dynamics of LuPO_4*
Journal of Alloys and Compounds **250** (1997) 573-576
- NOIREZ L., PEPY G., LAPP A. - *From phase orientation to phase destruction opposite shear flow induced effects*
Physica B **234-236** (1997) 252-253
- NOIREZ L., LAPP A. - *Shear flow induced transition from liquid-crystalline to polymer behavior in side chain liquid crystal polymers*
Physical Review Letters **78** (1997) 70-73
- NOIREZ L., LAPP A. - *Observation of the structure and the deformation of a liquid crystalline polymer under shear flow*
Mol. Cryst. Liq. Cryst. **303** (1997) 1705-1710
- NOIREZ L., BOEFFEL C., DAOUD-ALADINE M.A. - *Scaling laws in side chain liquid crystalline polymers : experimental evidence of main-chain layer hopping in the smectic phase*
Physical Review Letters **80** (1998) 1453-1456
- NUDING M.A., LAMPARTER P., STEEB S., BELLISSENT R. - *Structure of hydrogenated amorphous $\text{Ni}_{56}\text{Dy}_{44}$*
J. Alloys and Compounds **253-254** (1997) 118-120
- OBERDISSE J., BOUE F. - *Mechanical reinforcements of a polymeric matrix by inclusion of small spherical silica particles : looking for modes of rearrangement*
Cahiers de Rhéologie (1998) 339-344
- ODIER P., GOTOR F.J., PELLERIN N., LOBO RPSM., DEMBINSKI K., AYACHE J., NOEL H., POTEL M., CHAMIBADE J.P., COLLIN G. - *Copper deficiency in $\text{YBa}_2\text{Cu}_3\text{O}_{7-x}$ ceramics, textured and single crystals*
Materials Science & Engineering B **52** (1998) 117-122
- OLEKSYN O., SCHOBINGER-PAPAMANTELLOS P., RODRÍGUEZ-CARVAJAL J., BRÜCK E., BUSCHOW K.H.J. - *Crystal Structure and Magnetic Ordering in ErFe_6G_6 by X-ray, Neutron Diffraction and Magnetic Measurements*
Journal of Alloys and Compounds **257** (1997) 36-45
- OLLIVIER J., ETRILLARD J., TOUDIC B., ECOLIVET C., BOURGES P., LEVANYUK A.P. - *Direct observation of a phason gap in an incommensurate molecular compound*
Physical Review Letters **81** (1998) 3667-3670
- OLSOVEC M., SCHWEIZER J., PAOLASINI L., SECHOVSKY V., PROKES K. - *Magnetization densities and uranium form factors in UNiGa and UNiAl*
Physica B **241-243** (1998) 678-680
- ÖNNERUD P., ANDERSSON Y., TELLGREN R., NORBLAD P., BOUREE F., ANDRE G. - *The crystal and magnetic structure of ordered cubic $\text{Pd}_3\text{MnD}_{0.6}$*
Solid State Communications **101** (1997) 433-437
- ONUFRIEVA F., PFEUTY P., KISSELEV M. - *Electronic topological transition in 2D electron system on a square lattice as a motor for the «strange-metal» behaviour in high- T_c*
J. Phys. Chem. Solids. **59** (1998) 1853-1857
- OSAKABE T., KOHGI IWASA K., NAKAJIMA N., MIGNOT J. M., GONCHARENKO I.N., OKAYAMA Y., TAKAHASHI H., MORI N., HAGA Y., SUZUKI T. - *Novel magnetic structures of the low-carrier system CeP under high pressure*
Physica B **230-232** (1997) 645-648
- OTT F., FERMON C. - *Magnetic depth profiles in strained nickel-iron thin films measured by polarized neutron reflectometry*
Journal of Magnetism and Magnetic Materials **165** (1997) 475-478
- OTT F., FERMON C. - *Spin analysis and new effects in reflectivity measurements.*
Physica B **234-236** (1997) 522-524
- OTT F., LUNNEY J. - *Quantum Conductance : a step by step guide.*
Europhysics News **29** (1998) 13-16
- OTT F., BARBERAN S., LUNNEY J.G., COEY J.M.D., DE LEON-GUEVARA A.M., REVCOLEVSCHI A. - *Quantized conductance in a contact between metallic oxide crystals*
Physical Review B **58** (1998) 4656-4659
- PAPPAS C., ALBA M., BRULET A., MEZEI F. - *Ferromagnetic critical correlations in AuFe reentrant ferromagnets*
Physica B **241** (1997) 594-596
- PAIXAO J.A., WAERENBORG J.C., ROGALSKI M.S., GONCALVEST A.P., ALMEIDA M., GUKASOV A., BONNET M., SPIRLET J.C., SOUSA J.B. - *Magnetization density in $\text{UFe}_{10}\text{Si}_2$*
J. Phys. : Condens. Matter **10** (1998) 4071-4079
- PAOLASINI L., HENNION B., PANCHULA A., MYERS K., CANFIELD P. - *Lattice dynamics of cubic Laves phase ferromagnets*
Physical Review B **58** (1998) 12125-12133
- PAOLASINI L., CACIUFFO R., ROESSLI B., LANDER G.H. - *Unusual Fe-Fe interactions in the itinerant magnet UFe_2*
Physica B **241-243** (1998) 681-683
- PAOLASINI L., DERVENAGAS P., VULLIET P., SANCHEZ J.P., LANDER G.H., HIESS A., PANCHULA A., CANFIELD P. - *Magnetic response function of the itinerant ferromagnet CeFe_2*
Physical Review B **58** (1998) 12117-12124

- PAPOULAR R.J., COUSSON A., PAULUS W., KAISER-MORRIS E. - *The Model-Free Quest for Disordered Protons in Solids*, Physica B **234-236** (1997) 72-73
- PAPOULAR R. - *Cristallographie et reconstruction d'images par maximum d'entropie*
Rapport CEA-R-5758 (1997) 1-8
- PAULUS W., COUSSON A., HEGER G., REVCOLEVSKI A., DHALENNE G., HOSOYA S. - *Oxygen Defect Structure in $\text{La}_2\text{NiO}_{4-x}$*
Physica B **234-236** (1997) 20-22
- PECHEV S., CHEVALIER B., LAFFARGUE D., DARRIET B., ETOURNEAU J. - *Magnetic structure of ternary germanide $\text{U}_3\text{Cu}_4\text{Ge}_4$*
Journal of Alloys and Compounds **271-273** (1998) 448-451
- PERES N., SOUHASSOU M., WYNCKE B., GAVOILLE G., COUSSON A., PAULUS W. - *Neutron Diffraction Study of the Paraelectric Phase of Ammonium Dihydrogen Phosphate (ADP): Hydrogen Bonding of NH_4*
J. Phys.: Condens. Matter **9** (1997) 6555-6562
- PEREZ-MATO J.M., AROYO M., HLINKA J., QUILICHINI M., CURRAT R. - *Phonon symmetry selection rules for inelastic neutron scattering*
Physical Review Letters **81** (1998) 2462-2465
- PETER S., WECKLER B., ROISNEL T., LUTZ H.D. - *Linear, bent and trifurcated OH...F- hydrogen bonds : neutron powder diffraction, infrared and Raman spectroscopies of $\text{Zn}(\text{OD})\text{F}$ I and $\text{Zn}(\text{OF})\text{F}$ Ia*
Bulletin Chemists Technologists of Macedonian **16** (1997) 21-32
- PETER S., SUCHANEK E., ROISNEL T., LUTZ H.D. - *Neutron powder diffraction study on highly deuterated $\text{Ca}(\text{IO}_3)_2\cdot\text{D}_2\text{O}$*
Acta Crystallographica **C54** (1998) 1064-1066
- PETIT S., MOUDDEN A.H., HENNION B., VIETKIN A., REVCOLEVSKI A. - *Spin dynamics study of $\text{La}_{2-x}\text{Sr}_x\text{CuO}_4$ by inelastic neutron scattering*
Physica B **234-236** (1997) 800-802
- PETIT S., MOUDDEN A.H., HENNION B., VIETKIN A., REVCOLEVSKI A. - *Neutron study of the spin dynamics in superconducting $\text{La}_{2-x}\text{Sr}_x\text{CuO}_4$*
Physica C **282-287** (1997) 1375-1376
- PETIT S., MOUDDEN A.H., HENNION B., VIETKIN A., REVCOLEVSKI A. - *New slow and short range magnetic correlations in superconducting $\text{La}_{2-x}\text{Sr}_x\text{CuO}_4$*
European Physical Journal B **3** (1998) 163-167
- PETITGRAND D., CASALTA H., BOURGES P., IVANOV A.S. - *Low-energy magnetic excitations in Nd_2CuO_4*
Physica B **234-236** (1997) 806-807
- PETRESCU A.J., RECEVEUR V., CALMETTES P., DURAND D., DESMADRIL M., ROUX B., SMITH J.C. - *Small angle neutron scattering by a strongly denatured protein : analysis using random polymer theory*
Biophysical Journal **72** (1997) 335-342
- PETRESCU A.J., CALMETTES P., RECEVEUR V., DURAND D. - *Excluded-volume effects on the configurational distribution of a strongly denatured protein*
Prot. Sci. **7** (1998) 1396-1403
- PIANT A., LODINI A., HOLDEN T., ROGER R., BRAHAM C. - *Stress measurements in shot peening plates by neutron and X-ray diffraction*
Proceedings of ICRS5, Linköping 1997, 244-249
- PIERRE J., GILLON B., PINSARD L., REVCOLEVSKI A. - *Polarized neutron study of the magnetization density in $\text{La}_{0.8}\text{Sr}_{0.2}\text{MnO}_3$*
Europhysics Letters **42** (1998) 85-90
- PICKEN S.J., NOIREZ L., LUCKHURST G.R. - *Molecular conformation of a polyaramid in nematic solution from small angle neutron scattering and comparison with theory*
Journal of Chemical Physics **1092** (1998) 7612-7617
- PINSARD L., RODRÍGUEZ-CARVAJAL J., MOUDDEN H. A., ANANE A., REVCOLEVSKI A., DUPAS C. - *Jahn-Teller effect and ferromagnetic ordering in $\text{La}_{0.875}\text{Sr}_{0.125}\text{MnO}_3$: a reentrant behaviour*
Physica B **234-236** (1997) 856-858
- PINSARD L., RODRÍGUEZ-CARVAJAL J., REVCOLEVSKI A. - *Structural Phase Diagram of $\text{La}_{1-x}\text{Sr}_x\text{MnO}_3$ for Low Sr Doping*
Journal of Alloys and Compounds **262-263** (1997) 152-156.
- PINTSCHOVIVUS L., SCHREIECK B., EIGENMANN B. - *Neutron, X-ray and finite-element stress analysis on brazed components of steel and cemented carbide*
Proceedings of MAT-TEC 97, A. Lodini (ed.) Reims (1997) 309-312
- PLUYETTE E., SPRAUEL J.M., PERRIN M., CERETTI M., TODESCHINI P., LODINI A. - *Neutron diffraction residual stress evaluation around a bimetal welded joint*
Proceedings of ICRS5, Linköping (1997) 604-611
- PLUYETTE E., SPRAUEL J.M., PERRIN M., CERETTI M., TODESCHINI P., LODINI A. - *Neutron diffraction residual stress evaluation around a bimetal welded joint*
Proceedings of MAT-TEC 97, A. Lodini (ed.) Reims (1997) 55-60
- PLUYETTE E., SPRAUEL J.-M., LODINI A., PERRIN M., CERETTI M., TODESCHINI P. - *Residual stresses evaluation near interfaces by means of neutron diffraction : modelling a spectrometer*
Fourth European Conference on Residual Stresses, edited by S. Denis et al., vol. 1 pp 153-163
- POGOSSIAN S.P., BEN-YOUSSEF J., LE GALL H., DESVIGNES J.M., MENELLE A. - *New neutron magnetic low index leaky waveguide coupler*
J. Appl. Phys. **81** (1997) 4281-4283
- POGOSSIAN S.P., MENELLE A., LE GALL H., DESVIGNES J.M., BEN-YOUSSEF J. - *Neutron low index thin-film waveguides with antiresonant high-reflection layers*
Physical Review B **56** (1997) 4971-4978
- POGOSSIAN S.P., MENELLE A., LE GALL H., BEN-YOUSSEF J., DESVIGNES J.M. - *Observation of neutron guided waves from the open end of a thin film waveguide and a waveguide interferometry*
J. Appl. Phys. **83** (1998) 1159-1162
- PRAGER M., HAVIGHORST M., CODDENS G., BÜTTNER H. - *Rotational tunneling and structural phase transitions of NH_3 adsorbed as a submonolayer on $\text{MgO}(100)$ surfaces*
Physica B **234-236** (1997) 170-172.
- PRAGER M., HAVIGHORST M., CODDENS G., BÜTTNER H. - *NH_3 on $\text{MgO}(100)$ surfaces: the concentration dependence of tunneling spectra*
J. Phys.: Condens. Matter **9** (1997) 43-52.
- PREM M., BLASCHKO O., ROSTA L. - *Structure functions in decomposing Cu-Rh systems*
Physical Review B **55** (1997) 1-10.
- PROKES K., BUSCHOW K.H.J., BRUCK E., de BOER F.R., SECHOVSKY V., SVOBODA P. - *Crystallographic and magnetic structures in UTSi compounds*
Physica B **230-232** (1997) 39-42.
- PROVILLE L., AUBRY S. - *Mobile bipolarons in the adiabatic Holstein-Hubbard model in 1 and 2 dimensions*
Physica D **113** (1998) 307-317
- RAMZI A., HAKIKI A., BASTIDE J., BOUE F. - *Uniaxial extension of end-linked polystyrene networks containing deuterated free chains studied by small angle neutron scattering : effect of the network chains and the size of the free chains*
Macromolecules **30** (1997) 2963-2977
- RANDL O.G., PETRY W., BUHRER W., HENNION B. - *Lattice dynamics and related diffusion properties of intermetallics : II. Ni_3Sb*
J. Phys. : Condens. Matter **9** (1997) 10283-10292

- RATHGEBER S., RICHTER D., ZIRKEL A., WILLNER L., BRULET A., FARAGO B. - *Dynamics of bimodal polymer melts in the crossover region from Rouse to Reptation like behaviour. A study with NSE-Spectroscopy*. Physica B **234-236** (1997) 258-259
- RATHGEBER S., WILLNER L., RICHTER D., APPEL M., FLEISCHER G., BRULET A., FARAGO B., SCHLEGER P. - *Polymer dynamics in bimodal melts* Polym. Mater. Sci. Eng. **79** (1998) 299-300
- RATY J.Y., GASPARD J.P., CEOLIN R., BELLISSENT R. - *A cinnabar local order in liquid II-VI compounds* Physica B **234-236** (1997) 364-366
- RATY J.Y., GASPARD J.P., CEOLIN R., BELLISSENT R. - *Evolution of the Peierls distortion in liquid $As_{1-x}Sb_x$ compounds* Journal of Non Crystalline Solids **232-234** (1998) 59-64
- RAYMOND S., REGNAULT L.P., KAMBE S., MIGNOT J.M., LEJAY P., FLOUQUET J. - *Magnetic correlations in $Ce_{0.925}La_{0.075}Ru_2Si_2$* Journal of Low Temperature Physics **109** (1997) 205-224.
- RECEVEUR V., CALMETTES P., SMITH J.C., DESMADRIL M., CODDENS G., DURAND D. - *Picosecond dynamical change on denaturation of yeast phosphoglycerate kinase revealed by quasielastic neutron scattering* Proteins Struct. Funct. Gen. **28** (1997) 380-387.
- RECEVEUR V., DURAND D., CALMETTES P. - *Structure properties of an unfolded protein* Eur. Biophys. Journal **26** (1997) 15.
- RECEVEUR V., DURAND D., DESMADRIL M., CALMETTES P. - *Repulsive interparticle interactions in a denatured protein solution revealed by small angle neutron scattering* FEBS Letters **426** (1998) 57-61.
- RECKO K., BIERNACKA M., DOBRZYNSKI L., PERZYNSKA K., SATULA D., SZYMANSKI K., WALISZEWSKI J., SUSKI W., WOCHOWSKI K., ANDRE G., BOUREE F. - *The crystal and magnetic structures of $UF_{x-1}Al_{12-x}$ alloys* Physica B **234-236** (1997) 696-697
- RECKO K., BIERNACKA M., DOBRZYNSKI L., PERZYNSKA K., SATULA D., SZYMANSKI K., WALISZEWSKI J., SUSKI W., WOCHOWSKI K., ANDRE G., BOUREE F. - *The crystal and magnetic structures of $UF_{x-1}Al_{12-x}$ intermetallic compounds* J. Phys. : Condens. Matter **9** (1997) 9541-9553
- REGNAULT L.P., BOURGES P., BURLET P. - *Phase diagrams and spin correlations in $YBa_2Cu_3O_{6+x}$* In « Neutron Scattering in Layered Copper-Oxide Superconductors » Ed. A. Furrer, vol. **85** (1998) 85-134
- REINECKE H., MIJANGOS C., BRULET A., GUENET J.M. - *Molecular structure in PVC thermoreversible gels: Effect of solvent type and tacticity*. Macromolecules **30** (1997) 959-965
- RENARD D., BOUE F., LEFEBVRE J. - *Protein-polysaccharide mixture : structure of the systems and the effect of shear studied by SANS* Physica B **234-236** (1997) 289-291
- RENARD D., BOUE F., LEFEBVRE J. - *Protein-polysaccharide mixture : structure and effect of shear studied by small angle neutron scattering* R. Soc. Chem. **192** (1997) 303-315
- RENARD D., BOUE F., LEFEBVRE J. - *Solution and gelation properties of protein-polysaccharide mixtures : signature by small-angle neutron scattering and rheology* R. Soc. Chem. **218** (1998) 189-201
- RENKER B., BRADEN M., HEID R. - *Fingerprints of solid-state chemical reactions in the dynamics of fullerenes* Physica B **241-243** (1998) 255-261
- REQUARDT H., LORENZO J.E., CURRAT R., MONCEAU P., HENNION B., BERGER H., LEVY F. - *Structural study of the charge-density-wave modulation of isoelectronically doped $(Ta_{1-x}Nb_xSe_4)_{21}$ ($0.1\% < x < 1.2\%$)* J. Physics : Condens. Matter **10** (1998) 6505-6514
- RETOUX R., RODRIGUEZ-CARVAJAL J., LACORRE P. - *Neutron diffraction and TEM studies of the crystal structure and defects of $Nd_4Ni_3O_8$* Journal of Solid State Chemistry **140** (1998) 307-315
- RIAL C., MORÁN E., ALARIO-FRANCO M.A., AMADOR U., MARTÍNEZ J.L., RODRÍGUEZ-CARVAJAL J., ANDERSEN N.H. - *Effects of extra oxygen on the structure and superconductivity of $La_{2-x}Ca_xCuO_{4+y}$ prepared by chemical oxidation* Physica C **297** (1998) 277-293
- RIOS S., QUILICHINI M., PEREZ-MATO J.M. - *Neutron scattering study of the antiferroelectric transition in TiD_2PO_4* J. Phys. Condensed Matter **10** (1998) 3045-3060
- RIOS S., PAULUS W., COUSSON A., QUILICHINI M., HEGER G. - *Isotope effect in TiH_2PO_4 and TiD_2PO_4* Acta Crystallographica B **54** (1998) 790-797
- ROCHE S., TRAMBLY DE LAISSARDIERE G., MAYOU D. - *Electronic transport properties of quasicrystals* Journal Math. Phys. **38** (1997) 1794-1822
- RODRIGUEZ-CARVAJAL J. - *Structural analysis from powder diffraction data : the Rietveld method* Ecole thématique « Cristallographie et neutrons », Journées Rossat-Mignod 1997, Cours - Tome I [32 pages]
- RODRIGUEZ-CARVAJAL J. - *An introduction to the program FullProf : Comments on the examples kit* Ecole thématique « Cristallographie et neutrons », Journées Rossat-Mignod 1997, Cours - Tome I [24 pages]
- RODRÍGUEZ-CARVAJAL J., HENNION M., MOUSSA F., PINSARD L., REVCOLEVSKI A. - *The Jahn-Teller Structural Transition in Stoichiometric $LaMnO_3$* Physica B **234-236** (1997) 848-850
- RODRÍGUEZ-CARVAJAL J. (Coordinator) et al. - *Solid State Chemistry* European Spallation Source (ESS 97-62-M), Contributions to the Development of the Scientific Case, pp 67-93 (1997), Ed. U. Steingenberger: Solid State and Structural Chemistry and Physics
- RODRÍGUEZ-CARVAJAL J. - *Crystallography and Magnetism Using Neutron Powder and Single Crystal Diffraction* Proceedings of the IAEA Technical Committee Meeting on Neutron Beam Research, pp 1-8, Lisbon, September 10-12, 1997.
- RODRÍGUEZ-CARVAJAL J., ROSENKRANZ S., MEDARDE M., LACORRE P., FERNÁNDEZ-DÍAZ M.T., FAUTH F., TROUNOV V. - *Neutron Diffraction Study of the Magnetic and Orbital Ordering in $^{154}SmNiO_3$ and $^{153}EuNiO_3$* Physical Review B **57** (1998) 456-464
- RODRÍGUEZ-CARVAJAL J., HENNION M., MOUSSA F., MOUDDEN A.H., PINSARD L., REVCOLEVSKI A. - *Neutron Diffraction Study of the Jahn-Teller Transition in Stoichiometric $LaMnO_3$* Physical Review B **57**, Rapid Communications (1998) R3189-3192
- RODRÍGUEZ-CARVAJAL J., ROUSSE G., MASQUELIER C., HERVIEU M. - *Electronic Crystallization in a Lithium Battery Material: Columnar Ordering of Electrons and Holes in the Spinel $LiMn_2O_4$* Physical Review Letters **81** (1998) 4660-4663
- ROEPKE M., HOLLAND-MORITZ E., CODDENS G., FITTER J., LECHNER R. - *Spin dynamics in the high T_c superconductor $La_{2-x-y}Sr_xRE_yCuO_4$* Physica B **234-236** (1997) 723-725.

- ROGL P., ANDRE G., WEITZER F., POTEL M., NOEL H. - *Nuclear and magnetic structure of $U_3Ga_2Ge_3$: a neutron powder diffraction study*
Journal of Solid State Chemistry **131** (1997) 31-42
- ROISNEL T., NUNEZ P., MASSA W., TRESSAUD A. - *Magnetic structures of antiferromagnetic chain fluorides $A_2MnF_5 \cdot xH_2O$*
Physica B **234-236** (1997) 579-581
- ROUF-GEORGE C., MUNCH J.P., SCHOSSELER F., POUCHELON A., BEINERT G., BOUE F., BASTIDE J. - *Thermal and quenched fluctuations of polymer concentration in Poly(dimethylsiloxane) gels*
Macromolecules. **30** (1997) 8344-8359
- ROUSSEAU M., DANIEL PH., TOULOUSE J., HENNION B. - *Evidence of disorder in the perovskite crystals $RbCaF_3$ and $Rb_{0.65}K_{0.35}CaF_3$. Investigation of phonon acoustic modes by inelastic neutron scattering*
Physica B **234-236** (1997) 139-141
- ROUSSEAU M., DANIEL PH., TOULOUSE J., HENNION B. - *The dynamic signature of highly anisotropic correlation near the phase transition in $KCaF_3$*
J. Phys. : Condens. Matter **9** (1997) 8963-8971
- RUFFLE B., ETRILLARD J., TOUDIC B., ECOLIVET C., CODDENS G., AMBROISE J.P., GUÉGUEN E., MARCHAND R. - *Comparative analysis of the fast dynamics in the supercooled nonfragile glass-forming liquid $Na_{0.5}Li_{0.5}PO_3$ observed by coherent neutron scattering*
Physical Review B **56** (1997) 11546-11552
- RUFFLE B., BEAUFILS S., ETRILLARD J., CODDENS G., TOUDIC B., ECOLIVET C. - *Fast dynamics of $Na_{0.5}Li_{0.5}PO_3$ observed by coherent neutron scattering*
Physica B **234-236** (1997) 391-392.
- RUFFLE B., BEAUFILS S., ETRILLARD J., GALLIER J., TOUDIC B., ECOLIVET C., CODDENS G., AMBROISE J.P., GEGUEN E., MARCHAND R. - *Dynamics of a non fragile glass forming liquid*
MRS Symposium Proceedings Series, **455** (1997) 151-155.
- SALAUN S., BULOUE A., ROUSSEAU M., HENNION B., GESLAND J.Y. - *Lattice dynamics of fluoride scheelites : inelastic neutron scattering in $YLiF_4$ and modelization*
J. Phys. : Condens. Matter **9** (1997) 6571-6968
- SAOUT-ELHAK A., BENHAMOU M., DAOUD M. - *Phase separation in polymer blends near a surface*
J. Physique II **7** (1997) 503-516
- SAUVAJOL J.-L., ANGLARET E., BORMANN D., AZNAR R., HENNION B. - *Inelastic neutron scattering investigation of CsC_{60} in its polymer and dimer phases*
Solid State Communications **104** (1997) 387-390
- SAUVAJOL J.-L., CHESNEL K., ANGLARET E., ALMAIRAC R., AZNAR R., BOUTROUILLE P., HENNION B. - *Inelastic neutron scattering investigation of quenched CsC_{60} phases*
Solid State Communications **108** (1998) 781-785
- SAUVAJOL J.-L., ANGLARET E., CHESNEL K., PALPACUER M., GIRARD A., MOREAC A., AMELINE J.C., DELUGEARD Y., HENNION B. - *Vibrational properties of polymer and quenched CsC_{60} phases*
J. Chim. Phys. **95** (1998) 1441-1444
- SAUVAJOL J.-L., ANGLARET E., HENNION B. - *Low frequency modes of CsC_{60} phases*
In « Electronic Properties of Novel Materials », edited by H. Kuzmany et al. (1998) pp. 318-321
- SCHENK T., KLEIN H., AUDIER M., SIMONET V., HIPPERT F., RODRIGUEZ-CARVAJAL J., BELLISSENT R. - *Structure of magnetism of the $\mu Al_x Mn_{1-x} Cr_{1-x}$ approximant phase ($0 \leq x \leq 1$)*
Phil. Mag. Letters **76** (1997) 189-198
- SCHEYER P., LEVELUT C., PELOUS J., DURAND D. - *Cross-link influence on the relaxations in glass- and gel-forming polyurethanes by neutron and Brillouin scattering*
Physical Review B **58** (1998) 11212-11222
- SCHIEBEL P., PRANDL W., WULF K., PAPOULAR R., PAULUS W., HEGER G. - *Quantum Mechanics of the Rotation-Translation Coupling of NH_3 -Groups in Metal Hexamine Salts*
Physica B **234-236** (1997) 64-65
- SCHOBINGER-PAPAMANTELOS P., RODRÍGUEZ-CARVAJAL J., BUSCHOW K.H.J. - *Atomic Disorder and Canted Ferrimagnetism in the $TbCr_6Ge_6$ Compound. A Neutron Study*
Journal of Alloys and Compounds **255** (1997) 67-73
- SCHOBINGER-PAPAMANTELOS P., RODRÍGUEZ-CARVAJAL J., PROKES K., BUSCHOW K.H.J. - *Mictomagnetic Behaviour of $CeNi_{0.84}Sn_2$. A Neutron Diffraction and Magnetic Study*
Physica B **234-236** (1997) 689- 691
- SCHOBINGER-PAPAMANTELOS P., RODRÍGUEZ-CARVAJAL J., BUSCHOW K.H.J. - *Ferrimagnetism and disorder in the RCr_6Ge_6 compounds (R= Dy, Ho, Er Y) : A neutron study*
Journal of Alloys and Compounds **256** (1997) 92-96
- SCHOBINGER-PAPAMANTELOS P., RODRÍGUEZ-CARVAJAL J., NIEUWENHUYTS G.H., LEMMENS L.W.F., BUSCHOW K.H.J. - *Structure and Magnetic Ordering in $CeNi_xSn_2$ Compounds*
Journal of Alloys and Compounds **262-263** (1997) 335-340
- SCHOBINGER-PAPAMANTELOS P., RODRÍGUEZ-CARVAJAL J., ANDRÉ G., BUSCHOW K.H.J. - *A Neutron Diffraction Study of Magnetic Ordering in $DyMn_{6-x}Cr_xGe_6$ compounds (I)*
Journal of Alloys and Compounds **265** (1998) 56-60.
- SCHOBINGER-PAPAMANTELOS P., RODRÍGUEZ-CARVAJAL J., ANDRÉ G., BUSCHOW K.H.J. - *A Neutron Diffraction Study of Magnetic Ordering in $DyMn_{6-x}Cr_xGe_6$ compounds (II)*
Journal of Alloys and Compounds **265** (1998) 61-69
- SCHOBINGER-PAPAMANTELOS P., RODRÍGUEZ-CARVAJAL J., BUSCHOW K.H.J. - *Magnetic Order in $TbCo_6Ge_6$ and $TbCo_2Ge_2$ compounds: a Neutron Study.*
Journal of Alloys and Compounds **274** (1998) 83-89
- SCHOBINGER-PAPAMANTELOS P., OLEKSYN O., RODRÍGUEZ-CARVAJAL J., ANDRÉ G., BRÜCK E., BUSCHOW K.H.J. - *Atomic Disorder, Magnetic Order and Phase Transitions of $TbFe_6Ge_6$ Studied by X-ray Neutron Diffraction and Magnetic Measurements (I).*
Journal of Magnetism and Magnetic Materials **182** (1998) 96-110
- SEPELAK V., TKACOVA K., BOLDYREV V.V., WISSMANN S., BECKER K.D. - *Mechanical induced cation redistribution in $ZnFe_2O_4$ and its thermal stability*
Physica **234-236** (1997) 617-619
- SEPELAK V., WISSMANN S., BECKER K.D. - *A temperature-dependent Mössbauer study of mechanically activated and non-activated zinc ferrite*
Journal of Materials Science **33** (1998) 2845-2850
- SEPELAK V., BUCHAL A., TKACOVA K., BECKER K.D. - *Nanocrystalline structure of the metastable ball-milled inverse spinel-ferrites*
Materials Science Forum **278-281** (1998) 862-867
- SEPELAK V., STEINKE U., UECKER D. CHR., WISSMANN S., BECKER K.D. - *Structural disorder in mechanosynthesized zinc ferrite*
Journal of Solid State Chemistry **135** (1998) 52-58
- SIDIS Y., BOURGES P., HENNION B., VILLENEUVE R., COLLIN G., MARRUCO J.F. - *Spin dynamics in the metallic state of $YBa_2(Cu_{0.98}Zn_{0.02})_3O_{6+x}$*
Int. J. of Modern Physics B **12** (1998) 3330-3334

- SIMONET V., KLEIN H., BELLISSENT R., HIPPERT F., AUDIER M. - *Magnetism and local order in AlPdMn liquid alloys*
Physica B **234-236** (1997) 594-595
- SIMONET V., HIPPERT F., KLEIN H., AUDIER M., BELLISSENT R., FISCHER H., MURANI A.P., BOURSIER D. - *Local order and magnetism in liquid Al-Pd-Mn alloys*
Physical Review **B58** (1998) 6273-6286
- SIMONET V., HIPPERT F., AUDIER M., TRAMBLY DE LAISSARDIERE G. - *Origin of magnetism in crystalline and quasicrystalline AlMn and AlPdMn phase*
Physical Review **B58** (1998) R.8865-8868
- SMITH J.C., LAMY A., KATAOKA M., YUNOKI J., PETRESCU A.-J., RECEVEUR V., CALMETTES P., DURAND D. - *Motions in native and denatured proteins*
Physica B **241-243** (1998) 1110-1114
- SPITERI M.N., BOUE F., LAPP A., COTTON J.P. - *Polyelectrolyte persistence length in semidilute solution as a function of the ionic strength*
Physica B **234-236** (1997) 303-305
- STOCKER P., GAY J.M., BIENFAIT M., CODDENS G. - *Anisotropy of translational diffusion in premelted methane films;*
Surface Reviews and Letters **4** (1997) 863-868.
- STURGIS J.N., GALL A., ELLERVEE A., FREIBERG A., ROBERT B. - *The effect of pressure on the bacteriochlorophylla binding sites of the core antenna complex from Rhodospirillum rubrum*
Biochemistry **37** (1998) 14875-14880
- SUARD E., MIREBEAU I., CAIGNAERT V., IMBERT P., BALAGUROV A.M. - *Influence of deoxygenation process on magnetic diagram of iron doped Yba₂Cu₃O₇ phases : a neutron diffraction study*
Physica C **288** (1997) 10-20
- SUARD E., MIREBEAU I., DAOUD-ALADINE A., NAPETROV A. - *Unusual succession of magnetic phases in Zn_{1-x}Mn_{2+x}As₂*
Physica B **241-243** (1998) 739-741
- SYROMYATNIKOV V.G., MENELLE A., SOROKO Z.N., SCHEBETOV A.F. - *Neutron double multilayer monochromator-polarizer Co/Ti*
Physica B **248** (1998) 355-357
- SZEFTTEL J. - *Short range correlated eigenstates in the many-electron problem*
Physica B **230-232** (1997) 482-485
- SZEFTTEL J. - *Off-diagonal long range order in many-electron problem*
Acta Physica Polonica A **91** (1997) 341-345
- SZEFTTEL J., LAURENT P. - *Localized vibrations and standing waves in anharmonic lattices*
Physical Review E **57** (1998) 1134-1138
- SZEFTTEL J., MOUDDEN H., KOCHARIAN A. - *On the physical significance of the high-dimensional Bethe ansatz*
Journal of Magnetism and Magnetic Materials **187** (1998) 261-267
- SZUSZKIEWICZ W., DYBKO K., DYNOWSKA E., GORECKA J., WITKOWSKA B., HENNION B. - *Selected properties of lattice dynamics of HgSe and b-HgS*
Acta Physica Polonica A **92** (1997) 1029-1032
- SZUSZKIEWICZ W., HENNION B., JOUANNE M., MORHANGE J.F., DYNOWSKA E., JANIK E., WOJTOWICZ T., ZIELINSKI M., FURDYNA J.K. - *Magnons in cubic MBE-grown A_{1-x}Mn_xTe layers (A=Cd, Zn, Mg)*
Acta Physica Polonica A **93** (1998) 583-587
- SZUSZKIEWICZ W., HENNION B., JOUANNE M., JULIEN C., DYBKO K., DYNOWSKA E., GORECKA J., WITKOWSKA W. - *Peculiarities of lattice dynamics of HgSe and β-HgS*
J. of Cryst. Growth **184-185** (1998) 1204-1208
- TARASIUK J., WIERZBANOWSKI K., BACZMANSKI A. - *New direct algorithm for the calculation of the orientation distribution function from pole figures*
Archives of Metallurgy **42** (1997) 257-272
- TARASIUK J., WIERZBANOWSKI K., BACZMANSKI A. - *Non destructive analysis of crystallographic texture heterogeneity*
Philosophical Magazine A **78** (1998) 819-834
- TARASIUK J., WIERZBANOWSKI K., BACZMANSKI A. - *New algorithm for the ODF calculation from pole figures*
Materials Science Forum **273-275** (1998) 133-138
- TARASIUK J., WIERZBANOWSKI K., BACZMANSKI A. - *Non destructive study of texture heterogeneity*
Materials Science Forum **273-275** (1998) 283-288
- TARASIUK J., WIERZBANOWSKI K., BACZMANSKI A. - *New algorithm of direct method of texture analysis*
Cryst. Res. Technol. **33** (1997) 101-118
- TASSAING T., BELLISSENT-FUNEL M.-C., GUILLOT B., GUISSANY Y. - *The partial pair correlation functions of dense supercritical water*
Europhysics Letters **42** (1998) 265-270
- TEIXEIRA J., ZANOTTI J.-M., BELLISSENT-FUNEL M.-C., CHEN S.-H. - *Water in confined geometries*
Physica B **234-236** (1997) 370-374
- TEIXEIRA J. - *The double identity of ice X*
Nature, News and Views **392** (1998) 232-233
- TEMST K., VERBANCK G., SCHAD R., GLADYSZEWSKI G., HENNION M. - *Structural and magnetic properties of Fe/Cr and Fe/Ag multilayers*
Physica B **234-236** (1997) 467-469
- TENEGAL F., BOUCHET B., BELLISSENT R., HERLIN N., CAUCHETIER M., DIXMIER J. - *Early stage of the pyrolytic crystallization in amorphous nanopowders of silicon carbonitrides Si₃C₂N₂ by combined wide-angle X-ray and neutron diffractometries*
Philosophical Magazine A **78** (1998) 803-817
- THIEBAUT S., PAUL-BONCOUR V., PERCHERON-GUEGAN A., LIMACHER B., BLASCHKO O., MAIER C., TAILLAND C., LEROY D. - *Structural changes in Pd (Rh,Pt) solid solutions due to ³He*
Physical Review B **57** (1998) 10379-10387
- TOPEVERG B., DORNER B., SONNTAG A., PETITGRAND P. - *Quantum paramagnetic fluctuations in RbFeCl₃ in a magnetic field applied perpendicular to the anisotropy axis*
Physical Review B **55** (1997) 983-993
- TRAN V. H., TROC R., DU PLESSIS P. V., ANDRE G., BOUREE F. - *Nonmagnetic-magnetic crossover in the URu_{1-x}Pd_xGa system*
Physical Review B **56** (1997) 11065-11072
- TRAN V. H., ANDRE G., BOUREE F., TROC R., NOËL H. - *Ac-susceptibility and neutron diffraction studies of the URu_{1-x}Pd_xGa system*
Journal of Alloys and Compounds **271-273** (1998) 503-507
- TRAN V. H., TROC R., ANDRE G. - *Magnetic ordering in URhSi and URhGe*
Journal Magnetism Magnetic Materials **186** (1998) 81-86
- TROC R., TRAN V. H., WOLCYRZ M., ANDRE G., BOUREE F. - *Crystal and magnetic structure of a novel compound UCu₅Al. Structural stability with Th substitution*
Journal Magnetism Magnetic Materials **190** (1998) 251-256
- TURQUIER F., HAIRY, P., FITZPATRICK M.E., EDWARDS L., CERETTI M., LODINI A. - *Stress measurements in a tool steel structure coated with plasma sprayed zirconia*
Proceedings of MAT-TEC 97, Reims, A. Lodini (ed.) (1997) 163-168
- UEMURA Y. J., GAULIN B.D., MEKATA M., MIREBEAU I., POUGET S., THOLENCE J.L. - *Neutron spin echo studies of SrCr₈Ga₄O₁₉*
Journal Magnetism Magnetic Materials **177-181** (1998) 701-702

- VAJDA P., ANDRE G., HAMMANN J. - *Magnetic structure of b - DyD_{2+x} : Modulated phases for $x=0$ and short range order for $x=0.135$*
Physical Review B **55** (1997) 3028-3032
- VAJDA P., ANDRE G., ZOGAL O.J. - *Long range and short range magnetic order in b - $HoH(D)_{2+x}$ ($x=0$ and $x=0.12$)*
Physical Review B **57** (1998) 5030-5036
- VAKHRUSHEV S., KIAT J.M., DAKHIL B. - *X-ray study of the kinetics of field induced transition from the glass-like to the ferroelectric phase in lead magnonionate*
Solid State Communications **103** (1997) 477-482
- Van der MAAREL J.R.C., KASSAPIDOU K. - *Structure of short DNA fragment solutions*
Macromolecules **31** (1998) 5734-5739
- Van DIJK N.H., FAK B., CHARVOLIN T., LEJAY P., MIGNOT J.-M., HENNION B. - *Magnetic excitations in $CePd_2Si_2$*
Physica B **241-243** (1998) 808-810
- VIDAL O., ROBERT M.C., BOUE F. - *Gel growth of lysozyme crystals studied by small angle neutron scattering : case of agarose gel, a nucleation promotor*
J. Crystal Growth **192** (1998) 257-270
- VIDAL O., ROBERT M.C., BOUE F. - *Gel growth of lysozyme crystals studied by small angle neutron scattering : case of silica gel, a nucleation inhibitor*
J. Crystal Growth **192** (1998) 271-281
- VIGOUREUX P., GUKASOV A., BARILO S.N., ZHIGUNOV D.I. - *Neutron Scattering study of the structural phase transition in Eu_2CuO_4*
Physica B : Cond. Matt. **234-236** (1997) 815-817
- VIGOUREUX P., PAULUS W., HENRY J.Y., PINOL S., HEGER G. - *Influence of the Reduction and of the Oxidation on $Nd_{2-x}Ce_xCuO_{4\pm\delta}$*
Physica B **234-236** (1997) 719-720
- VIGOUREUX P., BRADEN M., GUKASOV A., PAULUS W., BOURGES P., COUSSON A., PETITGRAND D., LAURIAT J.P., MEVEN M., BARILO S.N., ZHIGUNOV D.I., AGELMANN P., HEGER G. - *Study of the Structural Phase Transition in $Gd_{2-x}Ce_xCuO_4$*
Physica C **273** (1997) 239-247
- VIRET M., GLÄTTLI H., FERMON C., DE LEON-GUEVARA A.M., REVCOLEVSCHI A. - *Magnetic coherence in the paramagnetic state of mixed-valence manganites*
Physica B **241-243** (1998) 430-432
- WHEELER J.C., PFEUTY P. - *Study of a novel tetracritical point*
Physica A **244** (1997) 476-483
- WIECHERT H., KORTMANN K.D., STUSSER N. - *Deuterium monolayers physisorbed on krypton-plated graphite : a two-dimensional Ising system*
Physica B **234-236** (1997) 164-166
- WIECHERT H., KORTMANN K.D. - *Ordering and phase transition in deuterium monolayers physisorbed on Krypton preplated graphite*
Journal of Low Temperature Physics **111** (1998) 561-568
- WINKLER B., HARRIS M.J., ECCLESTON R.S., KNORR K., HENNION B. - *Crystal field transitions in $Co_2[Al_4Si_5]O_{18}$ cordierite and $CoAl_2O_4$ spinel determined by neutron spectroscopy*
Phys. Chem. Minerals **25** (1997) 79-82
- WINKLER B., KAISER I., CHALL M., CODDENS G., HENNION B., KAHN R. - *Dynamics of $N(CH_3)_4GeCl_3$*
Physica B **234-236** (1997) 70-71
- WISNIEWSKI P., HENKIE Z. - *Crystal growth and magnetic anisotropy of resistivity of U_3X_4 pnictides*
Wiad. Chem. **51** (1997) 571-591
- WOCHOWSKI K., BURLET P., ANDRE G., BOUREE F., SUSKI W. - *Structure and element distribution in the $UFe_{10-x}Al_xSi_2$ system*
Journal of Phase Equilibria **19** (1998) 423-425
- WOLCYRZ M., HORYN R., ANDRE G., BOUREE F. - *Crystal structure and magnetic properties of $Bi_{0.267}Pr_{0.733}SrO_{3.4}$ via neutron diffraction*
Journal of Solid State Chemistry **132** (1997) 182-187
- WOLCYRZ M., HORYN R., ANDRE G., BOUREE F. - *Crystal and magnetic structures of $Bi_{0.2}Tb_{0.8}SrO_3$ via neutron diffraction*
Physical Review B **55** (1997) 14335-14340
- WUTTKE J., SEIDL M., HINZE G., TOELLE A., CODDENS G. - *Mode-coupling crossover in viscous toluene revealed by neutron and light scattering*
European Physical Journal B **1** (1998), 169-172.
- YOSHIDA M., MORI S., YAMAMOTO N., UESE Y., YAMADA Y., KIAT J.M. - *Transmission electron microscope observation of relaxor ferroelectric PMN*
J. of the Korean Phys. Soc. **32** (1998) S993-S995
- ZAHARKO O., SCHOBINGER-PAPAMANTELLOS P., RITTER C., RODRÍGUEZ-CARVAJAL J., BUSCHOW K. H. J. - *Influence of Thermal History on Crystal Structure, Microstructure and Magnetic Properties of $TbFe_6Ge_6$ (II)*
Journal of Magnetism and Magnetic Materials **187** (1998) 293-308
- ZANOTTI J.M., BELLISSENT-FUNEL M.-C., PARELLO J. - *Dynamics of a globular protein studied by neutron scattering and solid state NMR*
Physica B **234-236** (1997) 228-230
- ZANOTTI J.M., BELLISSENT-FUNEL M.-C., PARELLO J. - *Dynamics of a globular protein studied by neutron scattering and solid state NMR*
European Biophysics Journal, **26** (1997) 42-43